

# Northumbria Research Link

Citation: Edge, Jerry (2001) Passive flow monitoring in heating system networks. Doctoral thesis, Northumbria University.

This version was downloaded from Northumbria Research Link:  
<http://nrl.northumbria.ac.uk/id/eprint/600/>

Northumbria University has developed Northumbria Research Link (NRL) to enable users to access the University's research output. Copyright © and moral rights for items on NRL are retained by the individual author(s) and/or other copyright owners. Single copies of full items can be reproduced, displayed or performed, and given to third parties in any format or medium for personal research or study, educational, or not-for-profit purposes without prior permission or charge, provided the authors, title and full bibliographic details are given, as well as a hyperlink and/or URL to the original metadata page. The content must not be changed in any way. Full items must not be sold commercially in any format or medium without formal permission of the copyright holder. The full policy is available online: <http://nrl.northumbria.ac.uk/policies.html>

Some theses deposited to NRL up to and including 2006 were digitised by the British Library and made available online through the [EThOS e-thesis online service](#). These records were added to NRL to maintain a central record of the University's research theses, as well as still appearing through the British Library's service. For more information about Northumbria University research theses, please visit [University Library Online](#).

# **Passive Flow Monitoring in Heating System Networks**

Jeremy Simon Edge

A thesis submitted in partial fulfilment  
of the requirements of the  
University of Northumbria at Newcastle  
for the award of Doctor of Philosophy

June 2001

# **Passive Flow Monitoring in Heating System Networks**

Jeremy Simon Edge

A thesis submitted in partial fulfilment  
of the requirements of the  
University of Northumbria at Newcastle  
for the award of Doctor of Philosophy

January 2001

## **Acknowledgements**

The main acknowledgement is to Dr. C.P. Underwood for his invaluable guidance and support. Without his patience and encouragement, this work would never have been completed.

I would also like to acknowledge the Department of Built Environment Technicians (especially Mr. John Brunton), for their enormous help with the test rig.

Thanks to my mother and father for their love and support over the years.

Finally, thanks to my wife and son for their love, and for putting up with me, particularly in the final stages of writing up.



## **Abstract**

This work deals with a "passive flow monitoring" technique which can be used to help determine the energy used by a building's heating system. The thesis first highlights the background and importance of energy monitoring in buildings. This work points out that energy monitoring is an important feature in the running of buildings today. In the past, the energy crisis in the 1970's made people aware of how important it was to have knowledge of how buildings consume energy. More recently, environmental issues have reinforced the importance of gaining good quality information on energy use in buildings. This thesis investigates the use of combined port flow characteristics/control signal relationships for three port control valves to predict system water flow rate in heating systems. A laboratory test rig was built and a range of three port valves were tested. A series of combined port flow characteristics/control signal relationships were developed from measurements from the test rig. Curve fit models were then applied to these relationships in the form of polynomial equations. Where practical relationships could not be measured for a valve, a theoretical valve model was derived. In order to validate the polynomial regression model and the mathematical model, the test rig was modified to take into account practical heating system characteristics. A series of flow characteristic results were produced from the modified test rig so that the performance of the two models (empirical and mathematical) could be evaluated.

It was found that the empirical model performed well in predicting combined port flow ratios with RMS errors ranging between 2.73% and 6.54%.

The mathematical model gave overall prediction errors between -2.63% and +9.25% which compare favourably with the performance of some flow meters.

The work then goes on to present an energy use algorithm which incorporates the valve model (empirical or theoretical) for use in BEMS.

## Contents

Chapter	Title	Page No.
<b>1.0</b>	<b>Introduction</b>	1
1.1	Aim and Objective	2
1.2	Background	3
1.2.1	The Requirement of Energy Use Data for the Validation of Computer Models	8
1.3	Thesis Structure	12
<b>2.0</b>	<b>Assessment of Energy Use in Buildings</b>	15
2.1	Energy Monitoring	18
2.2	Energy Metering	24
2.3	Flow Meters	33
2.4	Summary	57
<b>3.0</b>	<b>Valve Modelling</b>	60
3.1	Background and Previous Work	67
3.2	Summary	84
3.3	Detailed Valve Model	85
3.4	Derivation of the Valve and Circuit Model	90
<b>4.0</b>	<b>A Practical Investigation of Valve Characteristics</b>	96
4.1	Introduction	96
4.2	A Practical Investigation of the Relationship Between Valve Flow Rate Characteristics and Incoming Control Signal	97
4.3	Philosophy of Test Rig Development	99
4.4	Laboratory Test Rig	102
4.5	Procedure	107
4.5.1	Initial Test Valve Set Up	107
4.5.2	Experimental Procedure	108
4.6	Results	110
4.7	Analysis	111
4.8	Initial Mathematical Model Comparisons to Measured Test Rig Flow Rate Data	116
4.9	Summary	117

<b>5.0</b>	<b>The Use of Flow Characteristics to Monitor Flow in a Practical Heating System</b>	<b>119</b>
5.1	Introduction	119
5.2	Mathematical Curve Fitting	120
5.2.1	Curve Fitting Results	121
5.3	Modification of Laboratory Test Rig	123
5.4	Procedure	126
5.4.1	Initial Test Valve Set Up	126
5.4.2	Experimental Procedure	128
5.5	Results Comparison	129
5.5.1	Summary of Results Comparison	135
5.6	Validation of Mathematical Valve Model	136
5.6.1	Summary of Results	140
5.7	Modification of the Valve Model	140
5.7.1	Further Model Modifications	142
5.8	Summary of Validation of Mathematical Model	146
5.9	Final Test of Valve Model Versions subjected to a Sinusoidal Control Signal Input	148
5.10	Summary	150
<b>6.0</b>	<b>Conclusions, Implementation and Recommendations for Further Work</b>	<b>152</b>
6.1	Conclusions	152
6.2	Implementation in Practice	155
6.3	Further Work	157
<b>References</b>		<b>211</b>
<b>Figures</b>		<b>159</b>

<b>Figure No.</b>	<b>Description</b>	<b>Page No.</b>
1a	Three Port Control Valve Mixing Arrangement	61
1b	Three Port Control Valve Diverting Arrangement	61
2	Linear/Equal Percentage Valve Characteristics	63
3	Rangeability of a Valve	65
4	Generalised Circuit Layout	90

5	Mathematical Model (Version 1.0)	93
6 - 8	Initial Results from Mathematical Model (Version 1.0)	160
9	Typical Compensated Heating Circuit	101
10	Typical Injection Circuit	101
11	3-port Valve Cross Section	102
12	Schematic of Test Rig	105
13 – 24	Initial Results from Test Rig	161
25 – 36	Hysteresis Errors for Initial Results	164
37 – 48	Comparison of Test Rig Results with Mathematical Model (Version 1.0) Predictions	167
49 – 56	Graphs Comparing Test Rig Results to Polynomial Regression Predictions	170
57	Mathematical Model (Version 2.0)	138
58 – 65	Graphs comparing Test Rig Results with Mathematical Model (Version 2.0) Predictions	173
66 – 105	Graphs comparing Test Rig Results with Mathematical Model (Version 2.1) Predictions	176
106 – 153	Graphs comparing Test Rig Results with Mathematical Model (Version 2.2) Predictions	185
154	Mathematical Model (Version 3.0)	144
155 – 164	Graphs comparing Test Rig Results with Mathematical Model (Version 3.0) Predictions	194
165 - 192	All Model Versions Integrated over Time Flow Profiles	197
193 -200	Comparisons of average prediction errors for valve Models	205
201	Energy Algorithm	208
<b>Tables</b>		<b>209</b>

<b>Table No.</b>	<b>Description</b>	<b>Page No.</b>
1	Flow Meter Classifications	34
2	Summary of $R^2$ Values	210
3	Summary of Prediction Errors	130

4	Valve Model Versions	137
---	----------------------	-----

<b>Appendices</b>		<b>221</b>
-------------------	--	------------

<b>Appendix</b>	<b>Description</b>	<b>Page No.</b>
1	Table A1, Flow Meters	222
2	Valve Model Derivation	224
3	Published paper as part of this work	228
4	Pictures (A1 – A6) of Test Rig	235
5	Fortran Program for Orifice Plate Flow Rates	238
6	Polynomial Curve Fit Graphs (A1 – A16) to Measured Data and Tables (A2 – A17) of Statistical Values	239
7	Table A18, Differential Pressure Transducer Readings Compared to Orifice Plate Readings	247
8	Figures A17 – A55, Mathematical Model Version 2.1 validation graphs (Hysteresis = 10%)	249

## List of symbols

$G_{inh}$	Inherent valve flow fraction
$G_o$	Valve let-by flow fraction
$G_{ins}$	Installed valve flow fraction
$P$	Valve stem (and inlet port plug) position (fraction), (Note that Letherman <sup>81</sup> , Weber <sup>115</sup> , and Hamilton <sup>89</sup> use the symbol $x$ for this in their respective equations)
$P_o$	Valve stem position at end of let by region
$P_{bypass}$	Bypass port plug position (fraction)
$c$	Equal percentage valve constant
$N$	Valve authority (fraction)
$\Delta p'_v$	Valve pressure drop at fully open (designated) position ( $\text{Nm}^{-2}$ )
$\Delta p'_s$	Design pressure drop in that part of the circuit influenced by the valve ( $\text{Nm}^{-2}$ )
$\Delta p_v$	Valve pressure drop ( $\text{Nm}^{-2}$ )
$\Delta p_s$	Circuit pressure drop ( $\text{Nm}^{-2}$ )
$\dot{V}_{inh}$	Valve inherent volume flow rate ( $\text{m}^3\text{s}^{-1}$ )
$\dot{V}'_{inh}$	Valve inherent volume flow rate at fully open (design rated) position ( $\text{m}^3\text{s}^{-1}$ )
$\dot{V}$	Circuit volume flow rate ( $\text{m}^3\text{s}^{-1}$ )
$\dot{V}'$	Circuit volume flow rate at design conditions ( $\text{m}^3\text{s}^{-1}$ )
$S$	Incoming control signal (fraction)
$G_{ins(inlet, S)}$	Inlet port installed characteristic at control signal $S$ (fraction)
$G_{ins(bypass, S)}$	Bypass port installed characteristic at control signal $S$ (fraction)
$\dot{V}_{(inlet, S)}$	Inlet port volume flow rate at control signal $S$ ( $\text{m}^3\text{s}^{-1}$ )
$\dot{V}_{(bypass, S)}$	Bypass port volume flow rate at control signal $S$ ( $\text{m}^3\text{s}^{-1}$ )
$\dot{V}_{(combined, S)}$	Combined port volume flow rate at control signal $S$ ( $\text{m}^3\text{s}^{-1}$ )
$\Sigma G, f$	Combined circuit flow ratio (this is given the symbol $f$ in the graphical output)
$k$	Constant for linear let-by model

$K_1 - K_4$	Constants for a given valve (Letherman <sup>81</sup> )
$Q$	Thermal Energy (kJ)
$T$	Time (secs)
$v$	Volume flow rate (m <sup>3</sup> /s)
$\rho$	Density (m <sup>3</sup> /kg)
$C_p$	Specific heat capacity (kJ/kg.K)
$t_i$	Water inlet temperature (°C)
$t_o$	Water outlet temperature (°C)

## **Chapter 1**

### **1.0 Introduction**

Adequate knowledge of energy use in buildings is important for a number of reasons. In the past fuel shortages and subsequent increases in fuel costs provided an incentive to building owners and businesses to lower the energy consumption of their buildings. This provoked interest in monitoring the energy use of buildings so that this knowledge could be used to identify low efficiency and high energy use areas so that improvements could be made and monitored. This helped to promote the efficient running of buildings so that costs could be reduced. More recently energy use has become an issue with respect to environmental issues. According to CIBSE<sup>1</sup>, “buildings consume nearly half the energy used in the UK”. They state that “an energy efficient building provides the required internal environment and services with minimum energy use in a cost effective and environmentally sensitive manner”.

A number of methods are used to monitor energy use in buildings, most of which are reviewed later in this thesis. With respect to heating systems (and chilled water cooling systems) one way to monitor energy use is to measure water flow rates and flow and return water temperatures over time. These could then be used in a simple energy balance equation to give energy use. This monitoring could be carried out by a Building Energy Management System (BEMS). Some sites do not have the facility to monitor water flow rate data. Some engineers do not allow for flow metering in their designs.



Cost cutting in the design stages of some projects precludes the use of flow meters in the final system installation. When flow meters are included, their accuracy may vary depending on the flow meter type and the way it is installed and maintained. Most heating (and cooling) systems use a modulating control valve to control the temperature/flow rate of the system water circulating. The positioning of these valves is often controlled from a control signal from a BEMS. This thesis investigates the possibility of using the control signals of these valves (from BEMS) together with the measured combined port flow characteristics of three port valves to predict system water flow rates, negating the requirement of separate flow metering equipment. Where practical valve information is not available for a valve, a theoretical valve model is proposed and tested.

### **1.1 Aim And Objectives**

The following sets out the aim and objectives for this study:-

#### **Aim**

To investigate the potential for the use of functional relationships between a control valve's characteristics and its positioning control signal as a means to assist in the monitoring of flow rates in heating system networks.

## Objectives

1. To design and build a test rig that is capable of testing a range of three port control valves in terms of measurement of flow characteristics with respect to valve control signal at different valve authorities.
2. To test a range of control valves and measure their combined port flow characteristics at pre-defined valve authorities.
3. From the results of point 2 above, use curve fitting techniques to create an empirical model of a valve.
4. Review existing theoretical equations and previous work to develop a mathematical model of a valve.
5. Modify the test rig so that the two versions of the valve model can be validated.
6. Develop an energy use algorithm that can be used in BEMS.

## 1.2 Background

At around the time of the outset of this work there was a concern regarding energy use in buildings.

For the efficient operation of any business, industry or organisation one factor to take into account is cost of energy use. In 1989<sup>2</sup> the Energy Efficiency Office stated that “the country’s fuel bills could be reduced cost-effectively by 20%, worth approximately £8 billion a year” and that this “would mean better profitability and lower costs for hundreds of companies and organisations”. They also stated that “Wasteful buildings, whether poorly designed or badly

run, can use many times more energy than similar efficient buildings”. They identified energy costs as the largest controllable factor in the running of office buildings and that these averaged about 22% of the total service costs. This was a large percentage of overall running costs and highlighted the significance of the cost of energy on the overall economic success of an organisation or business. They argued that energy savings of the order of 30% could often be achieved by improved good housekeeping, the efficient use of existing equipment and by cost effective investment.

The increase in concern for energy use and its respective costs appears to have begun in the 1970’s. Santangelo<sup>3</sup> refers to the energy crisis in the 1970’s affecting the attitude of industry towards energy use. Santangelo explained that the combination of shortage of supply and increase in energy costs made industry aware of the importance of energy monitoring and conservation where previously little effort was made to conserve, nor was there any real concern. It is revealed that in the overall design of industrial buildings energy was only considered as a means of supplying a facility. Santangelo points out “that the dramatic increases in energy prices in the 1970’s provided an incentive to reduce energy costs”.

Graves<sup>4</sup> also refers to the mid 1970’s in that up until this time energy management as a standard management function was, for the most part, non-existent. The dramatic increase in energy costs is given as the primer for energy management activities to provide a great opportunity for reducing costs in commercial, institutional and residential properties. According to Graves an

energy monitoring system can determine the effectiveness of an energy management programme and be used to help maintain the energy efficiency levels obtained through the programme.

Lyberg and Fracastoro<sup>5</sup> highlight the oil crisis in 1973 in that after this, efforts were made to save energy in buildings. They note that many proposed energy conservation measures did not perform as expected, because these were often based on simple calculation schemes for the prediction of energy cost savings. They then explain two approaches commonly applied to investigate the differences between measured and predicted energy consumptions. The first approach is the detailed monitoring of the energy consumption with use of comprehensive instrumentation, and the subsequent analysis of this data by computer models. The second approach is the reduction of the detail and number of measurements within an individual building, but to base these over many buildings under different climatic conditions so that the effects of some wider influences on energy consumption can be determined.

Olsen<sup>6</sup> stated in 1980 that “energy conservation is becoming increasingly important and therefore efficient installation and operation are becoming imperative. Previously, developers and speculative builders have placed all emphasis on initial cost of construction and little or no interest at all was shown on the cost of operation or on maintenance”. He pointed out that “as the energy crisis becomes more acute, more emphasis must be placed on operating costs and proper maintenance of operating efficiency to utilise available energy more efficiently”.

Huusom<sup>7</sup> stated in 1983 that “the interest in accurately measuring energy consumption has increased considerably over most of Europe due to the rise in energy prices ....”.

More recently the importance of the consideration of environmental issues also became a factor. The BRE<sup>8</sup> (Building Research Establishment) stated that “good building design can contribute considerably to reducing pollution and improving the environment”. They provided an assessment method which specifies criteria for a range of issues concerning the global, neighbourhood and internal environment.

“The use of buildings is responsible for more external air pollution than any other activity. The use of energy in buildings accounts for half of the UK’s annual production of greenhouse gases”. They identified buildings as being responsible for a large proportion of the emission of sulphur dioxide and dioxides of nitrogen and the use of CFC’s.

Carbon dioxide caused by the burning of fossil fuels was highlighted as being one of the main greenhouse gases. Also, sulphur dioxide, emitted when burning some fossil fuels, was referred to as being the main cause of acid rain. Two of the oxides of nitrogen - NO and NO<sub>2</sub> - arising from combustion appliances, were also identified as contributing to the cause of acid rain. It was stated that “reducing the energy consumption of buildings lowers the emissions of greenhouse gases and can reduce the emission of sulphur dioxide and the oxides of nitrogen”.

Some interesting facts emerged from the report<sup>8</sup> at the time: “Carbon dioxide emissions are estimated to contribute 50% to the effect of global warming.

Half of the carbon dioxide emitted in the UK results from the use of energy in buildings for heating, lighting and air conditioning.” It was stated that “a consequence of energy use is long term fossil fuel depletion. In the medium term, this will probably lead to an increase in fuel costs as extraction becomes more difficult”.

This concern is still evident today with the UK Government<sup>9</sup> stating that “The scientific evidence is growing that man-made greenhouse gas emissions are having a noticeable effect on the earth's climate. Globally, seven of the ten warmest years on record were in the 1990's. In the future, the earth's climate could warm by as much as 3°C over the next 100 years. The social, environmental and economic costs associated with this could be huge.”

It is, therefore, important to consider energy use and conservation in both new and existing buildings. With new buildings, some form of building energy prediction and analysis is required to estimate the possible energy consumption for the constituent parts and for the total building so that changes can be investigated and improvements may be made at the design stage. For existing buildings, energy monitoring and analysis is required to identify the consumption's of the constituent parts and for the total building so that areas can be identified for possible improvement and an energy conservation strategy can be made. Ongoing monitoring and analysis is required to assess the effects of the implementation of this strategy.

The amount of energy consumed within and by a building is generally due to the way it is used, the climate, the building construction, and the building's services engineering systems. It is therefore essential to be able to analyse and/or predict the effect of these factors on a buildings energy use. Shavit and Spethman<sup>10</sup> agree in stating that “to analyse the energy consumption in buildings, it is necessary to study the energy consumption as a function of the building envelope, mechanical system, and the control system”.

### **1.2.1 The Requirement of Energy Use Data for the Validation of Computer Models**

Computer models are used to predict and analyse energy use by systems and buildings. Indeed Miller<sup>11</sup> states that “in the building industry, the primary emphasis in the evaluation of means for reducing energy use has been on simulations that represent relatively long term characteristics”.

A generation of these programs have been developed which predict, with varying degrees of sophistication, the likely energy exchanges within a building subject to a given climate. The available methods for predicting energy consumption vary from very simple degree-day calculations, to detailed finite difference models for the building response. Bowman and Lomas<sup>12</sup> state that “these dynamic thermal models work from first principles, require a very detailed building and system description, and have a variety of output options

that include the variation with time of internal temperatures, heating loads and energy fluxes”.

With the widespread use of these models it is important that their performance is validated using empirical energy use data. Empirical validation is widely accepted as a method of validating computer simulation models. Bloomfield<sup>13</sup> agrees in stating that “comparison with real building performance represents the ultimate test of the validity of a model”. Bowman and Lomas<sup>12</sup> concur in stating that “empirical validation . . . is the ultimate stage in any validation process”. They identify more than 130 comparisons of computer model predictions and actual building performance revealed by work carried out at the then Leicester Polytechnic (now De Montfort University). In reviewing previous validation work they highlight the difficulty, costliness, and time, required for validating dynamic thermal models.

Bowman and Lomas<sup>12</sup> report that the Solar Energy Research Institute (SERI) established a data-base which contains actual measured building response data from test cells and residences in the USA. However, they argue that for the validation of simulation algorithms, a more detailed data set is required. In their review of previous validation work they highlight the inadequacy of empirical data in many attempts of empirical validation of a number of computer simulation software packages.

Other work carried out includes a comparison by Diamond and Hunn<sup>14</sup> of DOE-2 ( Department of Energy Building Energy Analysis Computer Program )



computer program simulations to utility company metered data for seven commercial buildings. It would appear that no sufficient end-use data was available as they argue that use of utility bill data is sufficient for the demonstration of the performance of the computer program. This comparison would not be valid for a true detailed validation of the program.

A study<sup>15</sup> was also made of the BLAST ( Building Loads Analysis and System Thermodynamics Program ) program predictions. This again used the energy consumption for two office buildings as indicated by the utility bills as a basis of comparison for the program predictions. Again this study is stated as a comparison not a true validation.

Riegel et al<sup>16</sup> report on the use of DOE2.1 computer simulation package as an interactive design/analysis tool. They identify the buildings massing, site and orientation as significantly affecting the ultimate building's energy consumption. They state that "the design team must have at their disposal the necessary design tools to adequately quantify climatic data and energy consumption levels so that intelligent cost-effective decisions can be made. Energy conscious design must be an integral part of the entire design continuum if a building's potential for energy savings is to be realised".

Lomas<sup>17</sup> investigates the availability of adequate empirical data for validation work. He concludes that "there are very few well documented high-quality data sets suitable for validating dynamic thermal models". Nevertheless, in later work he goes on to report on two empirical validation exercises. The first was

based on the validation of the ESP program. The results were not encouraging though some fault was identified with the empirical data used. The second, a validation of a number of simulation programs, found that “the work was valuable in identifying errors and approximations in simulation programs that would otherwise have remained undetected”. This work was based on the modelling of test rooms and the subsequent comparison of the model results with empirical data taken from the rooms.

Metered energy consumption by end-use and time of day are typically unavailable for commercial buildings<sup>18</sup>. Indeed, it is also evident that these data tend to be unavailable for most other types of buildings other than single room test cells or very simple dwellings. Previous validation work also suggests this.

The importance of obtaining good quality empirical data from buildings is demonstrated by the work carried out in this area. From this work it is evident that there is a distinct lack of time series, measured data from sites in order to perform model validations. The detailed monitoring of energy use is therefore a necessity for the empirical validation of computer simulation models.

The next chapter reviews methods for obtaining and monitoring energy use in buildings and their effectiveness. The performance of heat meters and in particular flow meters is addressed.

### 1.3 Thesis Structure

This chapter has provided some background on the requirement and importance of knowledge of energy use in buildings. The validation of computer simulation programs was also highlighted as a use for good quality information on how energy is used in buildings. The aims and objectives of this work have also been stated.

Chapter 2 reviews current methods of monitoring and assessing energy use in buildings from use of energy bills, heat metering and use of flow meters. It emphasises the need for good quality end use data so that a detailed knowledge of how energy is actually used in buildings can be gained. A number of research papers assessing the performance of heat metering devices and flow meters are reviewed. The majority of these papers help to express some doubt as to the reliability and accuracy of these devices (depending on type of device, maintenance, and installation conditions).

Chapter 3 details the theory behind control valve selection and performance and reviews work carried out with regard to valve modelling. It was found that most of the work in this area incorporated a valve model as part of a system to investigate the short term dynamic response and control characteristics of the overall system. No work had been carried out on the performance of the individual valve model, especially with regard to model accuracy in predicting flow characteristics.

Chapter 3 gives a theoretical treatment of control valve performance. A theoretical valve model is defined based on standard equations for inherent and installed characteristics of a valve. Initial results from the model are presented.

Chapter 4 describes a practical investigation of valve combined port flow ratios with respect to control signal. It details the philosophy and design of a test rig, together with the experimental procedure carried out on a range of test valves. Results from the test rig are presented and analysed. The results from the rig show the relationship between the control signal to a valve and the combined port flow ratio at different valve authorities. At the end of the chapter a comparison is made between the initial mathematical model detailed in chapter 3, with results from the test rig. These initial comparisons were encouraging.

Chapter 5 details the mathematical curve fitting procedure applied to the empirical data from the test rig. This was carried out so that the relationships could be incorporated into an energy use algorithm in a BEMS. The test rig was modified to simulate control signal and data monitoring as it would occur in practice so that the rig could be used to validate the mathematical curve fits and the mathematical model. Experimental procedure for the revised rig is detailed together with the validation results and comparisons to the flow ratios predicted by the curve fits and to the flow ratios predicted by the mathematical model. The initial mathematical model showed poor agreement at low control signals so a number of modifications were made to the model to try and improve its performance. Three versions of the model were tested.

Flow ratio predictions for each of the versions of the model are compared to the validation test rig results.

Chapter 6 gives the overall conclusions of the study together with details of how the empirical model and theoretical model could be implemented in practice to predict system flow rates and hence energy use (when combined with flow and return temperatures). Recommendations for further study are then discussed.

## Chapter 2

### 2.0 Assessment of Energy Use in Buildings

Traditionally, energy use in buildings is found from utility bills, or by direct measurement and monitoring of system water flow rates and flow and return water temperatures by either a Building Energy Management System (BEMS) or a heat meter, by computer simulation, or some other form of energy use assessment.

The use of utility bills for the assessment of energy use does not express the effects of system conversion efficiencies and, depending on system layout, does not give sufficient detail of energy use by individual systems or buildings, especially in the case of multi-building sites with a central source of heating hot water. The relative effect of the buildings' micro-climate, operation, structure and occupancy on energy use is therefore ignored.

Mazzucchi<sup>18</sup> states that “actual end-use energy consumption must be collected to understand how commercial buildings really use energy if the design and operation of these buildings for cost-effective energy consumption is ever to become the rule rather, than the exception”. It is also needed for a meaningful comparison or validation of building and system modelling design programs which are used commonly today. He points out that “these simulations . . . are generally validated only against monthly utility billings”.

Lyberg and Fracastoro<sup>5</sup> argue that “if applicable, direct measurement is generally the method to be preferred”. They claim that errors are often small compared to when another data gathering technique is used and that a disaggregation of the end use of energy can be achieved. They also claim that direct measurements having a small resolution in time, allows the study of the dynamic building performance. They continue that the disadvantage of direct measurement is cost.

Bisesi<sup>19</sup> recognises the significance of properly setting up a system as the first step in energy conservation. Successive measurement and comparison is the essential basis for energy monitoring.

Energy cannot be well managed unless there is a way to identify the major users and then easily trend the consumption patterns to identify the potential reductions in energy per unit of production or per service performed<sup>20</sup>.

Stebbins<sup>20</sup> reports on highly efficient energy metering and trend analysis techniques. Stebbins holds the view that a carefully constructed utilities metering/monitoring and trend analysis process is an essential first step toward effective energy control. The importance of the response of people is stressed in that meters only indicate and record what is happening and do not save energy by themselves. Experience shows that substantial savings can result from metering and trending<sup>20</sup>. The importance of the provision of historical energy consumption data is identified to aid in projecting future loads and developing standards for subsequent years. Such data are a fundamental requirement in order to formulate financial forecasts and operating budgets.

Gadsby et al<sup>21</sup> state that “measurements in the piping systems of . . . multifamily buildings requires expensive plumbing and valving arrangements to introduce flow measuring sensors”. Indeed this would appear to be the case for all types of buildings, although this warrants further investigation.

Ideally, the system may be analysed by considering the fuel entering the building or site, and the energy conversion, distribution and utilisation with losses at each stage within the system. In order to monitor the energy used by a hot water heating or chilled water cooling system it is necessary to measure water flow rates and flow and return water temperatures. Indeed, Haberl and Watt<sup>22</sup> state that “flow measurement is an important part of the analysis of building energy use whenever thermal energy use is being investigated. In a building accurate, yet affordable liquid flow measurements are required for the analysis of chilled water, hot water and steam condensate use”. Flow and return water temperature monitoring is a normal function of a Building Energy Management System (BEMS).

Water flow rates can be measured by a flow meter. A wide range of flow meters are available today with varying degrees of accuracy and reliability. The capital costs and installation requirements of these flow meters may lead to the exclusion of them in the final installed system, particularly where cost cutting during the system design period is required.



Haberl and Watt<sup>22</sup> reinforce this view by stating that “unfortunately, the need for accurate measurement is often stifled . . . due to tight budget constraints where the building owner may not be willing to pay the additional five to ten per cent cost for the detailed measurement . . .”. In existing buildings, where there is no facility for flow metering, the costs and extra complication of the installation of a flow meter into an existing system could lead, again, to their exclusion. In both these cases utility bills are usually relied upon to give an indication of overall energy consumption.

Surveys of many existing buildings serviced by conventional hot water heating and chilled water cooling reveal that all of the energy utilised usually passes at some stage through a modulating control valve. Valve position data, again, is a normal function of a BEMS control algorithm (where control signals are calculated centrally), or is detectable (i.e. if local autonomous control is used where stand alone controllers are used at plant level, which communicate with the BEMS host). Valve position data is also furnished by computer simulation analysis.

## **2.1 Energy Monitoring**

One area of building services engineering which has sought to monitor energy use for many years is district heating. This is an essential application for billing purposes.

Various methods are used in district heating schemes and multiple occupancy buildings to assess energy use.

Hegburg<sup>23</sup> reviews various energy allocation devices previously defined by McClelland<sup>24</sup>. These devices are used to allocate costs to users of energy in these district heating schemes and multiple occupancy dwellings. The review lists them as follows :-

1. Individual electric and natural gas meters which measure the electricity or natural gas entering each apartment. These are owned by the utility company who reads and maintain the meters and bills the residents.
2. Electric and natural gas submeters which are installed, owned, maintained and read by the apartment management.
3. Heat meters, (in the USA sometimes referred to as Btu meters), used with hot or chilled water systems which are accurate but expensive to install.
4. Volumetric heat meters which measure only the volume of water flow without temperature sensors meaning that they are easier to install but less accurate than 3.
5. Heat evaporation meters which are inexpensive and easy to install but because the liquid evaporates so slowly they must be read annually to ensure a satisfactory level of accuracy.

Goettling and Kupplers<sup>25</sup> paper on ‘electronic allocation’ systems pointed out that, amongst other things, “heating cost distribution by calibrated heat metering is expensive”. They list three metering methods :-

1. Integrating heat meters with measurement of volume and temperature.
2. Non-calibratable surrogate method where either volume flow is measured and a constant temperature change is assumed, or temperature change is measured and a constant volume flow is assumed.
3. Auxiliary surrogate method using principles of apportioning.

They explain that confusion occurs when one tries to compare the different methods in terms of accuracy or error, because there is no way to define, measure, or calibrate these for ‘apportioning’ (i.e. sharing out energy costs between dwellings), whereas it is relatively easy for calibratable meters.

Hegburg<sup>23</sup> also reviews five types of heating cost allocation systems previously defined by Hewitt et al.<sup>26</sup> as follows:-

1. Time Meters

Described as not actually measuring the amount of heat delivered but rather providing an estimate by recording the hours and minutes the thermostat zone valve is opened. Differences in water flow temperature are not accounted for and it was found that for a drop in 10K in flow temperature the heat output

from the same type and length of emitter is 12% less, thus giving no true indication of actual energy consumed. Also, because of valves being closed when thermostats are calling for heat, and transportation lags in delivering hot water this would appear to be an unsatisfactory method of monitoring true energy consumption.

## 2. Heat Meters

These are much more expensive than time meters but actually determine the amount of heat delivered to each apartment (depending on piping design and meter position). Hegburg: “the accuracy of (heat) meters (are), in general, (of) decreased accuracy when the flow temperature drop across the radiation (the heat emitter) was decreased”.

European regulations are referred to by Hewett et al<sup>26</sup> which set standards of accuracy of thermal meters, “some doubt was expressed as to whether these standards were being met in practice”.

## 3. Time plus Temperature (Allocation System)

“Some of these measure the emitter supply and return temperature to calculate the mean emitter temperature and combine this with the ambient room temperature to estimate heat flow rates, while some attempt to place a single sensor so that the approximate mean emitter temperature is measured directly” (taken from Goettling and Kuppler<sup>25</sup>). Hegburg states that “others are simplified

further by assuming a room temperature rather than measuring. . . . These systems improve on the accuracy of the time meters but cost less than the heat meters. They take the water temperature into account, which time meters do not, without requiring the measurement of a small temperature difference as heat meters do”.

#### 4. Ambient Temperature Monitors (Allocation System)

Hegburg states that “this entirely different approach is to monitor the ambient temperature or comfort level of an apartment”. “Some of these systems monitor the space temperature at a representative location and integrate the temperature over time, while others measure room thermostat set point and not the actual space temperature” (taken from Goettling and Kuppler<sup>25</sup>).

#### 5. Evaporative Monitors (Allocation System)

Hegburg describes that this method “is based upon the evaporation of a specific liquid in a vial attached to the radiator which is removed after a year’s usage and measured to determine the relative heating usage per radiator”.

Evaporative monitors are economical heat monitors for hot water systems and are limited to showing relative consumption over a years period. The time plus temperature method does not take into account heat emitter size and is dependent on sensor location and accuracy. The ambient temperature monitor

does not take into account variations in energy use due to the numerous factors affecting heat loads in individual apartments such as location, area of external facade, orientation, size, etc.

Fisk and Eastwell<sup>27</sup> examine the performance of evaporative heat metering in district heating schemes in a report carried out for the Building Research Establishment (BRE) in the U.K. In this report, they compare the evaporative radiator heat meter, which is the most commonly used in district heating schemes in the U.K., with other methods of allocating heating consumption costs. Specially calibrated integrating heat meters were used as a comparison for accuracy.

They found that 15% of the dwellings had readings greater than 20% of their true value when an evaporative heat meter was used, whereas only 4% of the dwellings had readings greater than 20% of their true value with the integrating heat meters. In their comparisons they identify the percentage of dwellings with readings of greater than 20% of their true value. Such large error margins would seem to be unacceptable, however it is argued that, as with other district heating metering principles the individual meter readings are usually totalled across the whole site annually and the readings of each dwelling are expressed as a fraction of this total. According to Fisk and Eastwell this method of apportionment relieves the need for a meter to have absolute accuracy, but the meters must remain consistent. This study also identified a problem with the correct installation of evaporative heat meters in that slack attachment to the radiator reduced the reading of the meter by 30%.

This is a major inaccuracy requiring regular checks to be made as to the correct fitting of these meters.

Fisk and Jebson<sup>28</sup> present three case studies in their assessment of the effect of heat metering on district heating energy consumption. In their final conclusions they state that “strong evidence exists that the introduction of metering results in a reduction of heat taken for the boiler house”. They use evidence from case studies to suggest that this reduction averages out to be 21% less than flat rate billing for the three case studies, after weather correction was applied. This would suggest that the merits of metering are not only assessment and billing of energy use, but also influence in effecting a reduction in actual energy consumed by the users.

By the very nature of ‘allocation systems’ and their comparative way of sharing out costs rather than measuring true end-use energy consumption, means that they are very limited and are a crude method of assessing end-use energy consumption in buildings. Indeed, only heat meters and properly equipped BEMS attempt to measure actual end-use energy consumption. This work concerns itself with such methods.

## **2.2 Energy Metering**

According to Heinemeier and Akbari<sup>29</sup>, the advantage of using BEMS data is that the continuous measurement of building demand can be carried out and, depending on how this data is handled, this can provide greater detail on

energy consumption than monthly utility bills. They also argue that because BEMS provide measured data they are more reliable than simulation results. They point out that the validation of simulation results can be carried out with the use of BEMS data. They add that BEMS take advantage of existing sensors and communication paths and that there is minimal additional cost for monitoring functions when compared to the cost of end-use sub-metering. They highlight possible limitations of using an existing BEMS for monitoring energy performance as many systems were originally installed for control and not evaluation of energy use and claim that the most direct way to monitor end-use energy is by end-use demand meters<sup>29</sup>.

A limitation of BEMS is identified in that the majority of BEMS do not monitor fuel energy use, but only monitor electrical energy use. In analysing BEMS data they point out that use of flow rates and temperature data can indicate the loads on certain HVAC equipment.

Their final conclusions include:

End-use demand data can be obtained less expensively from many existing BEMS's than from dedicated sub-metering.

Relatively minor alterations in the design of BEMS's can greatly enhance their monitoring functions.

A BEMS that integrates data monitoring and analysis with control functions encourages utility load management, intelligent system operations, and building energy research.

This would suggest that a BEMS is a good means of energy use monitoring and analysis for both new and existing buildings. Hurley<sup>30</sup> would possibly disagree with this in identifying possible limitations of the BEMS: "laboratory and field experience, and surveys have clearly indicated that computerised



laboratory and field tests and HVAC installations enhanced with (BEMS) often experience problems related to the accuracy and reliability of the systems instrumentation". He draws attention to one particular area that could be a cause for concern in stating that "in monitoring the performance of building services systems one of the most difficult parameters to measure and control is the flow of the various fluids. As a consequence, in BEMS, the flow rate or the total quantity of flow is often the least accurate measurement".

Stebbins<sup>31</sup> holds a similar view in stating that "all instruments, regardless of their characteristics and principles, depend upon careful attention to installation, strict attention to operating instructions and to in-service inspection, plus a program of systematic service and preventative maintenance". Stebbins contends that the more closely these principles are followed, the better the results that can be expected from any instrument and points out that "these requirements demand pre-installation training, maintenance clinics and proper instruction at all levels of instrument application". It follows that if any of these procedures and requirements are not performed satisfactorily then a problem with performance and accuracy of readings could occur.

It is essential to monitor system water flow rates when analysing thermal energy consumed by a buildings space heating system. A device which monitors this flow rate as well as flow and return temperatures or temperature difference is the heat meter. Because this device is especially designed for energy monitoring it will not encounter the same problems as those found with the BEMS.

Heat meters have been well used in the district heating industry in order to allocate costs to users. They are also commonly used in Europe to meter energy consumption of heating systems. Another application of the heat meter is for energy cost allocation to multiple occupancy buildings. Heat meters use a number of different types of metering device in order to monitor water flow rate. These devices all have differing degrees of accuracy and installation requirements.

Stebbins<sup>31</sup> discusses the general problems associated with metering and states that “energy cannot be managed and conserved unless there is a way to identify the major users and determine where the emphasis should be placed”. He identifies typical problems with energy metering including; cost, poor flow device location due to valve and piping arrangements, inability to shut down loads for installation of devices, poor accessibility to meters, lack of trained calibration and maintenance personnel, design engineer unfamiliar with requirements, cost of maintenance and spare parts. Stebbins claims that monitoring and reporting energy consumption allows for close control while minimising expenses as well as to provide historical energy consumption data to help in the prediction of future loads and the development of standards for the next year.

More detailed work on the performance of heat meters has also been carried out. Guinn and Hummer<sup>32</sup> tested approximately thirty-five 20mm (¾”) heat meters in a specially built test facility, before they were installed in active solar domestic hot water systems. They found that “the tests indicated wide

variations in meter accuracy generally ranging from 1% to 30% for totalised “Btu’s” and 1% to 20% for totalised flow at flow rates and differential temperatures ranging from 0.03l/s to 0.19l/s and 5.6°C to 55.6°C” . One of the causes of measurement error was found to be flow sensors not sensitive to low flow rates. Another cause of error was quality control. The flow sensors used in the meters were either the turbine type or positive displacement type. Manufacturers stated accuracy’s for the turbine types were either 1.5% over the full range of flow or  $\pm 1\%$  of full scale.

The stated accuracy for one of the positive displacement meters was  $\pm 0.75\%$  of the flow rate when operated between 15% and 80% of the span. For one of the turbine meters it was stated that the flow medium must remain relatively free of contaminants for reliable operation. It was found that one turbine meter in particular had a problem with low flow rates in that it tended to stop or operate unreliably. Another one was found to be measuring 50% high at the start of a test and 70% low during the latter part of the same test. There was also a problem with one flow sensor caused by poor meter assembly. A weigh counter and scales were used in the test to verify flow rates. The quality of the water used in the test would appear to be clean, though this was not stated. Also the time period of testing was not given. The test facility used was limited to a maximum flow rate of about 0.19l/s. This facility was then rebuilt to increase the flow capacity to 1.58l/s which is adequate for testing meters up to 50mm (2”) in size.

Guinn and Quick<sup>33</sup> used this new facility to test meters of 50mm (2”), 38mm (1.5”) and 20mm (0.75”) diameters. The test results of six meters were

reported. The stated overall system accuracy's of the meters were typically either  $\pm 3\%$  or  $\pm 2\%$ . The stated accuracy's of the flow sensors within these meters were typically  $\pm 2\%$  or  $\pm 1\%$ . Some results were quoted as very erratic due to poor meter assembly. An interesting point to note is that the variation of flow water temperature between  $4.4^{\circ}\text{C}$  and  $26.7^{\circ}\text{C}$  resulted in variation of the product of fluid density and fluid specific heat capacity ( $\rho c_p$ ) of less than  $0.6\%$ . Fluid density varies with fluid temperature which can effect the accuracy of some types of meter. They claim that this is hardly sufficient to justify the cost and reliability penalty associated with temperature compensation. However, they also found that wider ranges of temperatures (e.g.  $21.1^{\circ}\text{C}$  -  $82.2^{\circ}\text{C}$ ) produced a larger variation of volumetric specific heat close to  $2.5\%$  and point out that this "might indicate the need for temperature compensation, depending on the application". The tests produced widely varying results of measurement accuracy. The results are given in terms of mean and standard deviation of all the data points. It was found that only "three of the five meters were capable of producing a flow-measurement error less than  $2\%$ , while only one in six could provide that accuracy for measurement of energy flow". This meter had the highest mean error,  $-30.79\%$ . "The smallest mean plus standard deviation error for flow was  $-2.18\%$ , and the largest,  $-14.03\%$ . The smallest mean plus standard deviation error for energy was  $6.14\%$  and the largest was  $32.41\%$ ".

These two papers alone highlight the wide ranging and sometimes erratic performance of some heat meters. Evidence from this work suggests that a possible major source for this disappointing performance is the flow meter element of the device. Indeed, the contact types of device examined in this

work, i.e. the turbine type and the positive displacement type of flow meter, where parts of the flow meter come into contact with the fluid medium to be measured, would appear to be somewhat unreliable. This is further reinforced by Talbert et al<sup>34</sup> who report on the measured accuracy's and operating characteristics of seven energy meters and their components. Their studies revealed that for energy meters a major source of error is the flow meter component. They observed that "the flow meters occasionally showed poor repeatability, and that their accuracy was affected by the water temperature" . Five out of the seven meters used multi-jet turbine meters, while one used a full bore turbine meter for flow measurement. With one meter, the type of flow meter was not stated. A specially designed test facility with a quoted maximum probable measurement error of  $\pm 0.3\%$  was used. From their study they conclude that 95% of the average readings from different meters are expected to be within  $\pm 5.6\%$  for a given temperature and flow if the meters were calibrated (uncalibrated  $\pm 9\%$ ).

Huussom<sup>7</sup> investigates the performance of a non contact flow metering device. He uses a test rig to investigate the performance of an electromagnetic flow meter. He states that there is "a need for a flow transducer which may be part of an energy or volume meter with reasonable accuracy over a large range". It was found that the performance of an electromagnetic flow meter over two years is stable within 1%, but at very low flow rates a small fall in accuracy is recognised. Huussom also investigated the influences of pH and conductivity of the fluid and found that short term effects (i.e. within a few minutes) were significant, but after a short period of time the meter adapts and performs

normally. How the flow meter manages to go through this adaptation process is not explained. Water quality also had an initial effect on accuracy, but after an adapting period “the transducers were found to perform as under initial calibration procedures”.

This study was performed under laboratory conditions. The meter is a non-intrusive type and so does not have direct contact with the flowing medium to be measured, but relies on the conductivity of that medium to monitor flow rate. The performance of this device appears promising in relation to the contact type of flow meters previously referred to. This could suggest that there might only be a problem with the contact type of flow meter where elements of the device come into contact with the fluid to be measured. Perhaps the general wear and tear concerned with this contact adversely affects the performance of this type of meter.

Westergren et al<sup>35</sup> provide a solution for monitoring energy consumption in single family housing. The internet is used to monitor building energy use at short time intervals and this is combined with statistical methods and climate data to give average annual energy use. They look at various statistical analysis methods in detail but do not specify exactly how the end use energy was measured apart from stating that sensors were used. An indication of typical energy use by a house over a year was sought by looking at a large data set of houses.

Murthy and Nagaraju<sup>36</sup> developed a thermal energy meter/controller for solar water heater systems. Amongst other things this meter monitors fluid flow rate

and fluid temperatures. They claim that the accuracy of energy measurement is  $\pm 1.5\%$ . The meter uses thermistors to monitor temperature and a turbine type flow sensor to monitor flow rate. They calibrate these instruments in ideal conditions and quote accuracy of the temperature sensor to be  $\pm 0.2^\circ\text{C}$  for differential temperature measurement and uncertainty of the flow meter to be typically  $\pm 0.25\%$ . They also take into account uncertainties in density and specific heat of the water. These factors all contribute to the overall quoted accuracy of the meter of  $\pm 1.5\%$ , however this is based on ideal installation conditions. They carry out a field test and find that use of the meter/controller improves the efficiency of a solar water heating system. No reference of how practical installation effects influence the accuracy of the meter is made.

Babus'Haq et al<sup>37</sup> look at the performance of a number of heat meters for use in CHP (combined heat and power) and district heating networks. They state that 'the measurement of flow rate causes by far the most significant uncertainty in the overall accuracy, despite the fact that the flow unit is the most expensive component of the heat meter.' They highlight the intensive maintenance and recalibration requirements of flow meters when compared to temperature sensors. They give maximum permissible errors taken from BS7234 for heat meters between  $\pm 10\%$  and  $\pm 2\%$  depending on the classification of the meter, the supply and return temperature difference and the range of flow rate measured. However they identify certain factors which can cause errors 'several times the specified uncertainty' given by the British Standard. These factors include air bubbles, leakage and turbulence.

## 2.3 Flow Meters

Literature on heat meters therefore would appear to suggest that there is some uncertainty in the performance and accuracy of one particular component of the heat meter; the flow meter.

Some emphasis will now be given on recent applications research on the development, use and limitations of these devices. Work in this area appears to concentrate on two major aspects; general application and performance of flow meters for various fluid states and conditions, and effects of installation conditions on the accuracy of flow meters. Other work reports on new and innovative flow meter designs. A problem in reviewing this work is that the majority of the work found was applied to the application of flow meters in the process industries. Some of this work was found to be still relevant to building services engineering applications and is included for discussion. Other work is also included to gain an overall impression of flow meter applications performance and to provide an overview of the use, successful or otherwise, of flow meters in general.

BS 7405<sup>38</sup> states that “there many different types of flow meter available commercially. No one meter type is ideal for all applications.....” It is beyond the scope of this work to describe each type of flow meter and each of their applications. BS 7405 arranges flow meters into “ten major closed conduit groups”, as given in the following table;



Flow meter classification	
Group	Description
1	Orifices, venturis and nozzles
2	Other differential pressure types
3	Positive displacement types
4	Rotary turbine types
5	Fluid oscillatory types
6	Electromagnetic types
7	Ultrasonic types
8	Direct and indirect mass types
9	Thermal types
10	Miscellaneous types

**Table 1: Flow meter classification.**

(the extract from BS7405: 1991 is reproduced with the permission of BSI under license no. 2000/SK0511.)

This standard then sub-categorises around 86 flow meters into these groups, shown in table A1 in appendix 1. It states that “the performance of flow meters can vary significantly depending on both the design and type of meter”.

With reference to flow metering in general, Hurley<sup>30</sup> states that “the deterioration of primary elements of the meter by abrasion and chemical and/or electrolytic reactions has been found to be a major problem in the continuous monitoring of fluids”. A problem of deterioration due to environmental conditions is also identified for the transducers used for the conversion of analogue to digital signals.

Flow meters are normally categorised in terms of their theory and method of operation. According to Bertschler<sup>39</sup> more accurate flow elements and transmitters within a category will almost certainly be incrementally more expensive, and that installation costs also have to be taken into account. This paper also identifies the possibility that costs of re-routing existing piping to

accommodate new or replacement instruments may go well beyond the normal installation cost. The addition of extra utilities is also considered in terms of extra cost. An example is given of installing a magnetic flow meter which will require an extra power supply to an area that may only have two wire or pneumatic transmitters. The factor of increased cost for more careful and more frequent calibration is highlighted<sup>39</sup>. The area of technician support is also raised in terms of specialist training and equipment requirements.

Barnes<sup>40</sup> discusses pipeline metering utilising positive displacement meters and turbine flow meters for liquid measurement. The paper compares flow ranges, accuracy, pressure drop and cost of the respective meters in order to aid the end user in the selection of the meter that will provide the best overall measurement system for his specific requirements. The paper also examines the effects of viscosity on these meters. The author identifies that with a turbine meter, as the viscosity increases, the minimum flow rate required to maintain a specific degree of accuracy also increases. Barnes adds that this is not the case with a positive displacement meter, because as viscosity increases so does the rangeability of the meter. A typical accuracy given for a positive displacement meter is  $\pm 0.25\%$  from 20% to 100% of maximum rate, (5:1 flow range), and a typical accuracy for a turbine meter is  $\pm 0.15\%$  from 10% to 100% of maximum rate, (10:1 flow range). A typical repeatability for a positive displacement meter is given as  $\pm 0.025\%$  compared to a typical repeatability for a turbine meter as  $\pm 0.015\%$ . The work considers some installation effects of the meters which affect their cost, accuracy and reliability. Typically, straight length

of pipe requirements are discussed for turbine meters, whereas this factor is identified as not being a requirement for positive displacement meters. From work carried out by Guinn and Hummer<sup>32</sup> and Guinn and Quick<sup>33</sup> the validity of these typical accuracy values is in question.

Grebe<sup>41</sup> considers volume flow rate measurement in full, closed pipes when a reasonable accuracy of 5% or better is needed. Grebe argues that the final flow meter choice must come as a result of weighing the economic benefits of each meter against the application requirements. The paper reviews the performance of various flow meters for different applications, mainly in the process industry. Some of the applications that are considered are:- two-phase flow, liquids with solids, Reynolds number range, viscosity and viscosity changes, density and density changes.

Mattingly<sup>42</sup> describes several new fluid metering research tools and establishes their capabilities in order to satisfy the requirements of fluid metering in the process industries. Mattingly holds the view that there is a need to go beyond the standard calibration techniques to maintain and improve meter performance by using new research tools and states that “in the chemical process industries, it is widely held that the primary elements of fluid meters i.e. the devices which interact with the flowing medium are the weak-links in the measurement and control network chains required to maintain or optimise productivity”. The paper briefly summarises existing<sup>1</sup> calibration techniques in which meter output is compared with an established value and finds that these techniques do not investigate the detailed fluid dynamic phenomena of the flow into or through

the tested device<sup>42</sup>. Mattingly elaborates by asserting that when the performance of the meter is not as expected, these flow fields logically become suspect and investigations using available tools are required<sup>42</sup>. A number of research tools are reviewed in order to carry out this task.

Spitzer<sup>43</sup> gives a users perspective of the important considerations for the application of vortex shedding meter technology. It is stated that “stable and predictable hydraulic conditions must be maintained both upstream and downstream of the flow meter to achieve optimum accuracy and minimise hydraulic effect such as swirl, turbulence and distortion of the velocity profile”. Spitzer explains that this is achieved by installing the flow meter with upstream and downstream straight runs in accordance with manufacturers recommendations. The author adds that some vortex shedding meter designs have stringent requirements regarding the quality of the pipe upstream and downstream of the flow meter installation to ensure that the proper hydraulic profile is developed. According to Spitzer this requirement is virtually always ignored by users, resulting in some loss of accuracy. The effects of installation and application of these meters are reviewed. Pipe vibration, thickness of pipe, temperature variation, excessive velocity are all identified as affecting the performance and accuracy of these meters.

Kayama and Witlin<sup>44</sup> investigate the effects of inner wall conductivity of adjacent connecting pipes on the signal of magnetic flow meters with short face to face length. The shortening of the face to face length of the meter tends to ease installation and save on costs, but was also thought to affect

span error depending on the conductivity of the inner wall of the adjacent pipes. They investigate this effect by theoretical analysis and from experimental results. The conclusion of the analysis is that, though there is a trade-off between face to face length and accuracy, the limit of face to face length is 1.3 pipe diameters minimum if  $\pm 0.2\%$  of span error is permissible.

Wilda and Arcara<sup>45</sup> examine various techniques used by the fuel gas industry in computing the energy flow at a measurement point. They show that the sampling interval and response of the measurement equipment can introduce errors into the energy flow computation.

Seruga<sup>46</sup> investigates the sizing and selection of modern water meters. It is stated that “proper selection involves both the size and type of meter. Too often, meter size is chosen merely to match the pipe diameter without recognising that oversized pipe may have been used to allow for possible growth in water use, or to reduce pressure loss in a long stretch of pipe”. This incorrect sizing and selection of a flow meter could also easily occur within the building services industry particularly because of the wide range of conflicting advice and information available from manufacturers.

Dahlin and Franci<sup>47</sup> describe a new type of coriolis mass flow meter which has been developed and put into commercial use. They claim that this meter overcomes the limitations of other instruments of this type, namely sensitivity to vibrations, air entrainment, fluid density change and stress corrosion. “It also offers lower pressure drop and accurate digital signal handling and diagnostics”.

They criticise mass flow measurements based on combined measurements of volumetric flow and density, or inference of density from temperature and pressure measurements, and argue that these measurements are typically a costly and complex system with relatively low accuracy. Quoted accuracy of the instrument in terms of a maximum error was  $\pm 0.15\%$  of reading over a dynamic range of 10:1, whereas over a range of 100:1 the accuracy was reduced to the order of  $\pm 1.5\%$  of reading, in most fluids. Amongst others, two applications presented are for flow laboratories for the calibration of turbine and electromagnetic flow meters for a variety of fluids including water.

Hickl and Furness<sup>48</sup> discuss two methods of mass flow measurement. A turbine meter for velocity sensing combined with high accuracy pressure and temperature transducers for calculation or 'inferal' of mass flow are described. They quote a measurement accuracy of better than 0.1% of volume flow rate for this meter, claimed by meter design specifications. A coriolis mass flow meter was also used. They report of operational difficulty with the measurement systems resulting initially from unclean lines. It is stated that "from experience with both types of mass metering systems in liquid and single component gas streams has demonstrated that measurement of most flows can be made and maintained with a maximum  $\pm 0.2\%$  of rate uncertainty when adequate attention is given to metering system design and maintenance". Again, these accuracy values rely on adequate installation conditions which can be generally unavailable in existing installations, and prohibitively expensive or simply impractical in new installations.

Harje and Gadsby<sup>21</sup>, in reviewing alternate methods for acquiring energy use, chooses the paddle wheel type flow meter for flow measurements for economic and range of measurement reasons as opposed to non-intrusive techniques. The reason given for this choice is that Doppler methods are unreliable where there is not a significant presence of air bubbles or particles.

Miller<sup>49</sup> reviews the history of flow measurement and discusses the present and possible future developments in flow metering. The paper refers to the Romans' for the first demonstration of flow metering when the free discharge orifice flow meter was used to meter the water used in the household. Miller informs that the first flow laboratory was not developed until the late 1880's when Hershey began his experiments to optimise the Venturi for measurement of water<sup>49</sup>. Miller states that "the orifice meter continues to be the meter most widely selected and far out numbers all other flow meter installations".

Mattingly<sup>50</sup> argues that "traditional testing methods for improving flow measurement performance have lead to progress, but are probably near a point of diminishing returns". It is argued that further improvement of flow meter performance depends on more detailed study of instrument behaviour. The paper reports on the availability of analytical and empirical tools that allow this more detailed analysis to be made. The work specifically refers to the orifice meter flows which have been modelled using these advanced tools and vortex meters which have also been studied. It is reported that "such capabilities may ultimately permit dry calibration of orifice meters to predict performance based only on geometry and inlet flow. This approach could prove to be more

accurate than modifying standard orifice parameters using discharge coefficients obtained from empirical tables or equations, for example in situations where the installation of the meter deviates from recommended practice". Mattingly adds that some of these results await experimental verification. Vortex shedding flow meters are identified as another area of study because of their possible application to a wide range of fluids and further work is required to empirically validate these computer models.

Feller<sup>51</sup> reviews the problems associated with the application of turbine meters and positive displacement meters including; a problem with turbine meters of measuring low flows, problems with erosion and abrasion of turbine meter components, good accuracy of positive displacement meters with good performance at low flow rates, problems with erosion and wear of positive displacement meter components. The effects of temperature variation or particles getting caught between moving parts causing meter stoppage are also discussed. The paper refers to a number of meters, such as the magnetic, ultrasonic, Doppler, vortex shedding, variable constriction and differential pressure, as being used to a small degree because of performance limitations or relatively high cost. Some new developments now offer improved performance and other characteristics along with reduced costs. The improved designs stress low construction costs and eliminate the requirement for the meter to directly drive a mechanical register. Only electrical output signals are provided; which is all that is required for most modern industrial, commercial and residential process control and consumption metering. Recent developments are reviewed:-



Sensing turbine rotation. Turbine flow meter designs using this method offer minimum resistance to the flow because of improved blade shape, and the rotor mass is relatively low, the bearing loading is light and bearing life is relatively long. Turbine flow probes are often used in medium to larger pipe sizes where their price advantage over full bore turbines is enormous. However, since they measure the flow rate in only small proportion of the cross sectional area of the pipe and do not straighten the flow before measurement, they often have relatively large errors. The errors are pronounced when the probe is located near elbows, tees and valves. Feller also reports of a technology which is claimed to greatly reduces turbine flow probe errors. This technology uses a second turbine rotor mounted below the first rotor. Test results are reported of measurement accuracy's within three per cent of the actual values over a 10:1 flow range. Feller argues that it is doubtful whether most conventional full bore turbine meters incorporating straightening vanes would perform as well. The author also reports on the inclusion of a temperature difference calibrating feature into the flow meter to minimise the temperature sensor error. Other heat meter improvements are described including compensation for specific heat variations of the heat transfer liquid over a temperature range and the measurement of positive (heating) and negative (cooling) heat transfer with a single installed heat meter<sup>51</sup>.

Fuller<sup>52</sup> describes a series of tests that were conducted to confirm the transfer of calibration from liquid to a gas for a type of coriolis mass flow meter. The flow meter was calibrated 0 - 4.5 kg/min on water against a scale. The calibration was checked at 25%, 50% and 100% of full scale flow with an

overall accuracy of  $\pm 0.25\%$  at the flow meter tested. It should be noted that these tests were carried out under laboratory conditions. The final conclusions state that “the accuracy of this method of direct mass flow measurement is better than  $\pm 0.4\%$  of actual rate over turndowns in flow of the order of 40:1 for any one size of flow sensor”.

Corpron<sup>53</sup> investigates the effect on installation conditions on the performance of a T - cross section vortex meter. It is stated that “although vortex meters are found to be linear and accurate when mounted in reference piping, there has been lack of published data on how these meters perform when they are mounted near commonly encountered flow profile disturbing elements such as valves and elbows”. A study of the effects of several disturbing elements on a 3” meter with a T-cross section bluff body were undertaken in this work. It was found that the meter factor shifts as great as 1.8% and linearity changes as great as  $\pm 0.6\%$  under extreme installation conditions<sup>53</sup>. The study also demonstrated that meter performance can be improved by increasing the length of straight pipe between the disturbing element and the meter<sup>53</sup>. In this study meter factor was defined as the ratio of vortex shedding frequency and the flow rate.

Corpron<sup>54</sup> also compares several Vortex meters calibrated in water, low pressure air and high pressure air. The paper documents the performance variation associated with using these meters to monitor the flow rate of a gas or liquid under controlled laboratory conditions. Five meters were calibrated.

It was found that at higher Reynolds numbers ( above  $1.5 \times 10^4$ ) linearities within  $\pm 0.5\%$  of water could be achieved with selected meters, over a range of flow rates and Reynolds numbers. At lower Reynolds numbers the meter factors tended to increase with decreasing Reynolds Numbers.

Trimmer<sup>55</sup> tested six ultrasonic flow meters in a hydraulics laboratory.

Accuracy's better than 2% were obtained with two transit time meters on 14 inch diameter steel tubing. Poorer accuracy's were found with 8 inch diameter PVC pipe. It is stated that the Doppler and eddy correlation meters tested did not perform well.

Ganni and Ibbotson<sup>56</sup> present a flow meter with no moving parts "capable of measuring liquid flow rates from 0.05 to 200ml/min". The meter uses a time of flight technique using thermal impulses. Problems of difficulty and low accuracy is highlighted in the measurement of liquid flow in these micro-flow ranges. A high precision of 0.1% is stated for this particular meter.

Walsh<sup>57</sup> reviews thermal flow sensing and states that "instruments using this principle have a very extensive dynamic range and have accuracy's which typically range from 1-3% of reading". The author adds that "the leading advantage of thermal flow sensing is that the direct measurement of mass flow can be made without the added complexity and cumulative inaccuracies involved in separate corrections of volumetric rate for temperature and pressure".

McConaghy et al<sup>58</sup> investigate the effects on measurement accuracy of orifice plate condition by carrying out experiments using natural gas. Various orifice plate conditions were used including damage at the orifice-plate edge, liquid and solid build-up on the orifice-plate face, and orifice plate surface roughness. Results showed that metering accuracy varies greatly with the condition. Large changes in flow rate occurred in some cases. This would suggest that these conditions effect the accuracy of orifice plates for liquid flow measurement to some extent as well.

Labs<sup>59</sup> identifies a greater role for the microprocessor in the development of sensors, improving their capabilities and flexibility by providing signal conditioning, compensation, scaling, units conversion etc. It is reported that choosing a flow meter for a given application can be complicated and that much of the problem stems from the wide variety of flow meter types available.

According to Labs the microprocessor has helped to reduce the price of some flow meters in that on-site calibration is achievable. Labs states that “before microprocessors each installation required factory set-up and calibration. Microprocessors have contributed to the accuracy and linearity of many flow sensor devices”.

Bloom<sup>60</sup> addresses the problem of accurately measuring ultra-low flow.

It is stated that “accurate flow measurement and control at low and ultra-low flow rates is difficult compared to higher flow regimes. Because the meters deal with relatively small volumes of fluid, minute measurement errors greatly

affect accuracy. Further, conventional meters cannot be simply be downsized, because many metering methods common in the moderate-to-high flow range do not work well at the low flow end". For this work the low to ultra-low flow region was considered as liquid flow rates less than  $0.00091 \text{ m}^3$  per minute. The performance of various flow meters are reviewed and some meters are identified which have good performance at low flows:-

Positive displacement devices (generally) have problems in measuring low and very low flow rates. (However, two makes of meter are identified which perform well at low flow rates).

Axial turbine meters are widely used for medium and high flow rate measurement, but seldom operate well below  $0.00095 \text{ m}^3$  per minute.

Variable area. One type is a rotameter. Typically low cost low accuracy, but some more sophisticated ..... designs are used in high accuracy meters. one variation of the rotameter can handle flow rates down to  $0.0000037 \text{ m}^3$  per minute ..... Accuracy is 0.5% of full scale.

Fixed area flow meters - orifices, nozzles and venturis - are common flow measurement devices for all flow ranges. Flow meters of this type tend to have limited range. For extremely low flow rates, orifices must be extremely small.

Schlatter<sup>61</sup> discusses advances in vortex metering technology and states that "typical present day expectations surpass a minimum of 10:1 flow range with a percent reading accuracy of  $\pm 0.8\%$  for liquids". A salient point is raised in that some meter designs allow sensor/transducer removal without requiring a

process shutdown. It is reported that “Vortex flow meter manufacturers today offer meter performance which is superior to head-type meters (orifice, pitot, venturi, target) and complimentary to other meter types for most common in-line applications. This superior meter performance is well grounded and is evidenced from test results and new meter installations”. A Comparison is made with orifice meter performance. Orifice accuracy's are quoted at 1 to 5% of full scale for liquids with a repeatability of  $\pm 0.25\%$  to 1% of full scale compared with  $\pm 0.1\%$  to 0.25% of reading for vortex meters. Most significant disadvantages were quoted as ‘noise’ sensitivity and low cut off for the vortex meter, and accuracy determined by the validity of assumptions made about the installation, fluid property changes, limited turndown, and ambient temp sensitivity for the orifice meter.

Zaitseva et al<sup>62</sup> state that “automatic metering and regulation devices increase the efficiency of heating systems”. They suggest a method of increasing the measurement accuracy of electronic heat meters. The heat meters they look at consist of a flow meter which measures the flow of the heat-transfer agent and two resistance thermal converters and a heat computing circuit. They explain that:

To reduce the error in measuring the quantity of heat energy in these meters, the change in the density of the heat transfer agent accompanying a change in the temperature is taken into account and the heat meters themselves employ electronic components in which the conversion error is reduced to minimum. It is well known that in electronic heat meters the signal from the flow meter, which is proportional to the rate of flow, and the signal from the resistance

thermal converters, which is proportional to the temperature difference, are fed into a computer in which the amount of heat in joules, released to the user over measurement time, is determined.

They report of a rapid increase in total error of the heat computing unit with a decrease in flow rate and temperature difference.

Ting<sup>63</sup> presents the effects on orifice meter measurement and accuracy of non-standard operating conditions for gas flow measurement. These conditions were; reversed orifice plates, bent orifice plates, orifice meter tube surface roughness, and liquid entrainment in the orifice tubes. Sonic flow nozzles were used as the flow rate reference device. Typical results were “reversed plates resulted in measured flow being less than the actual flow by 12% to 17%. The flow rate measured by bent plates deviated up to 4.5% lower than true flow. Meter surface roughness and liquid accumulation in the meter also contributed to errors on the order of 0% to 2%”. Note that this study was for gas flow measurement and so inaccuracies of some order would also be expected for liquid flow measurement.

Dall and Lowes<sup>64</sup> investigate the application of a portable, ultrasonic flow metering system for metering water in the Australian water supply system. They apply it to large diameter pipes where magnetic flow meters are generally used with an average size of 500mm diameter. A problem is identified in maintaining accuracy of existing equipment i.e. the magnetic flow meters in that often they cannot detect small error changes (<10%) in large flow meters. They add that the expense and time required to remove some of the larger

meters if a problem is found is considerable. A number of tests were carried out on the accuracy of ultrasonic meters in order to help in solving this problem.

They report that the tests showed that both Doppler units tested failed to achieve the expected performance, as they were very sensitive to mounting position, and to achieve any acceptable degree of flow correlation with the reference meter, they had to be initially calibrated with the reference meter at a given flow rate. However, they also report that they found that the time of flight meter performed well within the manufacturers specification. Though they explain that it offered no performance or price advantage over magnetic flow meters. Manufacturers of the time of flight instrument stated an accuracy of  $\pm 1.5\%$  of rate. The worst error recorded during the tests was  $-0.93\%$  and the best was  $+0.13\%$ .

Gaertner and Stark<sup>65</sup> state that “for heat supplies over long and short distances, reliable and verifiable heat measuring instruments are required”. They report on a new heat meter developed by Siemens for such applications. The meter uses an ultrasonic-design flow measuring element, temperature measurement with platinum film resistors and control and processing by a microcomputer. No detailed performance information is included.

Murphy et al<sup>66</sup> describe the use of an integrated turbine metering system for the calibration of on-line circulating water flow measurement devices. They state that “the circulating water flow rate is often a difficult parameter to measure in power plants”. Two methods of using a differential pressure



monitor to measure flow rate on-line are described :- (a) the first approach is to measure the differential pressure across the naturally occurring orifice between the outlet water box and the outlet circulating water pipe, (b) the second approach is to measure the differential pressure across the inner and outer radii of an elbow. Once installed, these devices must be calibrated empirically. It was found that the sensitivity of differential pressure monitors to density changes does not usually have a significant effect. The calibration of these devices required a high accuracy. The turbine flow meter system that was used for calibration was able to measure flow rates with an accuracy of  $\pm 1.0\%$  or better, depending on system characteristics, with a repeatability of  $\pm 0.25\%$ .

Bennet<sup>67</sup> reports on the design of three fuel-metering valves for use in aircraft engines. One of the valves used an oscillating jet flow meter with no moving parts, the others used turbine flow meters. The dynamic performance and flow characteristics were tested for the valves. Hysteresis was determined to be less than 0.25% throughout the position control range. Flow characteristics were determined and a pressure regulator was used to control the pressure across the metering valve. Controlling the pressure drop across the valve to a fixed value allowed volumetric flow to be determined by valve position (metering data). Position accuracy and hysteresis were demonstrated in hysteresis plots. It was found that position accuracy for the valves was well within the requirements. An examination of flow command versus actual flow ( as measured by a lab standard turbine meter) for a typical operating cycle deviates from the requirements at low and high flow rates across the required operating range.

Yeh and Mattingly<sup>68</sup> study the pipe flow profile and its influence on orifice coefficients downstream of a reducer experimentally. They state that “this arrangement is known to be the cause of metering inaccuracies for meters installed in the downstream piping near these reducers”. The study revealed that the flow has profile characteristics that can strongly affect the performance of an orifice flow meter. Their results showed significant deviations from the ideal discharge coefficient characteristics for some flow meters and that different velocity profiles produced by different pipe configurations can significantly affect flow meter performance<sup>68</sup>.

Ifft and Mikkelsen<sup>69</sup> state that “lengthy upstream piping required by many types of flow meters can substantially increase the cost of flow meter installations”. This is especially true when flow meters are added to existing systems. They investigate the effects of a single 90° elbow and close coupled double 90° elbow out of plane on the accuracy of a V-cone flow meter. It was found that this particular meter can be installed close to either single or double elbows out of plane without affecting the stated accuracy of the meter more than 0.3%. They add that if the straight lengths required by some meters cannot be accommodated then the design engineer can usually come to a compromise, with associated accuracy or permanent pressure loss sacrifices<sup>69</sup>.

Laws<sup>70</sup> demonstrates that a flow conditioning device may be designed to operate as a differential pressure flow meter. It was found that the device is less sensitive to installation effects than the basic orifice plate and that there is

scope for the device to be installed with minimal installation lengths. The type of flow conditioning device used was a perforated plate.

Flaska and Kosla<sup>71</sup> point out that “pipe elbows can create flow disturbances which inhibit accurate measurement”. They describe the flow in an ordinary pipe elbows and the flow through a pipe elbows using a rotation vane installed ahead of the elbow to eliminate flow disturbances, in order to improve flow meter accuracy. They conclude that the required meter run for such an installation is reduced to less than 5 diameters. This could suggest a possible solution in some cases where adequate lengths of straight pipe are required, but not available. However, in existing installations there could be a problem in installing the rotation vanes, and there is still a requirement for some straight lengths of pipe work with this solution. A small effect on capital cost is also incurred.

Ton et al<sup>72</sup> describe “feed-water and condensate flow measurements which were performed to explain a reactor thermal power discrepancy and to optimise electrical output”. They use the cross correlation and the chemical tracing technique for flow measurements. They state that “the main advantage of this technique is that it is totally non-intrusive and that measurements do not require any changes to the unit configuration. This particular meter was chosen because of its proven high temperature capability, ease of transducer installation, and the high accuracy that was possible with the proper meter calibration”. They give an estimate of meter accuracy, taking into account fluid density, meter repeatability, and uncertainty in pipe cross-sectional area amongst

other things, to be about  $\pm 2\%$ . They point out that “whilst differential pressure devices are more susceptible than others, the sensitivity of flow meters to their installation condition is a general problem of concern to both flow meter manufacturers and users”.

Laws et al<sup>73</sup> state that “because of the wide variation in pipe installation geometry’s which can occur, it is difficult to achieve the ideal operating conditions in practice without including long upstream lengths of straight pipe between the source of disturbance and the flow meter or introducing some form of flow straightener or conditioner into the pipe network”. This shows agreement with the work carried out by Flaska and Kosla<sup>71</sup>.

Lynch and Horciza<sup>74</sup> investigate the accuracy of portable, clamp-on, ultrasonic flow meters by comparing their performance against a laboratory standard, ( a weighing tank - calibrated Universal Venturi Tube ), and against eight-path ultrasonic systems. They found that the portable clamp-on meter flow measurements were within 0.6% of the venturi tube measurements on all tests and within 1% of the eight-path systems measurements. Previous work suggests that these accuracy values might not apply in practice.

Hanson and Schwankle<sup>75</sup> report on the performance of flow meters on irrigation systems. They explain that “flow meters provide information on the application rate and the total amount of water applied to a field, both of which are necessary for good water management”. They identify difficulty in many irrigation pumping plants in achieving the required straight length of pipe

before and after the flow meter and claim that large errors in flow measurements may occur for those pumps. They conducted a literature review and failed to find information about the source of the straight length of pipe recommendations and about expected errors under non-optimal flow conditions. They investigated a variety of non-optimal upstream conditions and their effect on a propeller meter, a paddlewheel meter, a Doppler meter, a pitot-tube meter and a velocity meter. The flow meter measurement was compared to flow rate measurement obtained with a volumetric tank and the percent relative error was calculated as :

$$RE = 100 * (meter - tank)/tank$$

They found that turbulence from a check valve had little effect on the propeller meters and one pitot-tube meter at two pipe diameters. The relative error of another pitot-tube meter was large compared to the control errors. A paddlewheel meter had large relative errors at two pipe diameters. Very large relative errors occurred for all distances, ( 2, 5, 10 and 15 pipe diameters ), for the other flow meters. They found that a partially closed butterfly valve caused generally large relative errors for the propeller meters at two pipe diameters for the lower flow rates. They also found large relative errors for the pitot-tubes at two pipe diameters. The paddle-wheel meters and the Doppler meter showed a wide variety of responses. At two pipe diameters, very large relative errors occurred for these meters. For distances of five, ten and fifteen diameters, relative errors fluctuated between positive and negative errors. In some cases, large relative errors occurred even at 10 and 15 pipe diameters.

The effect of a 90° elbow generally was not significant at 2 pipe diameters for all the flow meters apart from the Doppler meter and the velocity gauge.

A combination of a 90° elbow and a partially closed butterfly valve caused very large relative errors at the low flow rates, regardless of distance downstream. Errors for one propeller meter exceeded 20%. However, as the flow rate increased, relative errors decreased and were similar at all distances downstream. For a given flow rate, relative errors were the highest at two pipe diameters, ranging from 12 to 38 % for the pitot tube meters.

The behaviour of the relative errors with flow rate and downstream distance of the Doppler meter and the point-measurement meters was highly sporadic compared to the above meters. Very large errors occurred at two pipe diameters. However at other pipe distances, relative error varied from small to large errors. One of the overall conclusions was; “Flow meters which measure flow water based on an integrated water velocity across the pipe diameter tend to be less affected by turbulence compared to meters which measure flow rate based on point measurements”.

Parker and O'Neil<sup>76</sup> investigate the “effect of a ninety degree elbow on the accuracy of a non-magnetic, insertion paddle wheel flow meter”. They identify the application of insertion type flow meters which “can be hot tapped into the piping” for existing installations so that shut down is not necessary. A major problem is highlighted in these retrofit installations in that the required straight lengths of piping upstream and downstream of the flow meter for its accurate operation is either hard to find, or not available. They state that “the costs to add a straight run for just the purposes of accurate flow metering are generally

prohibitive”. Flow meter performance is compared to flow rate measured from a tank mounted on load cells in a test facility. They find that “locating a flow sensor in the immediate downstream vicinity of a ninety degree elbow significantly disturbs the accuracy of the flow sensor in general. However, by correct sensor rotation placement, these errors can be greatly reduced”. They include a cautionary statement for application of their results to low flow rates because of the uncertainty involved in measuring these<sup>76</sup>.

Krassow et al<sup>77</sup> present a novel flow meter based on an orifice and a differential pressure sensor. Unlike other meters incorporating an orifice where an external differential pressure sensor is used, they include a micro sensor within the device itself making it much more compact for ease of use. This meter was tested for water flow measurement accuracy using an experimental test rig and its performance was compared to conventional meters and simulation. They found that the experimental results had good agreement with the simulation results and that the novel meter had an equivalent performance to meters with a conventional design. This research was done on a comparative basis and no absolute accuracies were quoted.

Installation effects are studied by Carlander and Delsing<sup>78</sup> in their study of an ultrasonic flow meter. They look at four different test configurations for the installation of the flow meter in a calibration test facility and compare the meter performance to an ideal installation test. Each of the configurations tested would be commonly found in installed pipe work systems e.g. reduction in pipe diameter. They found that each of the configurations caused an error in

flow measurement. Typical maximum errors were quoted as 2-4% of flow rate measured in the ideal case.

## 2.4 Summary

It is essential to monitor energy use in buildings for energy efficiency and for validating computer models. A number of methods are currently in use, each of which has its own advantages and disadvantages. The cost allocation methods used in district heating schemes do not monitor actual end-use energy and have inherent inaccuracies in their principles of operation. These inaccuracies are generally accounted for in that the heating energy costs are totalled and shared out across the users according to an overall comparison of monitored readings. There is, therefore, no requirement for a meter to have an absolute accuracy as long as consistency is achieved.

The only true method of monitoring energy use is by direct measurement of fluid flow rates and flow and return temperatures and integrating these over time. The two monitoring methods that have been identified that carry out this task are heat meters and BEMS equipped with the relevant data monitoring equipment. It has been found from experience that not all BEMS are capable of monitoring fluid flow rates. Both these methods are limited in their accuracy by the type of flow measurement and temperature sensing devices that they use. Previous work suggests that flow metering could be the largest source of error for these energy monitoring methods. Indeed evidence suggests that the types of flow measurement device used in these methods can be



unreliable and have wide ranging errors in their readings, particularly at low flow rates.

The performance and accuracy of a flow meter depends on a number of factors. Proper selection is important and the wide variety of flow meters available today from different manufacturers make it difficult for the engineer to make the most appropriate selection for a particular application. Furness and Heritage<sup>79</sup> state that “the correct selection and application of flow meters becomes more complex each time new techniques and new products appear, with the result that probably the majority of meters now purchased and used are not the correct meter for that duty”. BS 7405 : 1991<sup>38</sup> is a guide for the selection and application of flow meters for the measurement of fluid flow in closed conduits. Within its introduction it is stated that “there are . . . many publications on flow meter applications that appear in numerous journals which show that no single flow meter is suitable for every application”. The literature review has demonstrated the widely ranging performance of various flow meters under different application conditions. The effect of installation conditions has been comprehensively investigated for a number of meters and it has been found that conditions which do not comply with the manufacturers recommendations can significantly affect the performance of some flow meters. It has also been identified that not all applications are able to achieve ideal installation conditions. In those applications where ideal installations are able to be achieved then added costs and extra space requirements are normally incurred. Some flow meters also require the addition of a utility supply. Once installed, the performance of some flow meters is likely to deteriorate with

time and therefore on-going maintenance and calibration may be required. Some flow meters require replacement of parts with the subsequent shutdown and isolation of the pipe work in question. The accuracy and reliability requirements of an application affect the capital cost and initial calibration costs of the meter. Increases in accuracy requirements normally mean an increase in capital cost. Some of the newer designs of meter available on the market today are more accurate than some of the traditional meter designs and perhaps overcome some of the installation requirements (e.g. vortex meter), but these tend to be more expensive than some of the less accurate traditional designs.

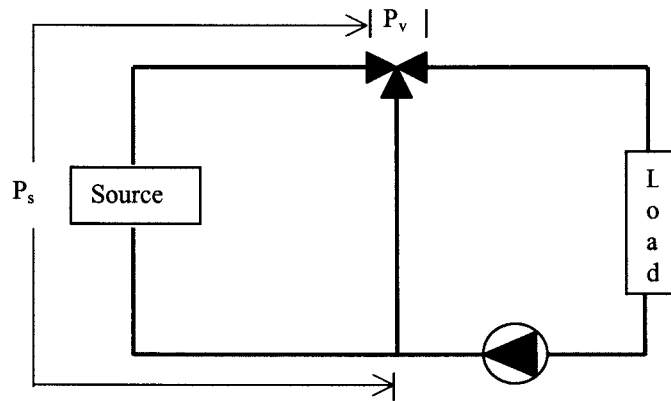
Fluid metering is an essential part of an energy monitoring/energy management system. The problems and costs of the selection, application and maintenance of flow meters have been highlighted and it would appear that, because of these factors, there is scope for a method of monitoring flow rate by some other means.

## Chapter 3

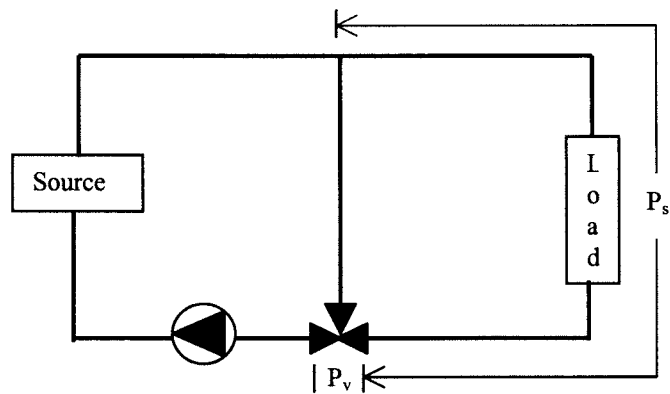
### 3.0 Valve Modelling

Valves are widely used in building services engineering applications for isolation, balancing, safety, and control. In hot water heating and chilled water cooling systems valves play an important part in the on-going adjustment of water flow rates and water temperatures in order to achieve the ultimately required correct performance and effective operation of a system to achieve comfortable conditions in buildings. Both two-port and three-port control valves are used to carry out this task.

Three-port valves are used in building services engineering for water temperature compensation to outside conditions, capacity control of hot water heating and chilled water cooling coils and other emission devices, and in injection circuits for the control of the injection water temperature. They may have either two inlet ports and one outlet port (mixing), or one inlet port and two outlet ports (diverting). Both these types of valve may be used in mixing or diverting applications depending on pipe work connections as demonstrated in figures 1a and 1b. They can provide either constant temperature variable flow control or variable temperature constant flow control in these applications. CIBSE<sup>80</sup> point out that most of the three-port valves used in building services engineering have two inlet ports and one outlet port.

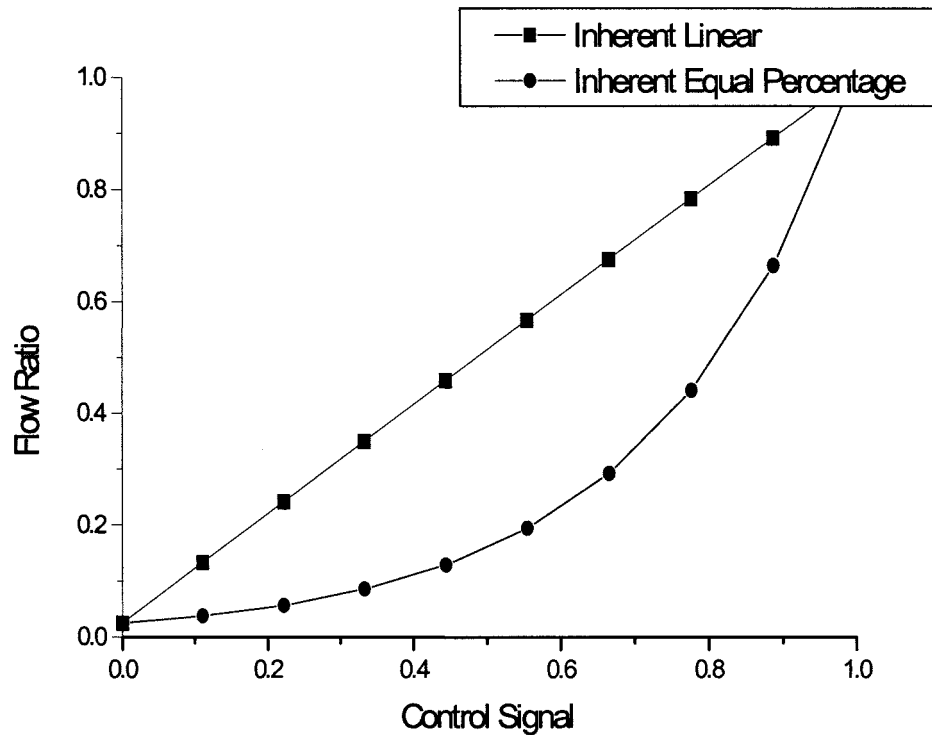
**Figure 1a. Mixing Application**

$$N = \frac{P_v}{P_v + P_s}$$

**Figure 1b. Diverting Application**

$$N = \frac{P_v}{P_v + P_s}$$

In order to model a control valve some knowledge is required of the relationship between the position of the valve stem and the corresponding flow rate passed by the valve. This relationship is called the valve characteristic. Valves are manufactured with a certain inherent characteristic which describes this relationship whilst a constant pressure drop is achieved across the valve. This is an ideal characteristic of the valve which expresses its performance without the influence of the associated pipe work system pressure fluctuations in which it is installed. A large range of inherent characteristics are available. For three-port valves the choice of inlet port (i.e. the port connected to the load) characteristic is normally governed by the 'non-linear' relationship between flow and heat emission of most heat exchange devices. The chosen characteristic offsetting this 'non-linear' characteristic in order to achieve an overall linear relationship between valve stem position and heat emission of the device. The bypass port characteristic is chosen to achieve a constant total flow through the valve at all valve stem positions. This, however, is rarely achieved in practice. Letherman<sup>81</sup> gives equations for three commonly used inherent characteristics, two of which are illustrated in figure 2 (over the page).

**Figure 2: Linear and Equal Percentage Characteristics.**

These take the following form,

$$\text{Linear,} \quad G_{inh} = K_1.x, \quad \dots\dots\dots(1)$$

$$\text{Equal percentage,} \quad G_{inh} = K_2.exp(K_3.x), \quad \dots\dots\dots(2)$$

Another common characteristic is,

$$\text{Parabolic,} \quad G_{inh} = K_4.x^2 \quad \dots\dots\dots(3)$$

where  $K_1$  to  $K_4$  are constants for a given valve.

This inherent characteristic is then used to express the valves installed characteristic which takes into account these pipe work system pressure effects.

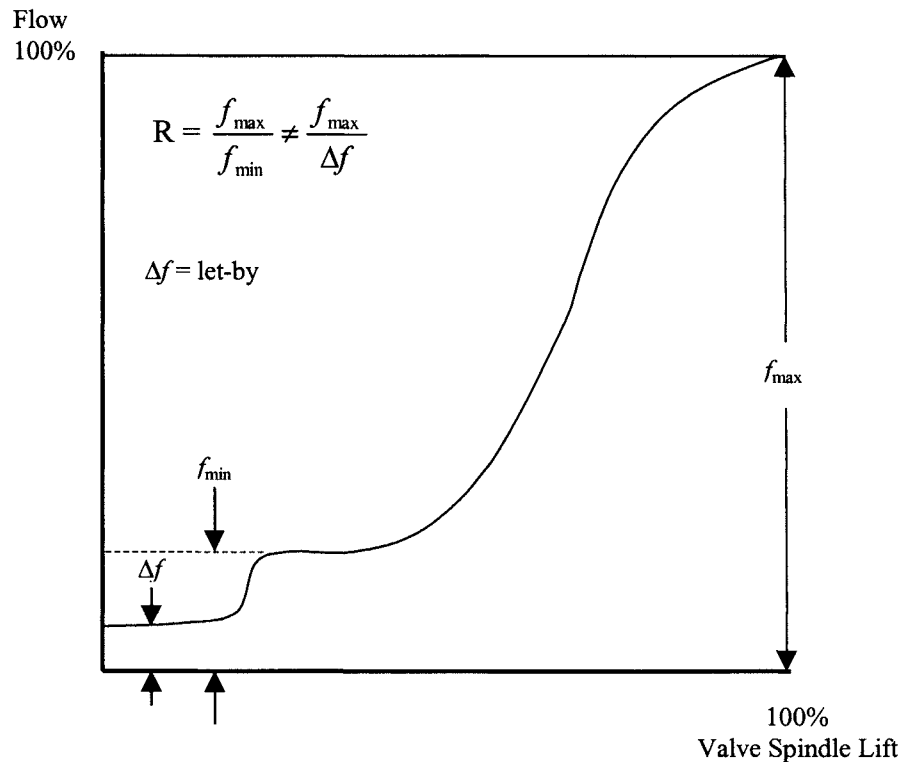
This installed characteristic is affected by the valve authority. Valve authority can be defined as “the ratio of the pressure drop across the valve when fully open to that across the circuit including the valve”. Referring to figures 1a and 1b for a three-port valve, for the corresponding pressure differences, this can be expressed as,

$$N = \frac{\Delta p_v}{\Delta p_v + \Delta p_s} \dots\dots\dots(4)$$

Note that for a three-port valve  $\Delta p_s$  refers to the pressure drop of that part of the circuit in which the flow is varying due to the action of the valve.

CIBSE<sup>80</sup> identify the importance of keeping the valve authority as high as possible so that the pressure drop across the valve is significant when compared to the pressure drop across the remainder of the circuit so that it may influence that circuit to exert good control. A higher authority will, however, require larger pumping power requirements. They state that “the authority should not be less than 0.5 for diverting . . . applications and not less than 0.3 for mixing applications”. Letherman<sup>81</sup> recommends that “a value of 0.4 (or 40%) at least is usually satisfactory, but a larger value is desirable”.

Other aspects of control valve performance which need to be considered when developing the valve model are its let-by and rangeability. Referring to figure 3 taken from CIBSE<sup>80</sup>, rangeability is defined as the ratio of the maximum controllable flow to the minimum controllable flow.

**Figure 3: Rangeability (R) and Let-by of a valve.**

This term is necessary because, when a valve is fully closed, there is still some fluid flow, or leakage, through the valve. This leakage is known as the valve let-by. Therefore, as the valve approaches its fully closed position the normal control characteristic of the valve is not followed.

The sizing and selection of a control valve is important in that control and system performance and energy use could be adversely affected by an inappropriate type and size of valve. Indeed, Tom<sup>82</sup> explains the importance of properly sizing control valves. He states that “no matter how precise the sensors, controllers, actuators and other control components are, if the . . . valves don’t perform properly the entire system will provide only poor control



at best”. He adds that “the fundamental purpose of a control valve is to modulate the flow of a liquid (typically water) through a piping network based upon a signal .....“. According to Tom, many systems being designed today have valves that are grossly oversized. He elaborates by asserting that an oversized valve will not control the flow through the system as well as one which is correctly sized.

McVann<sup>83</sup> discusses the performance of control valves in terms of deterioration of performance and failure. The consequences of a poorly performing valve are highlighted in that control and comfort are adversely affected as well as the occurrence of energy wastage. He observes that detecting valves which are not performing as required is a difficult task. Preventive maintenance is discussed as the primary means of discovering defects. Some of the problems also discussed are inappropriate valve capacity, excessive pressure drops and wrong valve characteristics for application. He states that “a good inspection and maintenance procedure program can forestall deterioration of control valves to the extent that replacement would become unnecessary and also avoid energy waste”.

Olsen<sup>6</sup> discusses control valve selection and states that “the proper sizing of control valves will normally result in the valve being smaller than the line size. A control valve which is oversized or selected for low pressure will ‘hunt’ and erratic control will result”.

### 3.1 Background and Previous Work

Many computer models attempt to model building and systems over relatively long periods of time in time increments of perhaps an hour or greater. Shavit and Spethman<sup>10</sup> agreed with this in stating that “all simulation programs to date do not have any capabilities to simulate the control systems and most of them are simulating the building in one hour increments”. Indeed, this statement can be applied to general building services engineering practice today. Although there are a number of simulation programs currently available for the analysis of short term system dynamics, these tend not to be used in the general building services design practice. Only long term analysis is carried out to determine design loads and internal comfort conditions. In reducing energy use it is also important to understand how buildings and systems, and individual components of systems and their control, perform and respond to each other over much smaller time intervals. Indeed Miller<sup>11</sup> states that “the ability to study these short-term characteristics, which occur on the order of seconds or minutes, through simulation is an important factor in the development of energy-reducing HVAC processes”. Thompson and Chen<sup>84</sup> reinforce this view in pointing out that “in order to evaluate the effect of room and control system dynamics on energy consumption, it is necessary to retain the short term dynamics of the room and HVAC system and to carry out the simulation with sufficiently short solution intervals to manifest these short term dynamics”. Shavit and Brandt<sup>85</sup> strengthen this argument by stating that “the success of implementing efficient energy management and control is coupled with understanding the performance of mechanical and control

systems". Work has therefore been carried out on modelling the dynamic performance of the mechanical and control systems involved in building services engineering. Some of this work includes the consideration and modelling of control valves to some extent.

The investigation of the dynamic response of building services engineering system components and their control began in the late 1960's. Some of this early work tended to focus on building envelope. The modelling of control valves has been included in some of the system modelling work, because of their influence on the dynamic response of the control of these systems.

Wapler and Pearson<sup>86</sup> analyse the dynamic behaviour of a water flow control valve and its connecting pipe work using a finite time step approach in order to investigate the reasons for water hammer in the valve. The actuation of the valve is by pressure from a stationary fluid exerted on a bellows connected to the valve stem. In this case the stationary fluid was refrigerant from a water-cooled condenser. In order for the valve to open a spring has to be compressed. A small damping coefficient also resists motion. A computer simulation is used for the analysis. They state that "theoretically it is possible to analyse the system by solving a complex second-order differential equation. However, the terms of the equation are highly non-linear, such as ... the relationship between the overall spring constant and the valve gap". Because of this they adopt a simulation evaluation using finite time steps. The valve under investigation was a two port disc type of control valve. They present equations for water velocity in the valve gap, upstream and downstream pressures, forces

acting on the valve stem and the size of the valve gap. As the model was used to investigate water hammer no discussion regarding the performance of the valve model was made. One of their conclusions was that “increasing the damping coefficient will . . . cure the symptoms of water hammer” without affecting the flow characteristics in the valve gap.

In investigating the control of a duct air temperature using a closed-loop control system, Zelenski et al<sup>87</sup> combined the dynamics of the heat exchanger, valve, actuator, controller and transducer in the forward block. A conclusion was that this block could be approximated by a dead time and time constant. It was further reported that the dominant time constant of a system containing one slow and other fast components strongly influenced the transient response of the system, while the effect of the fast elements was a simple delay or dead time.

Mehta and Woods<sup>88</sup> state that “to reduce energy consumption in buildings, design and analysis of building systems should be based on a dynamic model”.

Hamilton<sup>89</sup> develops mathematical models for a pneumatic actuator, a pneumatic line and a two port control valve as part of his overall model for a discharge air temperature control system. The basis for his actuator model is a spring - mass -damper system and a number of assumptions are made to simplify the mathematical model. A pneumatic line model proposed by Rohmann and Grogan<sup>90</sup> is used, but simplified to fit the particular pneumatic line being used. Standard equations are used, similar to those given by Letherman<sup>81</sup>, to

represent an ideal linear and ideal equal percentage valve, with approximate models presented for the let-by region where the ideal characteristic of the valve breaks down. Hamilton also includes a density correction for differing water temperatures.

Hamilton, Leonard and Pearson<sup>91</sup> include a two port valve model as part of their system model for a discharge air temperature control system. The valve could have equal percentage or linear characteristics. The flow characteristics were obtained by fitting curves to the valve characteristic curves and applying corrections for varying water density and varying pressure drops across the valve other than the standard values where the valve capacity index was determined. They also provide a second order differential equation for the pneumatic valve-actuator assembly as well as the pneumatic line model previously developed by Rohman and Grogan<sup>90</sup>. The valve-actuator model is the same as that presented by Hamilton<sup>89</sup>. They found experimentally that the model could be “simplified by neglecting the acceleration and velocity terms”. This was determined from a comparison of the speed of response of the actuator and the speed of response of the controller. The experimental tests also revealed a binding force which resisted the opening of the valve which was not present on the closing stroke of the valve. Thus they include a binding force component in their model which was found experimentally.. Later, in deriving the water circuit model, it was assumed that the water density was constant to simplify the equations.

Hamilton, Leonard and Pearson<sup>92</sup> investigated the dynamic responses near full load and part heating load of a discharge air temperature control system. It was emphasised that design criteria based on the dynamics of the components of the loop should be developed to aid the designer in selecting components for HVAC systems. Within this study they look at the effect of linear and equal percentage valves on system performance. In their model of the equal percentage valve they assume a linear characteristic for the let-by region.

Mehta and Woods<sup>88</sup> developed a rational model for dynamic responses of buildings and coupled it to different types of HVAC systems to derive dynamic models for buildings. They use transfer functions for a valve and actuator previously defined in an unpublished piece of work by Mehta as part of their overall system model. No detail of these models (valve and actuator), or their performance are given as the intent of this work was to demonstrate how the overall rational model could be used to “develop models which can describe dynamic interactions between the building envelopes, HVAC systems, building occupants, and the exterior environments”.

Mehta and Kharsa<sup>93</sup> state that “control system dynamics have a strong influence on the energy consumption patterns of a building environmental control system and the study of control system dynamics can lead to the derivation of energy saving strategies”. They investigate the influence of proportional control dynamics on energy consumption and identify complex energy transfers between interior and exterior environments resulting from the interaction of controllers, HVAC components, building envelopes, building occupants, and the exterior

environment. They highlight the importance of understanding the dynamics of these interactions in order to reduce energy consumption in buildings.

Thompson<sup>94</sup> simulated the dynamics of a room with a fan and coil heating system. A model is developed for each element of the system based on the physical characteristics of the elements. Amongst the models presented is an equal percentage valve and pneumatic actuator. The actuator model is based on air pressure exerting a force on a diaphragm which moves the actuator against the force of a mechanical spring. A linear relationship between change in pressure and the displacement of the actuator is used. For the valve model it was found from the test facility that the installed characteristic of the valve was linear in that the flow rate through the valve was proportional to the valve displacement. For the valve and actuator model they found that the force on the stem caused by the pressure drop across the valve and the inertial forces caused by the mass of the valve and actuator were not significant. However, friction forces were found to cause hysteresis in the displacement of the actuator. Thompson takes into account this hysteresis in the actuator displacement which was found from the test facility. The parameters for the valve and actuator models were established from the results of the tests<sup>94</sup>. For establishment of the linear model parameters a simple least squares technique was used. For non linear dynamic parameters an extension of Thompson and Kohr's least squares method<sup>95</sup> was applied.

Thompson and Chen<sup>84</sup> model a room with a fan-coil two-pipe heating system. They include models for pneumatic transmission lines, a pneumatic controller

with a proportional control action, a pneumatic valve actuator and a two port valve. The pneumatic transmission line model given by Rohman and Grogan<sup>90</sup> is presented with “assumptions that the end effects are negligible and that the resistance, inertance and capacitance parameters are distributed uniformly throughout the pneumatic line”. They also present a simplified transfer function of this model for long transmission lines (over 30m). They compare the room time constant with the frequency of the pressure signal and conclude that for short transmission lines, “the model can be approximated to unity”. The actuator was represented as a damped spring mass system, including hysteresis and flow force on the stem. This model is similar in form to the model presented by Hamilton<sup>89</sup>. They point out that “response times of pneumatic valve-actuators are typically less than 30secs which is negligible compared to the room constant” and so they use this factor to simplify their model. The model for the valve represented an equal percentage characteristic of exponential form. They apply the model in a piece-wise form and apply constants in the model based on a typical valve characteristic curve. In their summing up of their study they state that “the response times of the pneumatic line, controller, valve actuator, valve, . . . are short enough to be negligible”.

In his study of HVAC process dynamics Miller<sup>11</sup> simulated single zone and four zone buildings and their associated multi-zone heating and cooling units. Miller found that the dynamics of the controls of an HVAC system can contribute to the reduction in energy use.



Stoecker et al.<sup>96</sup> and Stoecker and Daber<sup>97</sup> model and simulate a discharge air temperature control system. The air temperature in this system was controlled by a three port mixing valve providing constant temperature variable flow hot water to the heat exchanger. A simple model was initially used, and discrepancies with the experimental results from a test rig were used to initiate changes to the parameters of the model with the aim of improving its performance. Hysteresis effects were included in the valve model. Stoecker and Daber identified the possibility that valve hysteresis “will aid stability . . . , although at the expense of precision in control”. Stoecker et al describe a test facility incorporating a three-port valve with linear characteristics controlled by a pneumatic actuator. The application of the valve was to achieve constant temperature and variable flow water through a heating coil. A turbine-type flow meter was used in the rig to measure water flow rate through the coil. The pneumatic pressure to the control valve was also measured via pressure transducers. With regards to the mathematical model of the valve they state that “a linear flow-to-control pressure characteristic was at first assumed . . . . Such a model proved to be an inadequate representation of the actual valve, so a further exploration of the valve characteristics disclosed the importance of incorporating hysteresis into the model”. The flow to pressure characteristics of the valve were determined from the test rig which identified a hysteresis pattern for the valve. The model for the valve was based on these results.

Shavit and Spethman<sup>10</sup> present a discussion of a building simulation program which takes into account the dynamics of the control systems. No detailed model was given in this discussion.

Shavit and Brandt<sup>85</sup> model the dynamic performance of a discharge air control system with proportional or proportional plus integral control. An actuator/valve (two port) is included in the model. The effect of valve characteristics (equal percentage and linear) is demonstrated, amongst other things, and also the system performance with and without valve positioners is investigated.

Hysteresis is taken into account when the actuator was not equipped with the positioner. The positioner normally provides “local feedback on the valve to guarantee it will move as a function of the pilot signal”. The mathematical model of the valve/actuator is in the form of an ordinary differential equation in terms of displacement of the valve with time, controller output and actuator time constant. The actuator response to a change in controller output is a simple lag. The water flow rate is determined from an equal percentage or linear curve as a function of the actuator position. The model is used to investigate system stability. They report of system instability caused by valve hysteresis (i.e. a valve without a positioner) and also on areas of instability affected by valve characteristic. Hysteresis was quoted at 10%.

May, Borresen and Hurley<sup>98</sup> study the direct digital control of a pneumatically actuated air handling unit. They describe a simplified model of the controller and air handling unit and compare the results of this with actual measurements. A modulating pneumatically controlled chilled water control valve is used in the system with a valve positioner. They present exponential equations for pneumatic lines with and without leakage and use a combined valve and coil model. In modelling the overall system they cite a technique used by Borresen in 1981 which they state “uses simple dynamic models comprised of elements

described by time constants, gains, and time delays". The electric-pneumatic system model input is a controller signal and the output is valve position. The combined valve and coil model input is coil discharge air temperature determined as a function of valve position and the output is discharge air temperature. They point out that these two elements of the overall model "could be characterised by time constants". This model makes an assumption that at steady state conditions air and water entering temperatures and water flow rates were constant for a given valve position. This assumption is not generally valid, but was necessary as the exact characteristics of the valve and coil were not known<sup>98</sup>. The valve equation used assumes a linear characteristic for the valve with a valve authority equal to unity. The model is used to investigate the performance of various controllers and their parameters. Part of the final conclusions was that "additional research was needed to develop better HVAC dynamic models and techniques for evaluating system characteristics in the field".

Hill<sup>99</sup> uses a simple three-way valve model as part of a detailed simulation of a large HVAC system. Theoretical equations identified by Hamilton et al.<sup>91</sup> for the valve characteristic are used. The frictional coefficients are modelled as an exponential function with the pressure drops across the valve as a standard function of flow rate squared. Hill points out that actuator hysteresis is modelled as "a linear variation of the valve position for increasing or decreasing control input with a user specified slack in the control action when the direction of travel changes". The overall simulation was successful in demonstrating the capabilities of modular simulation program<sup>99</sup>.

Clark, Hurley and Hill<sup>100</sup> use a simple equation relating pressure change to flow rate squared, with flow resistance coefficient defined as function of normalised valve position, for a dynamic model of a valve. They use flow resistance equations for linear and equal percentage valves previously derived by Hamilton<sup>89</sup> from standard valve equations. The three-port valve supplies constant flow variable temperature water to a heating coil. Valve actuators are represented by first order time constants, and hysteresis effects are modelled using a hysteresis subroutine<sup>100</sup>. They state that “this subroutine takes as input a control signal between 0 and 1 and a parameter indicating the degree of hysteresis. When the time derivative of the input control signal changes sign, the output control signal remains constant until the mechanical slack represented by the hysteresis parameter has been taken up”. They identify a problem in modelling and studying the valve on its own, because “the system in which the valve is installed determines the authority of the valve”. The whole system was therefore simulated in order to examine the valve model. A comparison was made between measured and simulated results and it was found that the simulation reproduces the outlet flow rate characteristics reasonably faithfully<sup>100</sup>. However, because the pressure loss coefficients were estimated using empirical procedures, they found that attempts “to improve the agreement between measured and simulated flow rates by trial and error modification of these pressure loss coefficients met with little success”. A difference was identified between the actual valve characteristics and the modelled equal percentage characteristics. One final conclusion of the paper is that some empirical curve fitting is required to model a valve in detail.

Clark and Borresen<sup>101</sup> present an extension of this work with more detailed comments on the valve model. In their heating coil simulation they state that “the relatively large steady state errors . . . can be attributed to differences between the control valve model and the experimental valve”. The three-port valve was connected to maintain a constant water flow rate whilst achieving variable water flow temperature in order to control the output of the heating coil. They investigate the effects of valve authority on three different valve types having different inlet port characteristic combinations. Simple linear and exponential characteristic equations are used to define frictional coefficients in terms of fractional leakage through the valve, normalised valve position and flow resistance of valve when fully open. These equations were previously used by Clark et al<sup>100</sup>. They avoid detailed definition of system pressure drop by referring to ‘high authority’ or ‘low authority’. The study is used to recommend valve characteristics and authorities for differing system requirements. It was found that an exponential/linear valve with a high authority should be used for slow-responding systems, whilst a linear/linear characterised valve with a high authority should be used for fast-responding systems. An exponential/exponential characterised valve was found to be unsuitable for this type of application.

Hittle and Birtles<sup>102</sup> examine “the control of supply water temperature from boilers and steam-to-hot water converters using water mixing valves”. They analyse steady state process gain to identify appropriate mixing valve characteristics. The valve model uses fractional flows and corresponding temperatures to give the overall supply water temperature to the building or

main distribution system. They present simple linear and equal percentage valve characteristic equations. They find that very high ( $N = 1.0$ ) and low ( $N < 0.2$ ) valve authorities (signified by the symbol  $N$ ) produce wide gain variations for a linear valve, whereas for an equal percentage valve a reduction in valve authority helps to reduce gain variations. However they state that for exponential valves “a high authority or very low authority are both undesirable”. A final conclusion of the work is that system gain is strongly influenced by valve characteristics.

Murray and Hanby<sup>103</sup> present a model for a thermostatic radiator valve and a panel radiator in a room. The room air flow, room load, radiator and thermostat are all modelled by first order systems and a stability analysis of the system was then performed.

In analysing flow conditions in integrated loop systems, Agnon<sup>104</sup> replaces three-way mixing valves with two interconnected and opposite acting two-way control valves installed in the branches in order to simplify the flow analysis. Each of the valves has a linear characteristic and so it is assumed that the sum of the flow rates in both branches remains constant which is not true for a three-way valve.

Underwood<sup>105</sup> simulates an electro-pneumatic transducer and a two port linear valve as part of his overall simulation of a heating coil. The model presented includes a directly proportional linear electro-pneumatic transducer and a linear two-port valve with hysteresis. Underwood cites some previous work carried

out by Rohrer in 1983 which “provides accurate correlation of valve hysteresis . . .” for the model. A simplified block diagram of the overall model is shown with no detail of mathematical equations included. Underwood uses the model to test four controllers and no further reference is made to the actual performance of the valve model.

Underwood and Crawford<sup>106</sup> present energy balance equations in order to model a hot-water-to-air heat exchanger. They use a digital computer, a digital to analogue converter, an electro-pneumatic transducer and two port control valve with pilot positioner to adjust the heat output of the hot water coil in their test facility. They ran a test on this arrangement to check that the pilot positioner decreased hysteresis on valve/actuator arrangement. They present results of this test with a graph of signal (in millivolts) received from a water flow meter in the line versus the signal sent from the computer and fit a third order polynomial to the data. It was found that virtually no hysteresis existed between the opening and closing strokes of the valve. As a result of the polynomial curvefit an equation for determining the mass flow rate of the water was found as a function of control signal. This equation assumed that the density of the water was constant. “It was found that the valve response can be reasonably approximated as a pure time delay of one time step for analysis and simulation purposes”.

Balasubramanian<sup>107</sup> describes a method of modifying a plug valve operated by a diaphragm actuator to meter liquid flow. This modification involves the addition of a metering pot between the actuator and the valve body. It is

stated that “when the valve has linear performance characteristics, the flow rate can easily inferred from the air pressure applied on the diaphragm of the pneumatic actuator”. He fails to point out that because of the influence of the system, the installed characteristics of the valve are different from the inherent characteristic and that to achieve an inherent characteristic a constant pressure drop across the valve must be achieved.

Pyotsia<sup>108</sup> develops a mathematical model for a quarter-turn control valve installed in a process pipeline. The valve position is determined by a pneumatic cylinder actuator. The valve model is derived from two basic equations. The first equation is a second order differential equation relating force to the distance covered by the actuator piston, taking into account the mass of the piston and lever mechanism. The second equation relates torque to valve turning angle and the inertia of the actuator and the valve. These equations are then used to develop a differential equation for the dynamics of the installed valve, taking into account such things as friction coefficients, damping forces, dynamic torque etc. in order to take into account the actual construction of the valve as well as its dynamics. The actuator friction coefficient was assumed to be constant in this mathematical model though it is pointed out that in practice this varies greatly as a function of velocity. A control valve simulation model, its testing and application is also described. Equations are presented for contact friction coefficients taking into account coefficients for accelerating and decelerating motion (static and dynamic). As a result of the analysis made by the program it is stated that “one of the most important factors affecting the dynamics of a control valve equipped with a



pneumatic cylinder actuator is the friction behaviour ...”. It should be noted that the great detail of the model included in this work was necessary because the model was to be used to develop products.

Fujiwara et al<sup>109</sup> present a mathematical model of a pneumatic control valve in their overall study of an intelligent valve positioner using new control method. Their specific interest was valve travel and so water flow rate and valve characteristics were not accounted for in the model. The model used takes a very similar form to the models previously identified by Hamilton<sup>89</sup> and Thompson and Chen<sup>84</sup> for a pneumatic valve actuator and takes into account viscous damping coefficient, spring constant, friction, mass of moving part, fluid force and pressure inside the air motor. They point out that “the characteristics of control valves ... are a non-linearity of Coulomb friction whose magnitude is variable and changeable disturbances caused by the fluid force”.

McCinnis et al<sup>110</sup> present a traditional mathematical model of a valve and incorporate this into a new modelling element which takes into account connector inertia, pipe friction effects and orifice characteristics. They claim that ‘it can be used to represent virtually any valve and pipe combination ...’ They do not consider three port valves and all the results of the model are expressed in terms of piezometric head at different pipeline locations of a water supply pipe network. No attempt is made at predicting system water flow rates.

Coughran<sup>111</sup> addresses the performance of control valves in the processes industries, particularly with reference to the installed dead band of control valves. He uses a test facility to look at the performance of several 2-port control valves. The valves are tested over three control cycles using small step changes of input signal. Volumetric flow rate (measured by a turbine flow meter), stem position (% of span) and input current (% of 4 – 20 mA) to position the valve are recorded. He states that ‘hysteresis is by definition a smoothly varying error, and tests show that hysteresis and linearity accumulate significantly only over large strokes. For closed-loop process control, these are rarely relevant.’ He therefore does not focus on this issue. He finds that very low dead bands required by the process industry cause a challenge for both design and testing. He concludes that testing valves on site is difficult ‘except in cases where noise and load disturbances can be eliminated.’

Wilton<sup>112</sup> examines the performance of a 2-port control valve in process applications. He specifically addresses valve performance when subjected to noise or disturbance in the flow pipe work. A theoretical analysis is developed in an attempt to explain the practical performance of control valves previously reported in other research papers. The theoretical model presented is in the form of a signal block diagram. The analysis concentrates on the dynamic control performance of the valve when subjected to differing load disturbances and does not address system fluid flow rates.

Champagne and Boyle<sup>113</sup> study the control loop performance of a control valve for use in the process industry. In particular, they look at ‘optimising valve

actuator parameters to enhance control valve performance.’ They develop a mathematical model to ‘assess the dynamic performance of a control valve, actuator and positioner ... assembly.’ With respect to valve performance their results are expressed as percentage valve travel corresponding to time. They find that the biggest influence on the speed of response of a control valve is the size of the supply pressure. They conclude that ‘the interaction of kinematics and fluid dynamics is, at times, not obvious.’

Atmanand and Konnur<sup>114</sup> look at the use of a 2-port control valve for the measurement and control of the flow of air. They state that ‘if a relationship is developed between the differential pressure produced by the control valve and the flow through it, the valve itself could function as a flow meter ...’ They establish a relationship for this based on an equation for control valve capacity. A number of terms are included in the equation because of the nature and compressibility of a gas. They determine values of  $C_v$  for a range of valve openings under laboratory conditions. They state that ‘the system works satisfactorily under laboratory conditions, its use in process control plant is yet to be established.’ They claim that ‘the unit was calibrated ... to an accuracy of  $\pm 1.5\%$ . They take no account of practical system characteristics which influence flow rate.

### 3.2 Summary

With the concern of saving energy in buildings and the affect of the performance of mechanical and control systems on this, some work has been

carried out on dynamic system modelling. Some of these models include control valves and their associated control mechanisms in order to investigate the short term response and control characteristics of the overall systems. The performance and accuracy of these valve models are not generally analysed or discussed in isolation as optimisation of the system control loop performance tends to be of more concern. No detailed work has been carried out with these models as to their accuracy in predicting flow rates.

### 3.3 Detailed Valve Model

Some of the earliest work on valve modelling was carried out by Hamilton<sup>89</sup> as part of an overall model of a discharge air temperature control system. He includes a model for a pneumatic line, a valve actuator and a two-port control valve.

Hamilton<sup>89</sup> presents an equation for the valve stem as follows,

$$m \cdot \frac{d^2 x}{dt^2} + \left( b \cdot \frac{dx}{dt} \pm f_c \right) + [K(X_{\max} - x)] = (P_a - P_{a \min}) A_p \dots \dots \dots (5)$$

where  $x$  = stem position,

$X_{\max}$  = valve stroke,

$b$  = viscous damping coefficient,

$f_c$  = friction force,

$P_a$  = pressure in the pneumatic line connecting the actuator to the controller,

$P_{amin}$  = pressure in the pneumatic line connecting the actuator to the

controller which produces a force equal to the pre-load force of the spring in the actuator,

$A_p$  = cross-sectional area of the piston in the actuator.

This model is based on a spring-mass-damper system. The model includes four force terms. These are; pressure force on the actuator piston from a pressure signal, spring force due to the actuator spring pre-load force and its compression, damping force due to friction and viscous damping caused by the valve packing, and a flow force caused by water on the valve plug<sup>89</sup>. He assumes that the pressure drop across the air fitting on the actuator is negligible. This would mean that the air pressure at the end of the pneumatic line would be the same as that entering the pneumatic actuator.

Hamilton found from experimental results that both the inertial term and the viscous damping term in this equation is negligible. He states that “it is . . . believed that other valve-actuator assemblies of the type studied here would exhibit the same characteristics . . .”. Hamilton uses a simplified form of Rohman and Grogans<sup>90</sup> model for his pneumatic line. His valve model uses ideal inherent characteristics which he incorporates into an overall water circuit model which includes a pump, heat exchanger, pipe work and a boiler. The inclusion of all these plant items introduces a large number of variables into the equation which are particular to the actual system being analysed which makes the model a little cumbersome to use and difficult to apply in general. It is recognised that this detail was necessary for Hamiltons study. The inclusion of valve authority to take into account system pressure effects would simplify the model greatly and allow its more general use. The treatment of

valve stem is very similar to that used by Weber<sup>115</sup> who presents an equation for a pneumatic valve actuator stem according to Newton's Law. The valve is a single seated control valve requiring air pressure to close the valve. He points out that the air pressure from the controller will be different from the air pressure in the valve motor "because of the resistance in the pneumatic transmission line and the capacitance of the valve motor". He considers five forces; the force on the stem by the diaphragm caused by air pressure in the valve motor, the force of gravity, the force of the spring acting on the diaphragm, the force caused by the fluid pressure acting on the valve plug, and a frictional force caused by the contact between the valve packing and the stem. The equation is as follows:

$$P.A_D + m.\frac{g}{g_c} - K.x - P_f.A_p - R.\frac{dx}{dt} = \frac{M}{g_c}.\frac{d^2x}{dt^2} \dots\dots\dots(6)$$

where  $P$  = pressure in the valve motor,

$A_D$  = area of diaphragm,

$g$  = acceleration of gravity,

$g_c$  = conversion constant,

$K$  = spring constant,

$P_f$  = fluid pressure at valve seat,

$A_p$  = area normal to valve plug,

$R$  = coefficient of friction between the stem and packing,

$m$  = mass of actuator piston, valve stem and valve plug.

The valve stem equation assumes a vertical stem with the downward direction taken as positive. He further simplifies the equation by ignoring the gravitational force term as it is constant and assumes a zero deviation in fluid pressure at the valve seat. This final assumption would be particularly valid for a double seated valve where the effects of flow force tends not to be experienced. This flow force in three-port mixing valves also does not normally create a problem. A transfer function of equation .....(6) is then obtained as follows,

$$\frac{x}{P} = \frac{A_D/K}{\frac{M}{Kg_c} s^2 + \frac{R}{K} s + 1} \dots\dots\dots(7)$$

He states that “the analysis ... has neglected static frictional forces, which cause hysteresis effects”.

In order to get a reasonable representation of the actual pressure in the valve, a model of the pneumatic line is required. Rohman and Grogan<sup>90</sup> provide a detailed mathematical model of a pneumatic transmission line which Hamilton<sup>89</sup> states “is cumbersome to use ...” in its original form. This model takes into account the non-isothermal behaviour of the air caused by a change in its pressure. For the purposes of this study a simplified model will be used, proposed by Weber<sup>115</sup>, which assumes isothermal behaviour for the air. This assumption would seem to be valid as a steady state signal is being investigated for the valve, not the short term dynamic response of the controller loop which could possibly be affected by this slight change in

temperature. Weber<sup>115</sup> applies the Equation of Continuity and Equation of Motion to the line and presents the following equation for a pneumatic line with a bellows termination,

$$\frac{P_i}{P_o} = \frac{1}{\cosh \sqrt{(R'.C'.s)} \times L} \dots\dots\dots(8)$$

Weber then expands the hyperbolic cosine in a series and retains the first two terms with the resulting equation,

$$\frac{P_i}{P_o} = \frac{1}{1 + \frac{R'.C'.L^2}{2}.s} \dots\dots\dots(9)$$

where  $P_i$  = controller sending end pressure,

$P_o$  = valve receiving end pressure,

$R'$  = resistance per unit distance of tubing,

$C'$  = capacitance per unit length of tubing,

$L$  = length of tube.

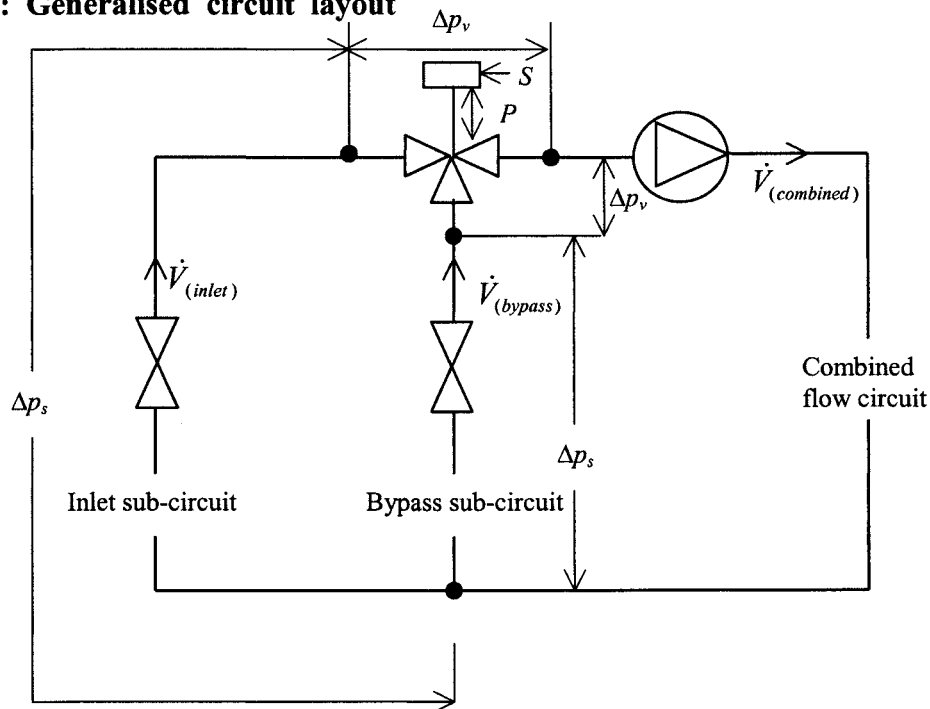
Which is a first order transfer function with a time constant. A bellows termination can normally be found on a pneumatic valve positioner which is used on the valves under study.



### 3.4 Derivation of the Valve and Circuit Model

A mathematical model for a three port control valve was developed based on the relationship between the flow rate passed by the valve and the position of the stem - the so called valve characteristic. As mentioned previously, the inherent characteristic of a valve expresses its idealised performance in the absence of accompanying system pressure fluctuations. This is then used to express the valve's installed characteristic which includes these associated system effects. In this work, the let-by (i.e. leakage across the valve seat at nominal closure) and hysteresis (i.e. error between the positioning signal and actual stem position due, mainly, to mechanical freedom in the actuator and stem linkage mechanism) are also accounted for. Figure 4 shows a generalised circuit layout.

**Fig.4: Generalised circuit layout**



Allowing for let-by (though usually very low in these types of valves), the inherent characteristic for a valve can be expressed as follows:

Inherent characteristic,  $G_{inh} = G_o + P.(1 - G_o)$  .....(10) for a linear valve and,

$$G_{inh} = G_o^{(1-P)} \text{ .....(11) for an equal-percentage valve,}$$

For a detailed derivation of the equal percentage case see appendix 2.

The installed flow characteristic, expressed as the fraction of flow passed by the valve at some position to that flow at the fully open position, can be related to the inherent flow characteristic with reference to a single valve port using the following expression the detailed derivation of which can also be found in appendix 2,

Installed characteristic,

$$G_{ins} = \frac{1}{\sqrt{1 + N \cdot \left( \frac{1}{G_{inh}^2} - 1 \right)}} \text{ .....(12)}$$

where  $G_o$  = valve let-by,

$P$  = valve stem (and inlet plug) position,

$N$  = valve authority.

These characteristic equations can be applied to the inlet and bypass ports of the three port valve. The final combined outlet flow rate of the valve as a function of incoming control signal is given as,

$$\dot{V}_{combined} = \dot{V}_{inlet} + \dot{V}_{bypass} \text{ .....(13)}$$

where inlet volume flow rate as a function of incoming control signal is given as,

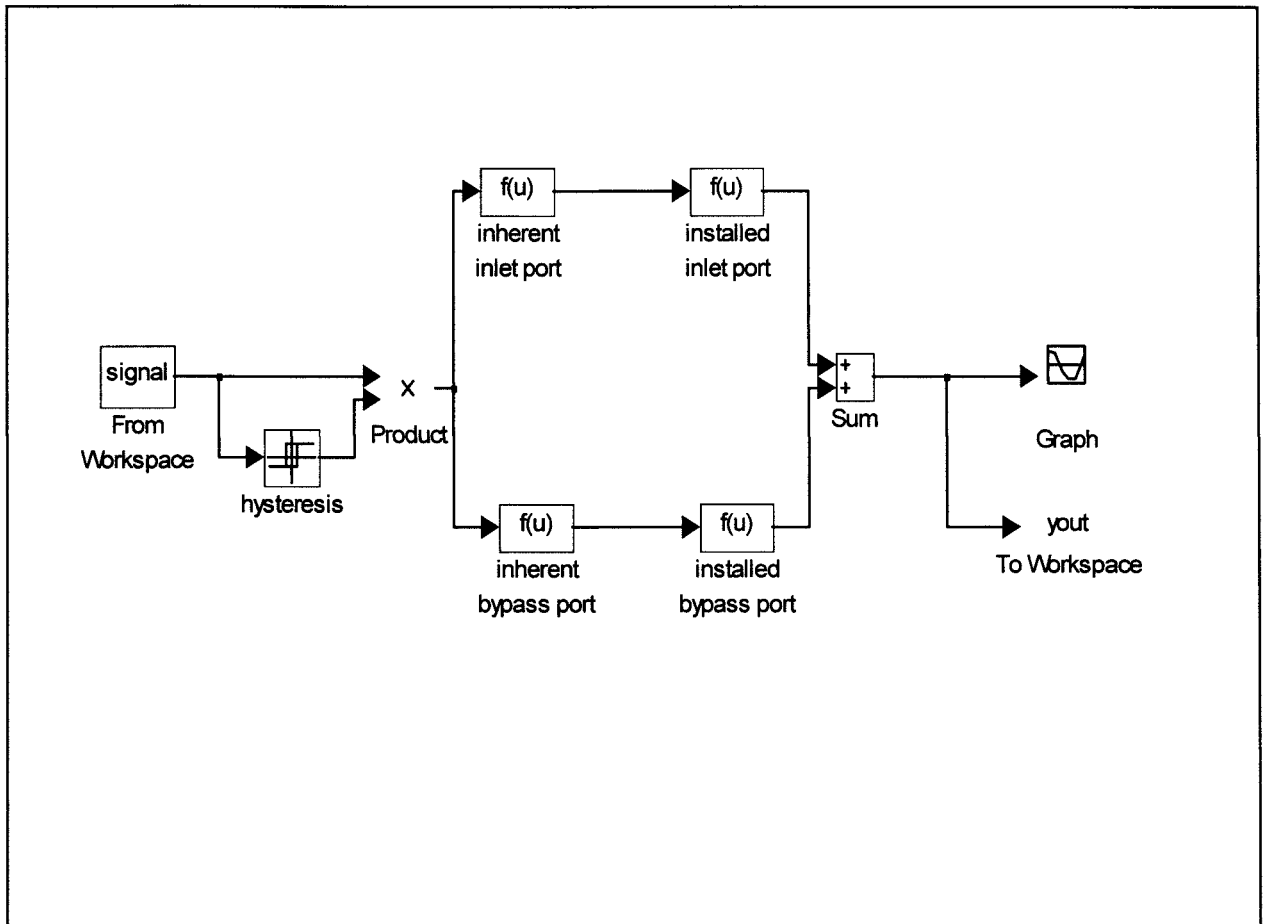
$$\dot{V}_{inlet} = \dot{V}' . G_{ins(inlet)} \dots\dots\dots(14)$$

and bypass volume flow rate as a function of incoming control signal is given as,

$$\dot{V}_{bypass} = \dot{V}' . G_{ins(bypass)} \dots\dots\dots(15)$$

In order to assess the adequacy of the simple valve and circuit model on its own, it was used as the initial model to predict combined port flow rates. It was thought that the short term dynamics of the pneumatic line and actuator assembly would not affect the steady state relationship between the control signal and the combined port flow rate. Equations for the pneumatic line and the actuator were not, therefore included in the initial mathematical model used.

Figure 5 (over the page) shows the model as it was represented in MATLAB Simulink.

**Figure 5: Mathematical Model (Version 1.0)**

This initial form will be referred to as version 1.0 of the model, as later in the thesis a number of modifications are made to the model in an attempt to improve its performance.

A control signal is generated from a Signal block available within the MATLAB Simulink software package. Hysteresis caused by mechanical slack and friction is modelled using a MATLAB Simulink “Relay” block. Both inlet and bypass ports of the three-port valve have inherent characteristics represented by equation .....(10) for a linear characteristic or equation .....(11) for an equal percentage characteristic. In all cases the output from the inherent

characteristic, which is the ideal normalised flow rate, is input to the installed characteristic of the inlet and bypass ports of the valve. This installed characteristic is described by equation .....(12). The output of these installed characteristic function boxes represents the actual normalised flow rate passing through the inlet and bypass ports of the valve. These two actual normalised flow rates are then added together to give the combined circuit flow ratios passing through the valve.

Figures 6 - 8 show the initial results from the model, both for linear/linear and equal percentage/linear control valves. It can be seen that the combined circuit flow when using an equal percentage/linear valve behaves in an opposing manner to that of the linear/linear case with significant shortfalls in total flow at all intermediate positions of the valve, especially at higher authorities.

Preliminary results were presented in Underwood and Edge<sup>116</sup> (1995, found in appendix 3). Clearly there is some disadvantage in using the equal percentage/linear valve from an overall circuit flow point of view, though this disadvantage seems to be outweighed by improved control on the load side of the valve as has been noted by Hamilton et al<sup>92</sup>. This does not suggest that the equal percentage/linear case offers any less potential for flow monitoring through control signal data than the linear/linear case, but that the valve characteristic and valve authority form the two dominant factors in assessing the appropriate model or performance relationship for the prospective use in flow monitoring of this kind.

In order to assess the adequacy of the model, a test rig was designed and built to achieve practical flow rate data so that comparisons could be made. This is described in the next chapter.

## **Chapter 4**

### **4.0 A Practical Investigation of Valve Characteristics**

#### **4.1 Introduction**

For the accurate assessment of energy use by hot water heating (and chilled water cooling) systems the monitoring of fluid flow is essential. A literature review on the application and performance of conventional flow meter devices suggests that there is scope for an alternative method for monitoring fluid flow.

Most heating pipe work systems include various types of valve capable of performing different functions, e.g. isolating and control. Common knowledge of valve performance is known within these circuits in terms of valve inherent characteristics and valve authority. Inherent characteristics are available from manufacturers data and are chosen by the designer, valve authority is also chosen in the design process. Valve inherent characteristics give some indication of flow rate entering the valve (at constant pressure drop across the valve). Valve authority gives an indication of the control valves influence on this flow rate in terms of a comparison of pressure drop across the valve and pressure drop across that part of the pipe work circuit in which the flow rate is varying. If more detailed information was available of the actual combined circuit water flow rate coming out of the valve with respect to valve signal

then this information could be possibly used for the monitoring of flow rate.

Valve signal data can normally be obtained from BEMS.

This chapter discusses the requirement of a practical investigation of the relationship between the incoming positioning signal to a valve and its effect on the outgoing flow rate characteristic of that valve. The development of a laboratory test rig is described together with the detailed methodology by which the investigation procedure is carried out. Results from the investigation are then presented and analysed. The chapter is concluded with a discussion of the results obtained and of their subsequent analysis.

## **4.2 A Practical Investigation of the Relationship Between Valve Flow Rate Characteristics and Incoming Control Signal**

As discussed previously, in selecting a three port control valve, an emphasis is made on the importance of the correct selection of the inlet port and bypass port characteristics of the valve and its pressure drop in order to achieve appropriate constant total flow conditions through the valve. These are called the inherent characteristics and are achieved with a constant pressure drop across the valve. Much of the existing work on control valve performance has concentrated on optimising control loop performance through the correct selection of a combination of parameters about the valve, including its pressure drop and inherent characteristics. When a valve is installed in a practical pipe work system this inherent characteristic is influenced by system pressure fluctuations so that this characteristic is not followed precisely. Hence, the



installed characteristic of a valve which take into account these pipe work system pressure fluctuations is defined.

The wider implications concerning the interaction between the valve and the pipe work circuit need to be considered. No work has been carried out to document the combined port flow rate performance of three port control valves. It is this knowledge of combined port outlet flow rate, as governed by the installed characteristics of a valve, with respect to valve stem position, or incoming control signal, that has been identified for the possible use in flow rate monitoring as an alternative to conventional flow measuring techniques. Specifically, the degree to which the three-port valve maintains a constant flow in the non-controlled part of the circuit, and at what fraction of design circuit flow this is maintained. Further investigation is required of the potential for the use of the relationships between a control valve's installed characteristic and incoming control signal for such "passive flow monitoring". The information obtained may then be used to consider how adequate a knowledge of the valve control signal would be in the monitoring of flow conditions in cases where conventional flow metering is impracticable or considered prohibitively expensive. Such a knowledge would provide a simple and low cost method of monitoring energy use in circuits equipped with control valves themselves positioned from signals processed in building management and computer-based control systems. In order to carry out this investigation an experimental test facility was developed.

### 4.3 Philosophy of Test Rig Development

The test rig was specifically designed to study the installed outlet port characteristic of the valve. In order to investigate consistency in performance for valves having different physical dimensions and flow capacity, a number of sizes of valve were required to be tested. Ideally, a number of combinations of valve inherent characteristics would also be investigated to determine the possible effects of these on the combined port outlet flow rate. The rig had, therefore, to be flexible in that it had to be able to accommodate a range of valve sizes together with their associated flow rates.

A factor which could effect the relationship between valve control signal and combined port outlet flow rate is hysteresis, caused by mechanical slack in the linkages and friction between stationary and moving parts. Indeed, depending on the size of this hysteresis error, possible differences in valve stem position corresponding to control signal for the upward or downward stroke of a valve could have a significant effect on this flow rate. The rig, therefore, had to quantify this effect in some way.

The effect of the interaction of a pipe work system with a valve had to be assessed. Each pipe work system has its own unique pressure drop characteristics. When selecting a control valve, the valve authority takes these pressure drop characteristics into account by relating them to the pressure drop across the control valve. In order to investigate the influence of valve authority, rig was designed with the facility to regulate the pressure drop

across the flow controlled part of the circuit. Thus the installed valve authority was adjustable so that the effect of valve authority and hence differing system pressure drops were able to be studied. Typically, valve authorities of 0.3 - 0.75 were chosen, to represent a range consistent with what might be expected in practice (ref. CIBSE<sup>80</sup> and Letherman<sup>81</sup>).

The design layout was chosen so that the three port control valve was connected as would be the case for a typical, mixing/injection circuit application commonly used to convert medium/high temperature hot water to low temperature hot water for use in heating systems. This application was found to exist for the three hospital sites previously studied. The same configuration is also applicable for a compensated heating system and indeed is used commonly in building services applications. The position of the three port control valve in both these circuit configurations is an ideal point of assessment of energy use as all of the heating water associated with the controlled circuit will travel through this valve. Figure 9 shows a typical compensated heating circuit and figure 10 shows a typical injection circuit (over the page).

**Fig.9: Compensated Heating Circuit (Simplified)**

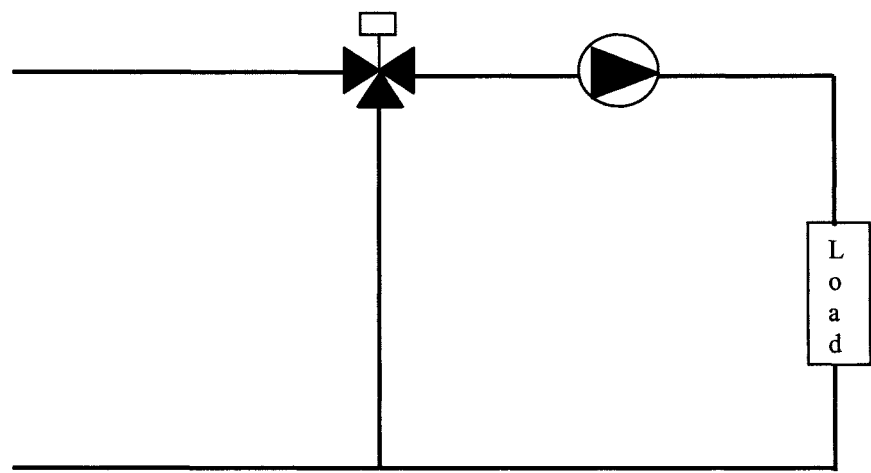
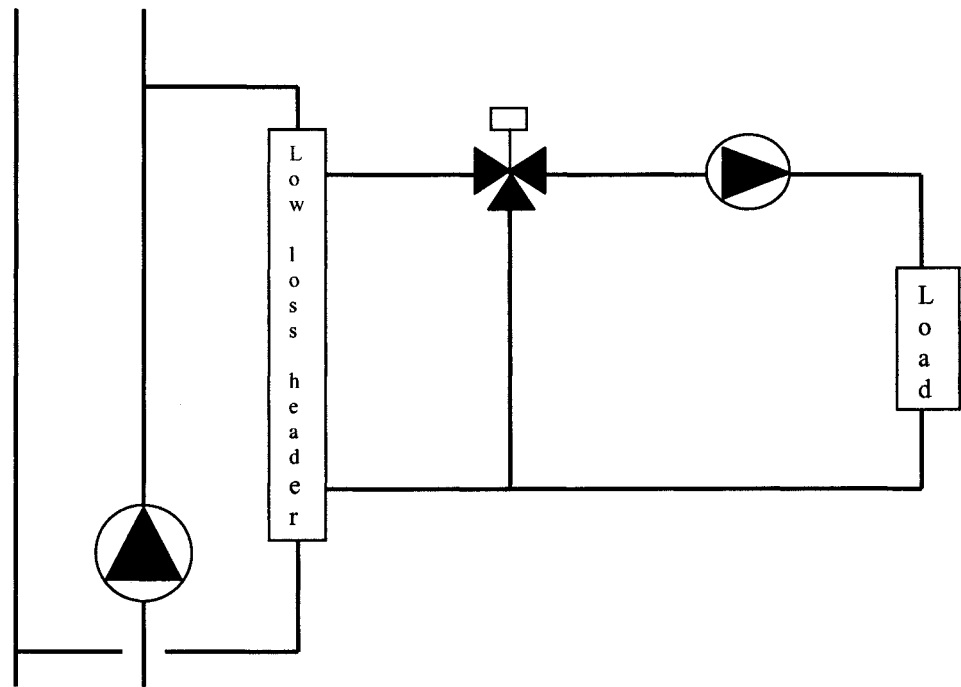


**Fig.10: Injection Circuit (Simplified)**

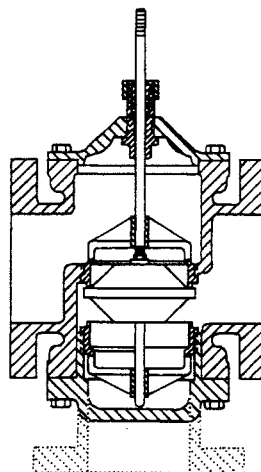


It should be noted that in both cases the flow rate at the combined outlet port of the valve is of interest as it is this flow rate that is transporting the energy around the heating system. This flow rate can then be used in an energy balance equation, together with flow and return temperatures normally provided by a BEMS, to provide the energy used by the system.

#### 4.4 Laboratory Test Rig

A range of pneumatically actuated three-port control valves were donated by an established valve manufacturer. Specifically, four valves were tested - 40mm and 50mm nominal bore Johnson figure no. V-5816 screwed cast iron valves, and 65mm and 80mm nominal bore Johnson figure no. V-5810 flanged cast iron valves. These valves are globe valves and are specifically designed for use in hot water, chilled water and steam applications. A typical cross section of the valve can be seen in figure 11.

**Fig. 11: Internal cross section of 3-port mixing valve  
(diagram from Johnson Controls<sup>117</sup>)**



They are especially designed for proportional control applications. All valves are equipped with a modulating valve plug. Johnson pneumatic diaphragm actuators were supplied with the valves. All the actuators were fitted with a Johnson figure no. V-9502 pilot positioner in order to provide stable and accurate control and limit the effects of hysteresis. This positioner was able to hold the test valve at the position imposed by the valve signal by compensating for flow surges, which exert force on the plug, and acting as a pneumatic relay device or a closed loop controller. The nominal spring range for the actuators was 9 to 14 psi (62 to 96 kPa). Valve stem position was monitored from a pointer on the valve stem and a graduated scale on the valve actuator. Manufacturers details<sup>118</sup> give details of the valves and actuators.

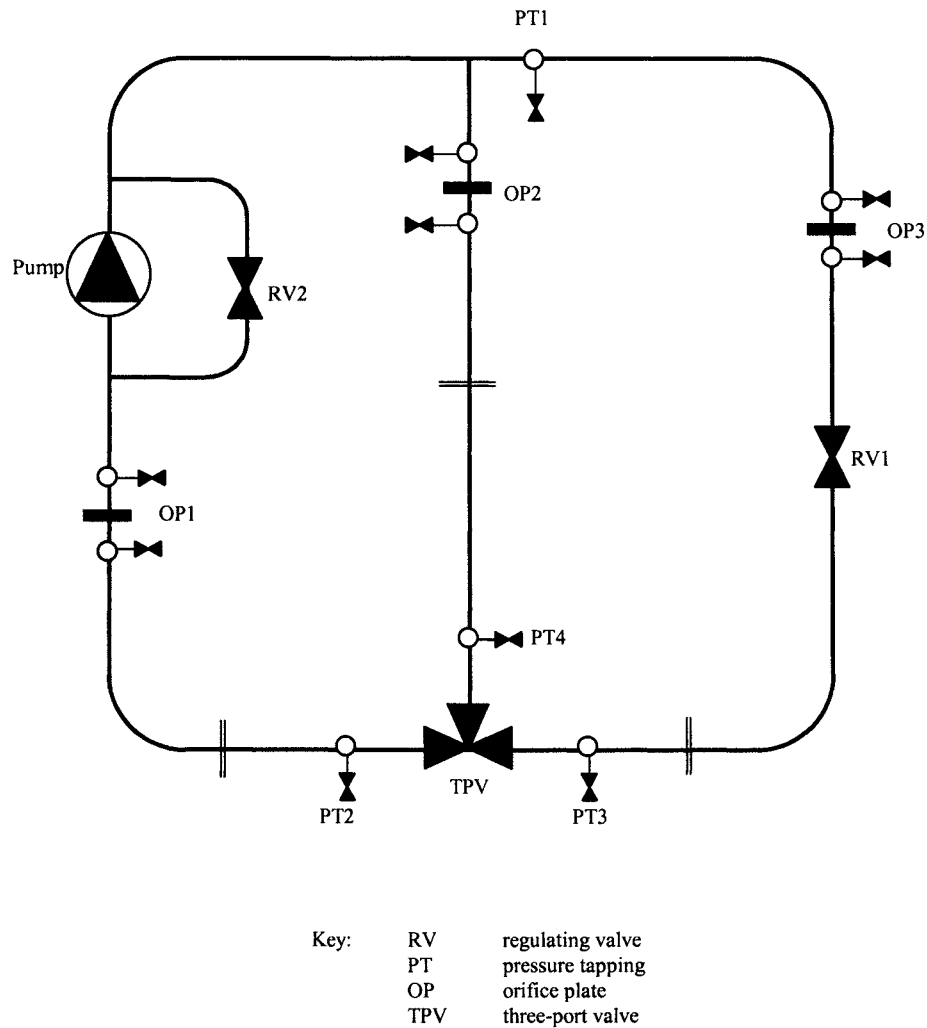
An air compressor, fitted with a regulating valve, RV3, and a Bourden tube pressure gauge, was used to power the valve actuator. This compressor plant was semi-automatic comprising of a twin cylinder, single stage compressor driven by a 3 phase electric motor and mounted on a vertical air receiver. The valve stems were of stainless steel. Each of the valves had a standard configuration of two inlet ports and one outlet port. The inherent characteristics of each of the two inlet ports on the valves were linear. All valves had a let-by rate of 0.05% of design rated flow.

The valves were installed in the rig for testing according to British Standard 5793 : 1981<sup>119</sup>. According to this standard,

“the upstream and downstream piping adjacent to the test specimen shall conform to the nominal size of the test specimen connection”.

The test rig was, therefore, built using welded mild steel tube with a nominal bore diameter of 80mm in order to accommodate the largest valve under test. This standard also specifies limiting straight lengths of pipe work to the final connections of the test specimen. Specifically, a minimum of twenty times the nominal pipe diameter for pipe work conveying flow into the test specimen, and a minimum of seven times the nominal pipe diameter conveying flow out of the test specimen. The final pipe work connections to the 80mm valve were designed to meet these requirements, whilst the pipe work connections to the smaller valves exceeded these specifications. The final pipe work connections to each of the test valves were of the same nominal bore as the test valve.

A schematic diagram of the rig is shown in figure 12 (over the page). In order to accommodate and test the range of valve sizes, flanged connections were made from the fixed part of the rig, to the final pipe work connections to the valve under test, so that the test valve and its required straight lengths of pipe work could easily be removed and replaced by another valve to be tested. Each of the test valves and their associated pipe work connections were therefore interchangeable. Pictures A1 - A6 in appendix 4 show the rig built and installed.

**Figure 12: Test rig schematic**

In order to have the facility to monitor the installed characteristic of the two inlet ports of the valve an orifice plate was installed in each inlet leg, OP2 and OP3, (80mm nominal diameter pipe work). An orifice plate, OP1, was also installed in the leg outlet port pipe work (80mm nominal diameter) in order to monitor the combined outlet flow characteristic, the main interest of this research. Each of the orifice plates had to be capable of monitoring full flow conditions for the situation of either a fully open or fully closed test valve, i.e. full flow through inlet port or full flow through the bypass port of



the valve. All the orifice plates were built and installed according to British Standard 1042<sup>120</sup>. This required amongst other criteria, that certain minimum lengths of straight pipe work existed, both upstream and downstream of the installed orifice plates, in order to ensure a smooth flow profile and minimise installed error. The orifice plates were square edged with D and D/2 pressure tapplings. Isolating valves were fitted to each pressure tapping to ensure ease of changeover and attachment to the manometer connections. A mercury filled 'U' tube manometer was used to monitor the pressure difference across each of the orifice plates.

The pump used was a Linepack LT65 close coupled electric motor driven, single stage, in line centrifugal pump, manufactured by Baric Pumps Ltd. In order to vary the flow rate in the rig a 50mm nominal bore pump bypass pipe was included with a 50mm regulating valve RV2.

An 80mm nominal bore regulating valve RV1 was installed in the fixed pipe work in a position such that it could be used to adjust the pipe work system resistance in the controlled part of the circuit. Thus the valve authority could be adjusted. To calculate valve authority, the pressure drop across the valve and the pressure drop across the varying flow rate part of the circuit had to be measured. The pressure drops were measured by mercury 'U' tube manometers. Hence, pressure tapplings PT2, PT3 and PT4, were installed in all three pipe work connections to the valve according to British Standard 5793 : 1981<sup>119</sup>. Another pressure tapping, PT1, for flow rate measurement was

included. Each of these pressure tappings also had isolating valves fitted for ease of changeover and attachment to the manometer connections.

## **4.5 Procedure**

### **4.5.1 Initial Test Valve Set Up**

With the pipe work rig drained, a test valve and its associated pipe work connections were fitted into place. At this stage the pump bypass regulating valve (RV2) and the system pressure drop valve (RV1) were fully open, to ensure that the rig could be filled efficiently with no possible air pockets collecting around a closed valve. Both regulating valves (RV1 and RV2) were manually adjustable with a scale and pointer arrangement incorporated on the valve stem to indicate valve position. All the plastic pipe work connections to the mercury manometers were then filled with water and attached to the relevant pressure tappings, carefully ensuring that no air bubbles existed. The air compressor was then connected to the pilot positioner and the valve actuator, and the compressor outlet gauge regulating valve was turned down to 0 p.s.i. This was to protect the actuator diaphragm against possible excessive air pressure damage when the compressor was switched on. The mains water isolating valve was then opened and the test rig was allowed to fill with water. Once full, the mains water isolating valve was closed to ensure that the rig was not pressurised. The pressure tapping isolating valves were then opened to allow the differential pressure manometers to monitor pressure drop across the relevant orifice plates, pipe work circuit and valve.

#### 4.5.2 Experimental Procedure

With the air compressor still operating, the compressor outlet gauge regulating valve was turned down to 0 p.s.i. and the circulating pump was switched on. In order to find the actual operating pressure range of the valve actuator and pilot positioner arrangement, air pressure was slowly applied by gradually opening the air compressor outlet gauge regulating valve until the test valve was fully open and observing the signal pressures at the two extreme valve stem positions, fully closed and fully open. A circulating water flow appropriate to the valve capacity under test was then established by adjusting the pump bypass regulating valve (RV2).

The next stage in the procedure was to adjust the valve authority to an appropriate value. Before this could be done the test valve had to be fully opened to ensure that full flow was circulating around the controlled part of the circuit. This was to ensure that a true indication of the maximum pressure drops across the test valve and the controlled part of the system was achieved. The air compressor outlet regulating valve was gradually opened until the test valve was in the fully open position (the inlet port was open and the bypass port was shut). An appropriate value of valve authority was then achieved by adjusting the controlled system pressure drop regulating valve (RV1) and monitoring the pressure drop across the valve, i.e. across pressure tappings PT2 and PT3, and the pressure drop across the controlled part of the circuit, i.e. across pressure tappings PT1 and PT3. Differential pressure readings were taken from the mercury manometers once they had achieved a steady level

after each regulating valve adjustment. Pressure drops were calculated using these values. These pressure drops were used in the standard valve authority equation previously identified. The valve was adjusted on a trial and error basis until an appropriate valve authority was achieved. Knowledge of the standard valve authority equation informed the valve (RV1) adjustment such that to achieve a lower or a higher valve authority, an increased or decreased value of the denominator of the equation was required. An increase or decrease in the controlled circuit resistance would achieve this. Thus the system regulating valve (RV1) was closed or opened by varying degrees in order to achieve the appropriate valve authority. Values of 0.3, 0.5 and 0.75 for valve authority were typically used for each test valve.

Once the valve authority had been set the test valve was closed by gradually closing down the air compressor outlet regulating valve. With the test valve fully closed, the initial differential pressure across the combined flow orifice plate (OP1) was noted. The test valve was then positioned at small equal increments of control air signal pressure until the inlet port was fully open, and then returned to the fully closed position at the same increments of signal pressure. This was achieved by gradual manual adjustment of the air compressor outlet regulating valve with reference to the air pressure gauge. By this process, it was possible to measure any hysteresis error between the valve stem and the incoming control signal. Care had to be taken during these gradual adjustments to ensure that there was no overshoot of the pressure signal, as a subsequent reduction in control air pressure to achieve the required control air pressure would cause a reversal of the direction of stem travel

which would affect the hysteresis measurements. Put simply, the direction of valve stem travel always had to be in the same direction on the upstroke of the valve; and the same condition applied for the down stroke of the valve. Any reversal of direction of the stem travel would affect the hysteresis measurements. At each pressure signal increment the mercury manometer levels were left to become relatively stable and then the column height values were recorded, as well as the corresponding air pressure control signal value. Column heights allowed the differential pressures across the orifice plate (OP1) to be calculated from which flow rates were deduced. This process was carried out for three different valve authorities for each test valve. This procedure allowed the actual installed characteristic of each valve as a function of valve authority to be obtained. Once the valve had been tested, the pump was switched off and the pressure tapping isolating valves were all closed. A hose was connected to the drain valve, which was then opened to allow the rig to empty to drain.

#### 4.6 Results

The differential pressures obtained from the orifice plate manometer (OP1) were converted to flow rate using the following standard formula given in British Standard 1042<sup>120</sup>,

$$q_m = CE\varepsilon \frac{\pi}{4} d^2 \sqrt{(2\Delta p \rho_1)} \dots \dots \dots (16)$$

which gives flow rate in kg/s.

An iterative procedure is used in the calculation and so a simple computer program was written in FORTRAN to perform the calculation. Appendix 5 gives details of this program.

Results were plotted of flow ratio versus normalised control signal as a series of line and symbol graphs to represent installed combined port flow rate characteristics for each valve at different valve authorities. Flow ratio defined in this case as;

$$f = \frac{\dot{V}}{\dot{V}'} \dots\dots\dots(17)$$

Referring to the graphs in figures 13 - 24, results for the combined plots of the upward and downward stroke flow characteristics at all valve authorities, for each valve, demonstrating the effect of valve authority on the installed flow characteristics of the valve.

#### 4.7 Analysis

Referring to figures 13 - 24, it can be seen that a constant combined port outlet flow rate is not achieved for any of the valves, with the majority of flow ratio values being in excess of unity, i.e. the design flow at fully open inlet port valve position. The deviance in actual to design flow rate tends to reduce with increasing valve authorities.

Specifically, for the 80mm test valve, deviance's of up to +25% occurring of the nominal design circuit flow rate were found for a valve authority of 0.3, with a mean deviance of +17.36%. The normalised control signal at which the maximum deviance occurred was 0.33. This deviance reduces for a valve authority of 0.5 to a maximum value of +17% and a mean value of +11.18% and reduced even further for a valve authority of 0.58 to a maximum value of +13%. The mean deviance at this valve authority was +7.96%. These maxima occurred at normalised control signals of 0.22, 0.33 and 0.44, for the 0.5 valve authority and 0.22, 0.33 and 0.44 for the 0.58 valve authority.

For the 65mm test valve, deviances of up to +55% of the nominal design circuit flow rate were found for a valve authority of 0.3, with a mean deviance value of 33.88%. The maximum deviance for this valve authority occurred at a normalised control signal of 0.375. This maximum deviance reduced to +27%, occurring at normalised control signals of 0.25 and 0.5, for a valve authority of 0.5, giving a mean deviance of +16.08%. A valve authority of 0.73 produced a deviance of up to +20%, with the maximum occurring at a normalised control signal of 0.5 for this valve, resulting in a mean deviance of +9.54%. Again this demonstrated the overall trend of the actual flow rate tending to approach the design flow rate for increasing valve authority.

This trend was confirmed by the performance of the 50mm valve. A deviance of up to +53% of the nominal design circuit flow rate, with a mean of +34.18%, was found for this test valve for a valve authority of 0.3. The

maximum deviance for this valve authority occurred at a normalised control signal of 0.22. Increasing the valve authority to 0.5 produced a similar reduction of maximum deviance to a value of +28% occurring at normalised control signals of 0.22 and 0.33, resulting in a mean deviance for this authority of +16.78%. A further increase of valve authority to 0.75 resulted in a further reduction in this deviance to a value up to +9%, with a mean of +3.79%. This maximum occurred at normalised control signals of 0.33 and 0.44.

For the smallest valve, with the 40mm nominal bore, a similar nominal design circuit flow rate deviance profile can be seen. For a valve authority of 0.3 a deviance of up to +50% of the nominal circuit design flow rate was observed, giving a mean deviance of +31.66%. The maximum deviance for this valve authority occurred at normalised control signals of 0.375 and 0.5. This deviance reduced to a maximum of +32% occurring at a normalised control signal of 0.375, and a mean of +17.97%, for a valve authority of 0.5. These values reduced again to a value of +8% maximum occurring at normalised control signals of 0.5 and 0.625, and +3.13% mean, when the valve authority was adjusted to 0.75.

From these observations it can be seen that the overall circuit characteristic tends towards unity with increasing valve authority, though this is more marked with the smaller bore test valves. The maximum deviance from the design flow rate tends to shift towards the zero value of normalised control signal with increasing valve size. For the individual valves, this maximum deviance



tended to occur at increasing normalised control signals for increasing valve authorities.

The results allowed the hysteresis error relative to control signal and flow rate to be evaluated. See figures 25 - 36. Specifically, for the 80mm test valve, with a valve authority of 0.3, the maximum hysteresis error for a single control signal value was found to be 8.7% with an overall mean hysteresis error of 3.18%. For the same valve, with an authority of 0.5, the maximum hysteresis error was 6.0% and the mean error was 2.23%. The maximum hysteresis error for this valve at a valve authority of 0.58 was 4.97% with a mean hysteresis error of 1.84%. Hence it would appear that the hysteresis error reduces with increasing valve authority. The overall mean hysteresis error for this valve taken across all three valve authorities was 2.42%.

For the 65mm test valve, with a valve authority of 0.3, the maximum hysteresis error was 26% with a mean hysteresis error of 7.97%. These percentage values were reduced to a maximum of 16.9% and a mean of 4.7%, when the valve authority was adjusted to 0.5. A further adjustment of the valve authority to a value of 0.73 resulted in a maximum hysteresis error of 17.3% and a mean hysteresis error of 3.6%. Again with this valve there was an overall reduction in hysteresis error as the valve authority was increased. The overall mean hysteresis error for this valve performance for all three valve authorities was 5.42%.

A similar hysteresis error profile was apparent for the 50mm test valve. At a valve authority of 0.3 the maximum hysteresis error was 17.3% with a mean hysteresis error of 4.78%. These values reduced to a maximum value of 4.85% and a mean value of 1.92% at a valve authority of 0.5. With an increase in valve authority to 0.75, the maximum hysteresis error for this valve was reduced to 3.1% with a mean hysteresis error of 1.15%. An overall mean hysteresis error of 2.62% occurs for this valve for its combined performance at the three valve authorities.

The performance of the 40mm test valve generally reinforces the hysteresis error profile tendency to reduce with increasing valve authority. At a valve authority of 0.3 the maximum hysteresis error for this valve was 11.84% with a mean hysteresis error of 2.87%. A valve authority of 0.5 produced a maximum hysteresis error of 9.07% with a slightly increased mean hysteresis error of 3.2% which was not expected. However, with a further increase in valve authority to a value of 0.75, the maximum hysteresis error reduced to 2.69%, and the mean hysteresis error reduced to 1.1%. The mean hysteresis error for the operation of this valve over the three valve authorities was 2.39%.

#### 4.8 Initial Mathematical Model Comparisons to Measured Test Rig Flow Rate Data

Results of circuit total flow characteristics obtained using the initial valve model (version 1.0) are compared with those measured from the experimental rig in figures 37 - 48.

In general, the experimental results were found to give good agreement with model results, especially at control signals greater than about 0.4 at the higher valve authorities. Mean absolute errors between these results were found to be 6.7% for the 40mm valve, 7.2% for the 50mm valve, 11.4% for the 65mm valve and 8.9% for the 80mm valve. The poorer agreement at low control signals is possibly due to the rangeability characteristic of the valve - in which the practical valve fails to maintain its ideal flow characteristic when approaching its seat. Hamilton<sup>89</sup> takes this into account to some extent by defining the let-by region for his valve model and giving it a separate inherent characteristic as follows,

$$G_{inbo} = G_o \cdot \frac{x}{x_o} \dots\dots\dots(18)$$

where  $G_{inbo}$  = inherent characteristic of the let-by region,

$x_o$  = valve stem position at the end of the let-by region.

The let-by region is defined as  $0 \leq x/X_{max} \leq x_o/X_{max}$ .

Subsequent refinement of the mathematical model is addressed in chapter 5 with a view to improving its performance.

#### **4.9 Summary**

A test rig was designed and built in order to investigate the relationship between the incoming control signal to a three port control valve and its outgoing combined port installed characteristic. Four sizes of test valve were used in the investigation, with control signal to flow rate relationships produced for three valve authorities for each valve.

The results show a wide variation of combined port outlet flow rate from the actual design flow rate of the valve at the fully open inlet port position. Mostly, the intermediate flow rates exceeded the design flow rate for all the test valves. This deviance reduced with increased valve authority.

Hysteresis error was found to reduce with increasing valve authority. With the exception of the 65mm valve, mean hysteresis errors were below 3% of the nominal circuit design flow rate suggesting that, for pneumatic valves fitted with pilot positioners, hysteresis effects in relation to the total circuit flow rate are not significant.

The results of this laboratory investigation allow an understanding of the relationship between the incoming control signal to a three port control valve and the resulting outgoing combined port flow rate at different valve

authorities. There is considerable potential for the use of this knowledge in determining flow rate in actual heating (and cooling) water circuits with a view to monitoring energy use. Comparisons with the initial mathematical model results are sufficiently encouraging to suggest that, with some further development and verification, a theoretical model could be used to predict flow conditions from control signal data. The next chapter investigates this application further by validating these control signal/flow rate relationships in a modified test rig. The mathematical model predictions are also validated by results from the modified rig.

## **Chapter 5**

### **5.0 The use of Flow Characteristics to Monitor Flow in a Practical Heating System.**

#### **5.1 Introduction**

Following the development of the test rig and the subsequent generation of some installed flow rate to control signal relationships for a range of three port valves at different valve authorities, this chapter will deal with the use of these relationships in a practical heating system for the monitoring of flow rate and hence energy use. The modification of the laboratory test rig in order to test the validity of the use of these relationships in the intended operating environment will be described together with the method by which the validation procedure is carried out. In order to incorporate these relationships into an energy use algorithm which could be included within a BEMS function, a series of mathematical curve fits to the flow/control signal relationships are made using polynomial regression analysis. Montgomery and Peck<sup>121</sup> state that “the most effective method of validating a regression model with respect to its prediction performance is to collect fresh data and directly compare the model predictions against it”. The modified validation test rig was used to validate the use of these regression models to predict water flow rate in a heating (or cooling) system and express an error band within which these relationships can be used. This chapter also investigates the adequacy of the use of a mathematical valve model in order to provide the flow/control signal

relationships and hence system flow rate and energy use, where detailed practical information on a control valve is not available. This adequacy is assessed by a comparison of the practical relationships between a typical control signal from a building energy management system, and system flow rate obtained from test rig, with the theoretical relationships obtained from the mathematical valve model.

## 5.2 Mathematical Curve Fitting

In order to investigate the possibility of incorporating the flow/control signal relationships into a Building Energy Management (BEMS) function, mathematical expressions were generated to describe the relationships using regression calculations in the Microcal ORIGIN Technical Graphics software package version 3.0. This package has a built-in least squares regression function. Because the measured result plots where of a curvilinear form a polynomial regression was considered to be appropriate. The aim of these calculations was to find a curve which best fits the empirical data so that the relationship between flow rate and control signal is appropriately described in a mathematical expression. In order to represent the measured data as accurately as possible, a separate polynomial regression least squares analysis was carried out for each upward and downward stroke for each test valve at each valve authority. The polynomial regression fitted data with a line of the form

$$y = A + Bx + Cx^2 + \dots \dots \dots (19)$$

where, in this case,  $y$  represents the normalised flow rate and  $x$  represents the normalised control signal. When curve fitting, a single polynomial expression of a fairly low order was aimed for. The strategy for choosing the order of the approximating polynomial was to successively fit models of increasing order and refer to a graphical comparison and the relevant statistical data in order to make a final selection. If these expressions did not provide a satisfactory fit, a piecewise polynomial was to be considered. This would involve dividing the range of  $x$  data into segments and fitting an appropriate curve to each segment. These would be jointed together to provide an overall expression for the data. The resulting piecewise polynomial expression, known as a spline, would normally be more complex than the single polynomial expression.

### 5.2.1 Curve fitting Results

The polynomial models were represented as curvilinear plots on two-dimensional graphs. The empirical data were plotted on the same axes of the same graphs so that comparisons could be made. Fifth order polynomial expressions were found to give a satisfactory fit for all the data curves. This order would appear to be a little high as good practice dictates that first or second order polynomial expressions are preferable. Mathematical text books suggest that higher orders do not enhance understanding and are not good predictors of the data. They also highlight the dangers of using these polynomial models for extrapolation. However, this data is within known limits of values measured on a laboratory test rig and our only interest lies in the



prediction of data within these limits. From our knowledge of control valve performance, any data occurring between the measured data points is strongly expected to follow the same overall data profile. The polynomial regression is not being carried out for further understanding of the data but merely to give as close a mathematical representation as possible of the actual data measured. Therefore, because the fifth order model carries out this task satisfactorily within the known limits, it is appropriate for this study. A more complex spline model was, therefore, not required. Referring to figures A1 – A16, in appendix 6 for the graphical comparisons, and the tables A2 – A17 in appendix 6 for the polynomial coefficients and the statistical data, it can be seen that good correlation between measured data and curve fit data was achieved. Coefficients of determination ( $R^2$ ) values were given for all the polynomial regressions. These ranged from a minimum value of 0.987 to a maximum value of 0.999 indicating the quality of fit of the regression model. This implies that, even for the worst case, up to 98.7% of the variability in the data is accounted for by the regression model. A value of  $R^2$  as close to 1.0 as possible was aimed for as this could indicate good agreement between the model and experimental data. However, it is well known that a value of  $R^2$  which approaches unity can be arrived at by simply adding enough terms to the model or by increasing the spread of  $x$  data. Care was therefore taken in its interpretation, with a graphical comparison carried out for each regression model in order to check the quality of fit. See table 2 for a summary of  $R^2$  values.

### 5.3 Modification of Laboratory Test Rig

The test rig previously described used a manual adjustment of control signal to the actuator of the control valve via a regulating valve on the air line from the compressor to the final control element. The air pressure signal was monitored on a Bourdon tube pressure gauge by visual inspection. A visual inspection of a mercury manometer allowed the differential pressure across the combined flow orifice plate to be evaluated.

In most heating systems today, monitoring and control is carried out by a Building Energy Management System (BEMS). Indeed, it is normally the task of the BEMS to issue control commands to control valves within the building services engineering systems. One of the ways in which this is done is by the output of an analogue signal, usually in the range of 4 - 20mA or 0 - 5Vd.c. via a transformer. In order to simulate a BEMS control signal, a Farnell stabilised power supply was used to give a variable analogue output d.c. current over a range of 4 - 20mA. In order to convert this electrical control signal to a proportional pneumatic control signal a Johnson EP-8000 electro-pneumatic transducer was used. Manufacturers<sup>122</sup> claimed that this was a high accuracy, low hysteresis device. This device is operated by a change in electrical input signal which moves an internal electric coil within a permanent magnetic field. The movement of the coil varies the amount of air exhausting from the control port which produces an output pressure. This output pressure is directly proportional to the input signal. The transducer was interfaced with the Johnson V-9502 pilot positioner.

In order to monitor the test valves combined outlet port flow rate automatically, the mercury manometer for the combined flow orifice plate (OP1) was replaced by a Siemens Sitrans PN160 differential pressure transmitter. The transmitter works by using a diaphragm to transmit a differential pressure to a silicone pressure sensor. The sensors measuring diaphragm is distorted by this differential pressure and the resistance of four piezo-resistors in a bridge circuit is changed. An output voltage is generated by this change in resistance which is proportional to the differential pressure. This voltage is then passed through an amplifier, a voltage/frequency converter and a micro controller, which corrects with respect to linearity and temperature, before being converted to an output signal by a digital/analogue converter. The transmitter was easily parameterised once installed without the need for any auxiliary instruments. This was achieved via three push buttons located on the outside of the instrument with settings displayed on an LCD located inside a housing on the device.

A low voltage d.c. supply was required to power the transmitter and this was provided by a Farnell stabilised power supply. The output signal from this differential pressure transmitter was 4 - 20mA d.c. This signal could have either a linear characteristic, proportional to the input pressure, or a square root characteristic, proportional to the flow. Manufacturers stated accuracy for this device was  $\leq 0.1\%$  measurement error, including hysteresis and repeatability, for a linear output characteristic, and  $\leq 0.2\%$  measurement error for a square root output characteristic. A linear output characteristic was used in these tests so that differential pressure values could be obtained. These differential pressure

values were then converted to flow rate using the previously written FORTRAN program, which uses the standard flow rate equation from British Standard 1042<sup>120</sup>, referred to in chapter 4, and which can be found in appendix 5.

The transmitter was installed below the pressure source and the connections made according to manufacturers instructions. The recommended manufacturers procedure for commissioning the pressure transducer was carried out in order to ensure the pipe work connections were full of the working fluid and adequately vented. All pipe work connections were made in 18mm nominal bore copper pipe work. The same orifice plate pressure tapings as the original rig were used for the connections to this test rig. Isolating valves were installed on the final connections to the test rig so that the main test rig could be drained down without affecting the differential pressure transmitter set up.

Data acquisition from the modified test rig was carried out by a Solartron ORION data logger. The logger, powered by 240V a.c. mains, provided the facility of receiving data, including results, and displaying this information in the appropriate physical units. An in built printing facility also enabled this data to be output in an appropriate hard copy analogue form. Only three input channels on the logger were used. The output control signal from the Farnell stabilised power supply to the electro-pneumatic transducer was connected to a channel, as well as the actual air pressure coming away from the electro-magnetic transducer, measured by a piezo-resistive gauge pressure sensor in the pneumatic line, though the latter was not used in the analysis. The final item

of data connected to a data logger channel was the output signal from the differential pressure transmitter on the combined flow orifice plate.

## **5.4 Procedure**

### **5.4.1 Initial Test Valve Set Up**

A test valve and its associated pipe work connections were installed in the test rig as detailed previously (in section chapter 4). Isolating valves on the pressure tapplings to the pipe work connections to the differential pressure transmitter and the orifice plates were closed at this stage. In order that the rig could be filled efficiently and to ensure minimal occurrence of air pockets, the pump bypass regulating valve (RV2) and the system pressure drop valve (RV1) were fully open. The air compressor outlet gauge regulating valve was closed and the compressor switched on. The compressor reservoir was allowed to fill, after which the outlet gauge regulating valve was slowly opened until the pressure gauge reading was at the maximum required to achieve full motion of the valve stem via the pneumatic actuator.

The Farnell stabilised power supply used for the input control signal (4 - 20mA) to the electro-pneumatic transducer was first adjusted to zero output to ensure that no excessive air pressures could damage the transducer. The output current from this supply was then gradually increased until the transducer allowed enough air pressure through to the positioner and actuator arrangement so that the three port test valve was approximately half open. This was to

ensure efficient and complete filling of the system. The mains water isolating valve was then opened and the test rig was allowed to fill with water. Once full, the mains water isolating valve was closed to ensure that the rig was not pressurised. The pressure tapping isolating valves were then opened to allow the differential pressure transmitter and the differential pressure manometers to monitor pressure drop across the relevant orifice plates, pipe work circuit and valve.

The Farnell stabilised power supply to the differential pressure transmitter was similarly first adjusted to zero output to ensure that no excessive voltages could damage the transmitter, then switched on and the output was gradually increased to the required voltage value to power the transmitter. A “blind” calibration of the transmitter was then made. This was achieved without the need of a calibrated pressure source, which was not available for this investigation. The start of scale was set as a percentage of the maximum measuring span of the transmitter. The maximum measuring span was set as a percentage of the maximum measuring span of the transmitter. Both these values were calculated from the previous knowledge of the test valves from the investigation detailed in chapter 4 of this work. The maximum measuring span of the transmitter was found from manufacturers data and was previously calibrated at manufacture. A zero point was also set for the transmitter, to compensate for the pressure difference between the positive and negative leg caused by installation effects.

### 5.4.2 Experimental Procedure

The circulating pump was switched on and the pump bypass regulating valve (RV2) was adjusted until an appropriate circulating water flow was achieved, as given by valve capacity information from manufacturers data. The stabilised power supply to the electro-pneumatic transducer was then adjusted until the three port test valve inlet port was fully open, (i.e. the bypass port was fully closed). An appropriate value of valve authority was achieved by adjusting regulating valve (RV1) and by carrying out the procedure previously detailed in chapter 4. In the previous set of tests valve authorities of 0.3, 0.5 and 0.75 were typically used. For these validation tests it was decided to limit the valve authorities to 0.3 and 0.5. These values were thought of as being more realistically achievable and common in practice, with high pumping power requirements normally being a prohibitive factor for the higher value of 0.75, though this value is more desirable for control purposes.

Once the valve authority had been set, the test valve inlet port was closed by gradually reducing the output current signal to the electro-pneumatic transducer from the stabilised power supply. The data logger was switched on and programmed to display and print data from the three channels at fifteen second intervals. In order to gain a better indication of the modulating characteristics of a control valve in practice, the output current signal from the stabilised power supply was increased to set the test valve so that its inlet port was half open at the start of the investigation. The output from the power supply was then adjusted at equal increments of control current signal output until the

valve inlet port was fully open. After each incremental adjustment the output display on the data logger was observed and allowed to become steady before the next incremental adjustment was made. This procedure was repeated until the valve inlet port was fully closed and then returned to the half open position again. Thus, the control signal from the stabilised power supply, the air pressure control signal emanating from the electro-pneumatic transducer, and the pressure drop across the combined flow orifice plate (OP1), were all recorded for each incremental adjustment of valve position for the full modulating range of the test valve. It should be noted at this stage that this method of positioning the valve is signal based (i.e. as would be the case from a BEMS), and that the previous method (on the unmodified test rig) was based on position (and manually adjusted).

This procedure was carried out at two valve authorities for each test valve. Flow rates were deduced from the orifice plate pressure drops given by the differential pressure transducer as described previously in chapter 4.

## **5.5 Results Comparison**

The results from the modified validation test rig were plotted on graphs of flow ratio versus normalised control signal for each test valve, at each valve authority. The control signal values from the modified test rig were used as an input to the polynomial regression equations in order to achieve corresponding predicted flow ratio values. These relationships were plotted on the same graphs using the same axes in order to perform a comparison of the original



polynomial regression expressions with practical valve performance, and hence assess the validity of the use of these expressions for the monitoring of water flow rate in heating (or cooling) systems. Referring to figures 49 - 56 for these graphs, and also to table 3 which summarises the results.

**Table 3: Summary of prediction errors**

Valve	Maximum Over Prediction Error	Maximum Under Prediction Error	RMS Error
80mm (N = 0.3)	+9.81%	-4.17%	4.03%
80mm (N = 0.5)	+8.23%	-2.93%	2.86%
65mm (N = 0.3)	+7.56%	-7.71%	5.29%
65mm (N = 0.5)	+3.30%	-5.37%	2.73%
50mm (N = 0.3)	+13.13%	-7.11%	5.85%
50mm (N = 0.5)	+3.73%	-8.77%	4.66%
40mm (N = 0.3)	+12.19%	-5.6%	6.54%
40mm (N = 0.5)	+1.19%	-6.97%	3.36%

For the 80mm valve,  $N = 0.3$ , the largest percentage prediction error was +9.81% for a control signal of 0.76. Hence a 9.81% over prediction of actual flow ratio was made at this control signal. The largest under prediction for this valve, ( $N = 0.3$ ), was by -4.17% of the actual flow ratio, occurring at a control signal of 0.31. In order to account for negative and positive errors (and the possibility of these cancelling each other out) the RMS (Root Mean Square) error was calculated for each of the valves. For this particular valve, ( $N = 0.3$ ), the RMS error was 4.03%.

For the 80mm valve,  $N = 0.5$ , the largest percentage prediction error was +8.23% for a control signal of 0.69. This again was an over prediction of actual flow ratio occurring at a similar control signal as the previous case. The largest under prediction for this valve, ( $N = 0.5$ ), was by -2.93% of the actual flow ratio, occurring at a control signal of 0.94, a dissimilar control signal

than the previous case. The RMS error for this valve, ( $N = 0.5$ ), was 2.86%. These error values represented a reduction in the maximum over prediction error, the maximum under prediction error and the RMS error for an increased valve authority.

For the 65mm valve,  $N = 0.3$ , the largest percentage prediction error was -7.71% for a control signal of 0.70. This value represents an under prediction of the actual flow ratio at this control signal. This was not a similar performance to the 80mm valve. The largest over prediction for this valve, ( $N = 0.3$ ), was by +7.56% of the actual flow ratio, occurring at a control signal of 0.80. This does appear to follow the trend for the maximum over prediction values and corresponding control signal of the 80mm valve. The RMS error for this valve, ( $N = 0.3$ ), was 5.29%.

The largest prediction error for the 65mm valve,  $N = 0.5$ , was -5.37% at a control signal of 0.30. This value represented an under prediction of the actual flow ratio at this control signal. This under prediction value occurred at a similar control signal to the maximum under prediction for the 80mm valve, ( $N = 0.3$ ), but was dissimilar to the other previously discussed cases. The largest percentage over prediction for this valve, ( $N = 0.5$ ), occurred at a control signal of 0.80, and was +3.30%. This occurred at exactly the same control signal for the largest percentage over prediction for the same valve with an authority  $N = 0.3$ . The RMS error for this valve, ( $N = 0.5$ ), was 2.73%. Again, these error values represented a reduction in the maximum over

prediction error, the maximum under prediction error and the RMS error for an increased valve authority for the 65mm valve.

The largest percentage prediction error for the 50mm valve,  $N = 0.3$ , was +13.13% at a control signal of 0.83. This value represented an over prediction of the actual flow ratio at this control signal and was the largest percentage error encountered for any of the valves during the validation procedure. This corresponding control signal was very similar to the control signal occurrence of the largest over prediction values of the 65mm valve and the 80mm valve. The largest percentage under prediction value for this valve, ( $N = 0.3$ ), was -7.11% at a control signal of 0.58. No similar trend was found from the previously discussed valves. The RMS error for this valve, ( $N = 0.3$ ), was 5.85%.

For the 50mm valve,  $N = 0.5$ , the largest prediction error was -8.77% at a control signal of 0.75. This represented an under prediction of actual flow ratio. The only similar control signal at which the largest under prediction value was encountered was for the 65mm valve, ( $N = 0.3$ , control signal 0.7). No other similarities were identified. The largest over prediction error value for this valve, ( $N = 0.5$ ), was +3.73% at a control signal of 0.34. This does not follow a possible trend for the previously discussed results of the largest over prediction value occurring at a control signal in the range of 0.69 - 0.83. The RMS error for this valve was 4.66%. Again, the findings for the 50mm valve demonstrate an overall reduction in the maximum over prediction error, the maximum under prediction error and the average percentage prediction error for

an increased valve authority. An examination of the validation results for the final test valve reinforce this last statement.

The largest percentage prediction error for the 40mm valve,  $N = 0.3$ , was +12.19% at a control signal of 0.75. This represented an over prediction and followed the general trend of over prediction occurrence at a control signal ranging from 0.69 - 0.83. Indeed these values also tended to occur on the upstroke of the valve. The largest percentage under prediction error for this valve, ( $N = 0.3$ ), was -5.60% at a control signal of 0.87. The under prediction values for all the test valves appear to occur at much more random values of control signal and no real trend could be identified. The RMS error for this valve, ( $N = 0.3$ ), was 6.54%.

For the 40mm valve,  $N = 0.5$ , the largest percentage prediction error was -6.97% at a control signal of 0.76. This represented an under prediction of the actual flow ratio. The largest percentage over prediction error for this valve, ( $N = 0.5$ ), was +1.19% at a control signal of 0.62 which lies slightly outside the suggested control signal range of a possible suggested trend occurrence of this value. The RMS error for this valve, ( $N = 0.5$ ), was 3.36%. The reduction of the largest over prediction figure and average percentage prediction error with increased valve authority for this valve strengthens the previously detailed percentage error profile concept. The increased largest under prediction error with increased valve authority for this valve opposes this trend. However, this was the only percentage error found, which failed to follow the trend.

The above detailed RMS errors range from 2.73% to 6.54% and were encouragingly low. The worst errors were a maximum percentage error of +13.13% found for the 50mm valve, ( $N = 0.3$ ), and a similar value of +12.19% found for the 40mm valve, ( $N = 0.3$ ), both representing over predictions by the regression model of the actual flow ratio. The maximum under prediction percentage error values were not as high, with the worst values of -8.77% for the 50mm valve, ( $N = 0.5$ ), and -7.71% for the 65mm valve, ( $N = 0.3$ ). Error values of this magnitude were not normally found, indeed, much lower error values were calculated for the majority of the control signal values applied to the range of valve regression models. When considering the operation of a three port control valve in practice its function requires it to be continuously modulating across its full control signal range. Therefore, the over and under predictions of flow ratio by the regression model should average or even themselves out to a certain extent, so that the RMS error values are more applicable. Consequently, a more accurate representation of flow ratio can be ascertained for the full modulating range of the control valve over time, without the instantaneous influence of an extreme percentage prediction error for a single control signal.

In light of some of these large errors it was decided to carry out a test of the Sitrans P pressure transducer which replaced a mercury manometer in the modified test rig. A comparison was made over a range of flow rates between the readings taken from the transducer and a mercury manometer. Specifically, connections were made from the pressure transducer to the inlet flow orifice plate pressure tapings on the test rig (OP3, see figure 12). Connections were also made from the mercury manometer to the same pressure tapings across

the orifice plate OP3. A typical test valve (TPV, figure 12) was installed in the rig and was adjusted to give a range of flow rates through orifice plate OP3. Readings were taken from the pressure transducer and the mercury manometer at each of the flow rates so that a direct comparison could be made. Table A18 in appendix 7 shows the comparisons.

It can be seen that over the range of flow rates measured the maximum difference between transducer readings and manometer readings was -3.86% i.e. the transducer reading was 3.86% less than the manometer reading – this was the worst case. The average difference between transducer and manometer readings was -0.756%. Hence for some of the individual readings these differences could be contributing to the error at individual signals. When analysing the full stroke of the valve, however, the average difference is more applicable and has less influence on the overall errors. These errors are within the modelling and regression uncertainties in all cases and therefore can be accounted for within the overall measurement prediction error.

### **5.5.1 Summary of Results Comparison**

The RMS errors for the polynomial regression models ranged from 2.73% to 6.54%. These low error values suggest that for the full stroke of a valve, from half open to fully open inlet port, from fully open to fully closed inlet port, and from fully closed to half open, at equal increments of control signal the overall prediction of flow rate accuracy is acceptable. Actual percentage prediction error values for individual control signals were as large as -13.13%

in one case and as small as +0.0053% in another, with percentage prediction errors ranging between these values for varying control signals. The modification of the test rig seems to have resulted in a 'phase shift' between the curve fit predictions and the measured data from the test rig. However, it could be argued that when the overall modulating range of the control valve is considered, the over and under predictions will tend to cancel each other out over time and therefore the RMS errors are more applicable. Valves operating in fixed positions for a large proportion of their operation time, could experience larger errors.

## **5.6 Validation of Mathematical Valve Model**

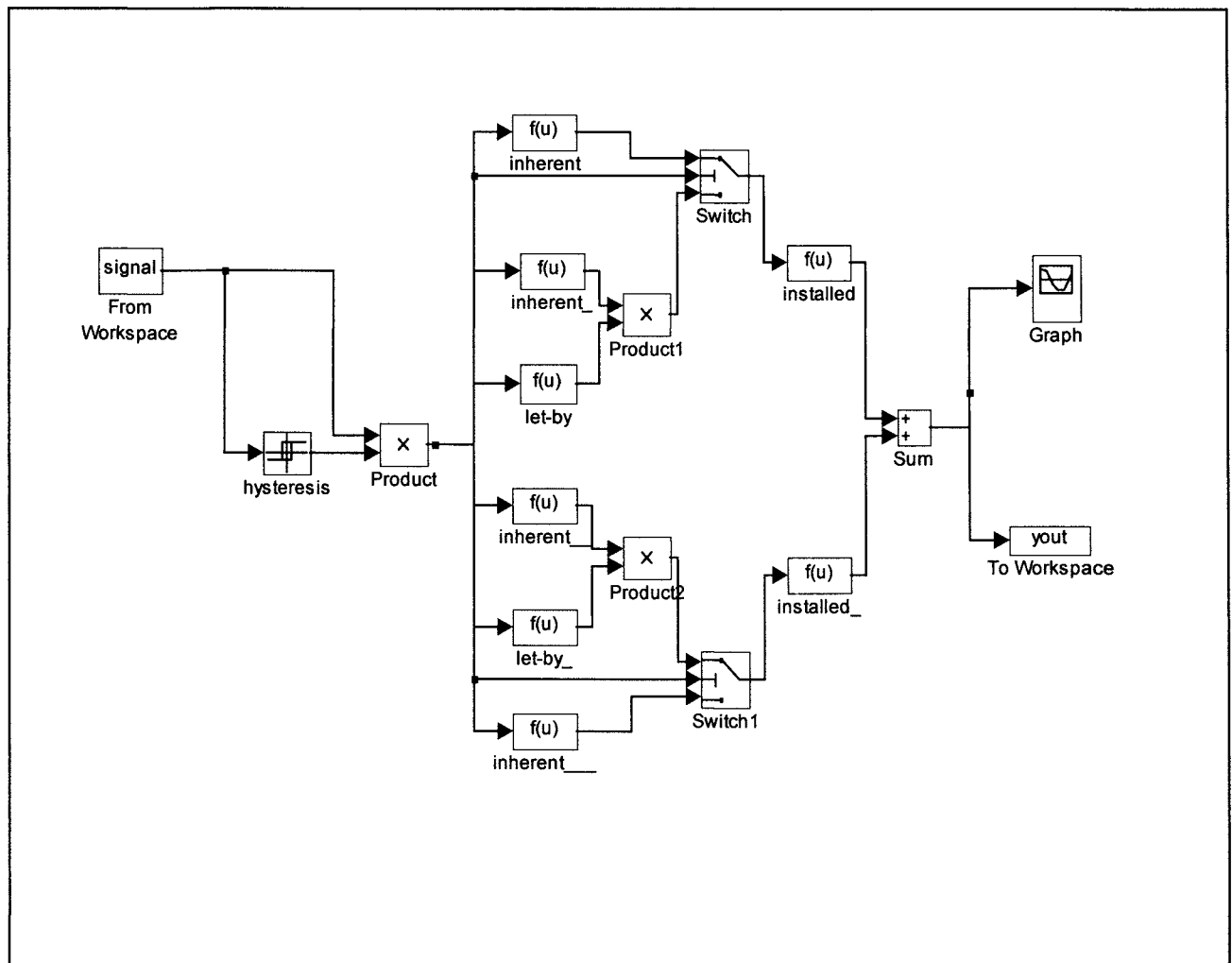
This section investigates the use of a mathematical model of a three port control valve to predict flow/control signal relationships where practical information is not available for a valve. The basic valve model (version 1.0) used in this study is detailed in chapter 4 of this work. A number of modifications and additions are made to this basic valve model and these are detailed in the following sections. A summary of the different versions of the valve model is given in table 4 over the page.

**Table 4: Valve model versions.**

Mathematical Model Version	Description
Version 1.0	Basic valve model
Version 2.0	Basic valve model with let-by region modelled by Hamilton's equation
Version 2.1	As version 2.0 with let-by in bypass port increased from 0.025% to 0.1%
Version 2.2	As version 2.0 with bypass port let-by equation replaced by a linear equation
Version 3.0	Pneumatic line and actuator models added and applied to versions 2.1 and 2.2

Early results from the basic model (version 1.0) suggest a poorer agreement with practical measurements at low control signals (typically  $< 0.4$ ). In an effort to improve this performance the model was changed to incorporate a let-by region previously suggested by Hamilton<sup>91</sup>. The revised model is shown in figure 57, and will be referred to as version 2.0 of the model (see over the page).



**Figure 57: Mathematical Model (Version 2.0)**

This model was run for a varying input control signal for valve authorities of 0.3 and 0.5. The mathematical model predictions were compared to experimental results from the modified validation test rig for the range of test valves. A series of graphs were plotted to show the comparisons.

Referring to figures 58 - 65 it can be seen that for the 40mm valve ( $N = 0.3$ ) a fair agreement is made in the overall shape of the curves though there does seem to be a 'phase shift' of the model results from the practical

measurements. The RMS error is 15.35%, with a maximum under prediction error of -19.9% occurring at zero control signal (i.e. the let-by region), and a maximum over prediction error of +21.8%, both quite high values.

For the 40mm valve ( $N = 0.5$ ) a better performance is evident. The RMS error is 4.82%. The maximum under prediction error is -8.8% and the maximum over prediction error is +7.2%. Again a large error occurs at a control signal of zero.

The 50mm valve ( $N = 0.3$ ) bears a comparable performance to the 40mm valve at the same valve authority. The RMS error for this model run is similar to the 40mm ( $N = 0.3$ ) valve with a value of 15.53%. The maximum under prediction error is -23.4% (at zero control signal) and the maximum over prediction error is +22.3%.

The 50mm valve ( $N = 0.5$ ) has an RMS error of 8.8%, a maximum under prediction error of -11.9% (at zero control signal) and a maximum over prediction error of +12.2%. This, as is the case for the 40mm valve, is better than the lower ( $N = 0.3$ ) authority model performance.

The RMS error for the 65mm valve ( $N = 0.3$ ) is 20.66%, the highest RMS value. The same pattern exists as for the previous valves, caused by this apparent 'phase shift', with a maximum under prediction error of -27.8% (again at zero control signal) and a maximum over prediction error of +27.2%.

The 65mm valve ( $N = 0.5$ ) has an RMS error of 10.37%, a maximum under prediction error of -13.0% (at zero control signal) and a maximum over prediction error of +18.5%.

For the 80mm valve ( $N = 0.3$ ), the RMS error is 14.12%. This valve has a maximum under prediction error of -20.3% (at zero control signal) and a maximum over prediction error of +18.2%.

The same valve (80mm) at a valve authority of  $N = 0.5$  has an RMS error of 12.4%, a maximum under prediction error of -6.5% and a maximum over prediction error of +20.2%.

### **5.6.1 Summary of Results**

The performance of all valve models is better at the higher valve authority ( $N = 0.5$ ). The physical shape of the model curves in most cases looks acceptable, however, all the model results tend to experience a 'phase shift' from the experimental data resulting in quite high over and under prediction errors. The 65mm valve has the highest error values. A major cause of error is at zero control signal in the let-by region of the valve. The use of Hamiltons<sup>91</sup> model for the let-by region of the valve has not improved the models performance at low control signals.

## **5.7 Modification of the Mathematical Model**

In an attempt to improve the performance of the mathematical valve model a number of modifications were investigated. Because of the error at zero control signal the valve let-by was changed. Specifically, the let-by on the inlet port and bypass port on the valve model was decreased from 0.05% to 0.01% to

see the effects. This change had negligible effect on the output results. Hysteresis was also changed from 5% to 10% but this also had negligible effect on the output results. Referring to manufacturers data for the valves the quoted let-by for the valves is 0.05%. No distinction is made as to which port this refers to, i.e. inlet port, bypass port or both ports. Obviously, this let-by value would have to apply to the inlet port as this influences the controlled part of the circuit. The bypass port let-by has less importance in terms of valve control performance so it was thought that manufacturing tolerances might mean that the let-by on this port might be larger. The valve model was therefore changed so that the inlet port let-by remained at 0.05%, but the bypass port let-by was increased to a value of 0.065%, then 0.075% and then 0.1%. This will be referred to as version 2.1 of the model. The results of these changes (as well as those for the model when  $G_o = 0.01\%$  for both ports) is demonstrated in figures 66 - 105. The effect of hysteresis was also investigated with model runs carried out for hysteresis values of 5% and 10%, however these changes produced a negligible effect on the model results, see appendix 8 (figures A17 – A55). It can be seen that there is no effect on predicted flow ratio at a control signal of zero. However, flow rates at control signals between zero and around 0.4 are significantly improved for most of the valves as the bypass port let-by is increased, with the best performance occurring at a bypass port let-by of 0.1%.

Following on from this modification to the by-pass port let-by value, in order to improve the model performance at zero control signal it was decided to change the equation which describes the let-by region for the by-pass port of

the model originally taken from Hamilton<sup>89</sup>, to a linear expression of the form:-

$$f = m.S + k \quad \dots\dots\dots(20)$$

This would allow some control of the predicted combined circuit flow ratio ( $f$ ) at zero signal by careful selection of the constant ( $k$ ). The inlet port let-by would remain unchanged. This will be referred to as version 2.2 of the model. The model was run for values of  $k$  equal to 2.5, 3, 3.5, and 4, with a value of let-by for the inlet port set at 0.05%, and a value for  $m$  chosen as 0.5. The value of  $m$  for the bypass port was then decreased to values of 0.03 and 0.035 for subsequent model runs, to see whether a change in this value would have any effect. Figures 106 - 153 show the results.

It can be seen that, for most valves, as the value of  $k$  increases, the combined circuit flow ratio model predictions at control signals from zero to about 0.4, improve. Changes to the value of  $m$  in the linear let-by equation do have a slight effect on the predicted flow ratios at low signals though this effect is not significant enough for further investigation.

### 5.7.1 Further Model Modifications

The previous modifications, to some extent, improve the model flow ratio predictions at low control signals (i.e. from zero to about 0.4). They do not address the apparent 'phase shift' between the test rig flow ratios and the

model flow ratios, which are causing errors at the higher control signals. The cause of this phase shift appears to be the modifications to the test rig. Early model comparisons with the unmodified rig were encouraging, as detailed in chapter 4, and did not experience this phenomenon.

The main changes to the rig concerned both the control signal and the data monitoring. Initial control signal adjustment was carried out manually by adjusting a regulating valve in the pneumatic line between the air compressor and the actuator of the valve. This was replaced by a signal generator and an electro-magnetic transducer. The data monitoring on the original rig was carried out by simple manual readings off mercury manometers and this was replaced by a pressure transducer and a data logger.

It was thought that the most likely area for the discrepancy in the results could be on the control signal side, perhaps caused by some sort of lag in signal through the pneumatic line and the pneumatic actuator.

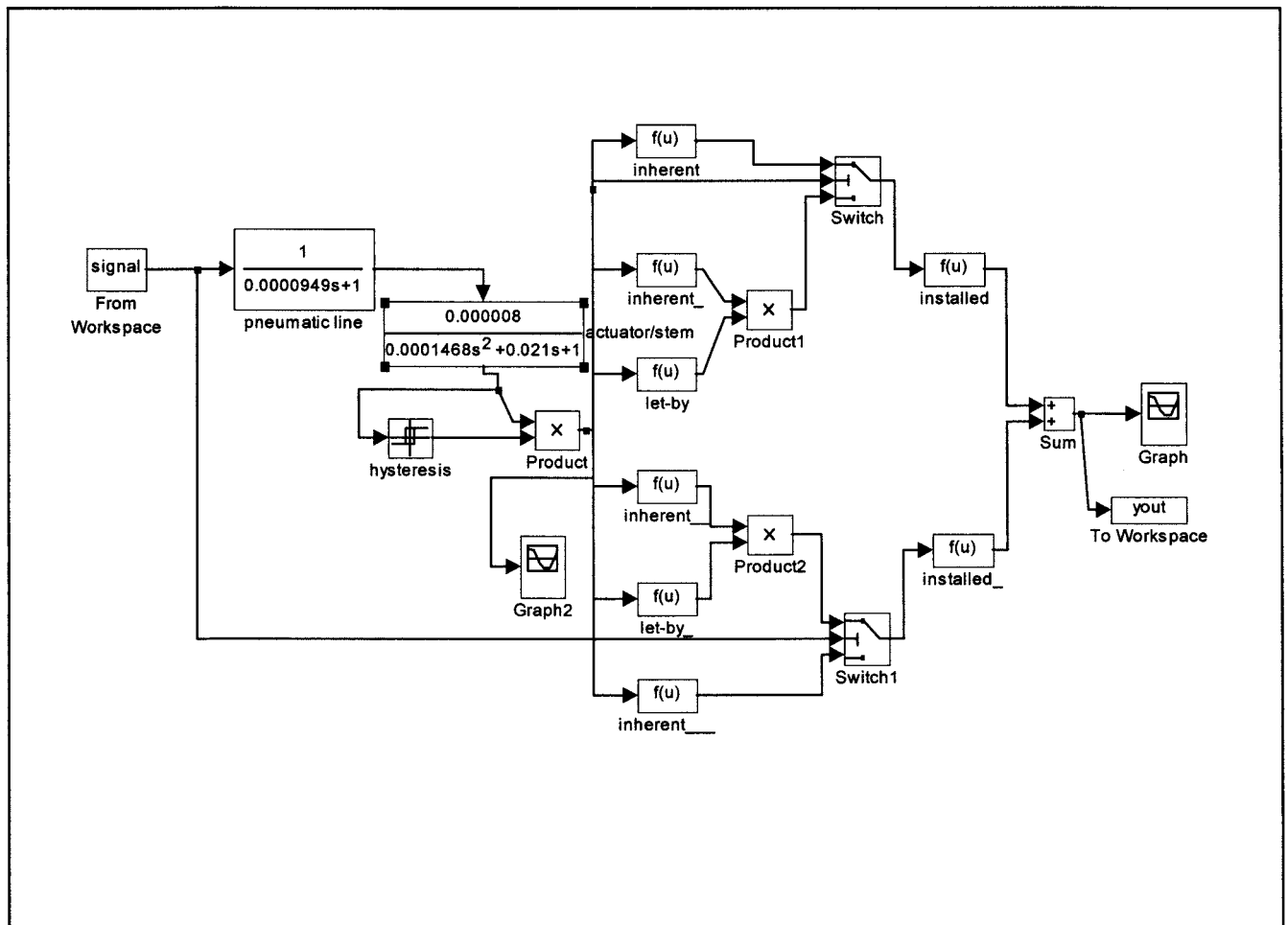
In order to investigate this the valve model was modified to incorporate the pneumatic line and actuator models proposed by Weber<sup>115</sup>.

Again, MATLAB was used to create the overall combined system model for the pneumatic line, pneumatic actuator and valve stem, and three-port mixing control valve.

Referring to figure 154, an input signal from a controller sends a pneumatic signal down a pneumatic line represented by equation ....(9), (found in chapter

4). The pneumatic signal leaves the pneumatic line and enters a pneumatic actuator represented by equation ....(7), (found in chapter 4).

**Figure 154: Mathematical Model (Version 3.0)**



This air pressure within the valve motor exerts a pressure on the diaphragm within the actuator which exerts a force on the valve stem which results in its movement to a new position. This valve stem position is the input to the previously detailed valve model (versions 2.1 and 2.2). This will be referred to as version 3.0 of the model.

Because the largest errors occurred at a valve authority ( $N$ ) of 0.3 the initial comparisons of this modified valve model were only made at this authority. At first, version 2.0 of the valve model was used with both inlet and by-pass port let-by regions modelled by Hamiltons' proposed equation and with let-by values of 0.05%. Then, this was modified by use of a linear equation to model let-by on the bypass port (model version 2.2). The first model run was performed for the 40mm valve ( $N = 0.3$ ). The model was run for values of  $k$  equal to 2.5, 3.5 and 4.5. Figures 155 - 158 show the results.

It can be seen that the results of using the linear let-by on the bypass port improves the models performance at the lower control signals. However, the addition of the pneumatic line and actuator models does not appear to solve the problem of the previously mentioned 'phase shift'. The results from the linear bypass port model show a very small improvement in using increasing values of  $k$  and percentage let-by. Because of this, the other valve sizes (50mm, 65mm and 80mm), were compared with the valve model which used both inlet and by-pass port let-by regions modelled by Hamiltons' proposed equation (as in model version 2.0) and with let-by values of 0.05% for the initial model run. This was modified again (as in version 2.2), by the use of a linear equation to model let-by on the bypass port and run only once for a  $k$  value of 4.5. Figures 159 - 164 show the results. Similar comments as for the 40mm valve can be made.



## 5.8 Summary of Validation of Mathematical Model

The proposed mathematical model results were compared to the measured combined port flow rate ratios from the modified validation test rig in a series of graphs. Various modifications were made to the basic model (version 1.0) in order to improve its performance.

Firstly, because of poor performance at low control signals a let-by term was introduced as proposed by Hamilton<sup>89</sup> (version 2.0). A fair agreement was made in the overall shape of the curves though they did appear to experience a phase shift from the test rig results. The inclusion of Hamilton's model for the let-by region of the valve did not improve the performance of the valve at low control signals. RMS errors were acceptable for this model, though under and over prediction errors at certain values of input control signal were high. The best performance was achieved for this model at the higher valve authority of  $N = 0.5$ . These model runs were carried out using the manufacturers quoted let-by of 0.05% on both ports.

It was then decided to investigate the effects of changing these values of let-by in order to improve the model performance. Firstly, the let-by values were changed to 0.01% for both ports. This had negligible effect on the output results. Then, the value of let-by of the bypass port was questioned. It was thought that perhaps the value could be larger than that quoted by the manufacturer (the manufacturers data only quoted a general let-by value non specific to a particular port on the valve). This value was increased to a value of 0.065%, then 0.075% and then 0.1% (version 2.1). It was found that this

did not improve the model performance at a control signal of zero. However, it did improve the model performance at control signals of between zero and 0.4. The best performance occurring with a bypass port let-by of 0.1%. For all these tests the inlet port let-by was maintained at 0.05%.

Following on from the moderate success of modifying the bypass port, in order to address the problem at zero control signal, it was then decided to change the let-by equation on the by-pass port from the one proposed by Hamilton<sup>89</sup>, to a linear one (equation -----20). The model (version 2.2) was run for values of  $k$  equal to 2.5, 3.0, 3.5 and 4.0. This improved the model performance at low control signals including zero control signal, with the best performance at  $k = 0.4$  for all valves. It did not address the problem of the shift in model predictions from the measured data from the rig.

This was thought to be caused by the modifications to the test rig, specifically on the control signal side. It was therefore decided to try to account for these by introducing the pneumatic line and actuator models proposed by Weber<sup>115</sup>. It was found that this model (version 3.0), combined with the linear let-by of the bypass port further improved model performance at low control signals but did not have any significant effect on improving the shift of model predictions from the test rig results.

## **5.9 Final Test of Valve Model Versions for a Sinusoidal Control Signal**

### **Input over Time.**

In order to compare the versions of the model to each other it was decided to subject the best performing model versions to a sinusoidal control signal input so that a comparison could be made. This would give an indication as to how the model would perform in practice over time if subject to a fully modulating control signal input.

The results were integrated over time to give the corresponding areas under the curves. This was used as a basis of comparison for accuracy of the mathematical model over time.

Figures 165 - 192 show the flow ratio profiles for each of the valves over time. Figures 193 - 200 show the performance of the models for each of the valves in terms of integral of absolute error.

It can be seen that for the 40mm valve ( $N = 0.3$ ), the best performing valve model was version 2.0 (error of +2.33%), and the worst performing was version 2.1 (error of +5.05%). Two other versions of the model also performed well, version 2.2 and version 4.0 of the model.

For the 40mm valve ( $N = 0.5$ ), the best performing valve model was version 2.2 (error of -0.61%), with model version 2.0 performing almost as well as this with an error of -0.97%. The worst performing model was version 2.1 (error of +1.83%).

The best performing model for the 50mm valve ( $N = 0.3$ ) was version 2.0 with an error of +0.41% with version 2.2 of the model performing almost as well with an error of +0.69%. The worst performing model for this valve was, again, version 2.1 (error of +3.2%).

Model version 2.0 was the best performing for the 50mm valve ( $N = 0.5$ ) with an error of +2.06%, however, as with previous valves, model version 2.2 performed close to this with an error of +2.31%. Version 2.1 was the worst performing model again with an error of +5.15%.

For the 65mm valve ( $N = 0.3$ ) the best performing model was version 2.1 with an error of +0.03%. Indeed for this valve all the model versions performed well - version 2.0 (error -2.63%), version 2.2 (error -2.29%), version 3.0 (error -0.38%) and version 2.1 (error -1.22%).

For the 65mm valve ( $N = 0.5$ ) the best performing model was version 2.0 with an error of +2.41%. The performance of model version 2.2 was close to this with an error of +2.72%. Model version 2.1 was the worst performing version with an error of +5.4%.

The 80mm valve ( $N = 0.3$ ) comparisons showed that version 2.0 was the best performing valve model with an error of +3.29%. Model version 2.2 showed a similar performance with an error of +3.55%. As demonstrated by the other results, model version 2.1 was again the worst performing valve model with an error of +6.29%.

For the 80mm valve ( $N = 0.5$ ) the best performing model was version 2.0 with an error of +9.01%. Version 2.2 of the model had a similar performance to this with an error of +9.25%. Worst performing model was, yet again, version 2.1, with an error of +12.4%.

### 5.10 Summary

These comparisons were made for a sinusoidal control signal input to the valve model versions over time. This was meant to simulate full motion of the valve with respect to time as would possibly occur in practice. If this is the case, then good agreement between overall model flow ratio predictions and measured values was achieved for most model versions for all valves at the two specified valve authorities. The best performing valve versions almost across all the comparisons, were versions 2.0 and 2.2, with version 2.0 having slightly lower errors. The errors for both these model versions were very good for all the valves. The worst performing model was version 2.1 in all cases but one. This shows that attempts at improving the original valve model were largely unsuccessful when overall errors are concerned. Some individual model versions did improve flow ratio predictions at low control signals but when looked at over the full range of input control signal, did not improve overall performance. Versions 2.0 and 2.2 of the valve model would be acceptable for predicting flow ratios for a fully modulating control valve in practice where practical information regarding the valve performance is not available. The performance of these valve models is not as good at certain individual control signals though, specifically at zero control signal, and so if the practical valve

performance tends to operate at fixed control signals for long periods of time then much larger errors in predicting flow ratios could occur (depending on which control signal is predominant in the working life of the valve).

## **Chapter 6**

### **6.0 Conclusions, Implementation and Recommendations for Further Work**

#### **6.1 Conclusions**

The importance of monitoring energy use in buildings has been identified.

CIBSE<sup>1</sup> have made a policy statement, the objectives of which are: “to mitigate the demands placed on the world’s reserves of fossil fuels; to reduce pollution of the environment caused by their consumption; to promote the use of renewable and sustainable energy sources.” They state that “whilst actively pursuing this policy it is accepted that any conservation measures must demonstrate that they are cost effective, can maintain set standards and do not give rise to any adverse consequences.” It is therefore essential to be able to gain as much detailed information about energy used by buildings as possible to identify areas of concern and to ensure that measures taken to save energy are successful. A number of methods of monitoring energy use in buildings have been reviewed. By far the most accurate method of monitoring energy use by space heating systems is to monitor system flow rates and flow and return temperatures. This is particularly true for large installations where a central boiler house services a number of buildings. Fuel bills will only give an indication of fuel consumed centrally, it will not give detailed knowledge of fuel consumed by the individual buildings it is servicing. The performance of heat meters and flow meters has been investigated. Evidence suggests that these devices could be inaccurate and unreliable. Surveys suggest that some buildings do not have the facility to monitor system flow rates. Indeed cost

cutting during the design stages of a project often precludes the specification of flow metering equipment. It is sometimes difficult to modify existing systems to include flow metering equipment. For buildings which do not have these devices installed there has been no other method for monitoring system flow rate information. As stated previously, many heating (and cooling) systems include a three port control valve through which all of the system water flows. These are normally controlled by a control signal from a BEMS.

This work has investigated the relationship between the incoming control signal to a valve and its combined port flow ratio. It has shown that, for valves that can be tested, a mathematical equation can be fitted to the flow ratio profile and that this equation can be used in conjunction with control signal values to predict the combined port flow rates in a pipe work system. This test data will possibly be available from manufacturers. Failing this, test results are relatively easy to obtain in laboratory conditions. The control signal data will generally be available in cases where the various control systems are under computer-based control, or a building management system is in use. These predictions can take into account the system resistance by specifying the authority ( $N$ ) of the valve. Validation results demonstrate that the average RMS errors for these curve fit equations range between 2.73% to 6.54%. Therefore, for a fully modulating control valve in practice, prediction of combined port flow ratios by these empirical models is very good compared to some flow meter performances. As noted previously, errors at individual control signals could be higher than this, so that if a control valve is not fully modulating in its operation i.e. it tends to remain in a fixed position for a long period of time,



then this prediction error could be higher (up to approximately -13% depending on the individual control signal value).

For situations where practical flow ratio information is not available for a valve then the use of a theoretical valve model was investigated. A number of versions of the model were tested against the test rig validation results.

Versions 2.0 and 2.2 of the model produced the best overall errors over time.

This work has demonstrated that a theoretical valve model can be used to predict combined port flow ratios over time with integral of absolute errors between -2.63% and +9.25%. Again, system resistances are taken into account by specification of valve authority in the model. These two values represent the two worst case overall error values for the range of valves and authorities.

Typically, the integral of absolute error for these two models was around  $\pm 2.0\%$ . Indeed a mean value of all the integrals of absolute errors for these two models was +2.14%. Therefore, for a fully modulating control valve in practice, prediction of combined port flow ratios by these theoretical models is good compared with some flow meter performances. As for the empirical model though, the theoretical model could experience higher errors at individual control signals, so that if a control valve is not fully modulating in its operation i.e. it tends to remain in a fixed position for a long period of time, then this prediction error could be higher (up to approximately  $\pm 20\%$  depending on the individual control signal value).

In summary, the empirical model performs better than the mathematical model.

It would be no great hardship for manufacturers to test all their valves in a similar manner to the test performed within this work. A simple test rig with

valve authority adjustment is all that is required. A new British Standard could be written for valve testing to set out this form of test so that manufacturers could supply their valves as ‘energy station calibrated’. This would mean that valves could be supplied with flow ratio signatures included in the manufacturers data for the valves, perhaps for a number of common valve authorities. These flow ratio signatures could be used within BEMS to predict combined port flow rates (see the following section 6.2 for implementation in practice). If all manufacturers carried out these simple tests then perhaps there would be no need for the mathematical model.

The dominant parameters relating the signal/flow relationship for a mixing valve of the type commonly used in UK applications (and therefore, its potential for use as a passive flow monitoring device) have been found to be the inherent characteristics of the two inlet ports, together with the valve authority in service. The actuator and stem linkage mechanism for pneumatic valves has been found to have only a minor effect on the relationship between valve control signal and output flow rate and whilst electromechanical linkages may well offer greater hysteresis error, these errors appear in general to have an insignificant bearing on these results.

## **6.2 Implementation in Practice**

It is intended that the empirical or theoretical model be included in an energy use algorithm to be used in a BEMS. Figure 201 shows how it could work. The control signal is fed in to the valve model. Valve authority and system design flow rates are required from the system designer. Valve authority can

be obtained from the three port valve sizing information and system design flow rate can be obtained from the system design calculations. This flow rate can be confirmed in the commissioning process for new systems and from commissioning records for existing systems. CIBSE<sup>123</sup> quote an accepted accuracy for commissioning the heating system water flow rates of +10%. This could have a bearing on the accuracy of the results. However, they also state that “it is up to the designer to specify flow rate tolerances appropriate to the particular design, installation and application.” These values are constants which are used in initially setting up the valve model for the system it is being applied to. Once in operation the control signal sent to position the three port control valve is also used as an input to the valve model. Output from the valve model is initially flow ratio ( $f$ ) but this can then be adjusted to actual volume flow rate ( $\dot{V}$ ) by multiplying the flow ratio by the system design flow rate ( $\dot{V}'$ ). Energy used at any instant in time is a function of system volume flow rate (which needs to be adjusted to mass flow rate by a density correction) and system flow and return temperatures. Density correction and specific heat capacity are temperature dependant and could be adjusted within the algorithm using the system water flow and return temperatures as inputs. The current valve models have been carried out for specific valve authorities (these remaining constant). They can therefore only be applied to systems which have a constant system resistance.

### 6.3 Further work

This work looked at the use of an empirical valve model and theoretical valve model to predict combined port flow ratios in heating systems. The empirical model was limited to the availability of valves that were tested on the rig. These valves had linear/linear inlet port characteristics. More tests should be carried out for linear/equal percentage inlet port characteristics. This would also allow a linear/equal percentage theoretical model to be compared with empirical data.

The valves tested also had pneumatic actuators. The overall effects of hysteresis were found to be small and could be neglected. Valves with an electro-mechanical actuator also need to be tested to see the effects of hysteresis with these actuators.

Further tests of the models should be carried out with data from an existing and appropriate site.

The existing models are restricted to systems where valve authority is constant. If enough information about a combined flow ratio for a valve over a full range of valve authorities was available then ongoing adjustments could be made to allow for changes in valve authority. This could also be appropriate for a mathematical valve model where, if valve authority was monitored on site, this could be used as an input to the valve model so that adjustments could be made to the installed characteristic equations within the model. Installations would have to include pressure tapings across the valve and

system so that valve authority could be monitored constantly so that the valve model could be adjusted as valve authority changed.

## Figures

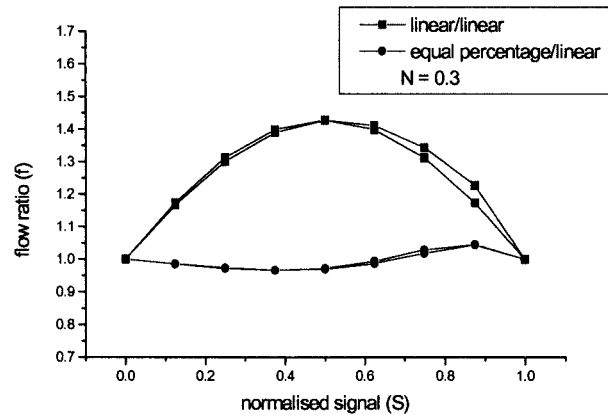


Fig.6: Combined circuit flow ratios for linear/linear and equal percentage/linear valves

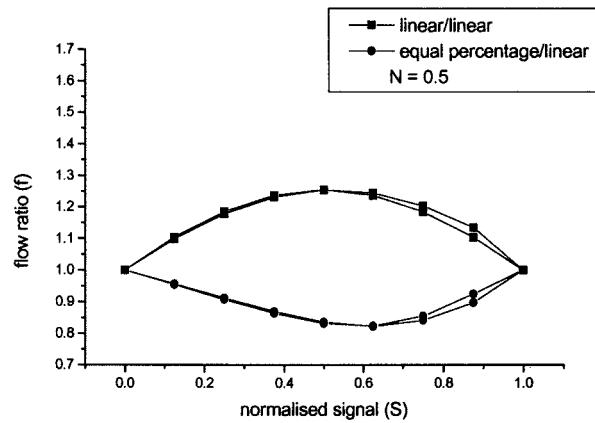


Fig.7: Combined circuit flow ratios for linear/linear and equal percentage/linear valves

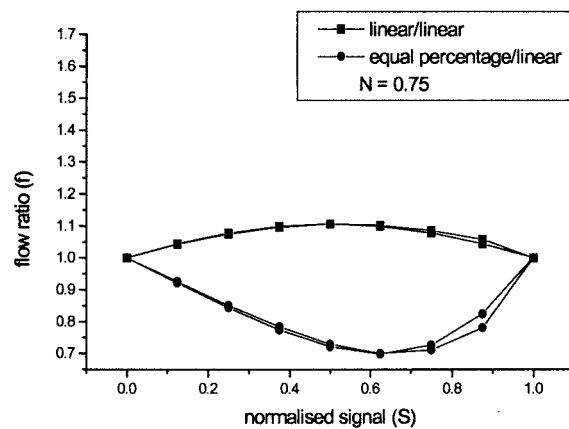


Fig.8: Combined circuit flow ratios for linear/linear and equal percentage/linear valves

**Figures 13 –24. Initial Results From Test Rig.**



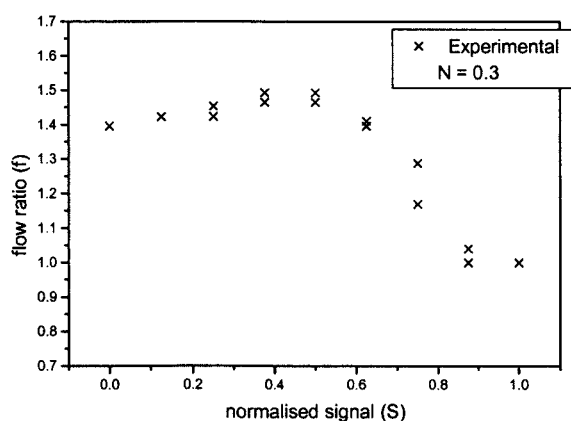


Fig.13: 40mm valve, initial results  
(unmodified test rig)

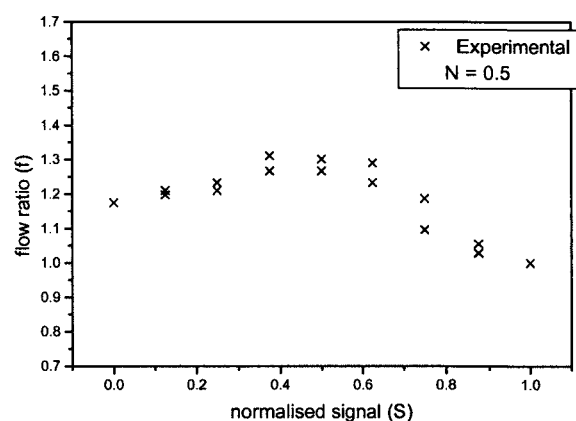


Fig.14: 40mm valve, initial results  
(unmodified test rig)

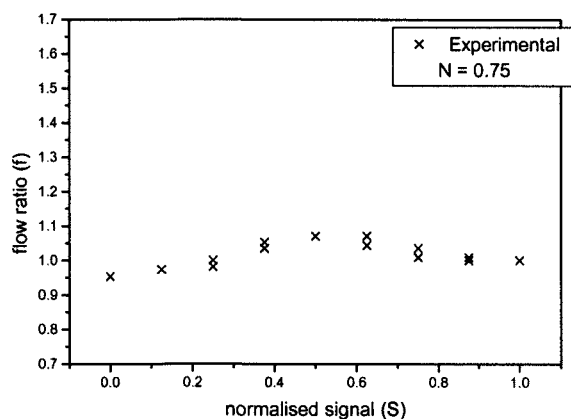


Fig.15: 40mm valve, initial results  
(unmodified test rig)

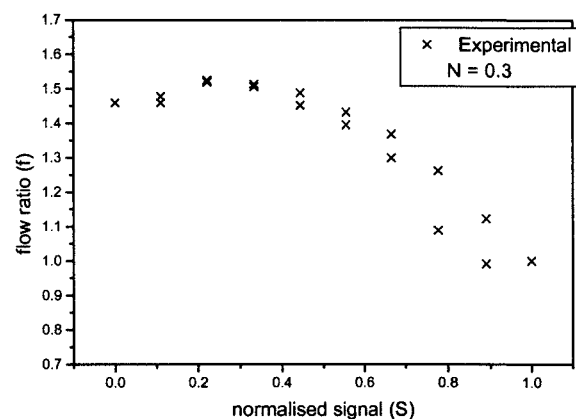


Fig.16: 50mm valve, initial results  
(unmodified test rig)

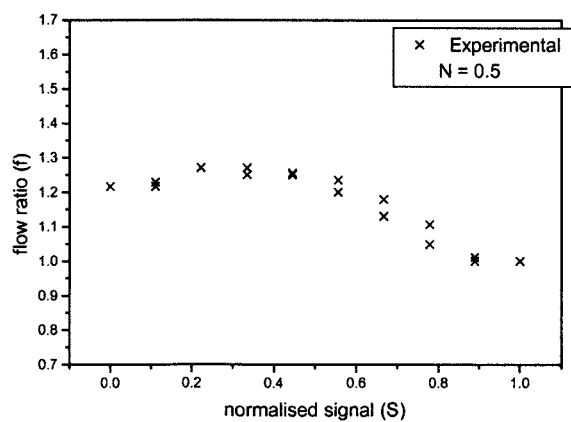


Fig.17: 50mm valve, initial results  
(unmodified test rig)

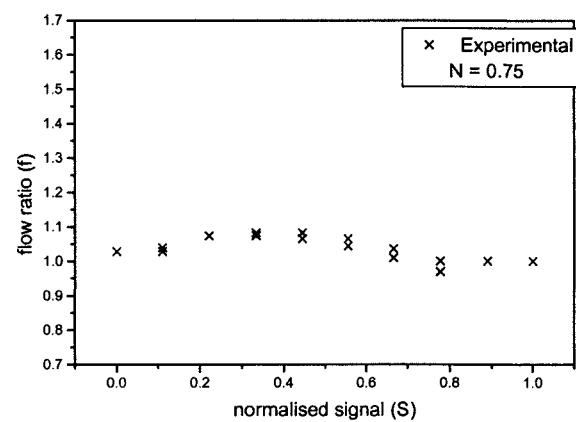


Fig.18: 50mm valve, initial results  
(unmodified test rig)

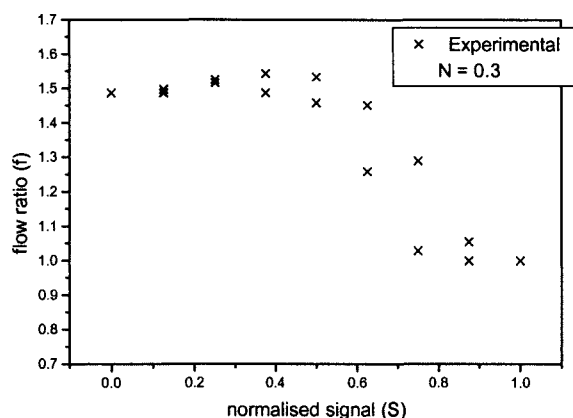


Fig.19: 65mm valve, initial results  
(unmodified test rig)

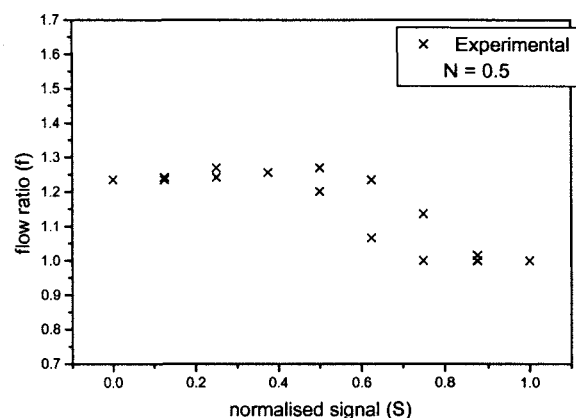


Fig.20: 65mm valve, initial results  
(unmodified test rig)

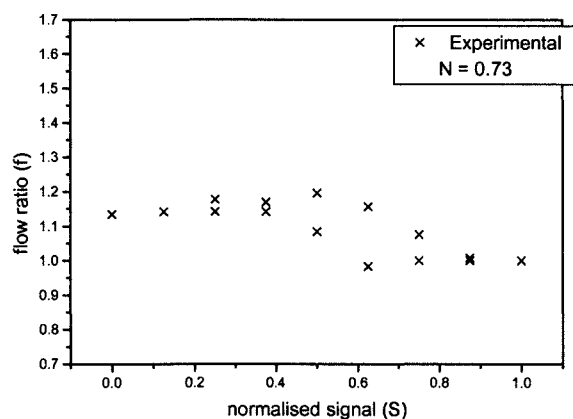


Fig.21: 65mm valve, initial results  
(unmodified test rig)

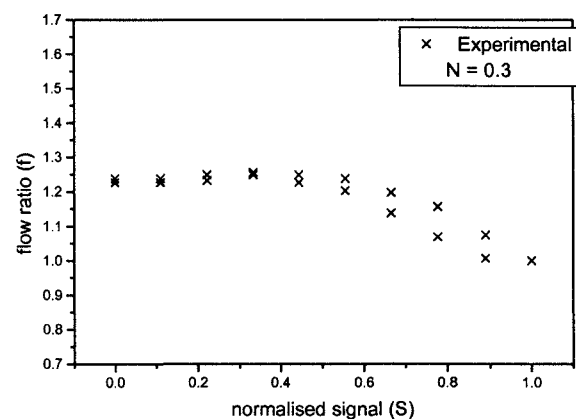


Fig.22: 80mm valve, initial results  
(unmodified test rig)

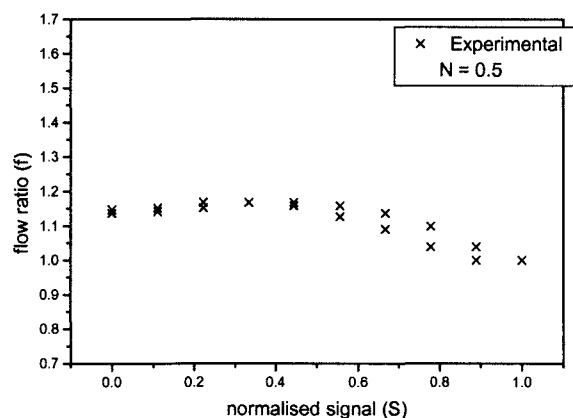


Fig.23: 80mm valve, initial results  
(unmodified test rig)

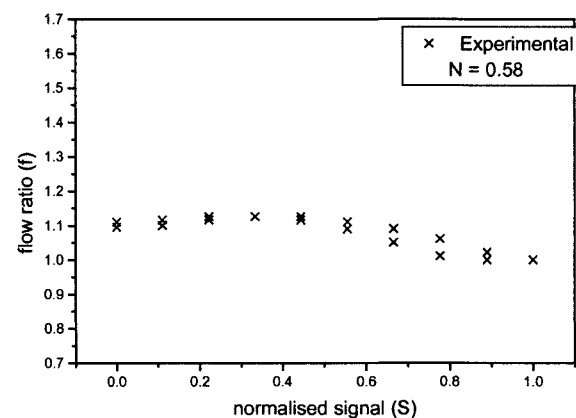
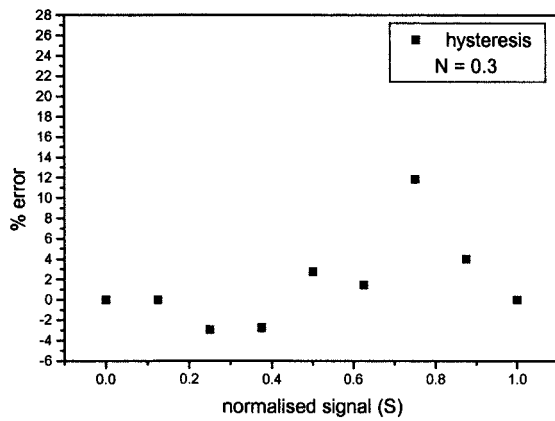
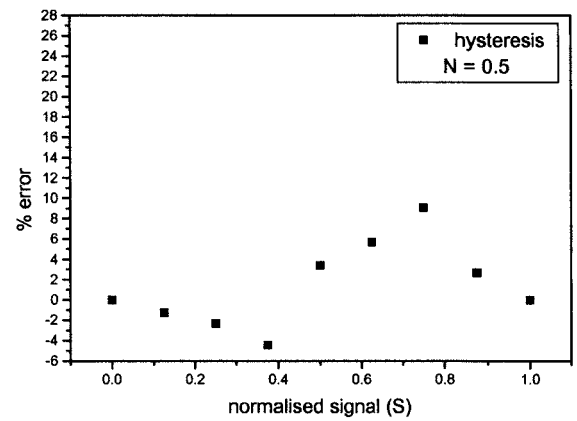
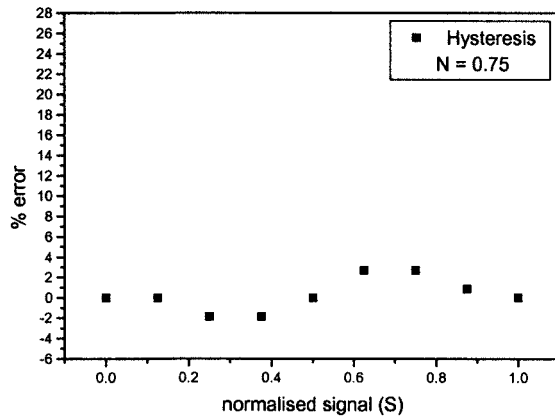
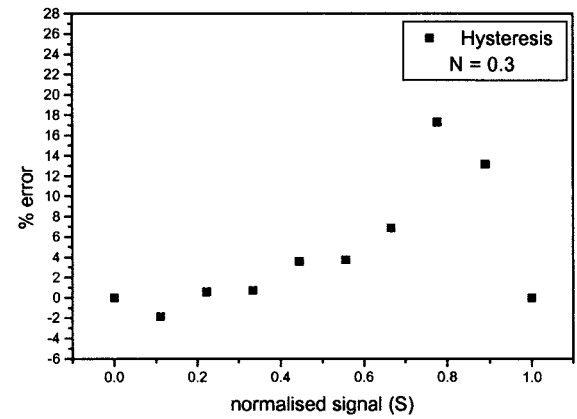
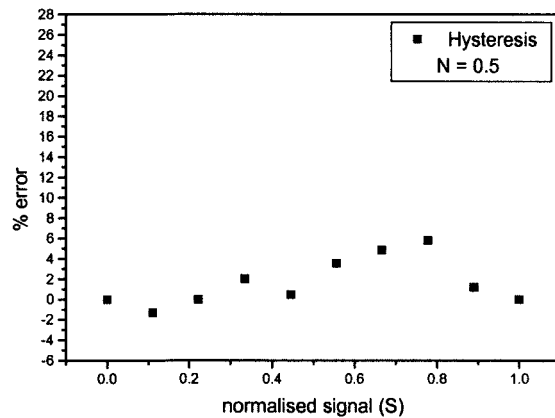
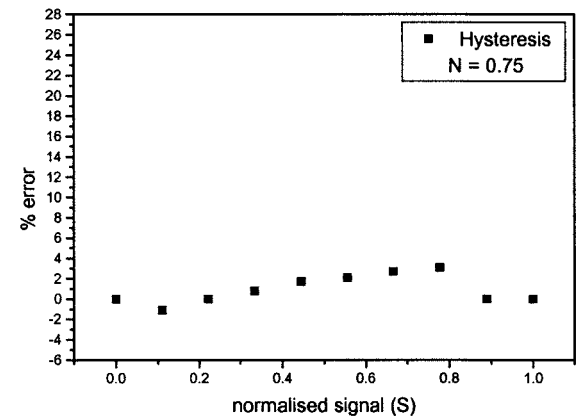
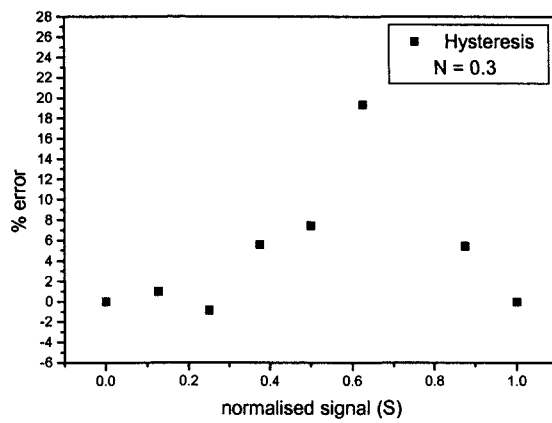
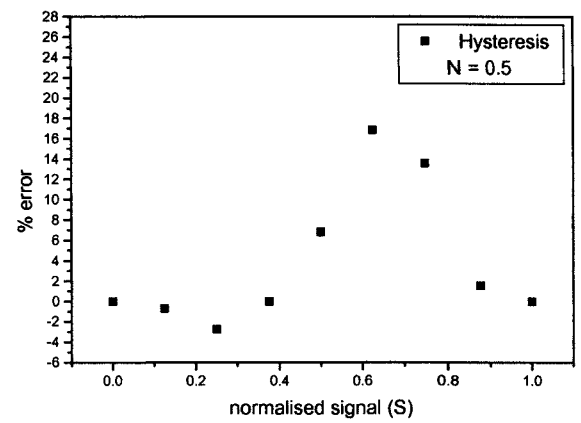
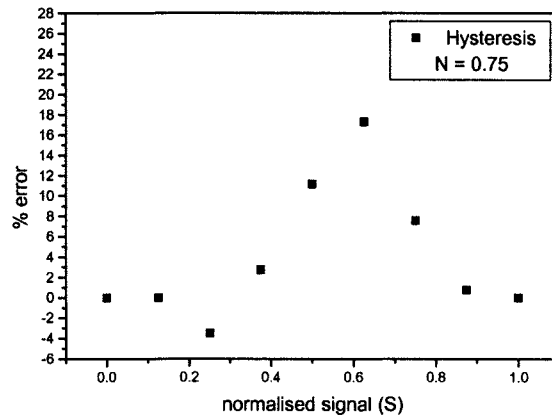
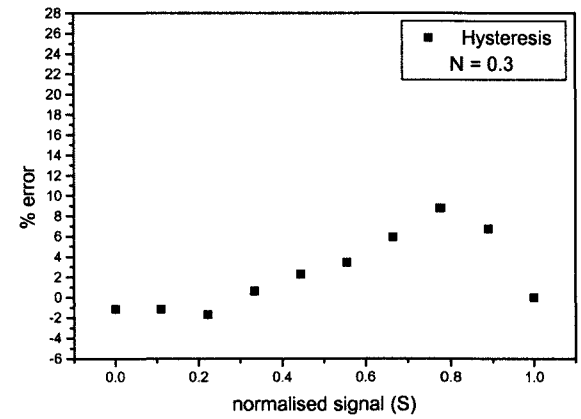
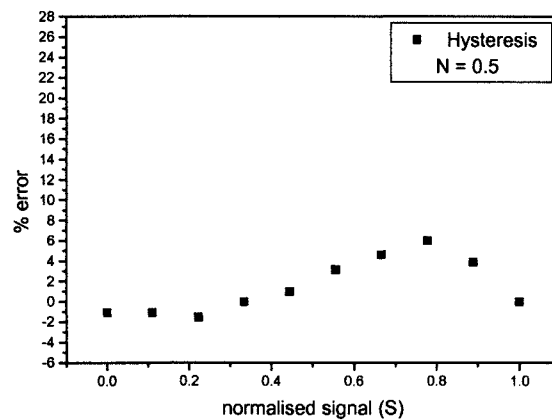
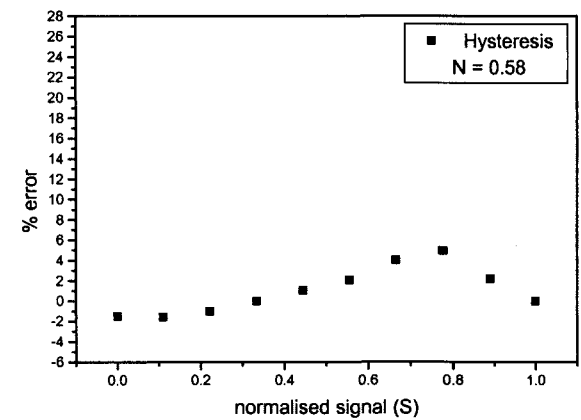


Fig.24: 80mm valve, initial results  
(unmodified test rig)

**Figures 25 - 36. Hysteresis Errors for Initial Results.**

Fig.25: 40mm valve, hysteresis error ( $H_{ys}$ )Fig.26: 40mm valve, hysteresis error ( $H_{ys}$ )Fig.27: 40mm valve, hysteresis error ( $H_{ys}$ )Fig.28: 50mm valve, hysteresis error ( $H_{ys}$ )Fig.29: 50mm valve, hysteresis error ( $H_{ys}$ )Fig.30: 50mm valve, hysteresis error ( $H_{ys}$ )

Fig.31: 65mm valve, hysteresis error ( $Hys$ )Fig.32: 65mm valve, hysteresis error ( $Hys$ )Fig.33: 65mm valve, hysteresis error ( $Hys$ )Fig.34: 80mm valve, hysteresis error ( $Hys$ )Fig.35: 80mm valve, hysteresis error ( $Hys$ )Fig.36: 80mm valve, hysteresis error ( $Hys$ )

**Figures 37 – 48. Comparison of Test Rig Results with Mathematical Model (Version 1.0) Predictions**

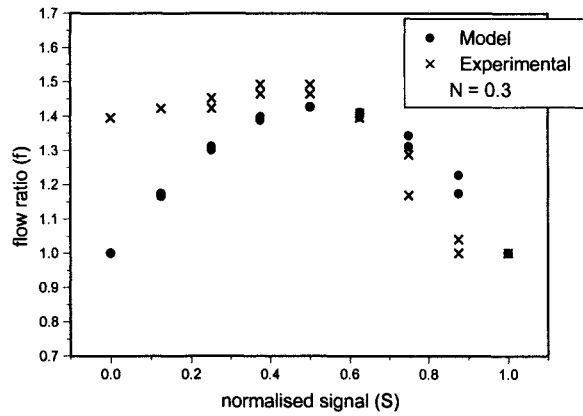


Fig.37: Combined circuit flow ratios for the 40mm test valve

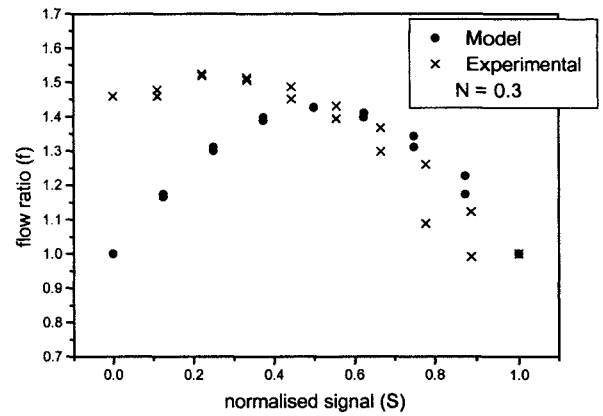


Fig.38: Combined circuit flow ratios for the 50mm test valve

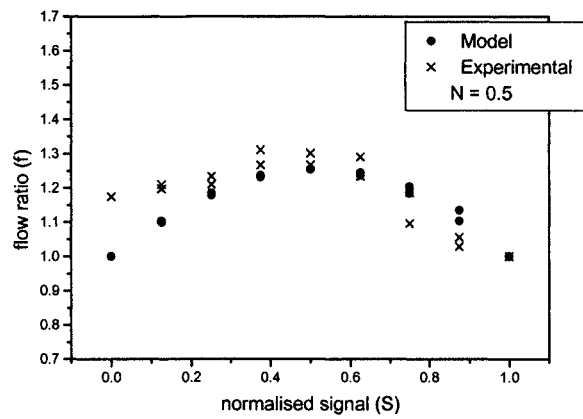


Fig.39: Combined circuit flow ratios for the 40mm test valve

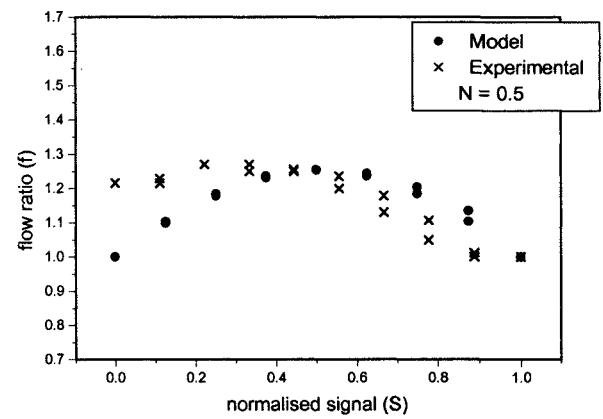


Fig.40: Combined circuit flow ratios for the 50mm test valve

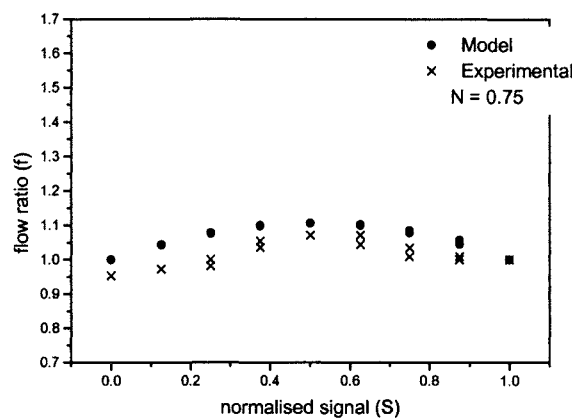


Fig.41: Combined circuit flow ratios for the 40mm test valve

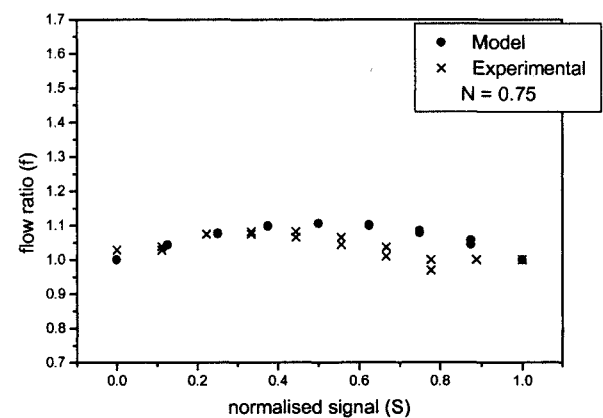


Fig.42: Combined circuit flow ratios for the 50mm test valve

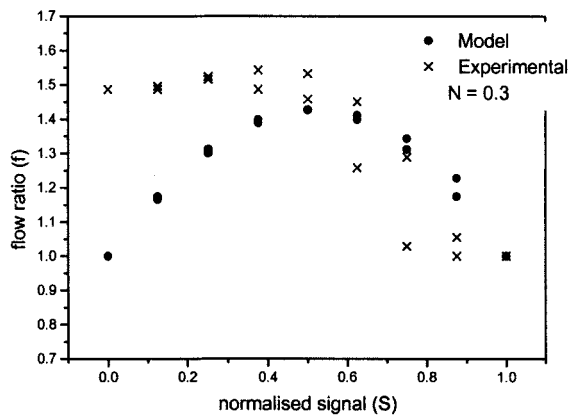


Fig.43: Combined circuit flow ratios for the 65mm test valve

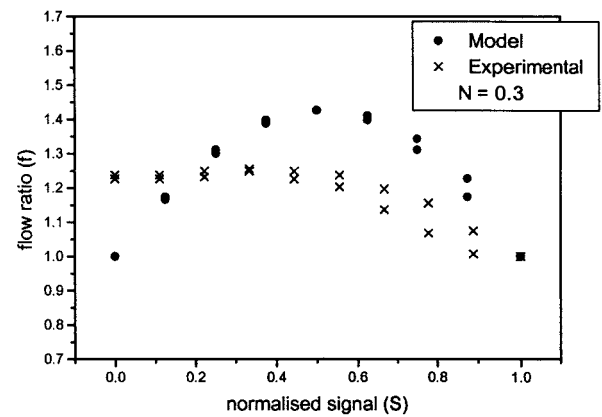


Fig.44: Combined circuit flow ratios for the 80mm test valve

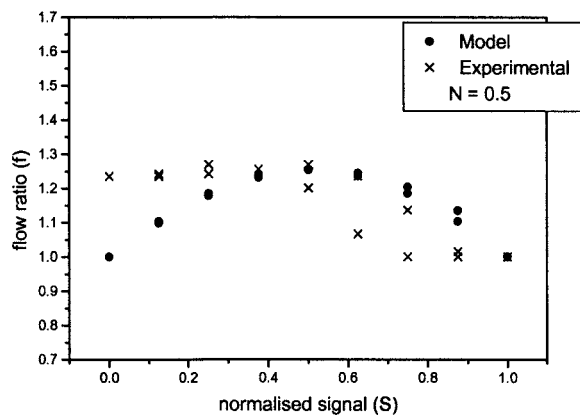


Fig.45: Combined circuit flow ratios for the 65mm test valve

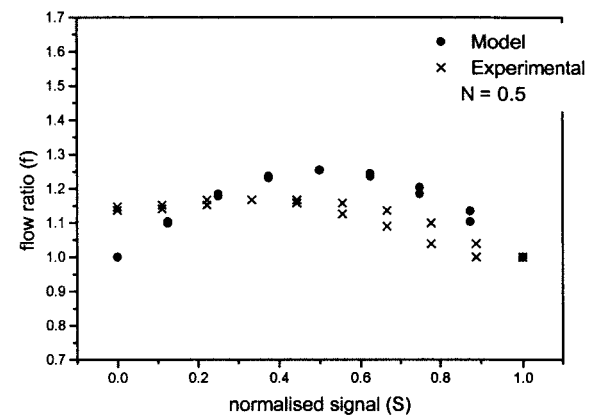


Fig.46: Combined circuit flow ratios for the 80mm test valve

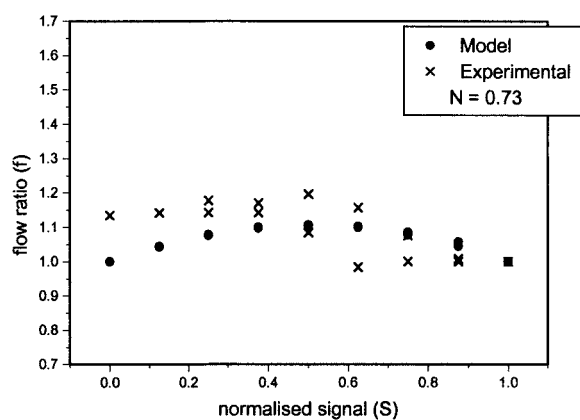


Fig.47: Combined circuit flow ratios for the 65mm test valve

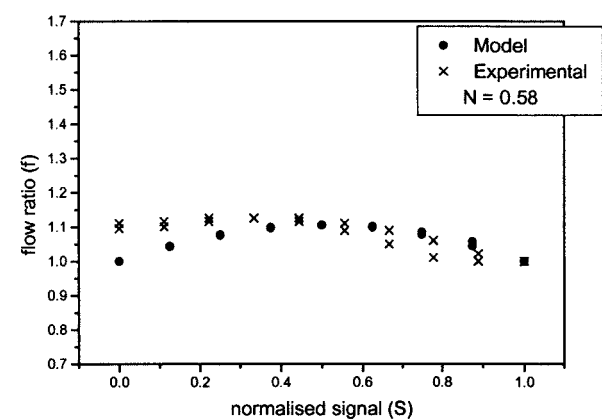


Fig.48: Combined circuit flow ratios for the 80mm test valve



**Figures 49 – 56. Graphs Comparing Test Rig Results to Polynomial Regression Predictions**

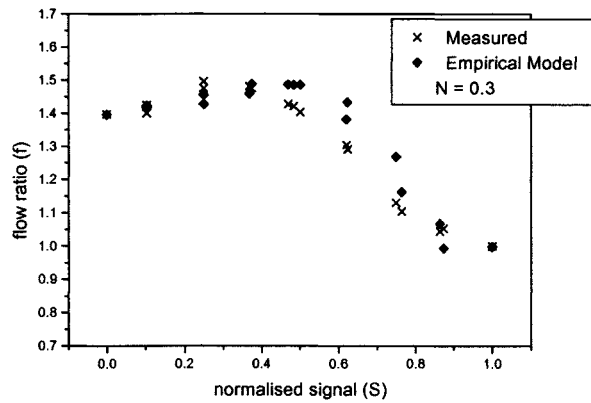


Fig.49: 40mm valve, comparison between measured flow ratios and predicted flow ratios from empirical model.

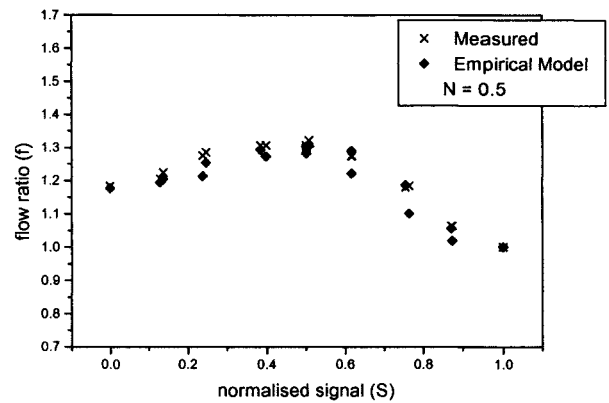


Fig.50: 40mm valve, comparison between measured flow ratios and predicted flow ratios from empirical model.

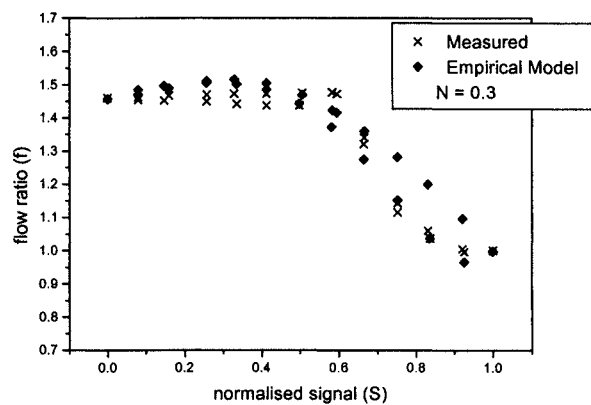


Fig.51: 50mm valve, comparison between measured flow ratios and predicted flow ratios from empirical model.

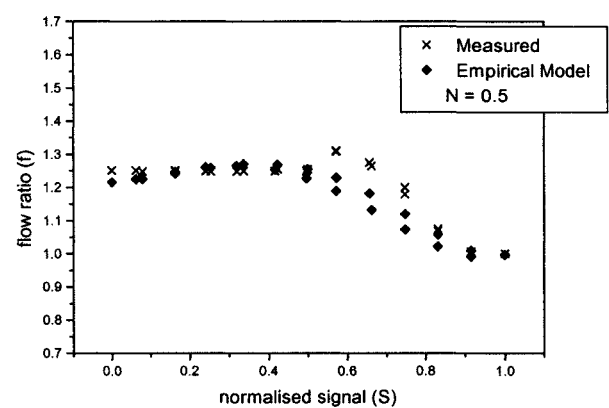


Fig.52: 50mm valve, comparison between measured flow ratios and predicted flow ratios from empirical model.

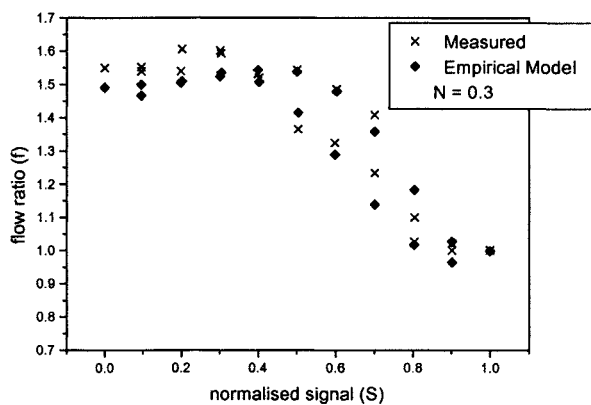


Fig.53: 65mm valve, comparison between measured flow ratios and predicted flow ratios from empirical model.

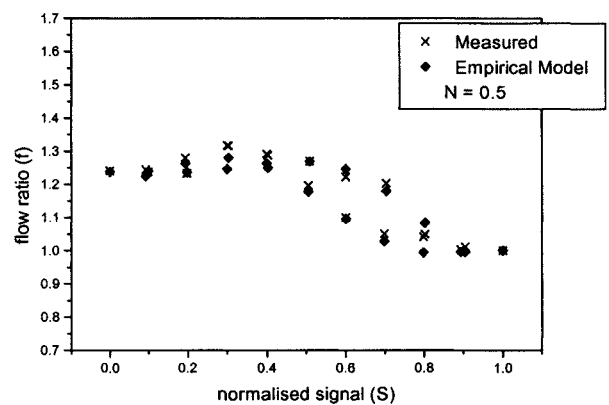


Fig.54: 65mm valve, comparison between measured flow ratios and predicted flow ratios from empirical model.

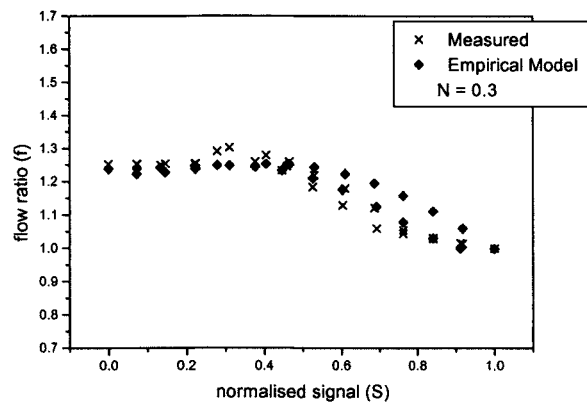


Fig.55: 80mm valve, comparison between measured flow ratios and predicted flow ratios from empirical model.

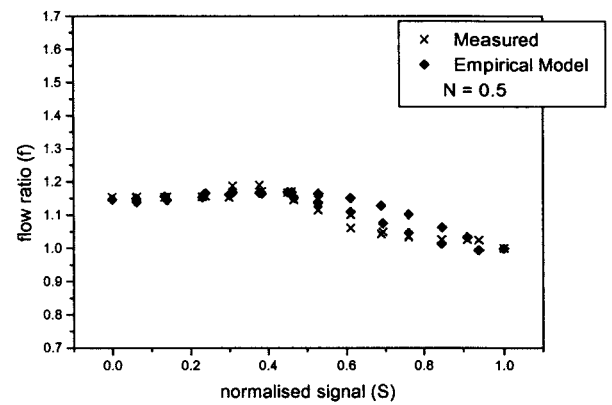


Fig.56: 80mm valve, comparison between measured flow ratios and predicted flow ratios from empirical model.

**Figures 58 - 65. Graphs Comparing Test Rig Results with Mathematical Model (Version 2.0) Predictions**

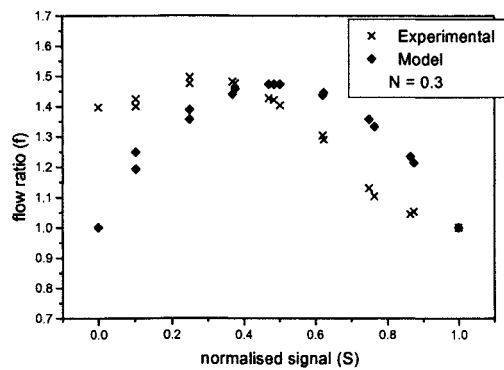


Fig.58: 40mm valve,  $hys = 5\%$ ,  
 $G_0 = 0.05\%$  inlet and bypass ports

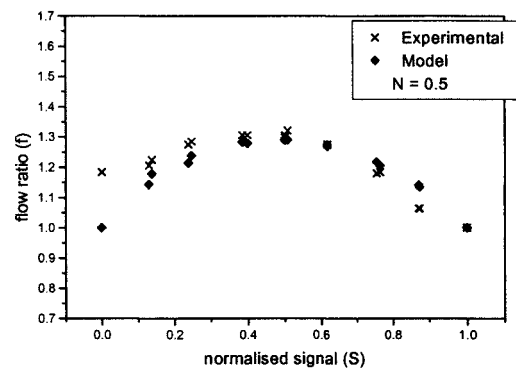


Fig.59: 40mm valve,  $hys = 5\%$ ,  
 $G_0 = 0.05\%$  inlet and bypass ports

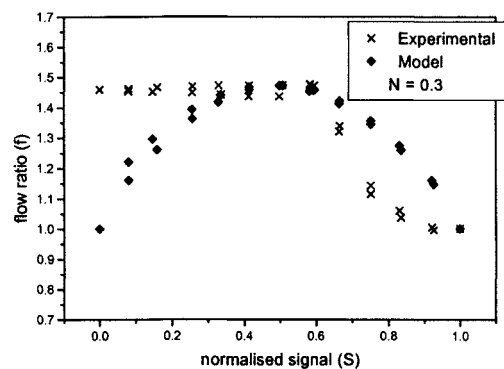


Fig.60: 80mm valve,  $hys = 5\%$ ,  
 $G_0 = 0.05\%$  inlet and bypass ports

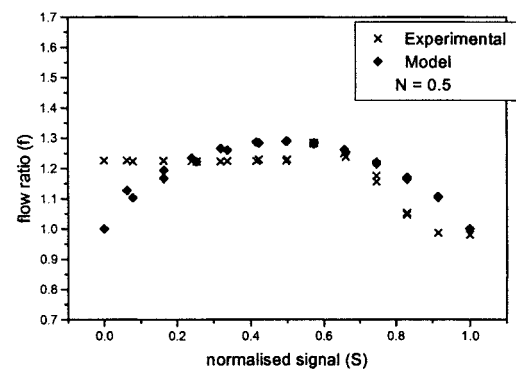


Fig.61: 80mm valve,  $hys = 5\%$ ,  
 $G_0 = 0.05\%$  inlet and bypass ports

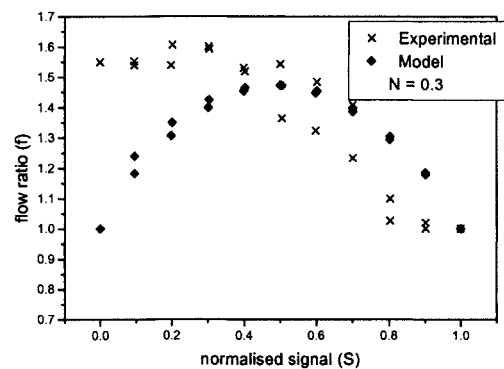


Fig.62: 80mm valve,  $hys = 5\%$ ,  
 $G_0 = 0.05\%$  inlet and bypass ports

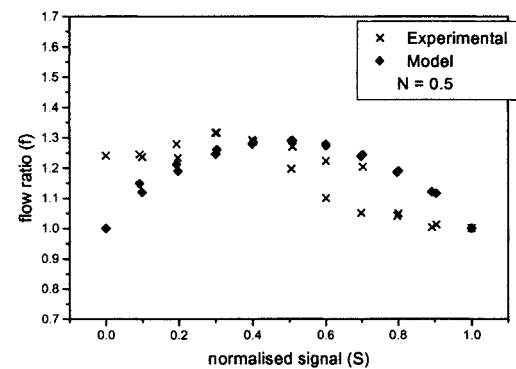


Fig.63: 80mm valve,  $hys = 5\%$ ,  
 $G_0 = 0.05\%$  inlet and bypass ports

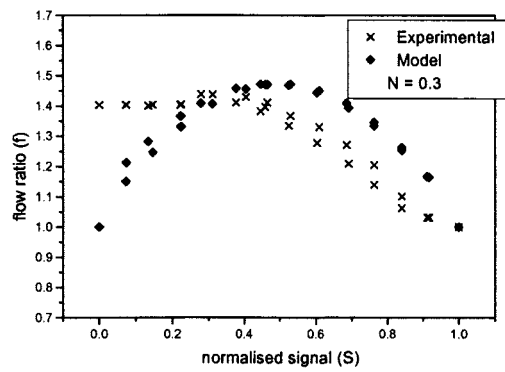


Fig.64: 80mm valve,  $hys = 5\%$ ,  
 $G_o = 0.05\%$  inlet and bypass ports

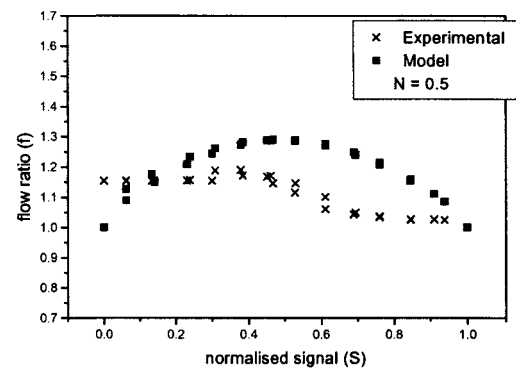


Fig.65: 80mm valve,  $hys = 5\%$ ,  
 $G_o = 0.05\%$  inlet and bypass ports

**Figures 66 - 105. Graphs Comparing Test Rig Results with Mathematical Model (Version 2.1) Predictions**

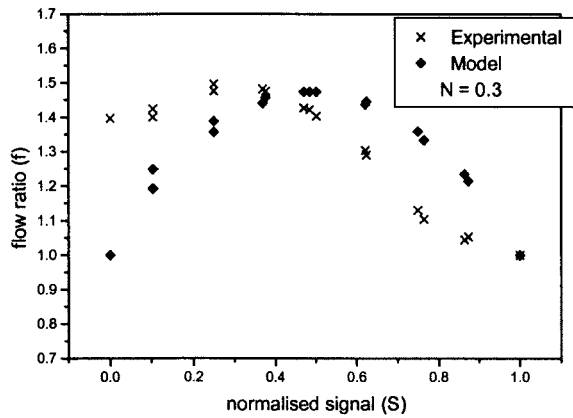


Fig.66: 40mm valve,  $hys = 5\%$ ,  
 $G_0 = 0.05\%$  inlet and bypass ports

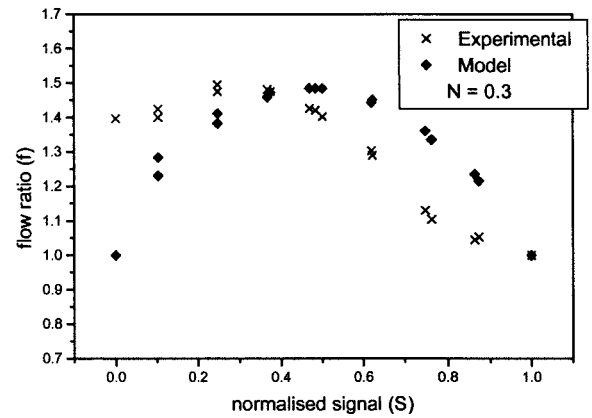


Fig.67: 40mm valve,  $hys = 5\%$ ,  
 $G_0 = 0.05\%$  inlet port and 0.065% bypass port

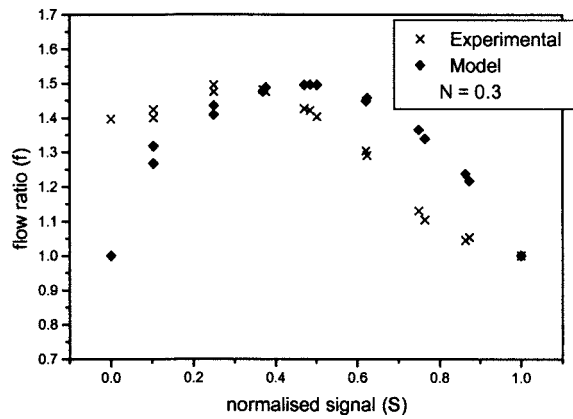


Fig.68: 40mm valve,  $hys = 5\%$ ,  
 $G_0 = 0.05\%$  inlet port and 0.075% bypass port

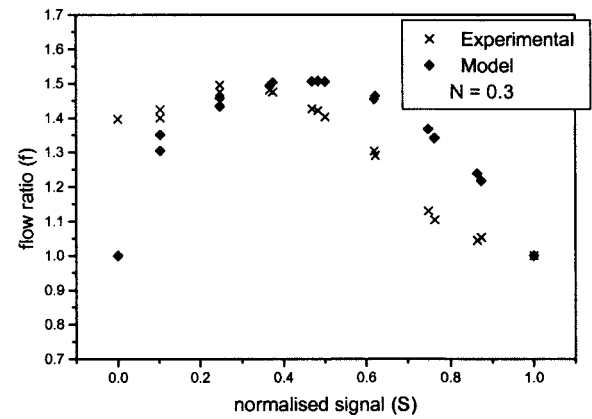


Fig.69 40mm valve,  $hys = 5\%$ ,  
 $G_0 = 0.05\%$  inlet port and 0.1% bypass port

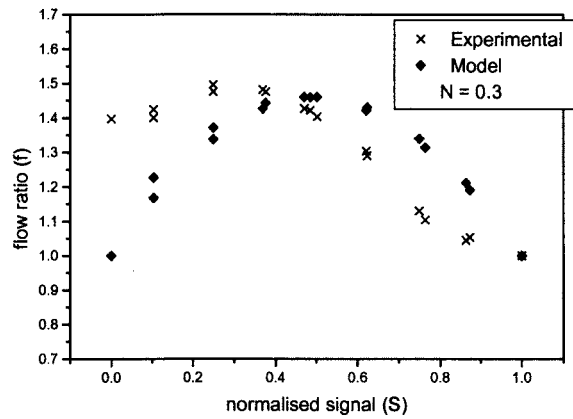


Fig.70: 40mm valve,  $hys = 5\%$ ,  
 $G_0 = 0.01\%$  inlet and bypass ports



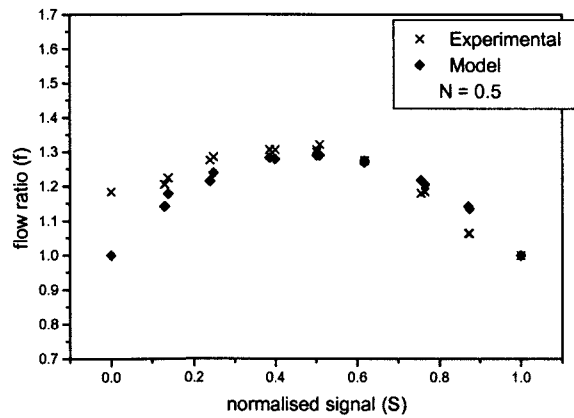


Fig.71: 40mm valve,  $hys = 5\%$ ,  
 $G_0 = 0.05\%$  inlet and bypass ports

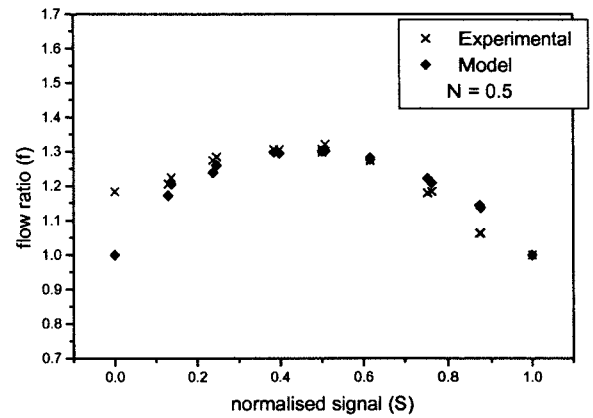


Fig.72: 40mm valve,  $hys = 5\%$ ,  
 $G_0 = 0.05\%$  inlet port and 0.065% bypass port

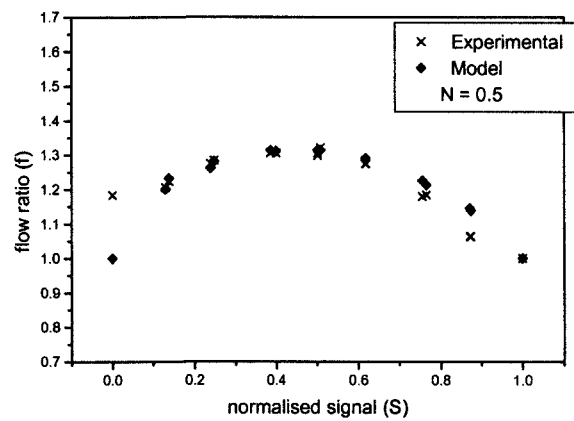


Fig.73: 40mm valve,  $hys = 5\%$ ,  
 $G_0 = 0.05\%$  inlet port and 0.075% bypass port

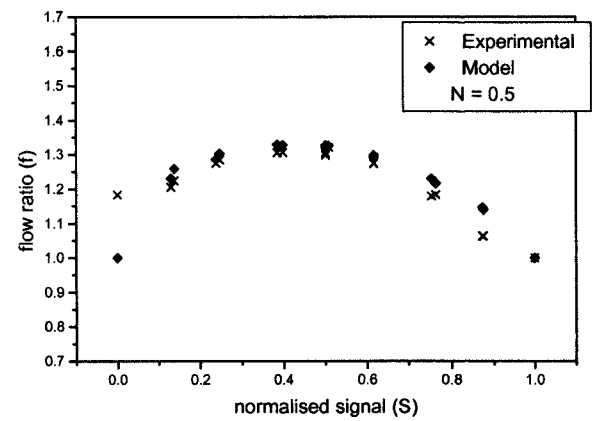


Fig.74: 40mm valve,  $hys = 5\%$ ,  
 $G_0 = 0.05\%$  inlet port and 0.1% bypass port

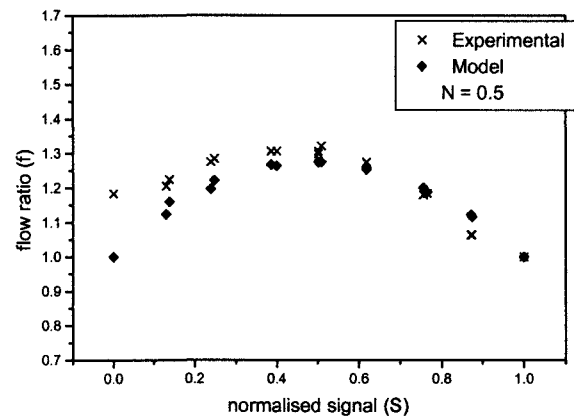


Fig.75: 40mm valve,  $hys = 5\%$ ,  
 $G_0 = 0.01\%$  inlet and bypass ports

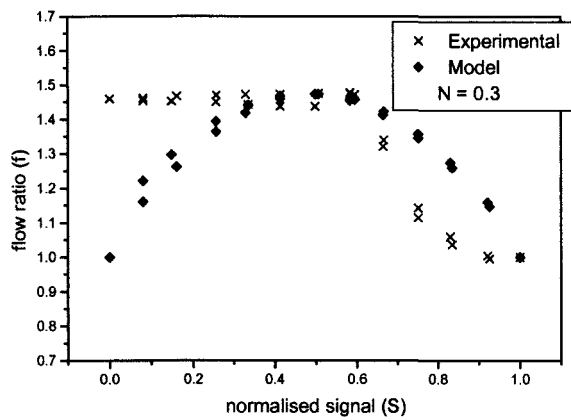


Fig.76: 50mm valve,  $hys = 5\%$ ,  
 $G_0 = 0.05\%$  inlet and bypass ports

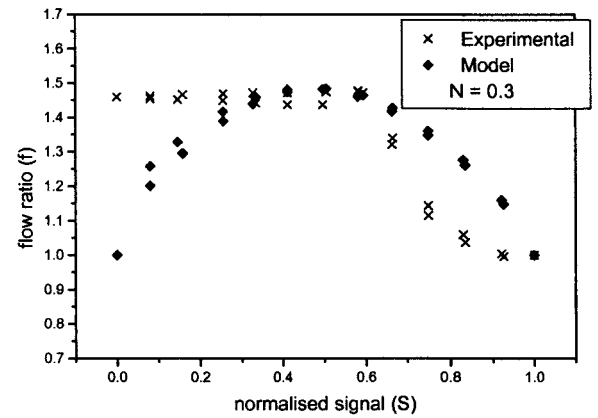


Fig.77: 50mm valve,  $hys = 5\%$ ,  
 $G_0 = 0.05\%$  inlet port and 0.065% bypass port

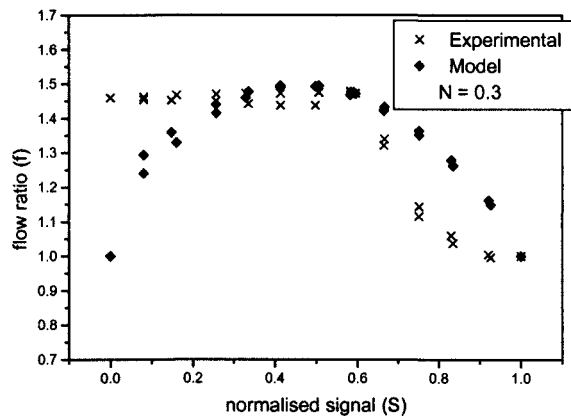


Fig.78: 50mm valve,  $hys = 5\%$ ,  
 $G_0 = 0.05\%$  inlet port and 0.075% bypass port

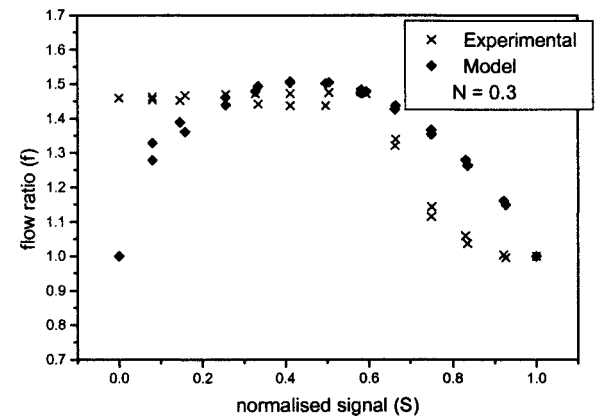


Fig.79: 50mm valve,  $hys = 5\%$ ,  
 $G_0 = 0.05\%$  inlet port and 0.1% bypass port

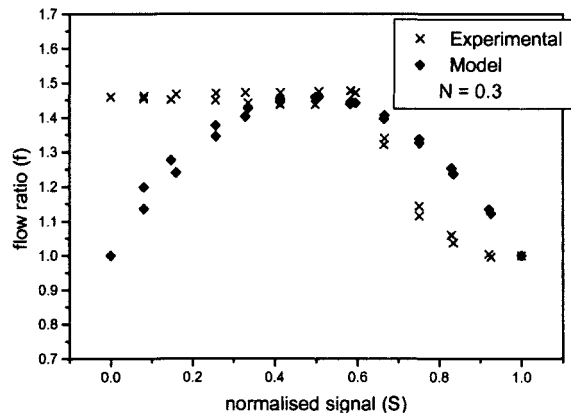


Fig.80: 50mm valve,  $hys = 5\%$   
 $G_0 = 0.01\%$  inlet and bypass ports

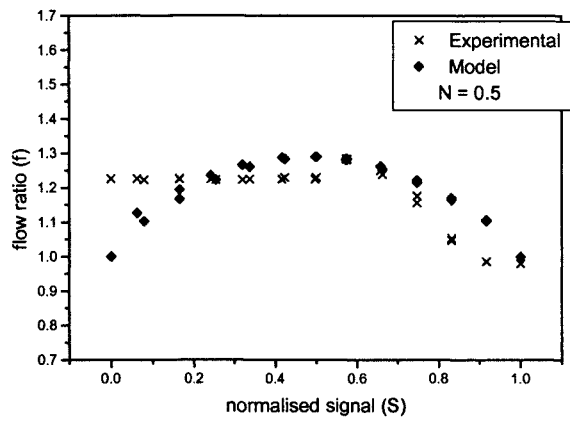


Fig.81: 50mm valve,  $hys = 5\%$ ,  
 $G_0 = 0.05\%$  inlet and bypass ports

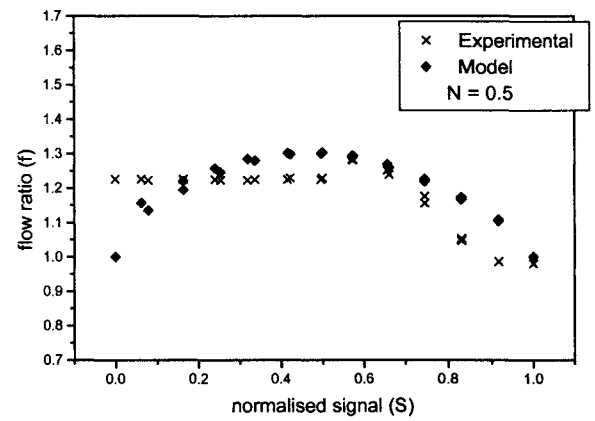


Fig.82: 50mm valve,  $hys = 5\%$ ,  
 $G_0 = 0.05\%$  inlet port and  $0.065\%$  bypass port

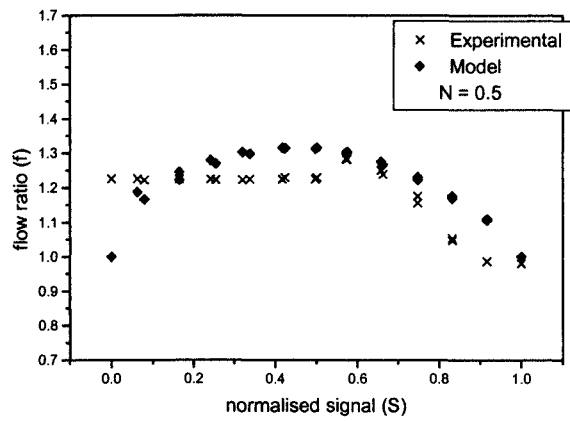


Fig.83: 50mm valve,  $hys = 5\%$ ,  
 $G_0 = 0.05\%$  inlet port and  $0.075\%$  bypass port

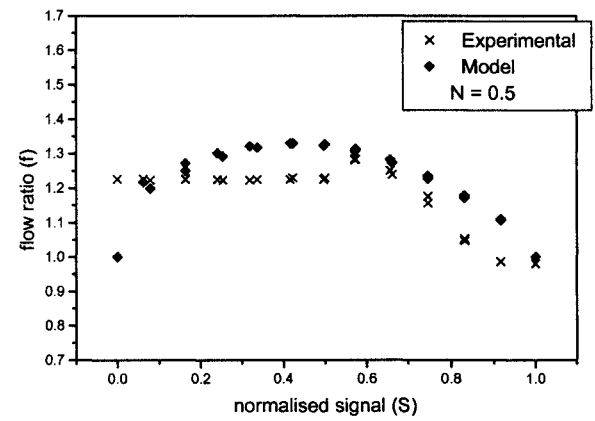


Fig.84: 50mm valve,  $hys = 5\%$ ,  
 $G_0 = 0.05\%$  inlet port and  $0.1\%$  bypass port

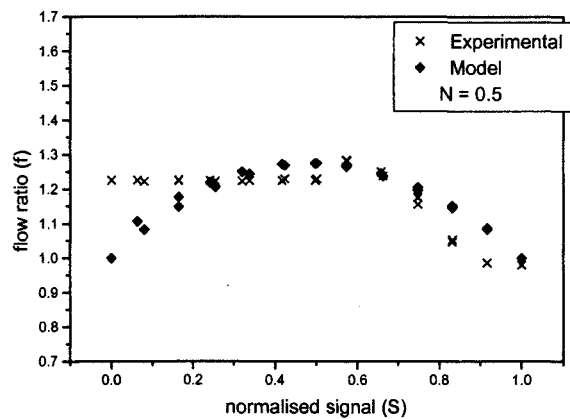


Fig.85: 50mm valve,  $hys = 5\%$ ,  
 $G_0 = 0.01\%$  inlet and bypass ports

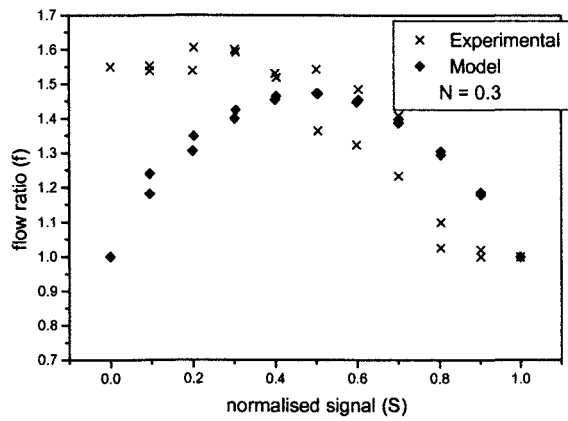


Fig.86: 65mm valve,  $hys = 5\%$ ,  
 $G_0 = 0.05\%$  inlet and bypass ports

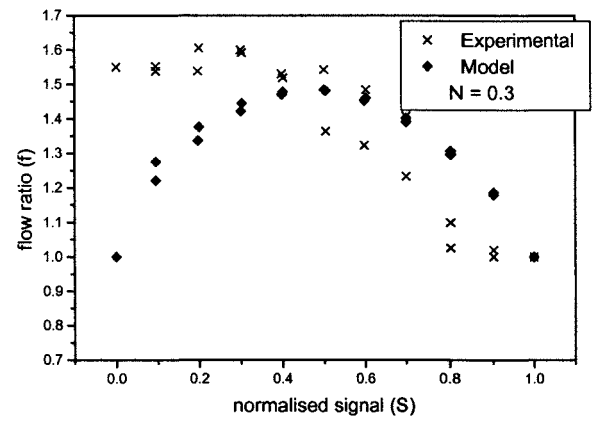


Fig.87: 65mm valve,  $hys = 5\%$ ,  
 $G_0 = 0.05\%$  inlet port and 0.065% bypass port

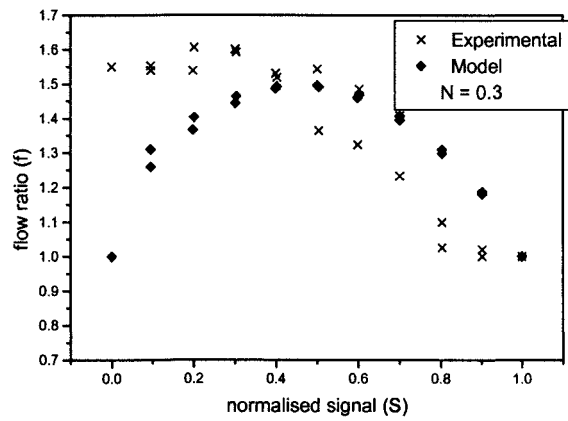


Fig.88: 65mm valve,  $hys = 5\%$ ,  
 $G_0 = 0.05\%$  inlet port and 0.075% bypass port

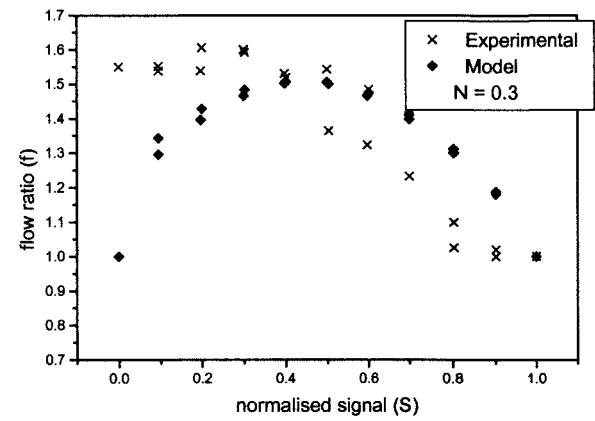


Fig.89: 65mm valve,  $hys = 5\%$ ,  
 $G_0 = 0.05\%$  inlet port and 0.1% bypass port

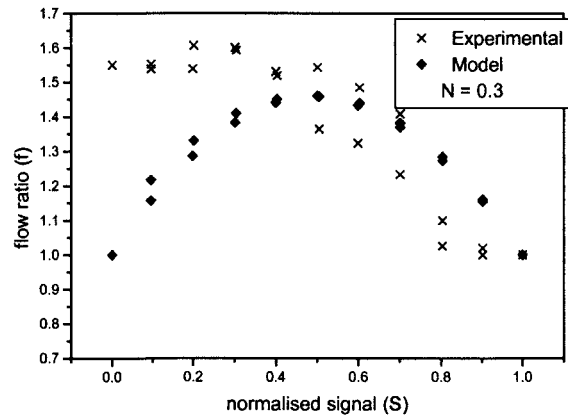


Fig.90: 65mm valve,  $hys = 5\%$ ,  
 $G_0 = 0.01\%$  inlet and bypass ports

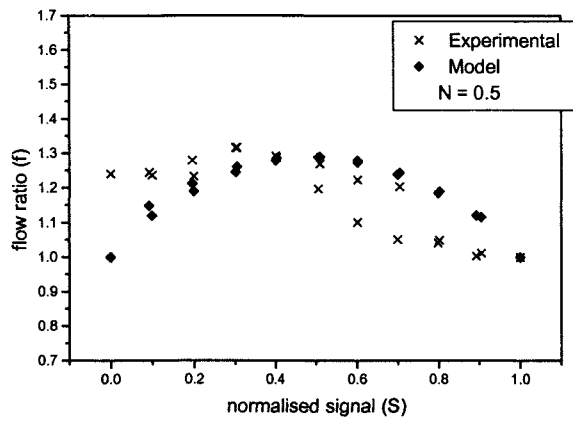


Fig.91: 65mm valve,  $hys = 5\%$ ,  
 $G_0 = 0.05\%$  inlet and bypass ports

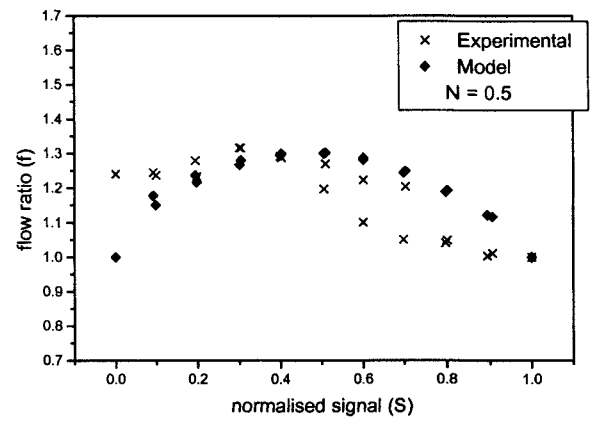


Fig.92: 65mm valve,  $hys = 5\%$ ,  
 $G_0 = 0.05\%$  inlet port and 0.065% bypass port

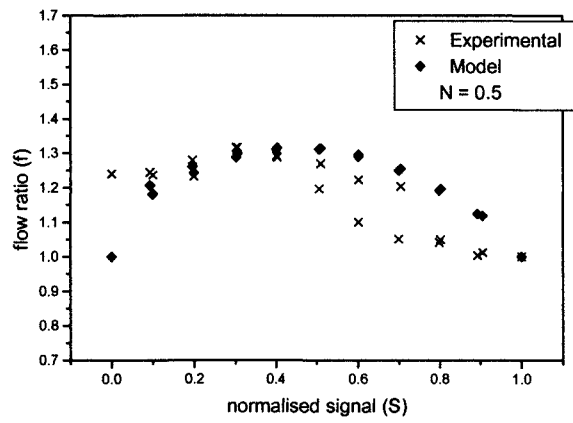


Fig.93: 65mm valve,  $hys = 5\%$ ,  
 $G_0 = 0.05\%$  inlet port and 0.075% bypass port

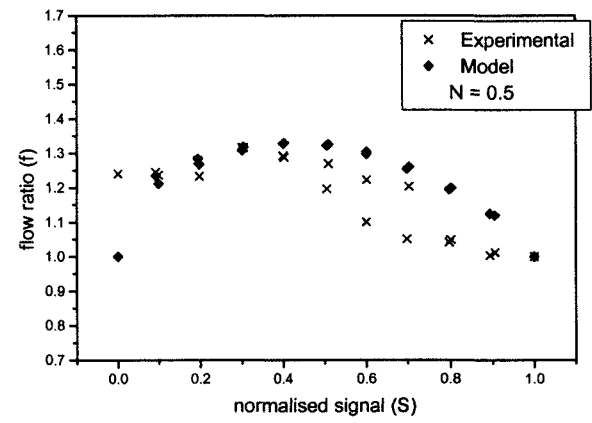


Fig.94: 65mm valve,  $hys = 5\%$ ,  
 $G_0 = 0.05\%$  inlet port and 0.1% bypass port

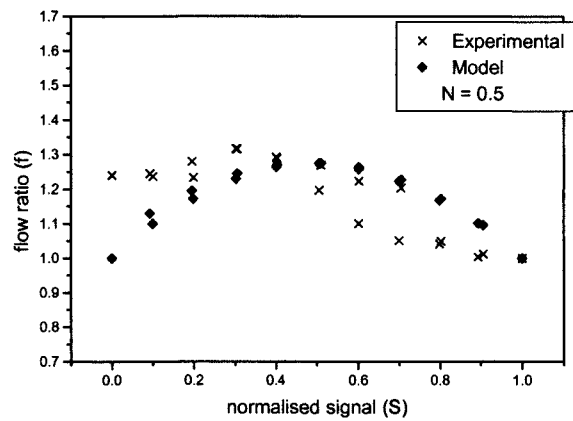


Fig.95: 65mm valve,  $hys = 5\%$ ,  
 $G_0 = 0.01\%$  inlet and bypass ports

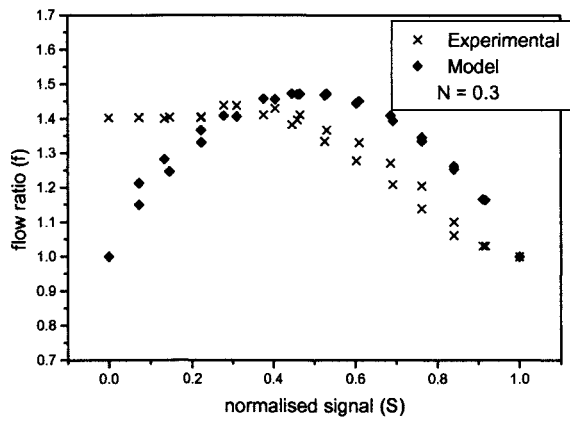


Fig.96: 80mm valve,  $hys = 5\%$ ,  
 $G_0 = 0.05\%$  inlet and bypass ports

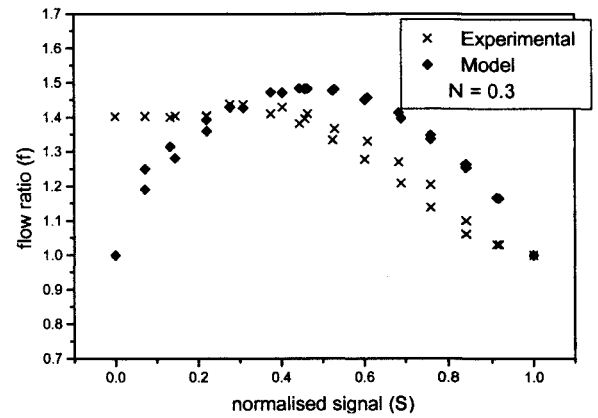


Fig.97: 80mm valve,  $hys = 5\%$ ,  
 $G_0 = 0.05\%$  inlet port and 0.065% bypass port

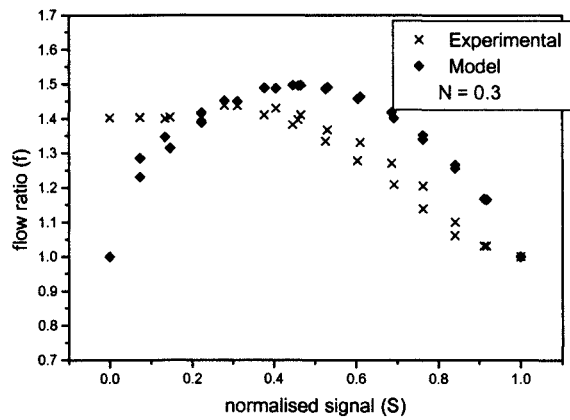


Fig.98: 80mm valve,  $hys = 5\%$ ,  
 $G_0 = 0.05\%$  inlet port and 0.075% bypass port

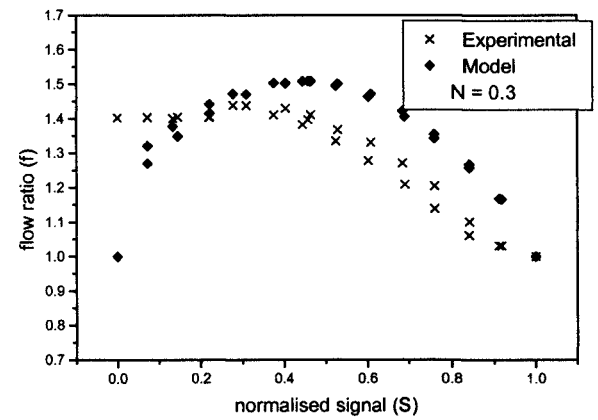


Fig.99: 80mm valve,  $hys = 5\%$ ,  
 $G_0 = 0.05\%$  inlet port and 0.1% bypass port

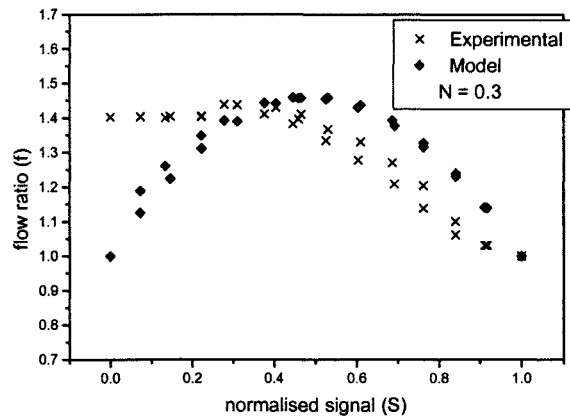


Fig.100: 80mm valve,  $hys = 5\%$ ,  
 $G_0 = 0.01\%$  inlet and bypass ports

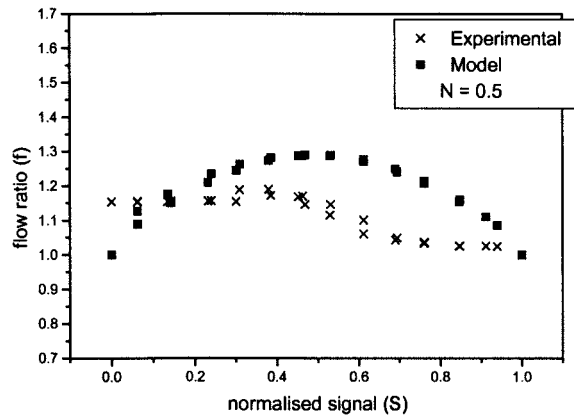


Fig.101: 80mm valve,  $hys = 5\%$ ,  
 $G_0 = 0.05\%$  inlet and bypass ports

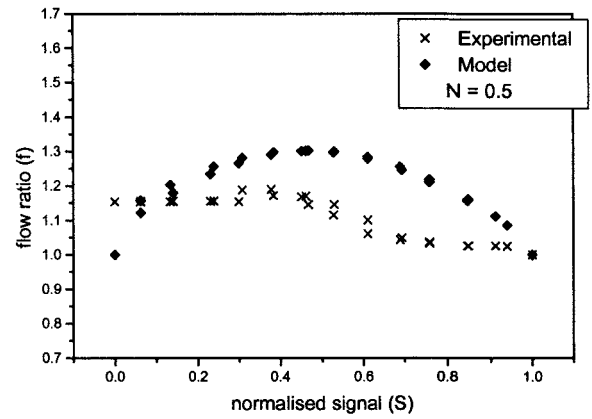


Fig.102: 80mm valve,  $hys = 5\%$ ,  
 $G_0 = 0.05\%$  inlet port and 0.065% bypass port

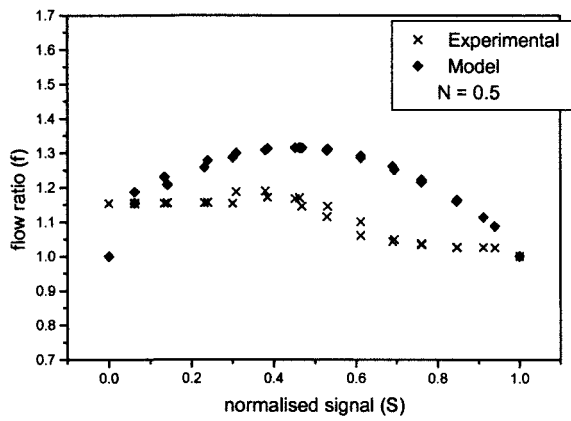


Fig.103: 80mm valve,  $hys = 5\%$ ,  
 $G_0 = 0.05\%$  inlet port and 0.075% bypass port

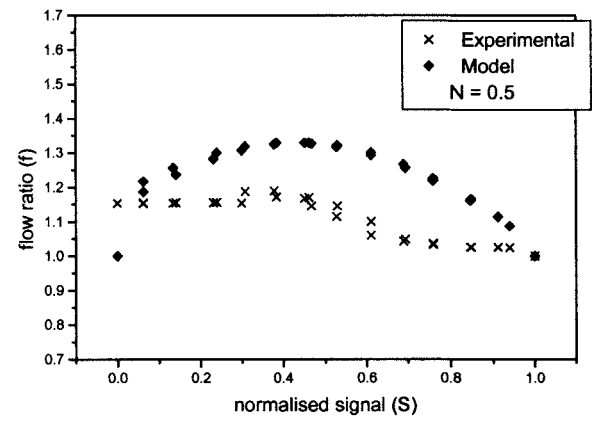


Fig.104: 80mm valve,  $hys = 5\%$ ,  
 $G_0 = 0.05\%$  inlet port and 0.1% bypass port

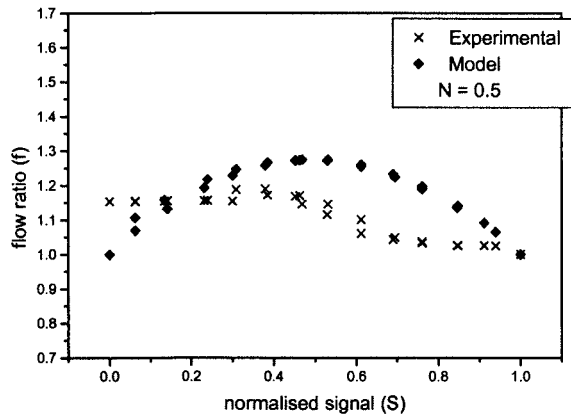


Fig.105: 80mm valve,  $hys = 5\%$ ,  
 $G_0 = 0.01\%$  inlet and bypass ports

**Figures 106 - 153. Graphs Comparing Test Rig Results with Mathematical Model (Version 2.2) Predictions**



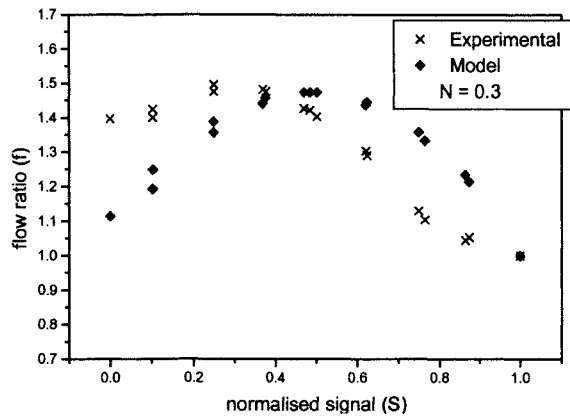


Fig.106: 40mm valve,  $hys = 5\%$ ,  
 $G_0 = 0.05\%$  inlet port, linear bypass  
 port,  $k = 2.5$ ,  $m = 0.5$

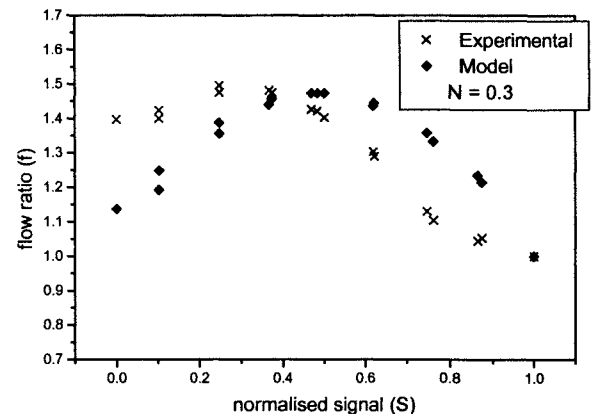


Fig.107: 40mm valve,  $hys = 5\%$ ,  
 $G_0 = 0.05\%$  inlet port, linear bypass  
 port,  $k = 3.0$ ,  $m = 0.5$

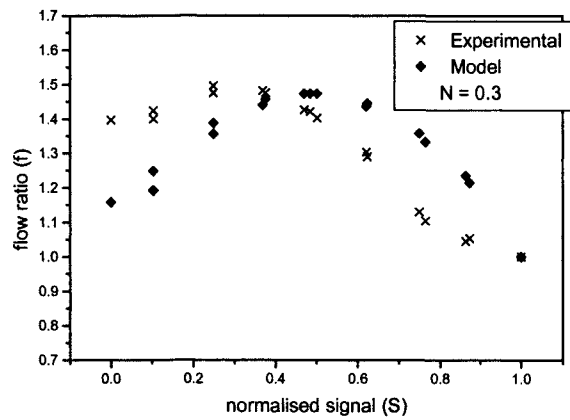


Fig.108: 40mm valve,  $hys = 5\%$ ,  
 $G_0 = 0.05\%$  inlet port, linear bypass  
 port,  $k = 3.5$ ,  $m = 0.5$

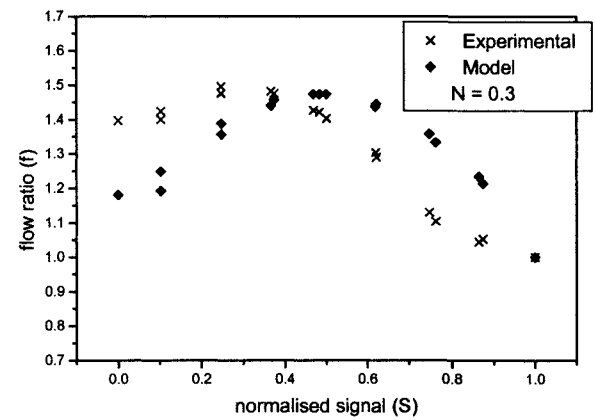


Fig.109: 40mm valve,  $hys = 5\%$ ,  
 $G_0 = 0.05\%$  inlet, linear bypass  
 port,  $k = 4$ ,  $m = 0.5$

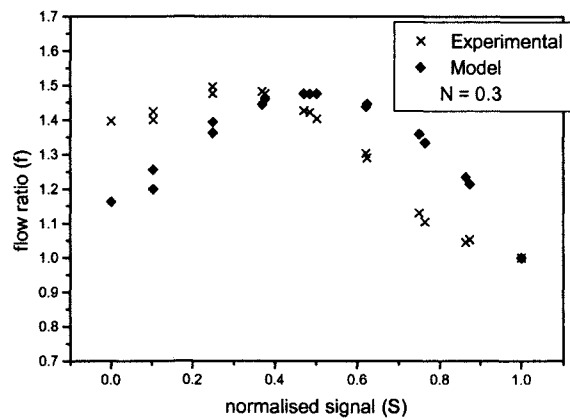


Fig.110: 40mm valve,  $hys = 5\%$ ,  
 $G_0 = 0.05\%$  inlet port, linear bypass  
 port,  $k = 3.0$ ,  $m = 0.03$

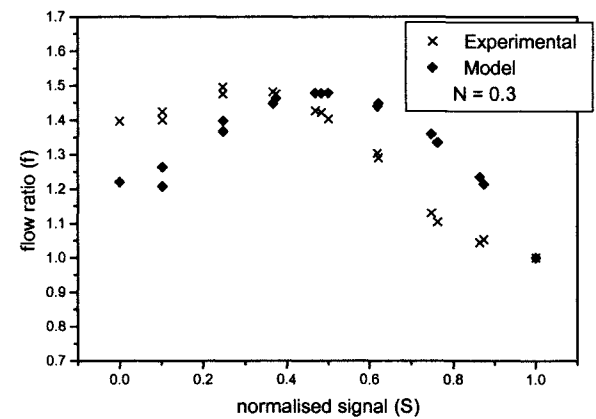


Fig.111: 40mm valve,  $hys = 5\%$ ,  
 $G_0 = 0.05\%$  inlet port, linear bypass  
 port,  $k = 3.5$ ,  $m = 0.035$

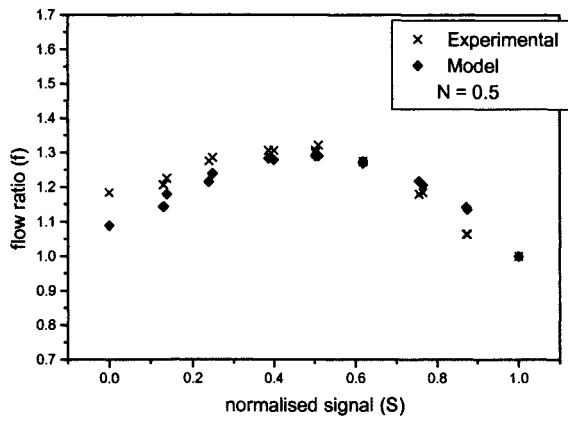


Fig.112: 40mm valve,  $hys = 5\%$ ,  
 $G_0 = 0.05\%$  inlet port, linear bypass  
 port,  $k = 2.5$ ,  $m = 0.5$

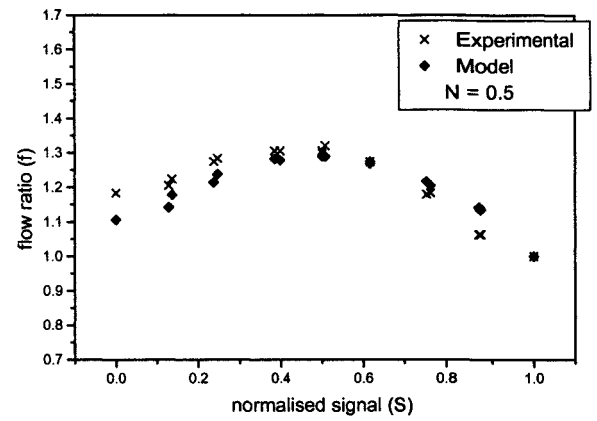


Fig.113: 40mm valve,  $hys = 5\%$ ,  
 $G_0 = 0.05\%$  inlet port, linear bypass  
 port,  $k = 3.0$ ,  $m = 0.5$

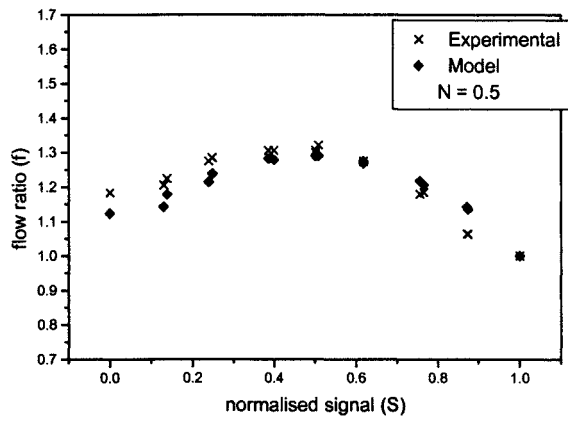


Fig.114: 40mm valve,  $hys = 5\%$ ,  
 $G_0 = 0.05\%$  inlet port, linear bypass  
 port,  $k = 3.5$ ,  $m = 0.5$

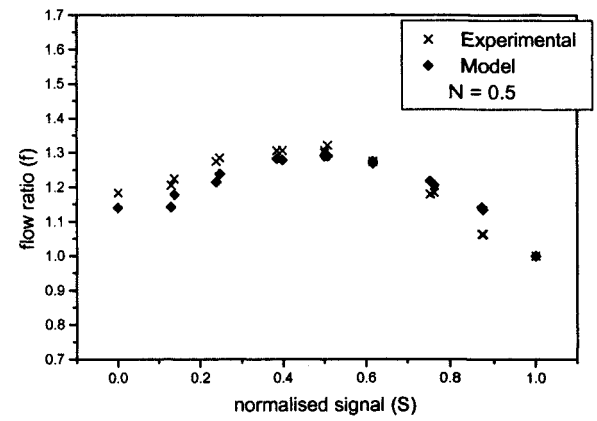


Fig.115: 40mm valve,  $hys = 5\%$ ,  
 $G_0 = 0.05\%$  inlet, linear bypass  
 port,  $k = 4$ ,  $m = 0.5$

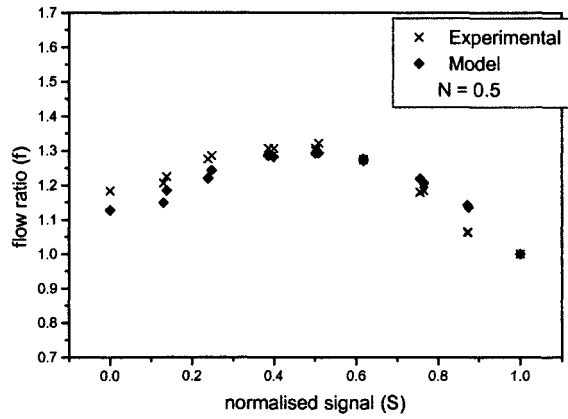


Fig.116: 40mm valve,  $hys = 5\%$ ,  
 $G_0 = 0.05\%$  inlet port, linear bypass  
 port,  $k = 3.0$ ,  $m = 0.03$

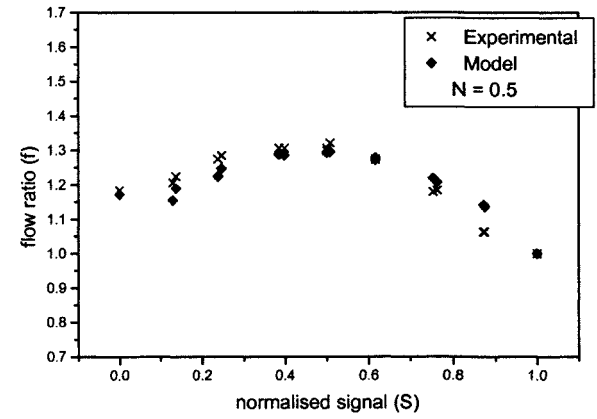


Fig.117: 40mm valve,  $hys = 5\%$ ,  
 $G_0 = 0.05\%$  inlet port, linear bypass  
 port,  $k = 3.5$ ,  $m = 0.035$

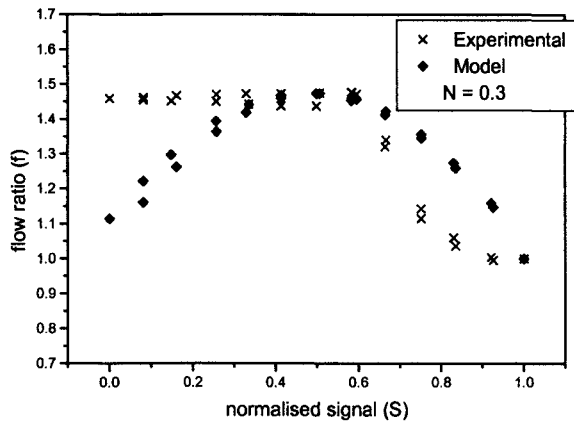


Fig.118: 50mm valve,  $hys = 5\%$ ,  
 $G_0 = 0.05\%$  inlet port, linear bypass  
 port,  $k = 2.5$ ,  $m = 0.5$

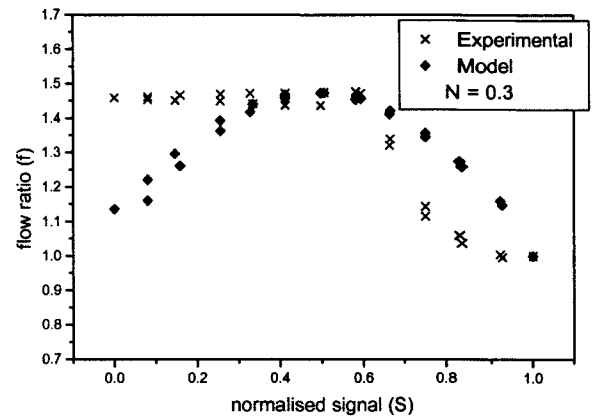


Fig.119: 50mm valve,  $hys = 5\%$ ,  
 $G_0 = 0.05\%$  inlet port, linear bypass  
 port,  $k = 3.0$ ,  $m = 0.5$

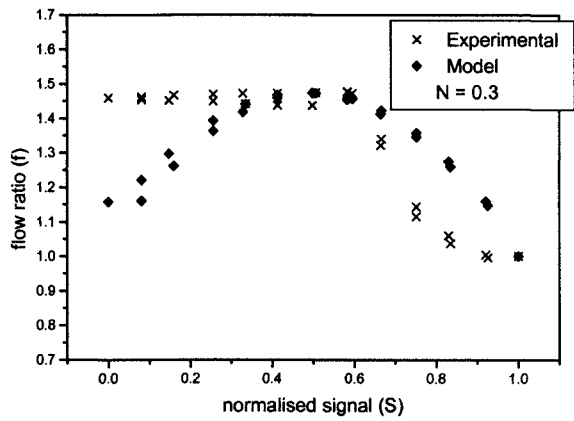


Fig.120: 50mm valve,  $hys = 5\%$ ,  
 $G_0 = 0.05\%$  inlet port, linear bypass  
 port,  $k = 3.5$ ,  $m = 0.5$

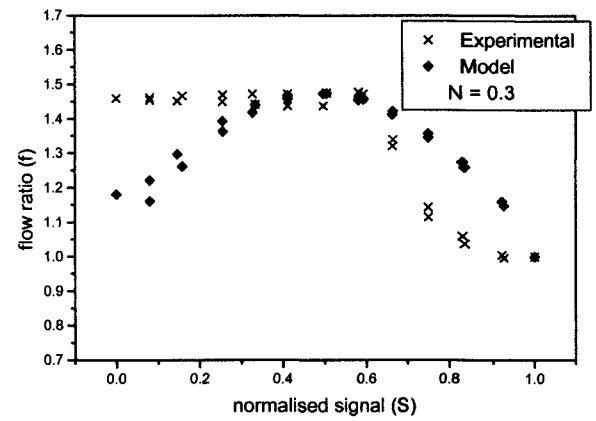


Fig.121: 50mm valve,  $hys = 5\%$ ,  
 $G_0 = 0.05\%$  inlet, linear bypass  
 port,  $k = 4$ ,  $m = 0.5$

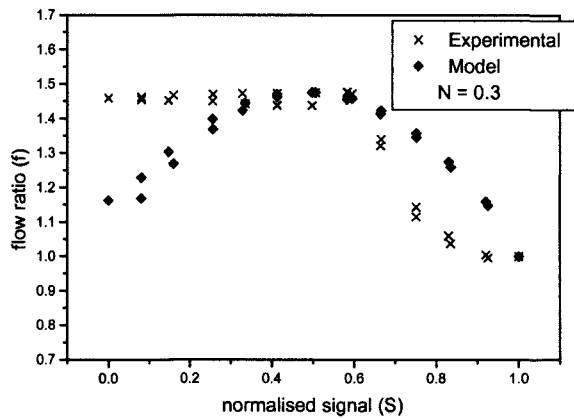


Fig.122: 50mm valve,  $hys = 5\%$ ,  
 $G_0 = 0.05\%$  inlet port, linear bypass  
 port,  $k = 3.0$ ,  $m = 0.03$

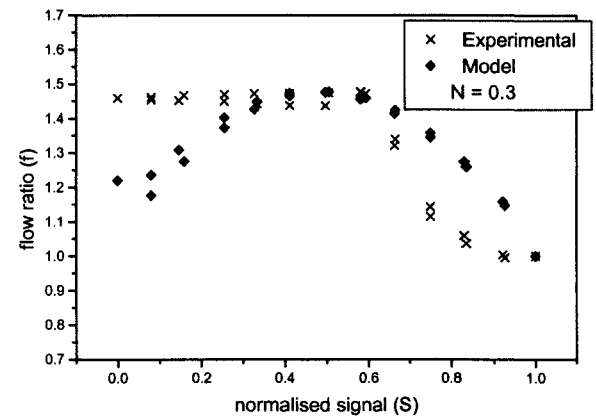


Fig.123: 50mm valve,  $hys = 5\%$ ,  
 $G_0 = 0.05\%$  inlet port, linear bypass  
 port,  $k = 3.5$ ,  $m = 0.035$

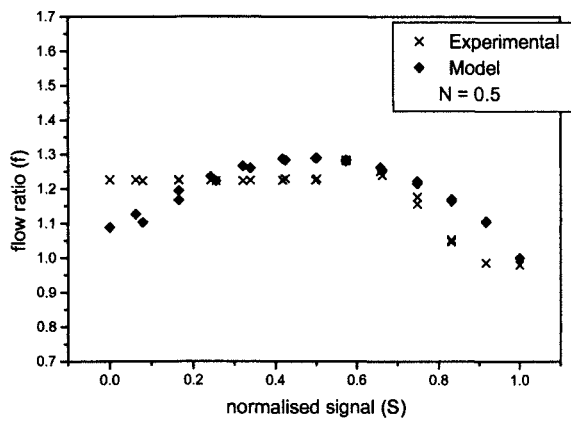


Fig.124: 50mm valve,  $hys = 5\%$ ,  
 $G_0 = 0.05\%$  inlet port, linear bypass  
 port,  $k = 2.5$ ,  $m = 0.5$

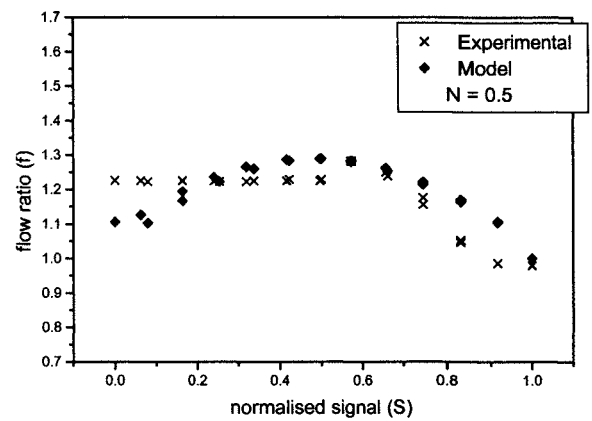


Fig.125: 50mm valve,  $hys = 5\%$ ,  
 $G_0 = 0.05\%$  inlet port, linear bypass  
 port,  $k = 3.0$ ,  $m = 0.5$

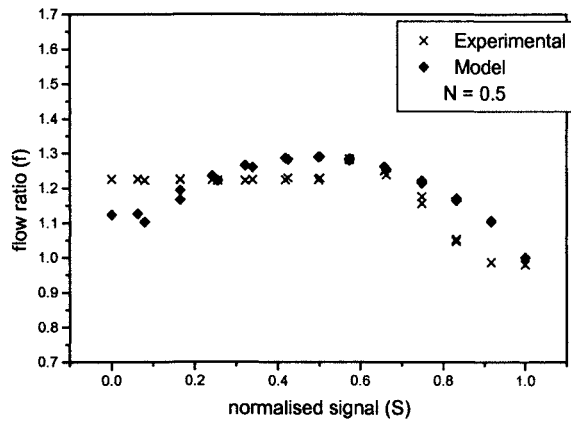


Fig.126: 50mm valve,  $hys = 5\%$ ,  
 $G_0 = 0.05\%$  inlet port, linear bypass  
 port,  $k = 3.5$ ,  $m = 0.5$

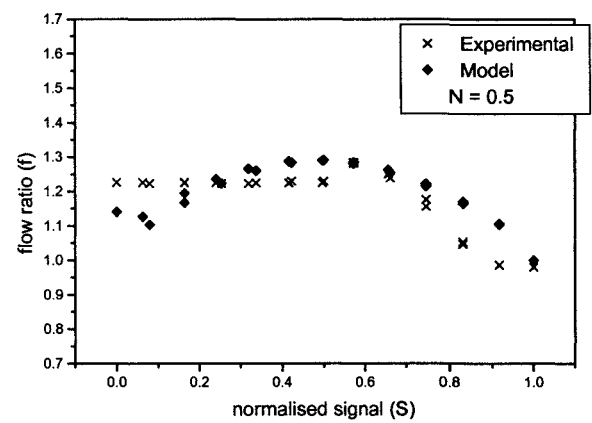


Fig.127: 50mm valve,  $hys = 5\%$ ,  
 $G_0 = 0.05\%$  inlet, linear bypass  
 port,  $k = 4$ ,  $m = 0.5$

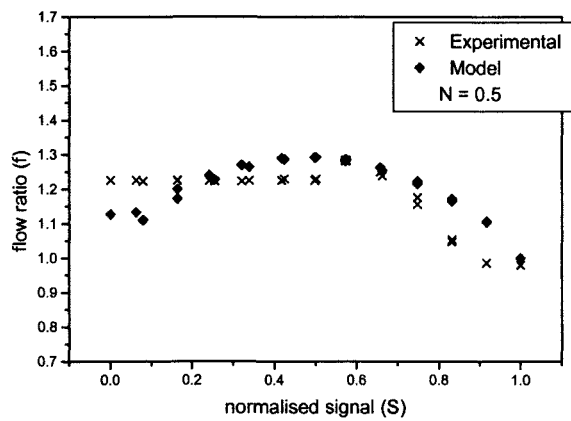


Fig.128: 50mm valve,  $hys = 5\%$ ,  
 $G_0 = 0.05\%$  inlet port, linear bypass  
 port,  $k = 3.0$ ,  $m = 0.03$

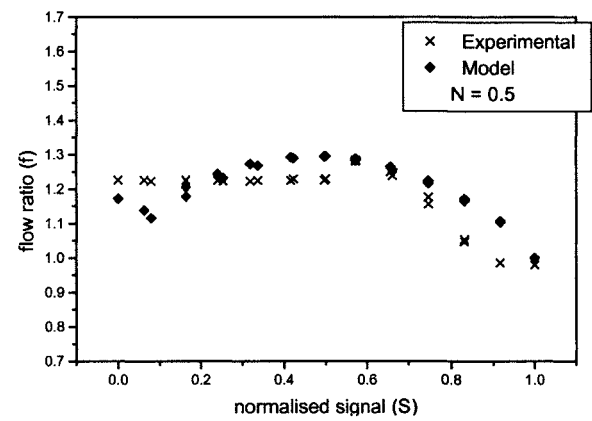


Fig.129: 50mm valve,  $hys = 5\%$ ,  
 $G_0 = 0.05\%$  inlet port, linear bypass  
 port,  $k = 3.5$ ,  $m = 0.035$

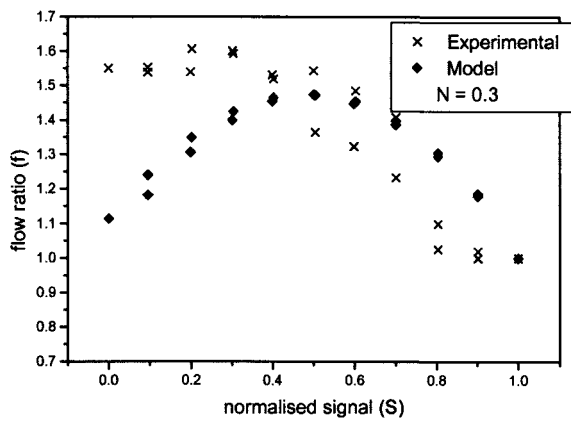


Fig.130: 65mm valve,  $hys = 5\%$ ,  
 $G_0 = 0.05\%$  inlet port, linear bypass  
 port,  $k = 2.5$ ,  $m = 0.5$

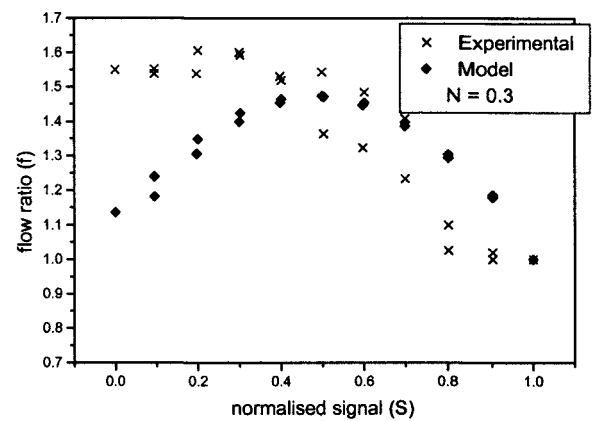


Fig.131: 65mm valve,  $hys = 5\%$ ,  
 $G_0 = 0.05\%$  inlet port, linear bypass  
 port,  $k = 3.0$ ,  $m = 0.5$

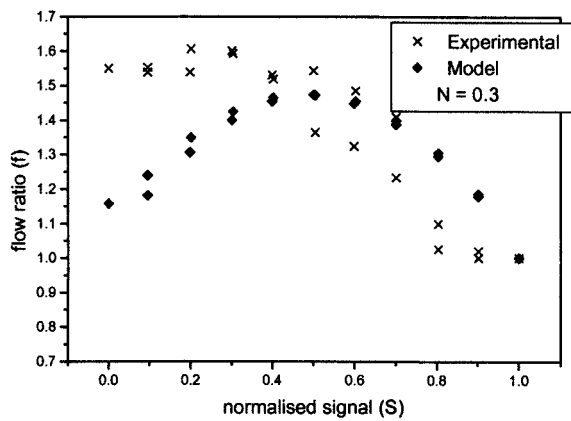


Fig.132: 65mm valve,  $hys = 5\%$ ,  
 $G_0 = 0.05\%$  inlet port, linear bypass  
 port,  $k = 3.5$ ,  $m = 0.5$

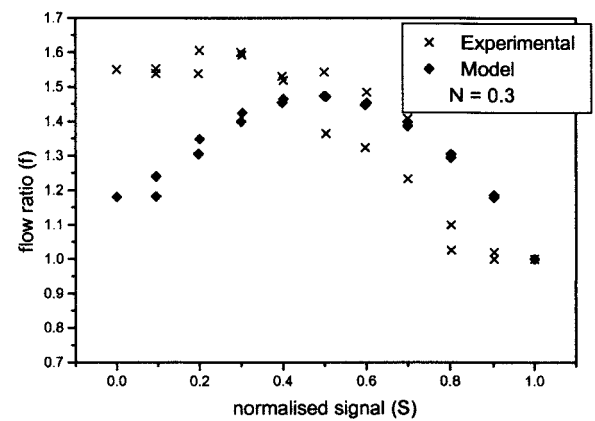


Fig.133: 65mm valve,  $hys = 5\%$ ,  
 $G_0 = 0.05\%$  inlet, linear bypass  
 port,  $k = 4$ ,  $m = 0.5$

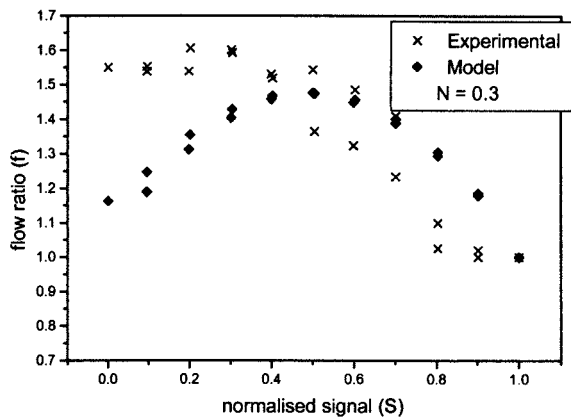


Fig.134: 65mm valve,  $hys = 5\%$ ,  
 $G_0 = 0.05\%$  inlet port, linear bypass  
 port,  $k = 3.0$ ,  $m = 0.03$

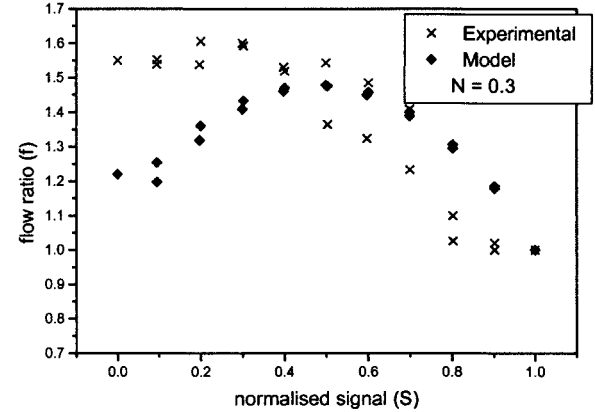


Fig.135: 65mm valve,  $hys = 5\%$ ,  
 $G_0 = 0.05\%$  inlet port, linear bypass  
 port,  $k = 3.5$ ,  $m = 0.035$

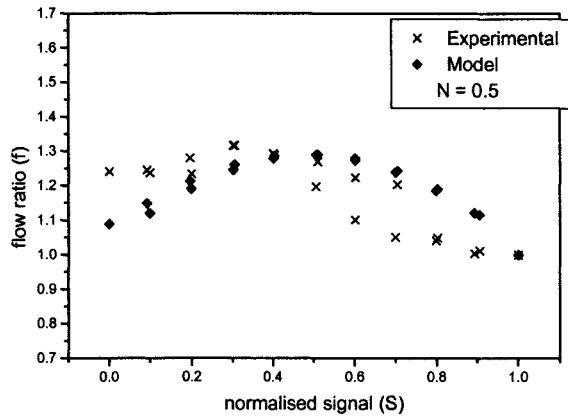


Fig.136: 65mm valve,  $h_{ys} = 5\%$ ,  
 $G_0 = 0.05\%$  inlet port, linear bypass  
 port,  $k = 2.5$ ,  $m = 0.5$

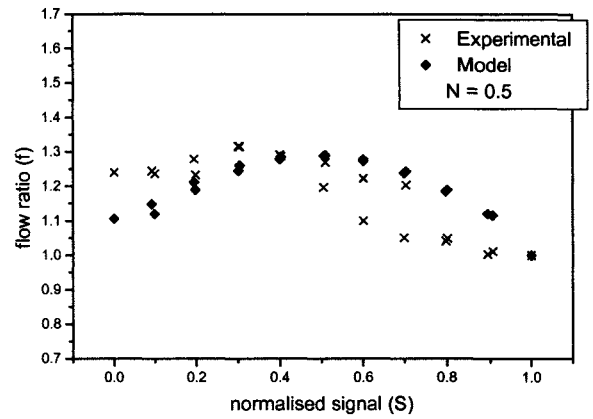


Fig.137: 65mm valve,  $h_{ys} = 5\%$ ,  
 $G_0 = 0.05\%$  inlet port, linear bypass  
 port,  $k = 3.0$ ,  $m = 0.5$

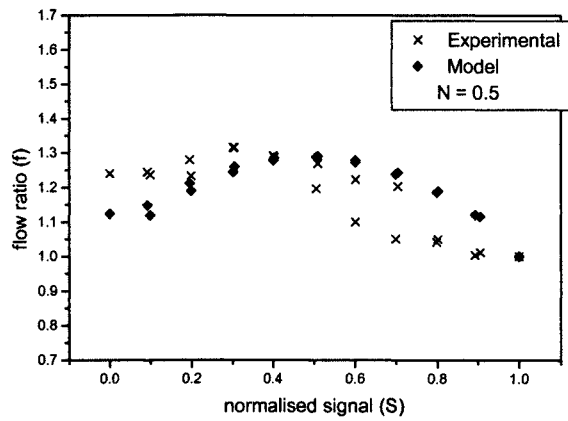


Fig.138: 65mm valve,  $h_{ys} = 5\%$ ,  
 $G_0 = 0.05\%$  inlet port, linear bypass  
 port,  $k = 3.5$ ,  $m = 0.5$

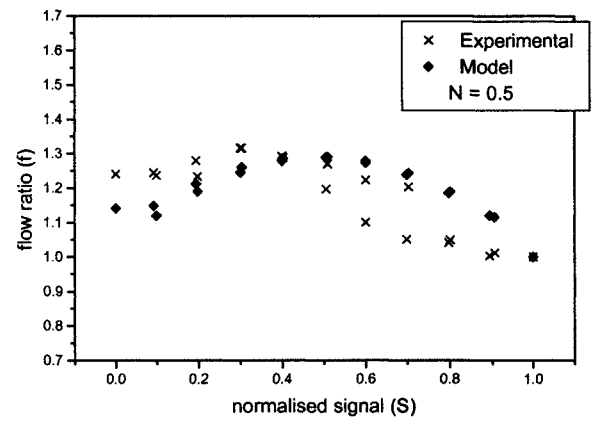


Fig.139: 65mm valve,  $h_{ys} = 5\%$ ,  
 $G_0 = 0.05\%$  inlet, linear bypass  
 port,  $k = 4$ ,  $m = 0.5$

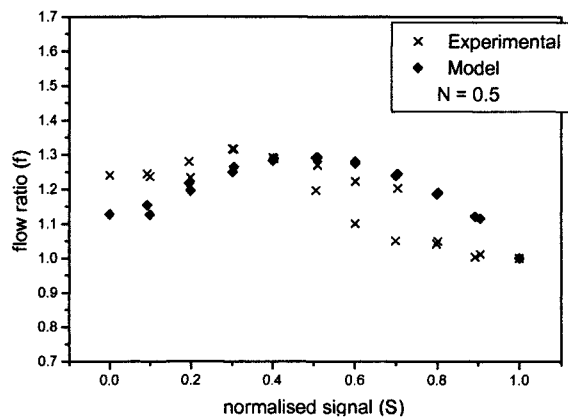


Fig.140: 65mm valve,  $h_{ys} = 5\%$ ,  
 $G_0 = 0.05\%$  inlet port, linear bypass  
 port,  $k = 3.0$ ,  $m = 0.03$

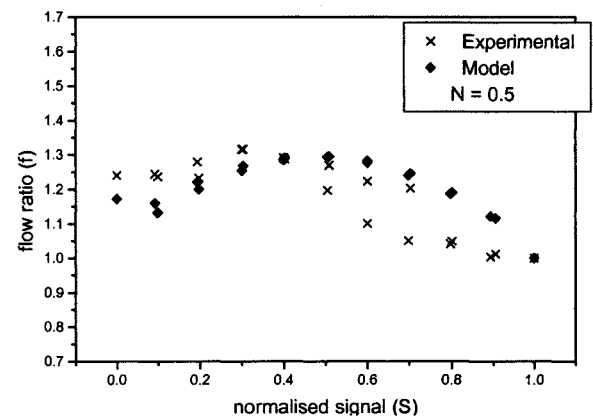


Fig.141: 65mm valve,  $h_{ys} = 5\%$ ,  
 $G_0 = 0.05\%$  inlet port, linear bypass  
 port,  $k = 3.5$ ,  $m = 0.035$

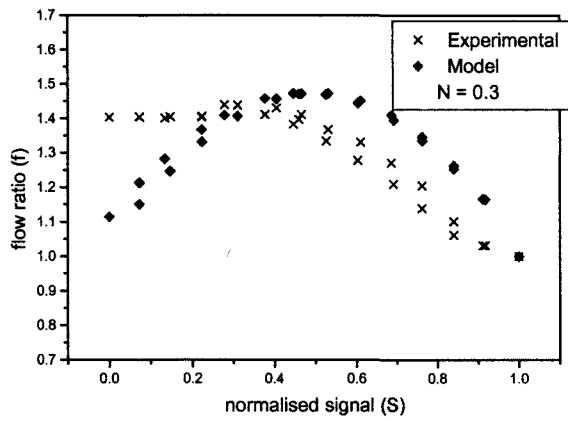


Fig.142: 80mm valve,  $hys = 5\%$ ,  
 $G_0 = 0.05\%$  inlet port, linear bypass  
 port,  $k = 2.5$ ,  $m = 0.5$

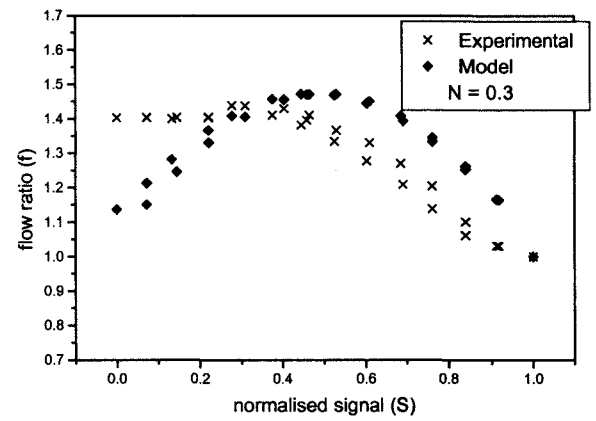


Fig.143: 80mm valve,  $hys = 5\%$ ,  
 $G_0 = 0.05\%$  inlet port, linear bypass  
 port,  $k = 3.0$ ,  $m = 0.5$

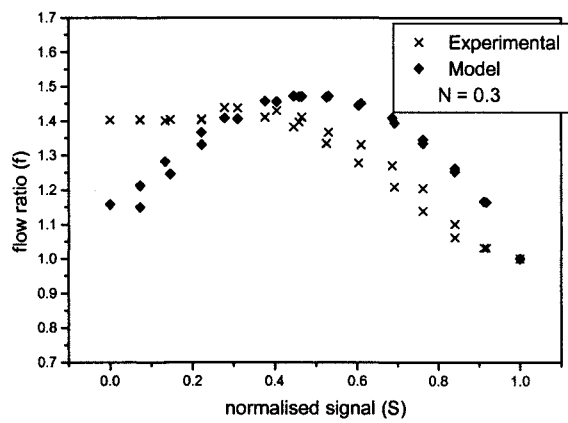


Fig.144: 80mm valve,  $hys = 5\%$ ,  
 $G_0 = 0.05\%$  inlet port, linear bypass  
 port,  $k = 3.5$ ,  $m = 0.5$

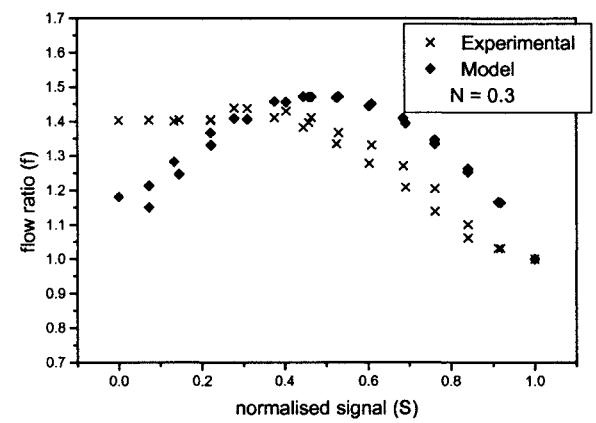


Fig.145: 80mm valve,  $hys = 5\%$ ,  
 $G_0 = 0.05\%$  inlet, linear bypass  
 port,  $k = 4$ ,  $m = 0.5$

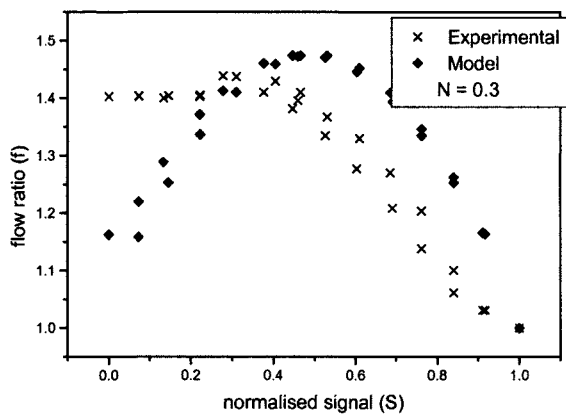


Fig.146: 80mm valve,  $hys = 5\%$ ,  
 $G_0 = 0.05\%$  inlet port, linear bypass  
 port,  $k = 3.0$ ,  $m = 0.03$

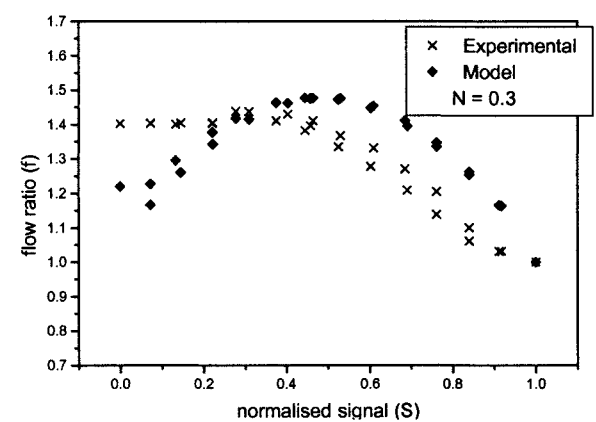


Fig.147: 80mm valve,  $hys = 5\%$ ,  
 $G_0 = 0.05\%$  inlet port, linear bypass  
 port,  $k = 3.5$ ,  $m = 0.035$

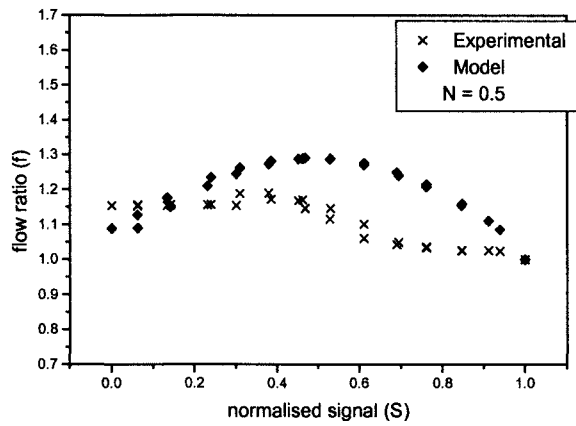


Fig.148: 80mm valve,  $h_{ys} = 5\%$ ,  
 $G_0 = 0.05\%$  inlet port, linear bypass  
 port,  $k = 2.5$ ,  $m = 0.5$

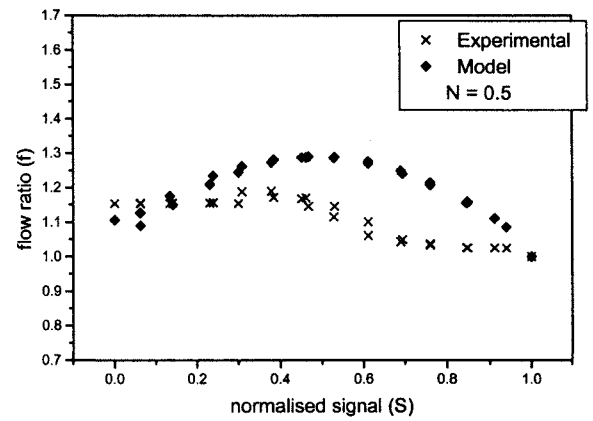


Fig.149: 80mm valve,  $h_{ys} = 5\%$ ,  
 $G_0 = 0.05\%$  inlet port, linear bypass  
 port,  $k = 3.0$ ,  $m = 0.5$

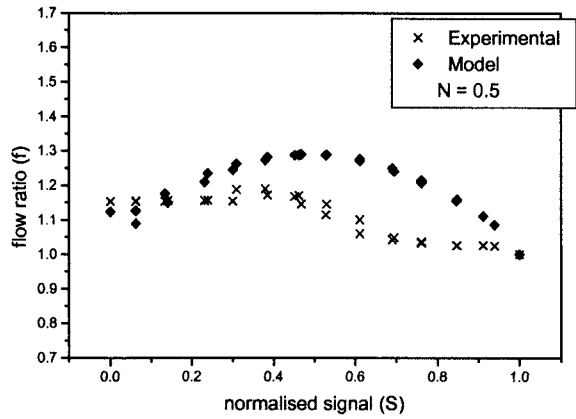


Fig.150: 80mm valve,  $h_{ys} = 5\%$ ,  
 $G_0 = 0.05\%$  inlet port, linear bypass  
 port,  $k = 3.5$ ,  $m = 0.5$

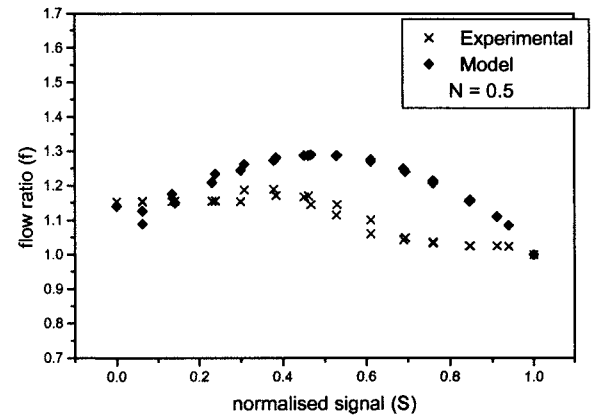


Fig.151: 80mm valve,  $h_{ys} = 5\%$ ,  
 $G_0 = 0.05\%$  inlet, linear bypass  
 port,  $k = 4$ ,  $m = 0.5$

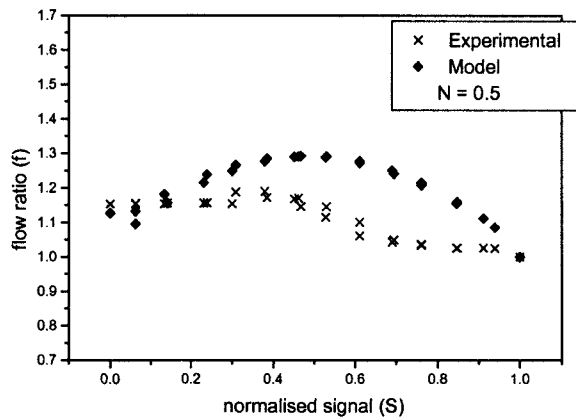


Fig.152: 80mm valve,  $h_{ys} = 5\%$ ,  
 $G_0 = 0.05\%$  inlet port, linear bypass  
 port,  $k = 3.0$ ,  $m = 0.03$

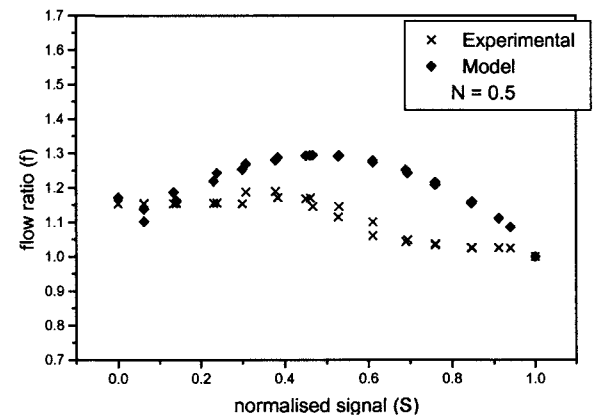


Fig.153: 80mm valve,  $h_{ys} = 5\%$ ,  
 $G_0 = 0.05\%$  inlet port, linear bypass  
 port,  $k = 3.5$ ,  $m = 0.035$



**Figures 155 - 164. Graphs Comparing Test Rig Results with Mathematical Model (Version 3.0) Predictions**

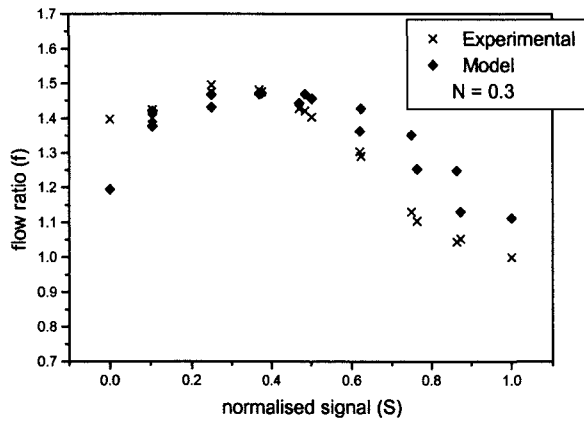


Fig.155: 40mm valve,  $hys = 5\%$ , pneumatic model,  
 $G_0 = 0.05\%$  inlet and bypass ports

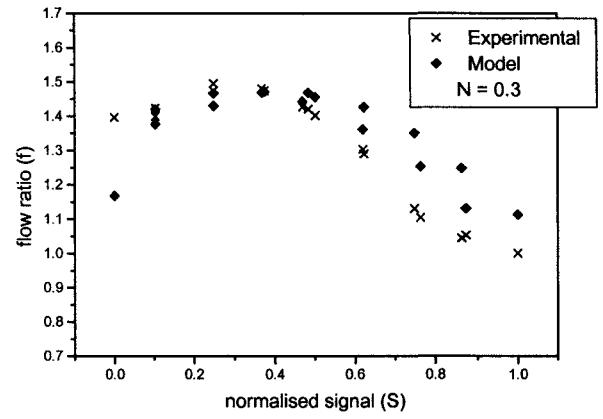


Fig.156: 40mm valve,  $hys = 5\%$ , pneumatic model,  
 $G_0 = 0.05\%$  inlet port, linear bypass port,  
 $k = 2.5$

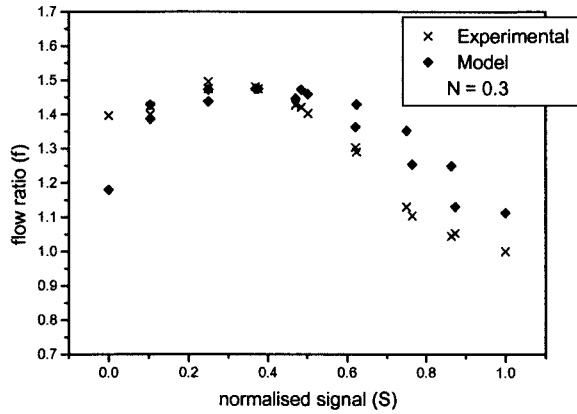


Fig.157: 40mm valve,  $hys = 5\%$ , pneumatic model,  
 $G_0 = 0.05\%$  inlet port, linear bypass port,  
 $k = 3.5$

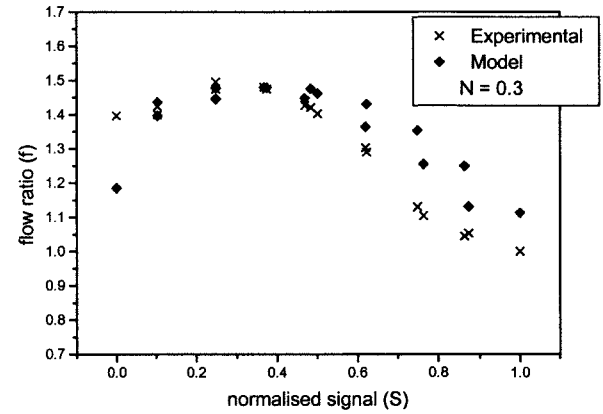


Fig.158: 40mm valve,  $hys = 5\%$ , pneumatic model,  
 $G_0 = 0.05\%$  inlet port, linear bypass port,  
 $k = 4.5$

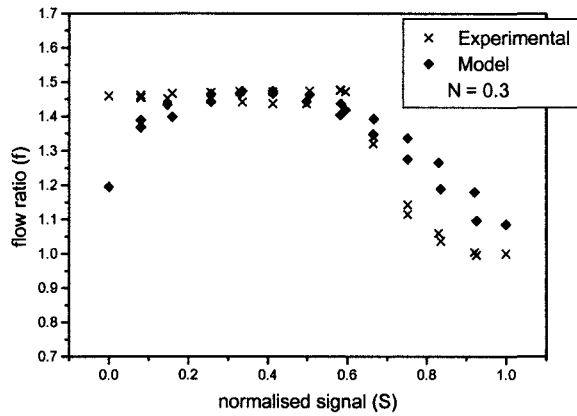


Fig.159: 50mm valve,  $hys = 5\%$ , pneumatic model,  
 $G_0 = 0.05\%$  inlet and bypass ports

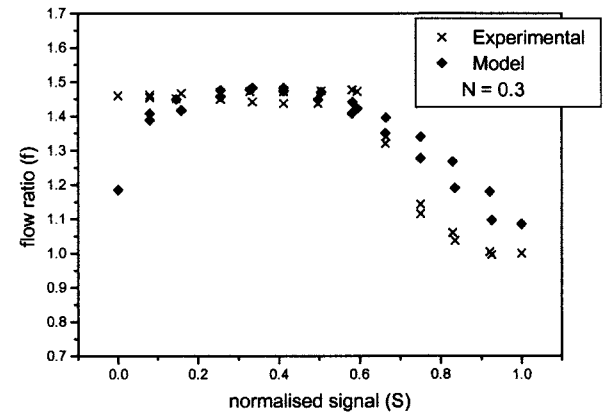


Fig.160: 50mm valve,  $hys = 5\%$ , pneumatic model,  
 $G_0 = 0.05\%$  inlet port, linear bypass port,  
 $k = 4.5$

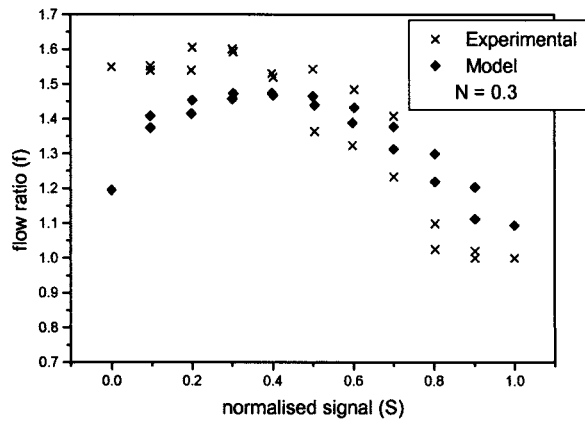


Fig.161: 65mm valve,  $h_{ys} = 5\%$ , pneumatic model,  $G_0 = 0.05\%$  inlet and bypass ports

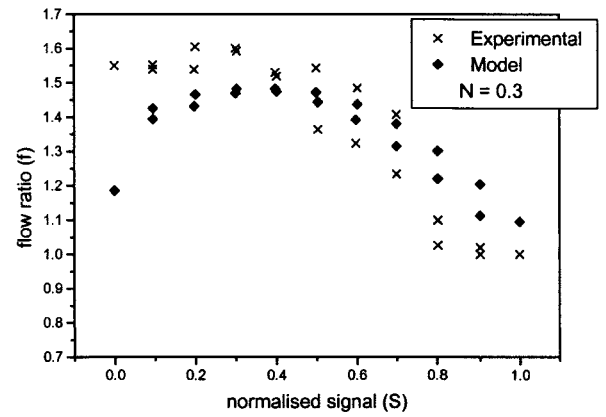


Fig.162: 65mm valve,  $h_{ys} = 5\%$ , pneumatic model,  $G_0 = 0.05\%$  inlet port, linear bypass port,  $k = 4.5$

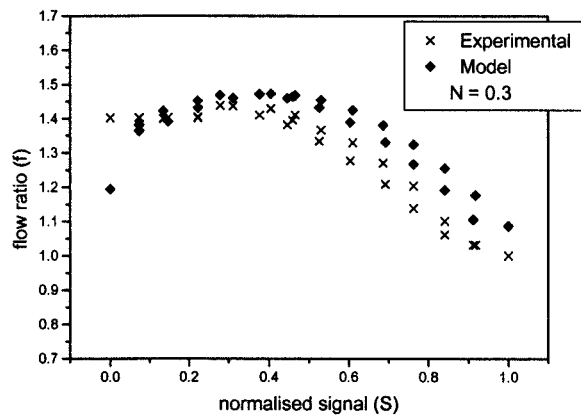


Fig.163: 80mm valve,  $h_{ys} = 5\%$ , pneumatic model,  $G_0 = 0.05\%$  inlet and bypass ports

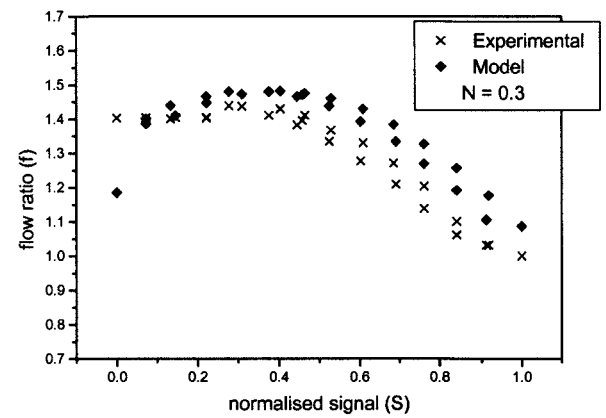


Fig.164: 80mm valve,  $h_{ys} = 5\%$ , pneumatic model,  $G_0 = 0.05\%$  inlet port, linear bypass port,  $k = 4.5$

**Figures 165 - 192. All Model Versions Integrated Over Time, Flow Profiles**

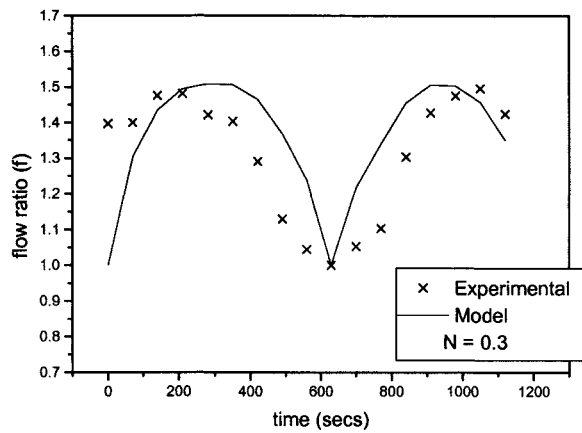


Fig.165: 40mm valve, model version 2.1,  
let-by = 0.05% inlet port, 0.1% bypass port

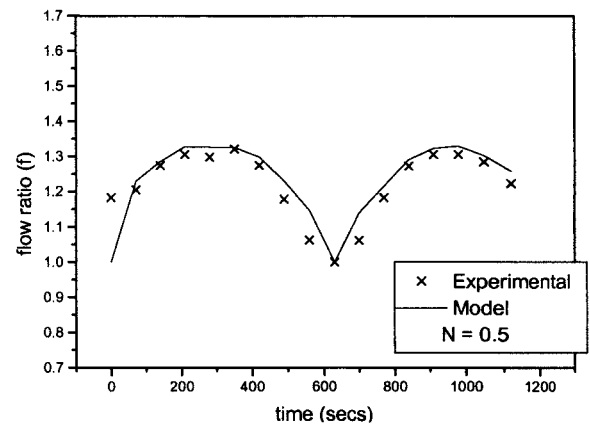


Fig.166: 40mm valve, model version 2.1,  
let-by = 0.05% inlet port, 0.1% bypass port

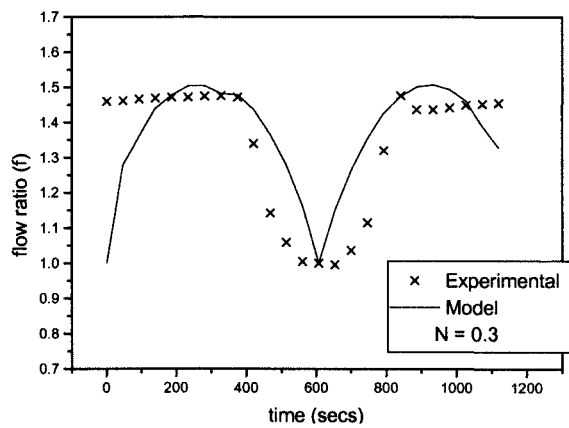


Fig.167: 50mm valve, model version 2.1,  
let-by = 0.05% inlet port, 0.1% bypass port

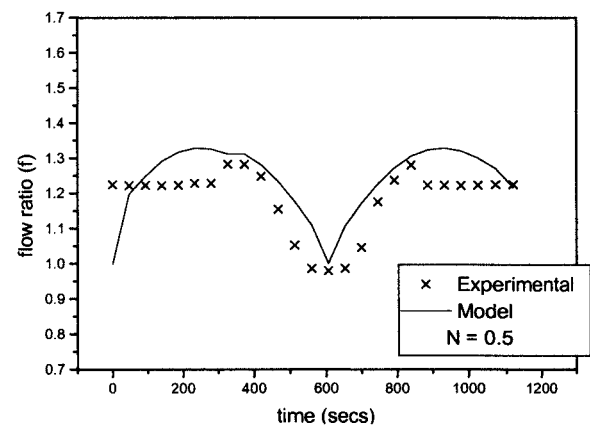


Fig.168: 50mm valve, model version 2.1,  
let-by = 0.05% inlet port, 0.1% bypass port

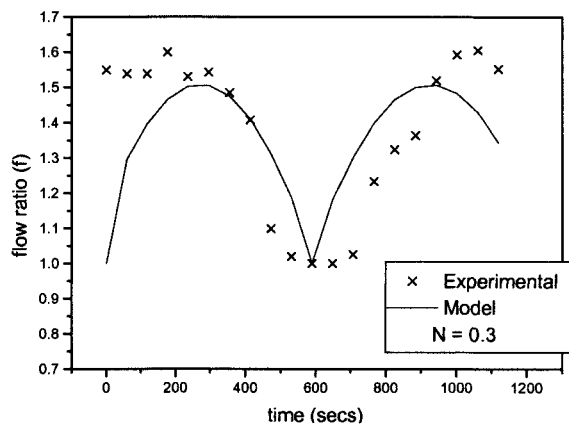


Fig.169: 65mm valve, model version 2.1,  
let-by = 0.05% inlet port, 0.1% bypass port

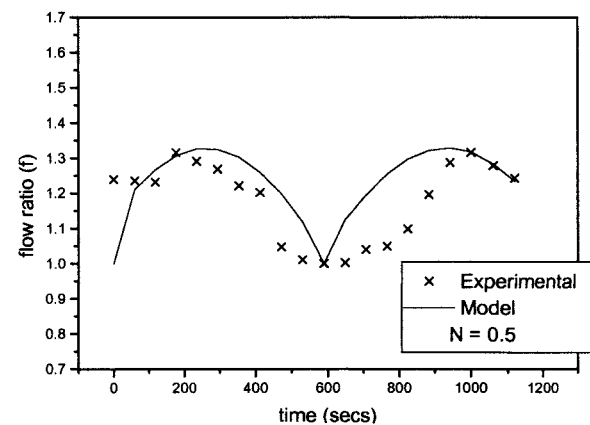


Fig.170: 65mm valve, model version 2.1,  
let-by = 0.05% inlet port, 0.1% bypass port

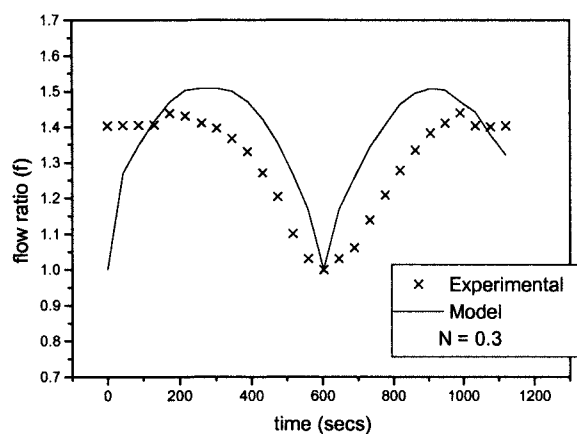


Fig.171: 80mm valve, model version 2.1,  
let-by = 0.05% inlet port, 0.1% bypass port

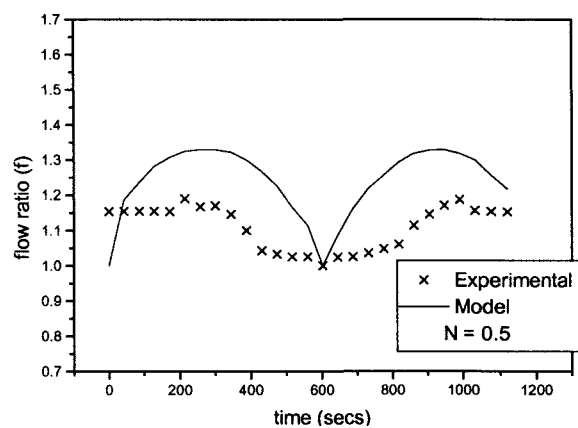


Fig.172: 80mm valve, model version 2.1,  
let-by = 0.05% inlet port, 0.1% bypass port

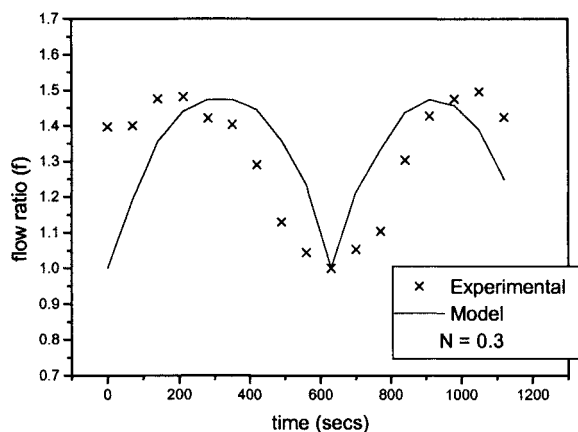


Fig.173: 40mm valve, model version 2.0,  
let-by = 0.05% inlet port and bypass port

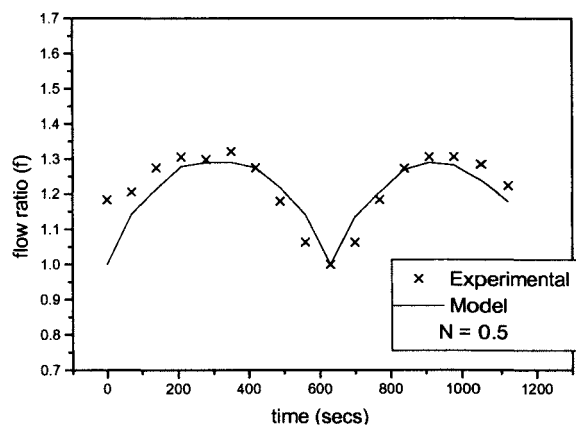


Fig.174: 40mm valve, model version 2.0,  
let-by = 0.05% inlet port and bypass port

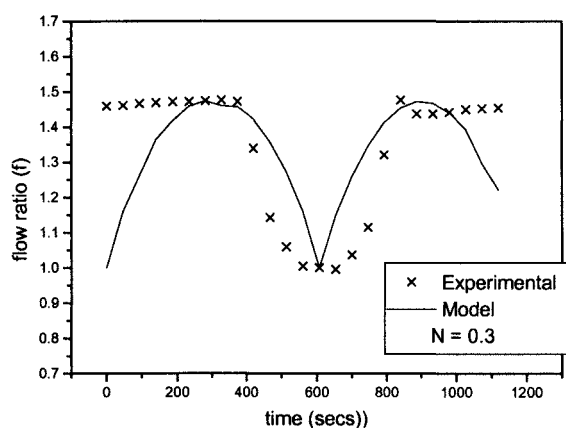


Fig.175: 50mm valve, model version 2.0,  
let-by = 0.05% inlet port and bypass port

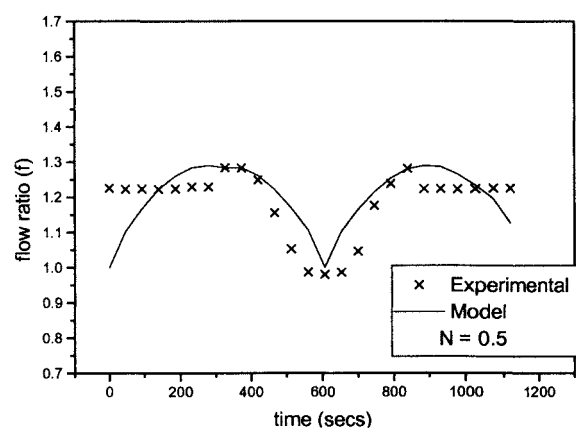


Fig.176: 50mm valve, model version 2.0,  
let-by = 0.05% inlet port and bypass port

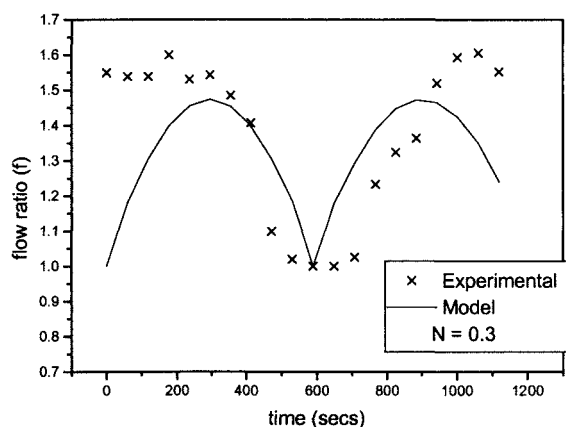


Fig.177: 65mm valve, model version 2.0,  
let-by = 0.05% inlet port and bypass port

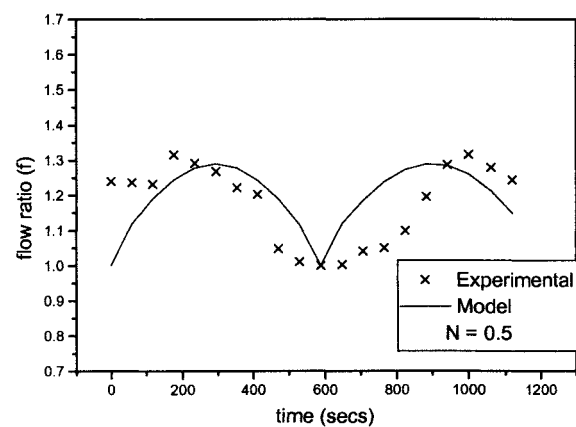


Fig.178: 65mm valve, model version 2.0,  
let-by = 0.05% inlet port and bypass port

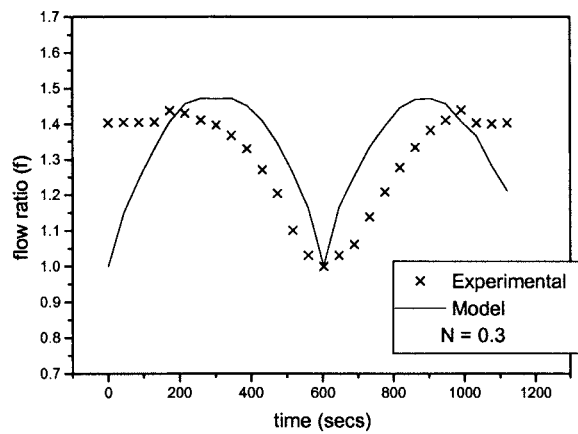


Fig.179: 80mm valve, model version 2.0,  
let-by = 0.05% inlet port and bypass port

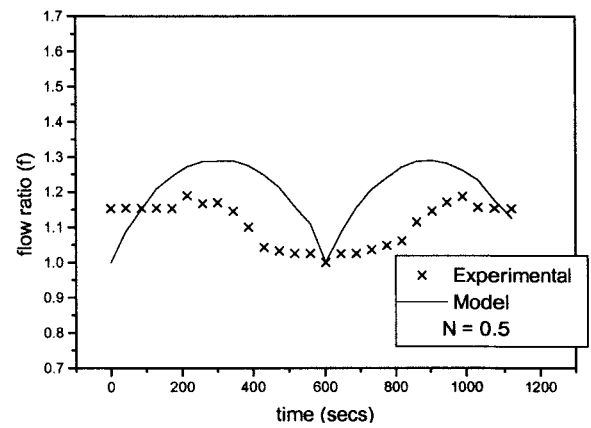


Fig.180: 80mm valve, model version 2.0,  
let-by = 0.05% inlet port and bypass port



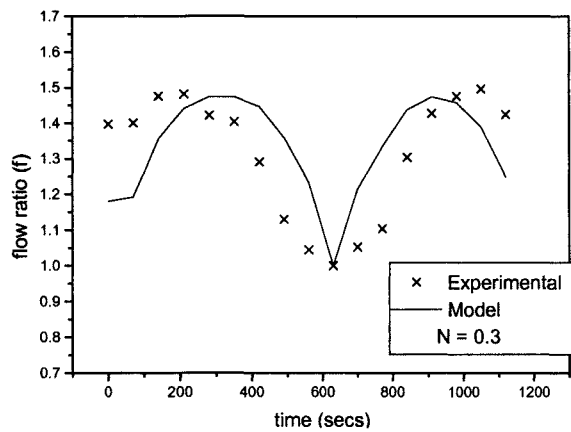


Fig.181: 40mm valve, model version 2.2,  
let-by = 0.05% inlet port and linear bypass port  
 $k = 4.0$

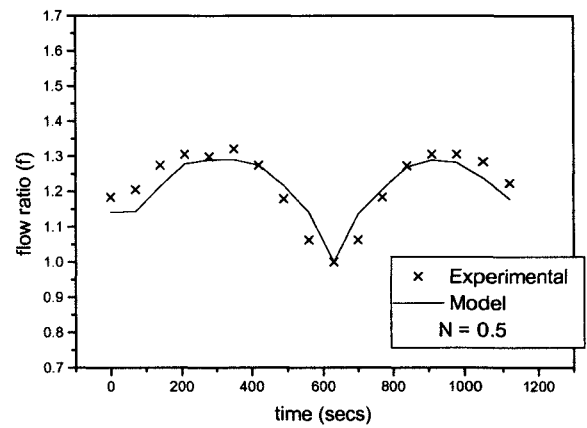


Fig.182: 40mm valve, model version 2.2,  
let-by = 0.05% inlet port and linear bypass port  
 $k = 4.0$

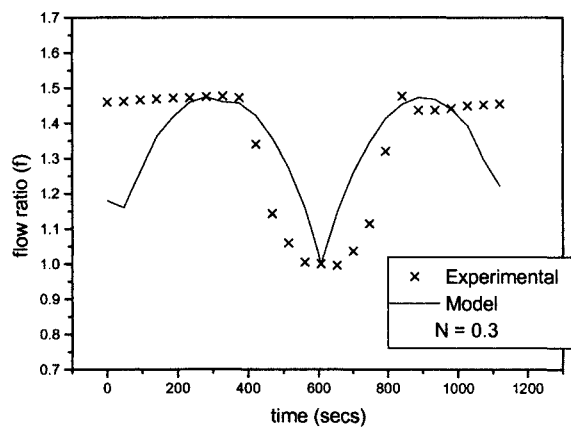


Fig.183: 50mm valve, model version 2.2,  
let-by = 0.05% inlet port and linear bypass port  
 $k = 4.0$

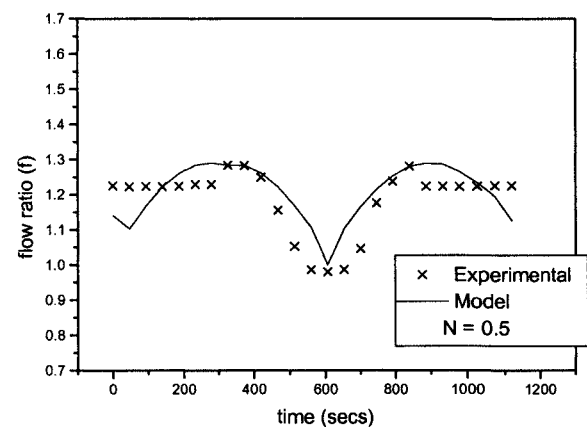


Fig.184: 50mm valve, model version 2.2,  
let-by = 0.05% inlet port and linear bypass port  
 $k = 4.0$

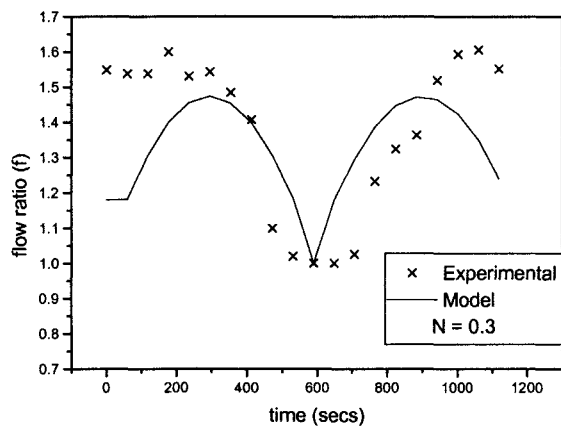


Fig.185: 65mm valve, model version 2.2,  
let-by = 0.05% inlet port and linear bypass port  
 $k = 4.0$

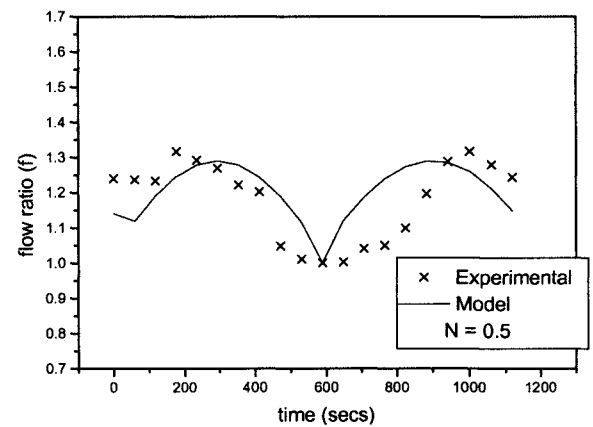


Fig.186: 65mm valve, model version 2.2,  
let-by = 0.05% inlet port and linear bypass port  
 $k = 4.0$

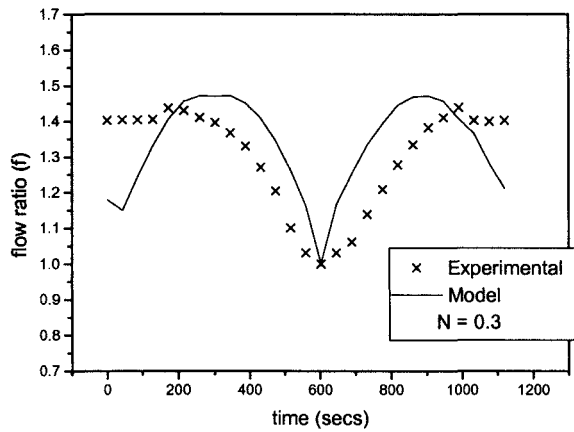


Fig.187: 80mm valve, model version 2.2,  
let-by = 0.05% inlet port and linear bypass port  
 $k = 4.0$

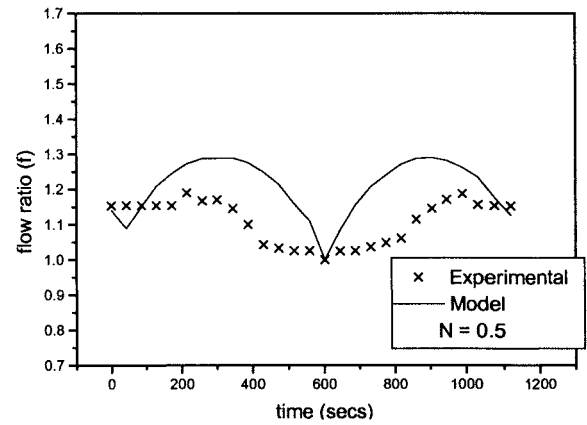


Fig.188: 80mm valve, model version 2.2,  
let-by = 0.05% inlet port and linear bypass port  
 $k = 4.0$

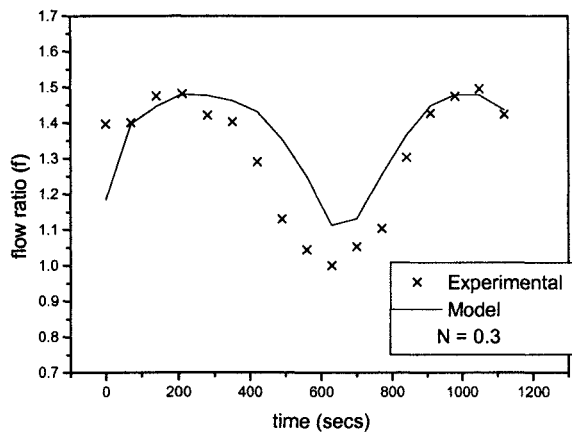


Fig.189: 40mm valve, model version 3.0,  
let-by = 0.05% inlet port and linear bypass port  
 $k = 4.5$

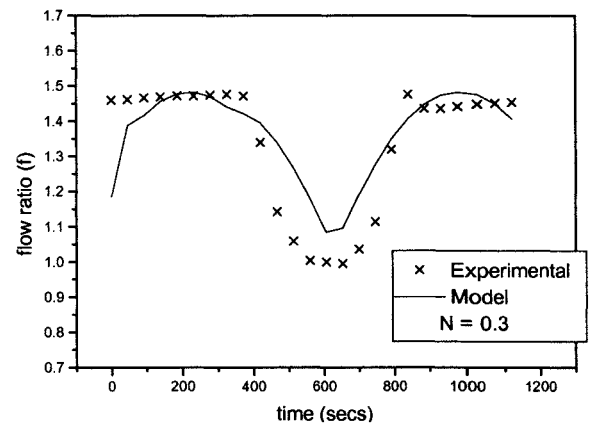


Fig.190: 50mm valve, model version 3.0,  
let-by = 0.05% inlet port and linear bypass port  
 $k = 4.5$

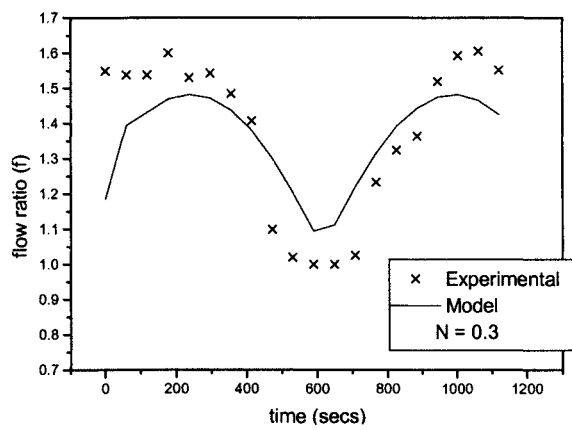


Fig.191: 65mm valve, model version 3.0,  
let-by = 0.05% inlet port and linear bypass port  
 $k = 4.5$

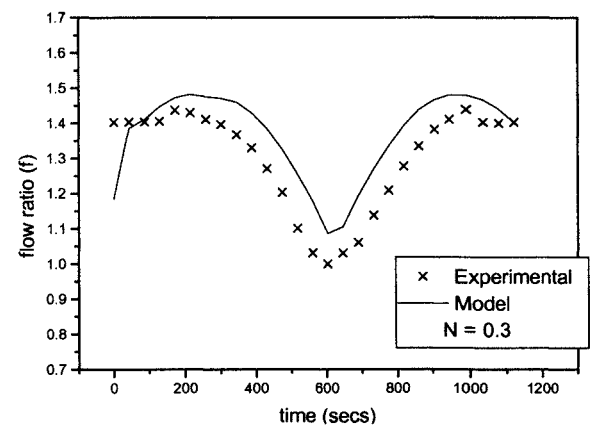


Fig.192: 80mm valve, model version 3.0,  
let-by = 0.05% inlet port and linear bypass port  
 $k = 4.5$

**Figures 193 - 200. Comparisons of Integrals of Absolute Error for Valve Models**

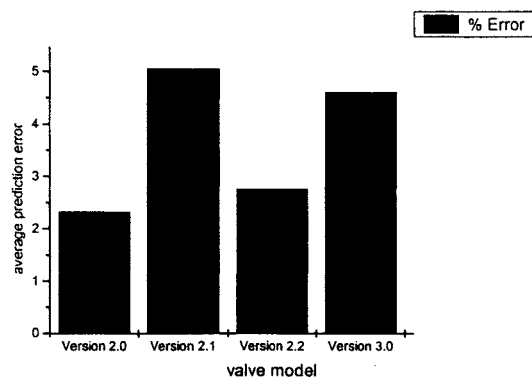


Fig.193: 40mm valve,  $N = 0.3$   
Average percentage prediction error over time

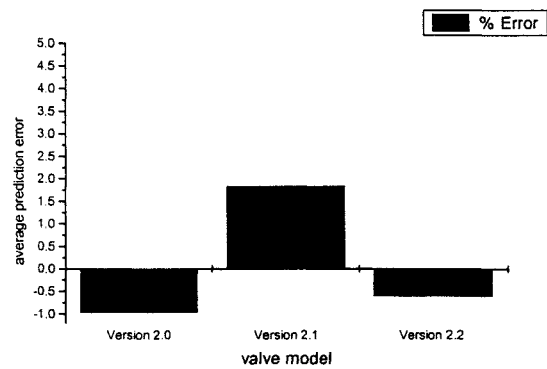


Fig.194: 40mm valve,  $N = 0.5$   
Average percentage prediction error over time

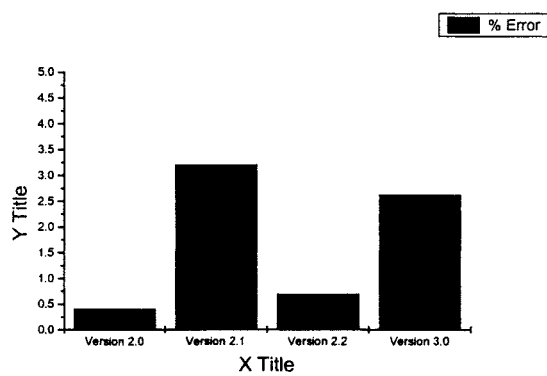


Fig.195: 50mm valve,  $N = 0.3$   
Average percentage prediction error over time

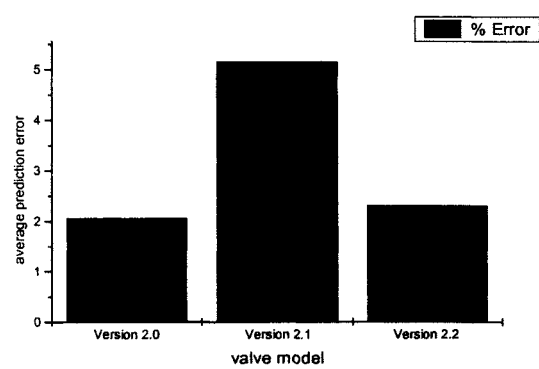


Fig.196: 50mm valve,  $N = 0.5$   
Average percentage prediction error over time

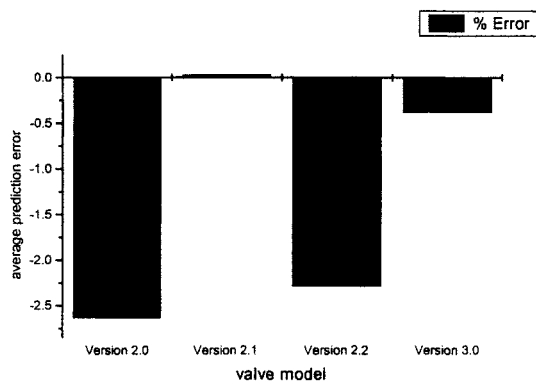


Fig.197: 65mm valve,  $N = 0.3$   
Average percentage prediction error over time

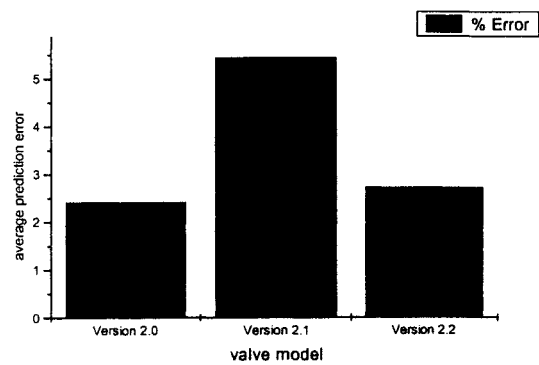


Fig.198: 65mm valve,  $N = 0.5$   
Average percentage prediction error over time

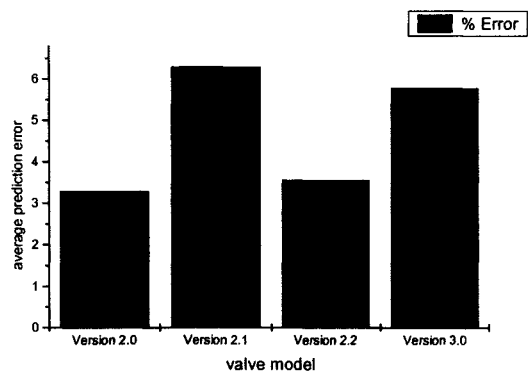


Fig.199: 80mm valve, N = 0.3  
Average percentage prediction error over time

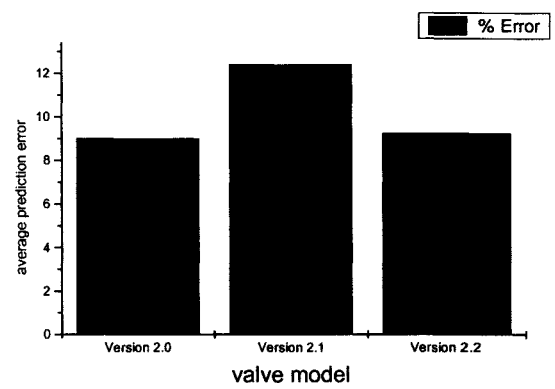
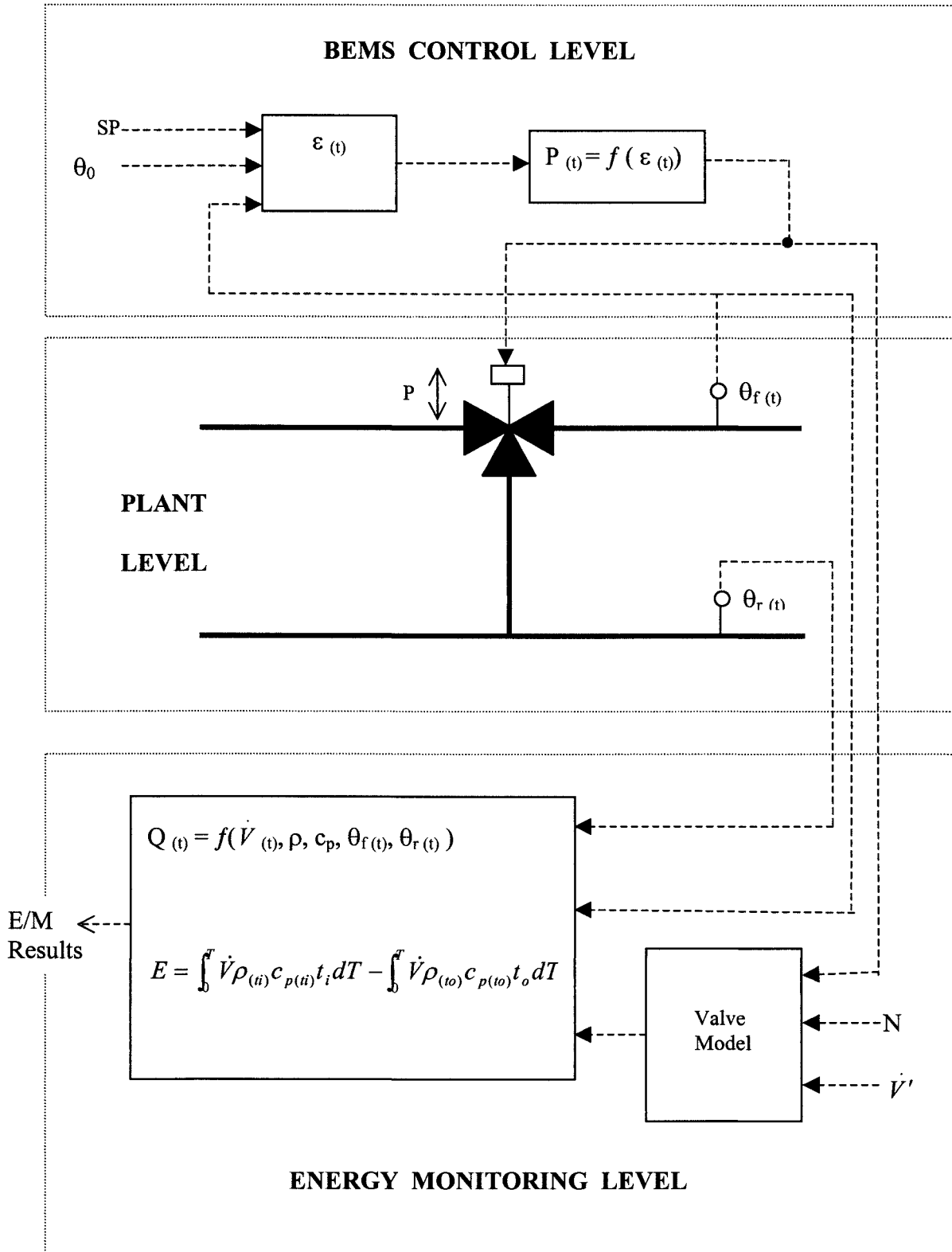


Fig.200: 80mm valve, N = 0.5  
Average percentage prediction error over time

**Figure 201: Energy Demand Algorithm.**

## Tables



**Table 2: Comparison of Fitted and Predicted  $R^2$  values**

Valve	$R^2_{\text{fitted}}$ (Upstroke)	$R^2_{\text{fitted}}$ (Downstroke)	$R^2_{\text{fitted}}$ (Average)
80mm (N = 0.3)	0.99867	0.99943	0.99905
80mm (N = 0.5)	0.99884	0.99955	0.99919
65mm (N = 0.3)	0.99961	0.99329	0.99645
65mm (N = 0.5)	0.99987	0.99686	0.99836
50mm (N = 0.3)	0.9981	0.99719	0.99764
50mm (N = 0.5)	0.99537	0.99777	0.99657
40mm (N = 0.3)	0.099795	0.99858	0.99826
40mm (N = 0.5)	0.99931	0.98988	0.99459

## References

1. CIBSE Guide, Energy Efficiency in Buildings, 1998.
2. Energy Efficiency Office. Energy efficiency in Buildings - Offices. March 1989
3. Santangelo, F.J. A current energy assessment for the industrial user. Conf. Advances in energy cost savings for industry and buildings. 6<sup>th</sup> World Energy Engineering Congress, Atlanta, U.S.A. 1983, p. 27-30. Conf. Code 06174.
4. Graves, P.T. Developing and monitoring a corporate energy management program. In: Annual Textile, Fibre and Film Industry Tech. Conf., Charlotte, NC, USA. Conf. code 16962. IEEE 1992.
5. Lyberg, M.D., Fracastoro G.V. An overview of the guiding principles concerning design of experiments, instrumentation and measurement techniques. Report from IEA Annex III: Residential Building Energy Analysis. The Swedish Council for Building Research, Document D11 : 1983.
6. Olsen, J.A. Hydronics and Control Valve Selection. ASHRAE Transactions vol. 80, pt. 2, 1980, p. 157-166, (No. 2597).
7. Huusom, J. An Electromagnetic Flow Meter Especially Designed for Flow Measuring of Heat Conveying Fluids. Flomeko Proc., Budapest, October 1983.
8. BRE Report. An environmental assessment for new office designs. BREEAM Version1/90. 1990
9. Department of the Environment, Transport and the Regions, Climate Change: Action to Tackle Global Warming, URL:<http://www.environment.detr.gov.uk/ga/01.htm>
10. Shavit, G., Spethman, D. A Dynamic Simulation Analysis of Alternate Control Strategies for a Typical Office Building. In: Proceedings of a Conference on Performance of HVAC Systems. West Lafayette, Purdue University, April 1976.
11. Miller, D.E. A Simulation to Study HVAC Process Dynamics. ASHRAE Transactions, vol. 88, pt. 2, 1982, p.809-825, (TO-82-6).
12. Bowman, N.T., Lomas, K.J. Empirical validation of dynamic thermal computer models of buildings. Building Services Engineering Research and Technology, vol. 6, No. 4. 1985.

13. Bloomfield, D. Appraisal techniques for methods of calculating the thermal performance of buildings. Building Services Engineering Research and Technology, vol. 6, No. 1. 1985.
14. Diamond, S.C., Hunn, B.D. Comparison of DOE-2 Computer Program Simulation to Metered Data for Seven Commercial Buildings. ASHRAE Transactions, vol. 87, pt. 1, 1981, p. 1222-1231, (CH-81-18).
15. Yuill, G.K., Philips, E.G. Comparison of BLAST Program Predictions with Energy Consumption's of Two Buildings. ASHRAE Transactions, vol. 87, pt. 1, 1981, p. 1200-1206, (CH-81-18).
16. Riegel, R.J., Windheim, L.S, Shanus, M.D. The use of DOE2.1 as an interactive design/analysis tool. IEEE 1992. Annual Textile, Fibre and Film Industry Tech. Conf., Charlotte, NC, USA, Conf. code 16962.
17. Lomas, K.J. Availability of monitored hourly building performance data for validating dynamic thermal models of buildings. Building Services Engineering Research and Technology, vol. 12, No. 2. 1991.
18. Mazzuchi, R.P. Design of a Large Scale Metering Project. In: Proc. National Workshop on Field Data Acquisition for Building and Equipment Energy Use Monitoring, Oak Ridge National Laboratory, Oak Ridge, TN, (1986).
19. Bisesi, P.J. Energy conservation through testing, adjusting and balancing. Conf. Advances in energy cost savings for industry and buildings. 6<sup>th</sup> World Energy Engineering Congress, Atlanta, U.S.A. 1983, p. 87-89, Conf. Code 06174.
20. Stebbins W.L. Highly efficient energy metering and trend analysis techniques for maximum control. IEEE Annual Textile, Fibre and Film Industry Tech. Conf., Charlotte, NC, USA, 1992. Conf. code 16962.
21. Harje, D., Gadsby, K.J. Diagnostics of energy related building problems using today's technologies. Energy Technology: Proc. of the Energy Technology Conference, 1984, p. 364-374.
22. Haberl, J., Watt, J. Thermal energy measurement with tangential paddle wheel flow meters. Solar Engineering, vol. 12. ASME 1995.
23. Hegburg, R.A. Monitoring Systems for Heating and Cooling Energy Allocation in Multiple Occupancy Dwellings. ASHRAE Transactions, vol. 95, pt. 1, 1989, p. 798-805, (CH-89-10-2).

24. McClelland, L. Encouraging Energy Conservation in Multi-Family Housing: RUBS and Other Methods of Allocating Energy Costs to Residents. Inst. of Behavioural Science, Univ. of Colorado, Boulder. 1980.
25. Goettling, D.R., Kuppler, F. Latest European Developments in the Field of Electronic Allocation of Costs by Hydronic Systems. ASHRAE Transactions, vol.87, Part2 . 1981.
26. Hewett, M.J., Emslander, H.L., Koehler, M.J. Heating Cost Allocation in Centrally Heated Rental Housing: Energy Conservation Potential and Standard Issues. Minneapolis Energy Office (Joint Research with MINNE GASCO). 1986.
27. Fisk, D.J., Eastwell, A.S. Field Performance of Evaporative Heat Metering in District Heating Schemes. BRE Report. 1981.
28. Fisk, D.J., Jebson, D.A. Influence of heat metering on district heating scheme consumption. Building Services Engineering Research and Technology, vol. 5, No. 3. 1984.
29. Heinemeier, K.E., Akbari, H. Capabilities of In-Place EMS for Remote Monitoring of Building Energy Performance - Case Studies. ASHRAE Transactions, vol. 93, pt. 2, 1987, p. 2321-2336, (NT-87-28-1).
30. Hurley, C.W. Measurement of Temperature, Humidity and Fluid Flow. National Bureau of Standards.
31. Stebbins, W.L. Utility monitoring and reporting systems: key to successful energy management. In: Advances in energy cost savings for industry and buildings. 6th World Energy Engineering Congress, Atlanta, U.S.A. 1983, Association of energy engineers, conf. code 06174.
32. Guinn, G.R., Hummer, L.L. Testing and Evaluation of Btu Meters for Measuring Solar System Performance. ASHRAE Trans. vol.88, Part 2, 1982, pp338-401.
33. Guinn, G.R., Quick, R. Experiences with Heat Meters for Evaluating the Performance of Active Solar Energy Systems. ASHRAE Transactions, vol. 93, pt. 1, 1987, p. 310-326, (No. 3033).
34. Talbert, S.G. et al. Evaluation of Thermal Energy Meters as Energy Allocation Devices. ASHRAE Transactions, vol. 99, pt. 1, 1993, p. 873-879, (CH-93-6-1).
35. Westergren, Karl-Erik; Hogberg, Hans; Norlen, Urban Monitoring energy consumption in single-family houses, Energy and Buildings, Volume 29, Issue 3, March 1999, Pages 247-257.

36. Murthy, C.N., Nagaraju, J. Intelligent thermal energy meter cum controller for solar water heating systems, Renewable Energy, Volume 17, Issue 1, May 1999, Pages 123-127.
37. Babus'Haq, R.F., Overgaard, G. and Probert, S.D., Heat-Meter Developments for CHP-DH Networks, Applied Energy, Volume 53, Issues 1-2, 1996, Pages 193-207.
38. BRITISH STANDARDS. BS7405 : 1991. Guide to Selection and Application of flow meters for the measurement of fluid flow in closed conduits.
39. Bertschler, G. Accuracy versus reproducibility in flow metering. In: Productivity Through Control Technology. Proc. of the 1983 Joint symposium, Houston, Texas. Conf. code 04408 87-89.
40. Barnes, G. Pipeline metering with liquid positive displacement and turbine flow meters. Advances in instrumentation, 1984, vol. 39 pt 1 499-506.
41. Grebe, G. Application Considerations for Selecting Flow meters. Advances in instrumentation. 1984 vol.39 no.2, Proc. of the ISA Int. Conf. and Exhib. Houston, Texas. 1984.
42. Mattingly, G.E. Fluid metering at NBS : New research tools and new opportunities. Advances in instrumentation, vol. 39, pt. 2, 1984, p. 1145-1169.
43. Spitzer, D.W. Vortex Shedding Flow meters - A Users perspective. Advances in Instrumentation, vol. 39, pt. 2, 1984, p. 1171-1180.
44. Kayama, N., Witlin, W.G. Effects of Inner Wall Conductivity of Adjacent Connecting pipes on the signal of magnetic flow meters. Energy Processing/Canada, vol. 78, no. 1, 1985, p. 1181-1192.
45. Wilda, D., Arcara, S. Modern Energy Flow Measurement. Advances in Instrumentation, vol. 39, pt. 2, 1984, p. 1345-1349.
46. Seruga, E. Sizing and selecting modern Water Meters. Water/Engineering Management. 1985, vol 132, pt. 8, p. 33-35.
47. Dahlin, E., Franci, A. Practical application of a new coriolis mass flow meter. Orifice plates, wedge elements, averaging pitot tubes, venturi tubes, and flow nozzles are influenced by changing densities. Proc. of the Annual Control Engineering Conference. 1985. p. 200-204.

48. Hickl, E.L., Furness, R.A. Mass Flow Measurement in the 80's. Proc. Ann. Symp. on Instrumentation for the process industries.1985. p. 49-52
49. Miller, R.W. History of flow measurement - Past, present, and future. Proc. Ann. Symp. on Instrumentation for the process industries.1985. p. 67-73.
50. Mattingly G.E. Improving flow measurement performance : Research Techniques and Prospects. INTUIT 1985, vol. 32, pt. 1, p. 57-65.
51. Feller, M.F. New developments in liquid flow and thermal metering. Energy engineering: Jn. of the association of energy engineers. Dec 1986- Jan 1987. vol. 84, Pt 1, p. 16-36.
52. Fuller, W.F. Direct mass flow measurement using the coriolis principle. Australian Journal of instrumentation and control. Series 2. 1987, vol. 2, pt. 2, p. 6-9.
53. Corpron, G.P. Vortex flow meter performance characteristics - Part A : The effect of installation conditions on the performance of a T - Cross section Vortex Flow meter. Experimental uncertainty in Fluid Measurements. FED - Vol.52, Presented at the Winter Annual Meeting of the ASME, Boston, Massachusetts, Dec. 13-18, 1987.
54. Corpron, G.P. Part B : Comparison of Several Vortex flowmeters calibrated in water. low pressure air and high pressure air. Experimental uncertainty in Fluid Measurements. FED - Vol.52, Presented at the Winter Annual Meeting of the ASME, Boston, Massachusetts, Dec. 13-18, 1987.
55. Trimmer, W.L. Ultrasonic flow meter testing. Conf. Planning now for irrigation and drainage in the 21st Century, Lincoln, NE, USA (conf. code 12235), 1988, p. 643-650.
56. Ganni, A., Ibbotson, J. Liquid flowmeter with no moving parts for 0.05 to 200 ML/min. Advances in instrumentation, vol. 43, pt. 3, 1988, p. 1277-1282.
57. Walsh, T.S. Mass flow sensing, data collection and signal processing. Sensors. (Peterborough, NH), vol. 6, pt. 12, 1989, p. 27-34.
58. McConaghy, B.J., Bell, D.G., Studinski, W. How orifice plate condition affects measurement accuracy. Pipeline industry, vol. 71, pt. 6, 1989, p. 21-26.
59. Labs, W. Flow meters. Accuracies are better, prices lower. Chilton's Instruments and Control Systems. Feb. 1990, vol. 63, pt. 2, p. 29-33.

60. Bloom, G. Accurately measuring ultralow flow. Machine Design. 1990, vol. 62, pt. 18, p. 103-107.
61. Schlatter, G.L. Advances in vortex metering technology. INTECH. 1990, vol. 37, pt. 3, p. 44-45.
62. Zaitseva, E.A., Dutchak, V.V., Tarsis, A.D. Increasing the measurement accuracy of electronic heat meters. Measurement Techniques. (English translation of IZMERITEL 'NAYA Tekhnica). June 1991, vol. 34, pt. 1, p. 56-58.
63. Ting, V.C. Effects of non standard operating conditions on the accuracy of orifice meters. In: Proc. SPE Annual Conf. and Exhibition. 1991, vol. pi, pt. 2, p. 479-486.
64. Dall, M., Lowes, L. Application of a portable, non-intrusive ultrasonic flow metering system for enclosed pipes. Australian Journal of Instrumentation and control. 1991, vol. 16, pt. 3, p. 14-25.
65. Gaertner, F., Stark, R. New measuring technology in heat meters. Fernwaerme International. 1991, vol. 20, pt. 11, p. 581-584.
66. Murphy, S. et al. Calibration of on-line circulating water flow measurement devices with an integrated Turbine Metering system. Instrumentation in the power industry. Proc. 1992, vol. 35, p. 583-599.
67. Bennet, J. Fuel metering valve design innovations Aerospace Engineering. 1993, vol.13, pt.10, p. 7-10.
68. Yeh, T.T., Mattingly, G.E. Pipe flow downstream of a reducer and its effects on flow meters. Fluid measurement and instrumentation forum - 1993, presented at the Fluids Engineering Conference, Washington D.C. June 20-24, 1993, ASME Fluids Engineering Division, vol. 161.
69. Ifft, S.A., Mikkelsen, E.D. Pipe elbow effects on the V-cone flow meter. Fluid measurement and instrumentation forum -1993, presented at the Fluids Engineering Conference, Washington D.C., June 20-24, 1993, ASME Fluids Engineering Division, vol. 161.
70. Laws, E.M. The development of a new differential flow measurement device. Fluid measurement and instrumentation forum -1993, presented at the Fluids Engineering Conference, Washington D.C., June 20-24, 1993, ASME Fluids Engineering Division, vol. 161.
71. Flaska, K., Kosla, L. Rotation vanes upstream of pipe elbows improves flow meter accuracy and decreases required straight pipe meter run lengths. Fluid measurement and instrumentation forum -1993, presented at the Fluids Engineering Conference, Washington D.C., June 20-24, 1993, ASME Fluids Engineering Division, vol. 161.

72. Ton, V. et al. Feedwater and condensate flow measurements at Pickering Nuclear Generating Power Station. In: Proceedings Ann. Conf. Canadian Nuclear Association. 1994, vol.1, p. 1-15.
73. Laws, E.M., Duazzane, A.K., Erdal, A. Short Installations for Accurate Orifice Plate Flow Metering. In: ASME FED Publication 1994, Proc. of the ASME FED Summer Meeting, Part 15 (of 18), Lake Tahoe, NV, USA. June 1994, Conf. Code 20869, vol. 93, p. 27-36.
74. Lynch, F., Horciza, E. Flow measurement using low cost portable clamp-on ultrasonic flow meters. In: Jn. Water Power - Proc. of the Int. Conf. on Hydropower. 1995, vol. 1, p. 766-773.
75. Hanson, B.R., Schwankle, L.J. Performance of flow meters on Irrigation Systems. International Water and Irrigation Review. 1995, vol.15, pt. 1, p. 29-31.
76. Parker, B., O'Neil, D.L. Effect of a 90° elbow on the accuracy of a non-magnetic, insertion paddle wheel flow meter. Solar Engineering. ASME 1995, vol. 2, p. 731-740.
77. Krassow, H., Campabadal, F. and Lora-Tamayo, E., The smart-orifice meter: a mini head meter for volume flow measurement, Flow Measurement and Instrumentation, Volume 10, Issue 2, June 1999, Pages 109-115.
78. Carlander, C. and Delsing, J., Installation effects on an ultrasonic flow meter with implications for self diagnostics, Flow Measurement and Instrumentation, Volume 11, Issue 2, June 2000, Pages 109-122.
79. Furness, R.A., Heritage, J.E. Commercially available flow meters and future trends. Measurement and Control, vol. 19, no. 5, 1986, p. 25-35.
80. CIBSE Guide. Volume B. Installation and Equipment Data. 1986.
81. Letherman, K.M. Automatic Controls for Heating and Air Conditioning: principles and applications. Oxford: Pergamon, 1981.
82. Tom, S.T. Control valve and damper sizing. ASHRAE Jn., October 1987, p. 30-34.
83. McVann, D. Control valve performance. Heating, Piping and Air Conditioning, vol. 55, no. 12, 1983, p. 79-81.
84. Thompson, J.G., Chen, P.N.T. Digital Simulation of the effect of Room and Control System Dynamics on Energy Consumption. ASHRAE Trans., vol. 85, pt. 2, 1979.



85. Shavit, G., Brandt, S.G. The Dynamic Performance of a Discharge Air Temperature Control System with a P-I Controller. ASHRAE Trans., vol. 88, pt. 2, p. 826-838, 1982, (TO-82-6).
86. Wapler, M., Pearson, J.T. Investigating the causes of water hammer in a water control valve. ASHRAE Trans., vol. 98, pt. 1, 1992, p. 107-115.
87. Zelenski, R.E., Lund, R.A. An Investigation of a Closed-Loop System for Duct Air Temperature Control. ASHRAE Trans., vol. 74, part 1, 1968.
88. Mehta, D.P. Woods, J.E. An Experimental Validation of a Rational Model for Dynamic Responses of Buildings. ASHRAE Trans., vol. 86, pt. 2, 1980, p. 497-520, (DV-80-4).
89. Hamilton, D.C. A Design Procedure for a Discharge Air Temperature Control System.  
A Thesis Submitted to the Faculty of Purdue University,  
May 1975.
90. Rohmann, C.P., Grogan, E.C. On the Dynamics of Pneumatic Transmission Lines. ASME Trans., Vol.79, 1957.
91. Hamilton, D.C., Leonard, R.G., Pearson, J.T. A System Model for a Discharge Air Temperature Control System. ASHRAE Trans., vol. 83, pt. 1, 1977, p. 257-268, (No.2446 RP143).
92. Hamilton, D.C., Leonard, R.G. Pearson, J.T. Dynamic Response Characteristics of a Discharge Air Temperature Control System at Near Full and Part Heating Load. ASHRAE Trans., vol. 80, pt. 1, 1974, (No.2303).
93. Mehta, D.P., Kharsa, J.E. Influence of proportional control dynamics on energy consumption in environmental control systems.  
IEEE Annual Textile, Fibre and Film Industry Tech. Conf., Charlotte, NC, USA, 1992, Conf. code 16962.
94. Thompson, J.G. The Effect of Room and Control System Dynamics on Energy Consumption. ASHRAE Trans., vol. 87, pt. 2, 1981, p. 883-896, (CH-81-9 No.2).
95. Thompson, J.G., Kohr, R.H. Modelling and Compensation of Non-linear Systems Using Sensitivity Analysis. Transactions of ASME, Journal of Basic Engineering, Vol. 90, No.2, 1968.
96. Stoecker, W.F. et al. Stability of an Air-Temperature Control Loop. ASHRAE Trans., Vol. 84, Part 2, 1978.

97. Stoecker, W.F., Daber, R.P. Conserving Energy in Dual Duct System by Reducing the Throttling Ranges of Air Temperature Controllers. ASHRAE Trans., vol. 84, pt. 1, 1978.
98. May, W.B., Borresen, B.A., Hurley, C.W. Direct Digital Control of a Pneumatically Actuated Air-Handling Unit. ASHRAE Trans., vol. 88, pt. 2, 1982, p. 857-874, (TO-82-6 No.4).
99. Hill, C.R. Simulation of a Multi Zone Air Handler. ASHRAE Trans., vol. 91, pt. 1B, 1985, p. 752-765, (CH-85-16 No.2).
100. Clark, D.R., Hurley, C.W. Hill, C.R. Dynamic Models for HVAC System Components. ASHRAE Trans., vol. 91, pt. 1B, 1985, p. 737-751, (CH-85-16 No.1).
101. Clark, D.R., Borresen, B.A. Dynamics of a heating control loop. In: Proc. International Symposium on the Performance of HVAC Control Systems in Buildings. Building Research Establishment, Garston, June 18-19<sup>th</sup>, 1984.
102. Hittle, D.C., Birtles, A.B. Control of Supply Water Temperature from Boilers and Steam-to-Hot-Water Converters. ASHRAE Trans., vol. 91, pt. 2A, 1985, p. 630-641, (No.2932).
103. Murray, M.A.P., Hanby, V.I. Component based simulation of HVAC systems. Proc. CIBS Technical Conference. 1985, p. 46-56.
104. Agnon, S. Analyzing Flow Conditions in Integrated Loop Systems ASHRAE Trans., vol. 88, pt. 1, 1982, p. 211-226, (No.2675).
105. Underwood, D.M. Resonse of Self-Tuning Single-Loop Digital Controllers to a Computer Simulated Heating Coil. ASHRAE Trans., vol. 95, pt. 2, 1989, p. 424-430, (VA-89-1-2).
106. Underwood, D.M., Crawford, R.R. Dynamic Non-Linear Modelling of a Hot-Water-to-Air Heat Exchanger for Control Applications. ASHRAE Trans., vol. 97, pt. 1, p. 149-155, (Research 3452).
107. Balasubrumanian, G.R. How to modify a control valve to meter liquid flow. Plant Engineering, vol. 40, no. 9, 1986, p. 60-61.
108. Pyotsia, J. Mathematical model of a control valve. Advances in Instrumentation, proc., vol. 47, pt. 2, 1992, p. 1341-1353.
109. Fujiwara, M., Kuroda, M., Shiga, T. Intelligent Valve Positioner employing new control method. Fluid control and measurement, Tokyo, Japan, Sept. 1985., Conf. code 10300, 1986, vol. 1, p. 101-106.

110. McInnis, Duncan A.; Karney, Bryan W.; Axworthy, David H., Efficient valve representation in fixed-grid characteristics method, Journal of Hydraulic Engineering, Volume 123, Issue 8, August 1997, Pages 709-717.
111. Coughran, M.T., Measuring the installed dead band of control valves, ISA Transactions, Volume 37, Issue 3, July 1998, Pages 147-154.
112. Wilton, S.R., Control valves and process variability, ISA Transactions, Volume 39, Issue 2, April 2000, Pages 265-271.
113. Champagne, R.P. and Boyle, S.J., Optimizing valve actuator parameters to enhance control valve performance, ISA Transactions, Volume 35, Issue 3, 1996, Pages 217-223.
114. Atmanand, M.A.; Konnur, M.S. Novel method of using a control valve for measurement and control of flow, IEEE Transactions on Instrumentation and Measurement, Volume 48, Issue 6, December 1999, Pages 1224-1226.
115. Weber, T.W. An Introduction to Process Dynamics and Control. Wiley-Interscience, 1973.
116. Underwood, C.P., Edge, J.S. Flow characteristics in circuits using three-port modulating control valves. Building Services Engineering Science and Technology. Vol. 16, no. 3, 1995, 127-132.
117. Johnson Controls, Valve and Actuator Manual 977, Valve Product Information Section, Product Bulletin VC, Issue Date 0596, Johnson Controls Inc., 1996, Page 3.
118. Johnson Controls Inc., Manufacturers data for valve series VP-7016, Catalogue Section D, (0185), valve series 5016, Catalogue Section V, (0881), and valve series V-5010, Catalogue section D, (1284).
119. British Standards, BS5793 : Industrial Process Control Valves, Parts 1 and 2, London : British Standards Institution, 1989.
120. British Standards, BS1042 ; Methods of Measurement of Fluid Flow in Closed Conduits, London : British Standards Institution, 1989.
121. Montgomery, D.C., Peck, E.A. Introduction to Linear Regression Analysis. Pub. Wiley 1982.
122. Johnson Controls Inc., Manufacturers data for EP-8000 Electro-pneumatic Transducer.
123. CIBSE, Code W : 1994, Commissioning Code, Water Distribution Systems. August 1994. The Chartered Institute of Building Services Engineers, London.

## **Appendices**

**Appendix 1.****Table A1: Group designations of flow meters.**

The extract from BS7405: 1991 is reproduced with the permission of BSI under licence number 2000/SK0511.

Group designations of flow meters	
Group	Metering technology
1	<i>Conventional differential pressure types</i> Sharp edged concentric orifice (corner tapping, D and D/2 pressure tapping and flange tapping designs) Venturi tubes (classical venturi tube and venturi-nozzle) Flow nozzles (ISA and long radius designs)
2	<i>Other differential types</i> Annular orifice Eccentric or segmental orifice Integral orifice Gentile tube Spring loaded aperture meters Elbow meter Linear resistance meter Dall tube Proprietary flow nozzles Multi-port averaging pitots Wedge Meter Pitot tube Variable area flow meter Target meter Sonic nozzles Conical entrance and ¼ circle orifice plates
3	<i>Positive displacement types</i> Reciprocating piston Sliding Vane Nutating disc Bi- and Tri-rotor designs Roots type meters Diaphragm meters Rotary piston Oval gear Helical rotor meter Liquid metering pumps Wet gas meters Bellows meters
4	<i>Rotary turbine type meters</i> Axial turbine meter Mechanical helix meter Bearingless turbine Propeller meters Insertion turbine Twin rotor turbine meter Multi jet or vane type meter Pelton wheels Cup anemometers

**Table A1: Group designations of flow meters.**

The extract from BS7405: 1991 is reproduced with the permission of BSI under licence number 2000/SK0511.

Group designations of flow meters	
Group	Metering Technology
5	<i>Fluid Oscillatory Types</i> Vortex shedding meter Swirlmeter Insertion vortex Fluidic oscillator Fluid deflection meter
6	<i>Electromagnetic types</i> a.c. types d.c. types Velocity probe types
7	<i>Ultrasonic types</i> Time-of-flight meters Sing-around Reflex meters Doppler meters Long wave acoustic
8	<i>Direct and indirect mass types</i> Indirect methods Angular momentum turbine Parallel venturi Gyroscopic meter Driven angular momentum Coriolis type Wheatstone bridge
9	<i>Thermal types</i> Heat loss types Hot wire film anemometers Thermal profile meters Calorimetric heat grid
10	<i>Miscellaneous types</i> Cross correlation meters Nuclear magnetic resonance Gas ionization Laser anemometer Tracer injection meters Weighting methods Velocity area techniques

## **Appendix 2**

## Appendix 2. Derivation of Valve and Circuit Model

Allowing for let-by, the inherent characteristic for the linear valve can be expressed as follows (figure 2):

$$\text{Linear, } G_{inh} = G_o + P.(1 - G_o) \dots\dots\dots(A1)$$

For the equal percentage case, equal increments of valve position will produce equal ratios of flow. Thus for an equal percentage valve under constant pressure conditions:

$$\frac{dG_{inh}}{G_{inh}} \propto dP$$

Introducing the proportionality constant  $c$  :

$$\frac{dG_{inh}}{G_{inh}} = cdP \dots\dots\dots(A2)$$

For a general solution with allowance for let-by:

$$\int_{G_o}^{G_o \leq G_{inh} \leq 1} \frac{dG_{inh}}{G_{inh}} = c \int_0^{0 \leq P \leq 1} dP \dots\dots\dots(A3)$$

From which:

$$\ln(G_{inh}) - \ln(G_o) = cP \dots\dots\dots(A4)$$

From the condition  $P = 1$ , when  $G_{inh} = 1$  :

$$c = -\ln(G_o),$$



i.e.,

$$G_{inh} = \exp[(1 - P) \ln G_0] \dots\dots\dots (A5)$$

Which reduces to :

$$G_{inh} = G_0^{(1-P)} \dots\dots\dots (A6)$$

The installed characteristic can now be derived; refer to the generalised circuit of figure 5. First the authority can be expressed as :

$$N = \frac{\Delta p'_v}{\Delta p'_v + \Delta p'_s} \dots\dots\dots (A7)$$

Assuming that the pressure developments around the circuit can be related to the square of the volume flow rate :

$$\frac{\Delta p_s}{\Delta p'_s} = \left( \frac{\dot{V}}{\dot{V}'} \right)^2 \dots\dots\dots (A8)$$

for the system, and :

$$\frac{\Delta p_v}{\Delta p'_v} = \left( \frac{\dot{V}}{\dot{V}'} \right)^2 \left( \frac{\dot{V}'_{inh}}{\dot{V}_{inh}} \right)^2 \dots\dots\dots (A9)$$

for the valve, where  $\dot{V}_{inh}$  refers to the inherent throughput of the valve.

It is required that the pressure drop across the valve and connecting circuit path remain constant under all conditions if the valve is to perform correctly, so that :

$$\Delta p_v + \Delta p_s = \Delta p'_v + \Delta p'_s = \left[ \Delta p'_s + \Delta p'_v \left( \frac{\dot{V}'_{inh}}{\dot{V}_{inh}} \right)^2 \right] \left( \frac{\dot{V}}{\dot{V}'} \right)^2 \dots\dots\dots(A10)$$

Noting that :

$$G_{inh} = \frac{\dot{V}_{inh}}{\dot{V}'_{inh}}$$

and

$$G_{ins} = \frac{\dot{V}}{\dot{V}'}$$

and that,

$$\Delta p'_s = \Delta p'_v \left( \frac{1-N}{N} \right),$$

then by substitution in equation A10 the installed characteristic can be expressed:

$$G_{ins} = \frac{1}{\left[ 1 + N \left( \frac{1}{G_{inh}^2} - 1 \right) \right]^{1/2}} \dots\dots\dots(A11)$$

**Appendix 3 : Research Paper by Dr. C.P. Underwood and J.S. Edge as part of  
This Work**

**Summary** This work has sought to identify the nature of the total flow characteristic in circuits controlled by three-port modulating valves. A theoretical model has been developed and compared with a small family of three-port control valves. The influence of valve signal/flow hysteresis error has been quantified, though no account was taken of valve wear. Good potential for the use of control valves as passive flow monitors has been identified, though further work is required to evolve a practical solution for this. The agreement between experimental data and theoretical results is encouraging, suggesting that a model has potential for use where measurements of valve performance are unavailable. The influence of signal/flow hysteresis was found to be insignificant.

## Flow characteristics in circuits using three-port modulating control valves

C P Underwood BSc PhD CEng MCIBSE and J S Edge BSc

Department of the Built Environment, University of Northumbria at Newcastle, Ellison Buildings, Ellison Place, Newcastle upon Tyne NE1 8ST, UK.

Received 23 May 1994, in final form 6 April 1995

### List of symbols

$G_{inh}$	Inherent valve flow fraction
$G_0$	Valve let-by flow fraction
$G_{ins}$	Installed valve flow fraction
$P$	Valve stem (and inlet port plug) position (fraction)
$P_{bypass}$	Bypass port plug position (fraction)
$c$	Equal-percentage valve constant
$N$	Valve authority (fraction)
$\Delta p'_v$	Valve pressure drop at fully open (designated) position ( $Nm^{-2}$ )
$\Delta p'_s$	Design pressure drop in that part of circuit influenced by the valve ( $Nm^{-2}$ )
$\Delta p_v$	Valve pressure drop ( $Nm^{-2}$ )
$\Delta p_s$	Circuit pressure drop ( $Nm^{-2}$ )
$\dot{V}_{inh}$	Valve inherent volume flow rate ( $m^3s^{-1}$ )
$\dot{V}'_{inh}$	Valve inherent volume flow rate at fully open (design rated) position ( $m^3s^{-1}$ )
$\dot{V}$	Circuit volume flow rate ( $m^3s^{-1}$ )
$\dot{V}'$	Circuit volume flow rate at design conditions ( $m^3s^{-1}$ )
$S$	Incoming control signal (fraction)
HYS	Valve stem/positioning mechanism hysteresis error (fraction)
$\Delta SP$	Slack in valve positioning mechanism (fraction)
$G_{ins(inlet, S)}$	Inlet port installed characteristic at control signal $S$ (fraction)
$G_{ins(bypass, S)}$	Bypass port installed characteristic at control signal $S$ (fraction)
$\dot{V}_{(inlet, S)}$	Inlet port volume flow rate at control signal $S$ ( $m^3s^{-1}$ )
$\dot{V}_{(bypass, S)}$	Bypass port volume flow rate at control signal $S$ ( $m^3s^{-1}$ )
$\dot{V}_{(combined, S)}$	Combined port volume flow rate at control signal $S$ ( $m^3s^{-1}$ )
$\Sigma G$	Combined circuit flow ratio

### 1 Introduction

Control valves are used extensively in the building services industry for applications covering flow isolation,

flow regulation and flow control in liquid and gas services. In this work, the influence on total circuit flow of three-port modulating valves connected to achieve 'diverting' and 'mixing' capacity control of heat emission processes has been investigated.

Three-port valves are widely used to control the capacity of hot water heating and chilled water cooling coils and other emission devices in UK buildings. Mostly, these valves are designed as mixing valves having two inlet ports and one outlet such that, with correct connection arrangements, variable-flow constant temperature control or variable-temperature constant flow control can be realised with respect to the emission device<sup>(1)</sup>.

These valves have inlet ports 'characterised' so that the relationship they exhibit between flow delivered and stem position attempts to offset the essentially non-linear characteristic between flow and heat emission of the heat exchange device. This represents a valve's *inherent characteristic* and, depending on the manufacturer, will be of a linear or equal-percentage form (Appendix 1, Figure A1). In turn, the bypass port is also characterised to ensure that the flow rate in the non-controlled part of the circuit remains constant, though in practice this can rarely be achieved. In practice the *installed characteristic* achieved by a valve depends on its inherent characteristic and the pressure drop across the valve<sup>(2)</sup>.

The effect of the installed characteristic of the valve on the overall flow characteristic of the circuit, and the potential use of this information for flow monitoring, forms the basis of the work reported here.

### 2 Previous work on control valve performance

Early work on control valve performance related to heating and air conditioning applications was due to Hamilton *et al.*<sup>(3)</sup> as part of an investigation into a discharge air temperature control system of a heating coil. Linear and equal-percentage two-port pneumatically actuated control valves were compared in an otherwise conventional duct-mounted hot water heating coil system. This work identified poor control with the linear valve at part load when compared with the equal-

percentage valve, though at near full load, control with the linear valve was marginally better than with the equal-percentage valve.

In a departure from what has become established UK practice, Clark *et al.*<sup>(4)</sup> considered the performance of coil control in a configuration similar to that investigated by Hamilton, but in which a three-port control valve was connected to mix with respect to the load—thereby achieving variable water flow temperature at constant flow rate. The work concluded that the combination of valve pressure drop, and the characteristics of both the inlet and bypass ports were critical. Valves with equal percentage/equal percentage characteristics were found to be unsuitable for this application. For slow-responding systems, valves with high authority (i.e.  $N > 0.5$ ) and equal-percentage/linear characteristics should be used, whilst for fast-responding systems, high authority and linear/linear characteristics should be used.

Reporting on the choice of valve characteristics for a variety of general control applications (not specific to heating and air conditioning cases), Siemers<sup>(5)</sup> concluded that the choice of inherent flow characteristic be determined from two control loop parameters—the loop gain and the time constant of control action. This, to some extent, agreed with the more specialist findings of Hamilton when comparing linear and equal percentage valves for the same control application.

### 3 Development of a control valve model

Mathematical models of control valves for liquids are generally based on expressing the relationship between the flow rate passed by the valve and the position of the valve stem—the so called *valve characteristic*. The inherent characteristic of a valve expresses its idealised performance in the absence of accompanying system pressure fluctuations. This is then used to express the valve's installed characteristic which includes these associated system effects. In this work, the *let-by* (i.e. leakage across the valve seat at nominal closure) and *hysteresis* (i.e. error between the positioning signal and actual stem position due, mainly, to mechanical freedom in the actuator and stem linkage mechanism) are also accounted for.

The installed flow characteristic, expressed as the fraction of flow passed by the valve at some position to that flow at the fully open position, can be related to the inherent flow characteristic with reference to a single valve port using the following expression the detailed derivation of which can be found in Appendix 1,

$$G_{ins} = \frac{1}{\left[1 + N \left( \frac{1}{G_{inh}^2} - 1 \right)\right]^{1/2}} \quad (1)$$

In the practical three-port valve case, as depicted in the generalised circuit layout of Figure 1, the valve authority,  $N$ , is calculated from equation A7 (Appendix 1) and will be the same for both inlet and bypass ports, assuming that the circuit is properly balanced during commissioning. Thus, in Figure 1 the system pressure drop,  $\Delta p_s$ , is the same for the inlet sub-circuit and the bypass sub-circuit. Equally, the valve pressure drop,  $\Delta p_v$ , is the same for both inlet port and bypass port paths.  $P$  is determined from the incoming control signal

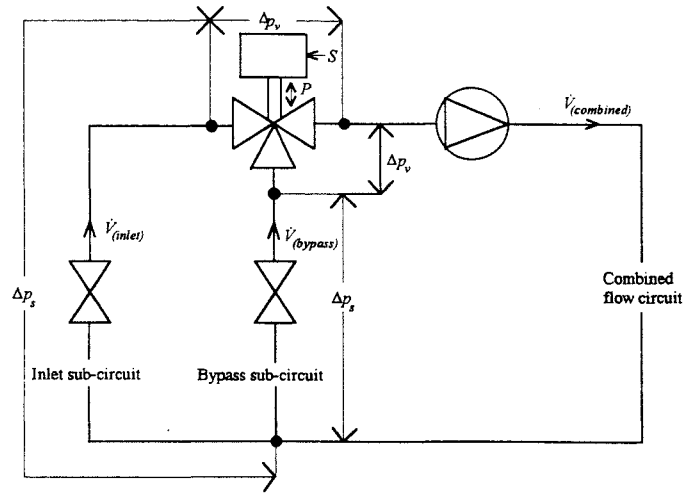


Figure 1 Generalised circuit layout

and the hysteresis of the valve and actuator linkage mechanism (from equations A13, A14 or A15—Appendix 1) and is relative to the inlet port of the valve. For the bypass port,  $P_{bypass} = 1 - P$ . The inherent flow characteristics, expressed as the fraction of flow passed by the valve to the maximum passed when fully open and are clearly position dependent, are then determined using the appropriate combination of equations A1 and A6 (Appendix 1) for the two ports and, finally, the installed characteristic can then be obtained.

The flow rate balance of the valve as a function of incoming control signal is then given as follows:

$$\dot{V}_{inlet, S} = \dot{V}' G_{ins(inlet, S)} \quad (2)$$

$$\dot{V}_{bypass, S} = \dot{V}' G_{ins(bypass, S)} \quad (3)$$

and

$$\dot{V}_{combined, S} = \dot{V}_{inlet, S} + \dot{V}_{bypass, S} \quad (4)$$

Finally, the combined circuit flow ratio:

$$\Sigma G = G_{ins(inlet, S)} + G_{ins(bypass, S)} \quad (5)$$

### 4 Experimental valve test facility

An experimental rig was developed in order to verify the installed total flow performance of a number of 'typical' three port control valves and to compare these results with those obtained from the theoretical model described earlier.

The rig, constructed in 80 mm nominal bore welded mild steel, was equipped with an orifice plate on each of the test valve ports, as shown in Figure 2. The rig was constructed in accordance with BS5793<sup>(7)</sup> for valve testing. The orifice plates conformed to BS1042<sup>(8)</sup>, and each connected to a mercury manometer via upstream and downstream pressure tappings.

Four three-port pneumatically actuated valves were tested—40 mm and 50 mm nominal bore Johnson figure no. V5816 valves, and 65 mm and 80 mm nominal bore Johnson figure no. 5810 valves. All valves were manufactured with linear/linear inherent characteristics and let-by rates of 0.05% of design rated flow. The signal range of all valves tested was 0.62 bar (9 psi)–1.24 bar (18 psi).

The following test procedure was adopted:

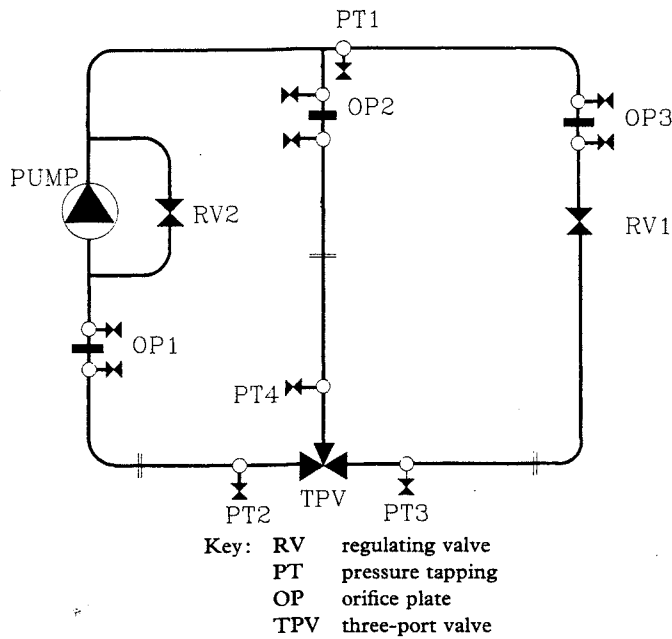


Figure 2 Valve test rig layout

- 1 Each test valve was connected into the rig in the position shown in Figure 2, and an instrument air supply connection made.
- 2 A circulating water flow (at room temperature) appropriate to the valve capacity under test was established,

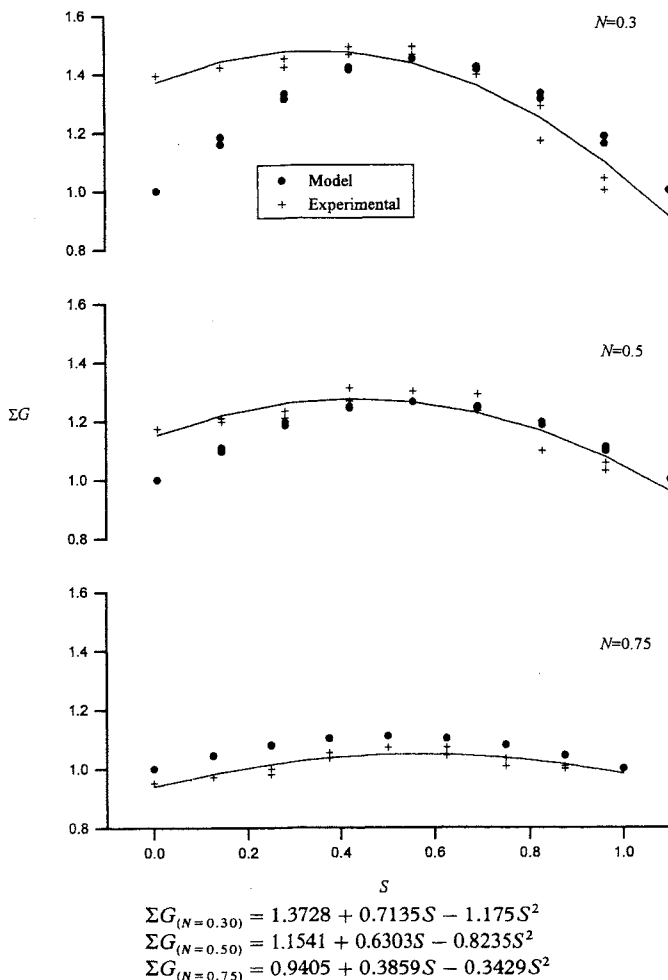


Figure 3 Combined circuit flow ratios for the 40 mm test valve

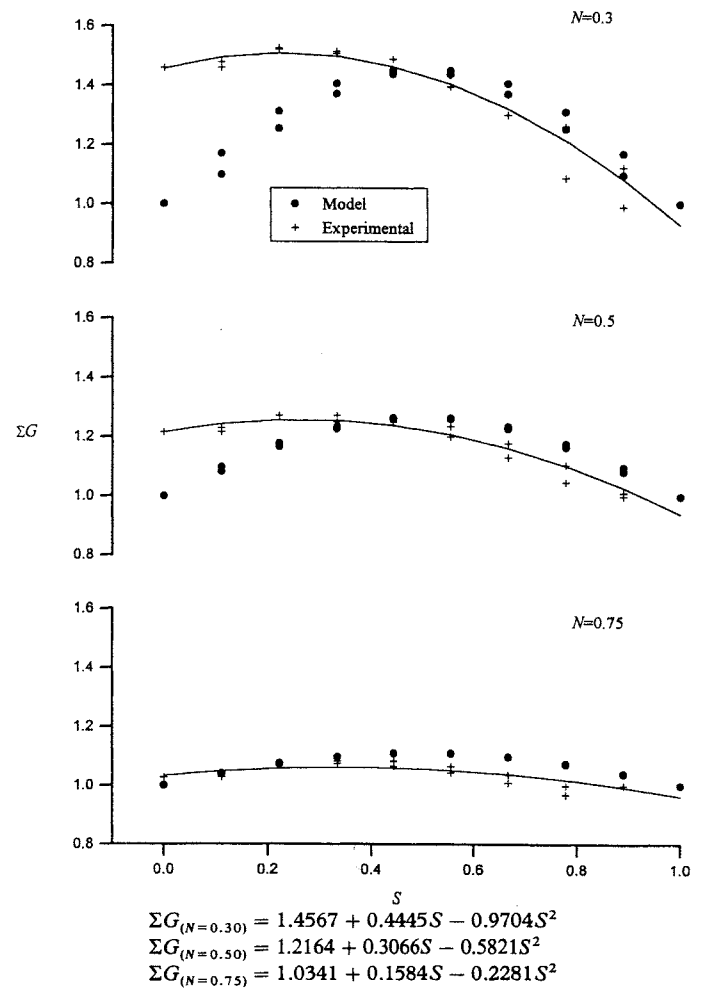


Figure 4 Combined circuit flow ratios for the 50 mm test valve

established, by adjusting the pump regulating valve, and a control air pressure signal was applied, corresponding to the fully open position of the valve. The controlled circuit regulating valve was adjusted until pressure losses across the valve and the controlled circuit were consistent with an appropriate test case valve authority. Results were generally conducted at valve authorities of 0.3–0.75, consistent with a range of what might be expected to be good practice<sup>(1)</sup>, though in the case of the 65 mm valve the maximum authority that could be achieved by the rig was 0.73 and, for the 80 mm valve, 0.58.

- 3 The valve was positioned at small equal increments of control air signal pressure until the inlet port was fully closed and then returned to the fully open position at the same values of signal pressure. Flow rates from orifice plate pressure losses were deduced at each increment. By this process, it was possible to measure any hysteresis error between the valve stem and the incoming control signal, as well as to obtain the actual installed characteristic of each valve as a function of valve authority.

## 5 Results

Results of circuit total flow characteristics obtained using the valve model are compared with those measured from the experimental rig in Figures 3–6.

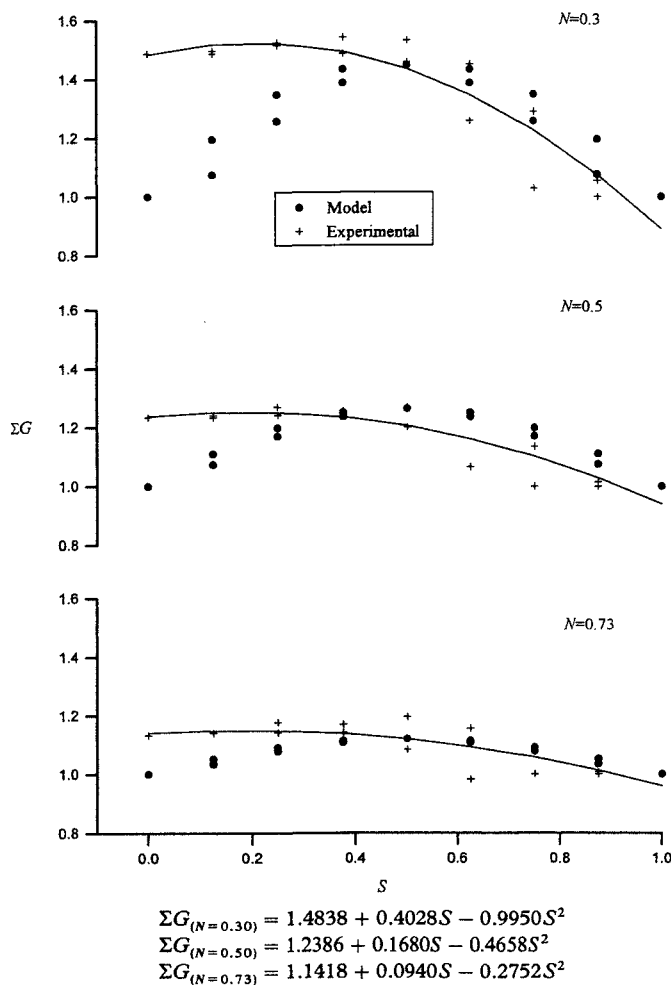


Figure 5 Combined circuit flow ratios for the 65 mm test valve

A second-order polynomial was found to give excellent fit to all experimental data. This form of expression was thus fitted to all experimental results and has been superimposed (in solid line) on all results shown.

The following conclusions can be drawn:

- From theoretical and experimental results, the overall circuit characteristic tends towards unity with increasing valve authority, though this is much more marked with the smaller bore valves considered. At a valve authority of 0.5, which would generally be considered good practice, elevations in flow of up to 20% of the nominal design circuit flow rate can be expected.
- Hysteresis errors were, in general, found to reduce with increasing valve authority. Mean absolute hysteresis errors were found to be 1.2% (40 mm valve), 2.6% (50 mm valve), 5.6% (65 mm valve) and 1.8% (80 mm valve). Hence, with the exception of the 65 mm valve, mean absolute hysteresis errors were below 3% of the nominal circuit design flow rate, suggesting that, for pneumatic valves, hysteresis effects in relation to the total circuit flow characteristic are not significant.
- For all valves tested, and at all values of valve authority investigated, a second-order relationship could be fitted to the experimental data describing total circuit flow with correlation coefficients of better than 0.8–0.9 (4 cases) and 0.9–0.97 (8 cases). This confirms that, for cases where practical valve

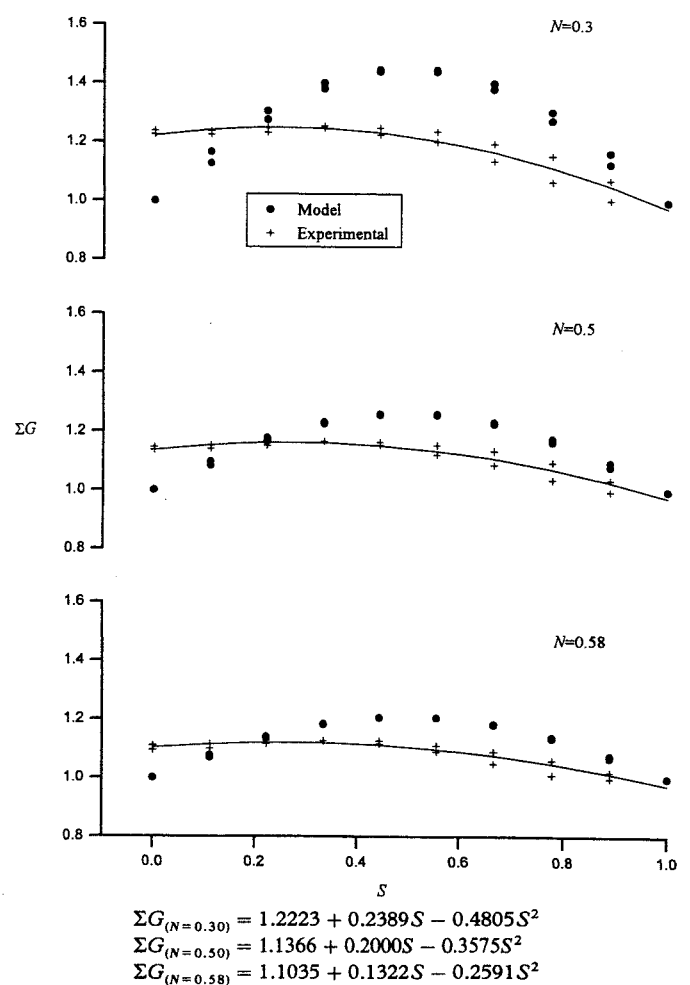


Figure 6 Combined circuit flow ratios for the 80 mm test valve

characteristics are known, together with the installed valve authority, the incoming control signal can be used as an acceptable basis for monitoring flow patterns within the controlled circuit.

- Experimental results were found to give good agreement with model results, especially at control signals greater than about 0.4 at the higher valve authorities (see Figures 3, 4, 5). Mean absolute errors between these results were found to be 6.7% for the 40 mm valve, 7.2% (50 mm), 11.4% (65 mm) and 8.9% (80 mm). The poorer agreement at low control signals is apparently due to the 'rangeability' characteristic of the valve—in which the practical valve fails to maintain its ideal flow characteristic when approaching its seat. Nevertheless, the overall agreement is sufficiently encouraging to suggest that, with some further development and verification, a theoretical model could be used to predict flow conditions from control signal data in practical cases where measured valve characteristics are unavailable.

## 6 Equal percentage case

The results described were obtained for linear/linear control valves. Another common format in UK practice is equal percentage/linear. To establish typical total circuit flow characteristics with this type of valve, the model was applied to the equal percentage/linear case with all other parameters identical to those of the 50 mm

Johnson linear/linear test valve. Experimental results were not obtained for this case.

Model results for both valves are compared in Figure 7. These confirm that the combined circuit flow when using an equal percentage/linear valve behaves in an opposing manner to that of the linear/linear case with significant shortfalls in total flow at all intermediate positions of the valve, especially at the higher valve authorities. Once again, the hysteresis error is only moderately significant at the low valve authorities.

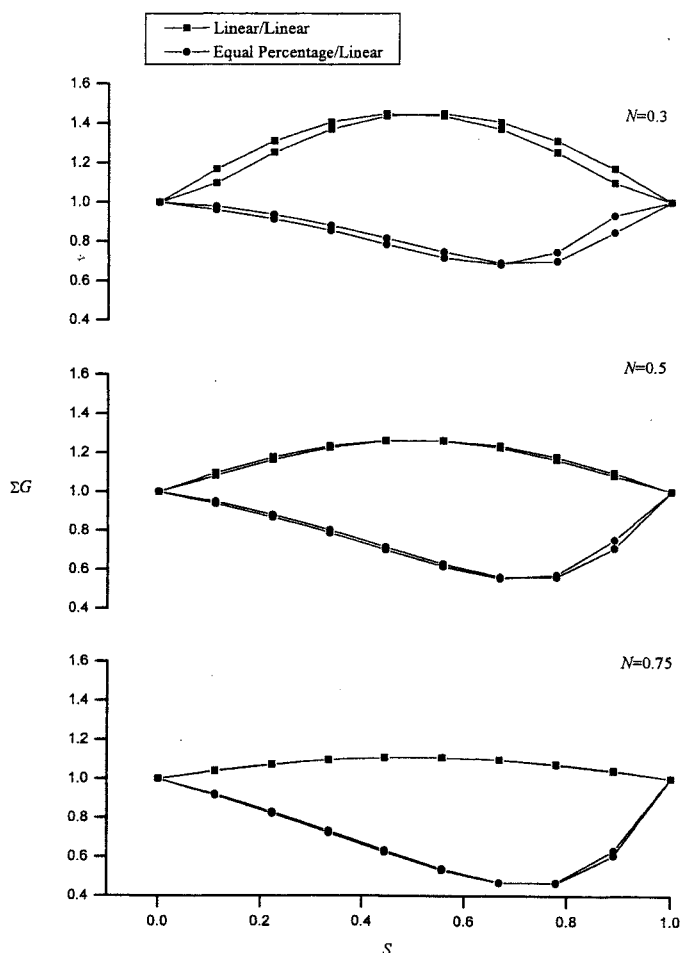


Figure 7 Combined circuit flow ratios for linear/linear and equal percentage/linear valves

Clearly there is some disadvantage in using the equal percentage/linear valve from an overall circuit flow point of view, though this disadvantage tends to be outweighed by improved control on the load side of the valve as has been noted by Hamilton *et al.*<sup>(3)</sup>.

This does not suggest that the equal percentage/linear case offers any less potential for flow monitoring through control signal data than the linear/linear case, but that the valve characteristic and valve authority form the two dominant factors in assessing the appropriate model or performance relationship for the prospective use in flow monitoring of this kind.

## 7 Conclusions

The potential for utilising an understanding of the combined flow characteristics of three-port control valves, together with the associated control positioning signal data for the monitoring of flow conditions in hot water

heating and chilled water cooling networks, has been explored.

Substantial potential has been found to exist in cases where the combined flow characteristics of the practical valve are known, together with the positioning signal data. In many cases, the former will normally be available from manufacturers' test data and, failing this, test results are relatively easy to obtain in laboratory conditions. The control signal data will generally be available in cases where the various control systems are under computer-based control, or a building management system is in use.

In cases where the precise performance characteristics for the valve are unavailable, considerable potential exists for the use of a theoretical model to generate these data, though some further work needs to be done in establishing precise flow characteristics at low control signals.

The dominant parameters relating the signal/flow relationship for a mixing valve of the type commonly used in UK applications (and, therefore, its potential for use as a passive flow monitoring device) have been found to be the inherent characteristics of the two inlet ports, together with the valve authority in service. The actuator and valve stem linkage mechanism for pneumatic valves has been found to have only a minor effect on the relationship between valve control signal and output flow rate and whilst electromechanical linkages may well offer greater hysteresis error, these errors appear in general to have an insignificant bearing on these results.

## Acknowledgement

The authors wish to thank Johnson Controls Inc. for providing the test case control valves used in the project.

## References

- 1 *Automatic controls and their implications for system design Applications Manual AM 1* (London: Chartered Institution of Building Services Engineers) (1985)
- 2 Tom S T Control Valve and Damper Sizing. *ASHRAE J.* 30-34 (October 1987)
- 3 Hamilton D C, Leonard R G and Pearson J T Dynamic Response Characteristics of a Discharge Air Temperature Control System at Near Full and Part Heating Load *ASHRAE Trans.* 80(1), 181-194 (1974)
- 4 Clark D R and Borresen B A Dynamics of a Heating Coil Control Loop *Proc. Symp. on Performance of HVAC Systems and Controls* pp 57-73 (Garston, UK: Building Research Establishment) UK (1984)
- 5 Siemers H Selecting Valves by Choosing the Optimum Flow Characteristic *Proc. BHR Group 3rd Int. Conf. on Valves and Actuators*, Oxford, UK pp 97-128 (1990)
- 6 Clark D R HVACSIM+ Building Systems and Equipment Simulation Program Reference Manual, Section 3.2 NBSIR 84-2996 (USA: National Institute of Standards and Technology) (1985)
- 7 BS5793: *Industrial Process Control Valves, Parts 1 & 2* (London: British Standards Institution) (1989)
- 8 BS1042: *Methods of Measurement of Fluid Flow in Closed Conduits, Part 1—Pressure Differential* (London: British Standards Institution) (1989)

## Appendix 1: Derivation of the valve and circuit model

Allowing for let-by (though usually very low in these types of valves), the inherent characteristic for the linear



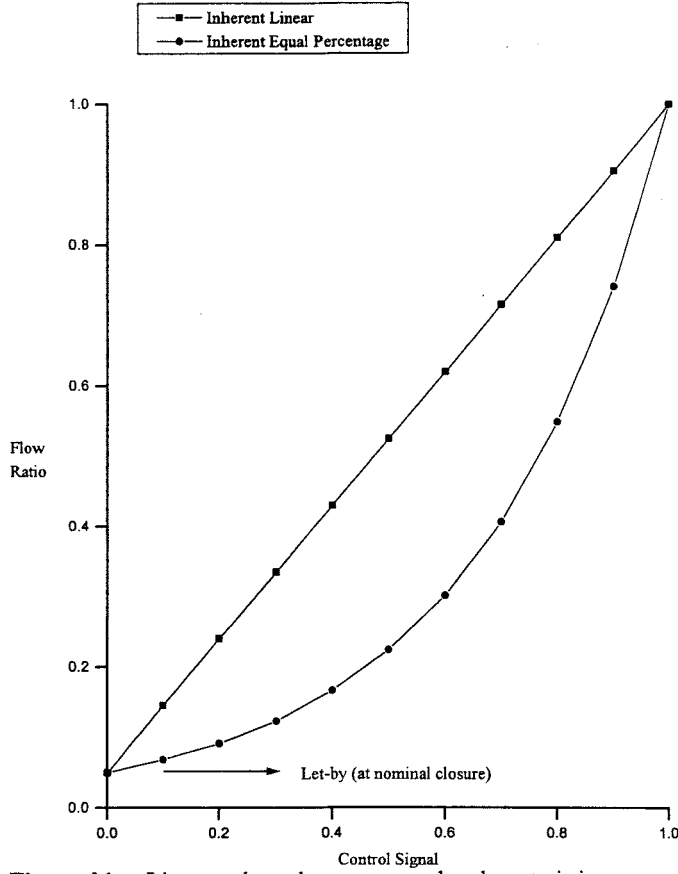


Figure A1 Linear and equal percentage valve characteristics

valve can be expressed as follows (Figure A1):

$$\text{Linear, } G_{inh} = G_0 + P(1 - G_0) \quad (A1)$$

For the equal percentage case, equal increments of valve position will produce equal ratios of flow. Thus for an equal-percentage valve under constant pressure conditions:

$$\frac{dG_{inh}}{G_{inh}} \propto dP$$

Introducing proportionality constant  $c$ :

$$\frac{dG_{inh}}{G_{inh}} = c dP \quad (A2)$$

For a general solution with allowance for let-by:

$$\int_{G_0}^{G_0 \leq G_{inh} \leq 1} \frac{dG_{inh}}{G_{inh}} = c \int_0^{0 \leq P \leq 1} dP \quad (A3)$$

From which:

$$\ln(G_{inh}) - \ln(G_0) = cP \quad (A4)$$

From the condition  $P = 1$ , when  $G_{inh} = 1$ :

$$c = -\ln(G_0), \text{ i.e.,} \\ G_{inh} = \exp[(1 - P) \ln G_0] \quad (A5)$$

Which reduces to:

$$G_{inh} = G_0^{(1-P)} \quad (A6)$$

The installed characteristic can now be derived; refer to the generalised circuit of Figure 1. First, the valve

authority can be expressed as:

$$N = \frac{\Delta p'_v}{\Delta p'_v + \Delta p'_s} \quad (A7)$$

Assuming that the pressure developments around the circuit can be related to the square of the volume flow rate:

$$\frac{\Delta p_s}{\Delta p'_s} = \left( \frac{\dot{V}}{\dot{V}'} \right)^2 \quad (A8)$$

for the system, and:

$$\frac{\Delta p_v}{\Delta p'_v} = \left( \frac{\dot{V}}{\dot{V}'} \right)^2 \left( \frac{\dot{V}'_{inh}}{\dot{V}_{inh}} \right)^2 \quad (A9)$$

for the valve, where  $\dot{V}'_{inh}$  refers to the inherent throughput of the valve.

It is required that the pressure drop across the valve and connecting circuit path remain constant under all conditions if the valve is to perform correctly, so that:

$$\Delta p_v + \Delta p_s = \Delta p'_v + \Delta p'_s = \left[ \Delta p'_s + \Delta p'_v \left( \frac{\dot{V}'_{inh}}{\dot{V}_{inh}} \right)^2 \right] \left( \frac{\dot{V}}{\dot{V}'} \right)^2 \quad (A10)$$

Noting that:

$$G_{inh} = \frac{\dot{V}'_{inh}}{\dot{V}'}, \text{ and } G_{ins} = \frac{\dot{V}}{\dot{V}'},$$

and that

$$\Delta p'_s = \Delta p'_v \left( \frac{1 - N}{N} \right),$$

then by substitution in equation A10 the installed characteristic can be expressed:

$$G_{ins} = \left[ \frac{1}{1 + N \left( \frac{1}{G_{inh}^2} - 1 \right)} \right]^{1/2} \quad (A11)$$

Hysteresis errors—resulting mainly from mechanical slack between the valve actuator and stem was included in the model in a manner similar to that used by Clark<sup>(6)</sup> and summarised as follows.

For an incoming control signal,  $S$ , the slack will be,

$$\Delta SP = S - P \quad (A12)$$

Thus, for

$$S > \text{HYS}, P = \frac{(S - \text{HYS})}{(1 - \text{HYS})} \quad (A13)$$

For

$$S < 0, P = \frac{S}{(1 - \text{HYS})} \quad (A14)$$

And for

$$0 \leq S \leq \text{HYS}, P = \text{constant} \quad (A15)$$

(In all cases,  $P$  will be subject to the limiting condition  $0 \leq P \leq 1$ , since the incoming control signal cannot be less than zero, and will 'saturate' above unity).

## **Appendix 4. Pictures of Test Rig**



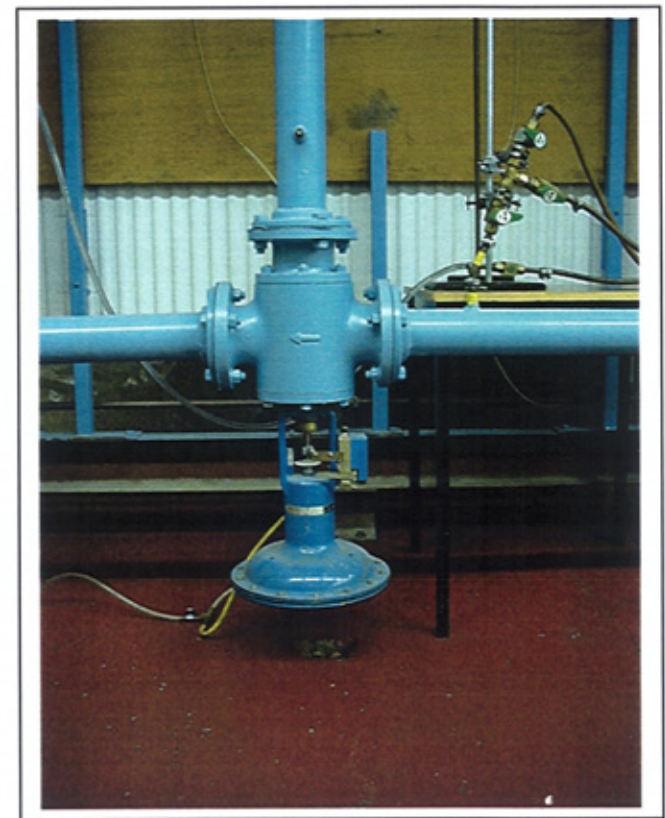
Picture A1: Test Rig



Picture A2: Test Rig

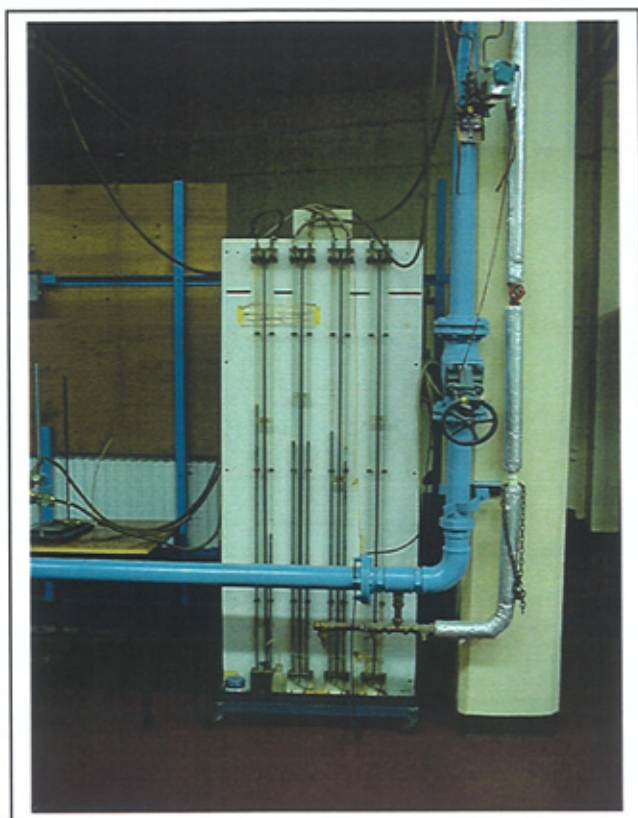


Picture A3: Test Rig



Picture A4: Test Rig (test valve)





Picture A5: Test Rig (manometers and regulating valve)



Picture A6: Test Rig (pump)

**Appendix 5: Fortran Program for Orifice Plate Flow Rates**

```

      program converge
      dimension Cd(300)
      integer j
      real a, e, c, do, rho, mu, beta, deltap, Re, flow, error, Cd
      data e, do, rho, mu, dp, beta/1.,0.05753,1000.,0.0082,0.082,0.701577/
c
c input orifice plate pressure drop
c
      print *, "Enter to orifice plate pressure loss (N/sq m)"
      read(*,*)deltap
c
c calculate flow constant
c
      a=e*do*do*(sqrt(2.*deltap*rho))/(mu*dp*(sqrt(1.-beta**4.)))
      cd(1)=0.5
c
c convergence loop
c
      do 100 j=1,300
      Re=Cd(j)*a
      c=0.5959+0.0312*beta**2.1+0.0029*beta**2.5*(1000000/Re)**0.75
      c=c+0.09*beta**4./(1.-beta**4.)-0.015839*beta**3.-0.184*beta**8.
      error=abs(c-Cd(j))
      if(error.le.0.001)go to 1000
      Cd(j+1)=Cd(j)+0.001
100  continue
      print *, "Unable to achieve convergence"
      go to 500
1000 flow=3.14159*mu*dp*Re/4.
      print *, "Flowrate for this case = ",flow," (kg/sec)"
      print *, "Cd = ",c
500  stop
      end

```

## **Appendix 6. Curve Fits to Experimental Results (Graphs)**

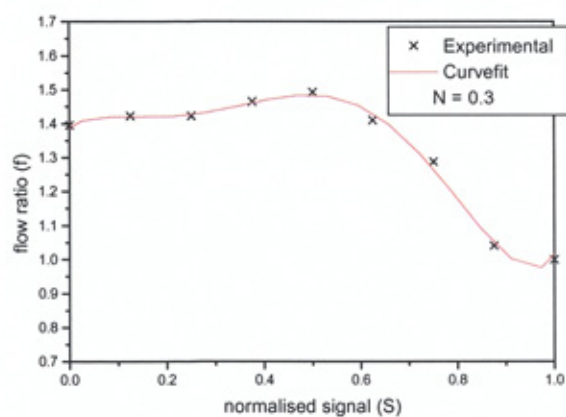


Fig.A1: 40mm valve, upstroke

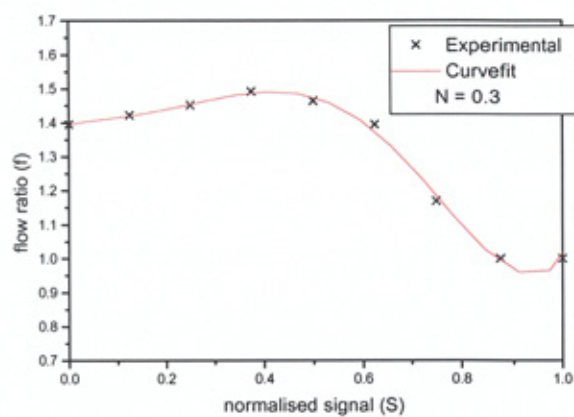


Fig.A2: 40mm valve, downstroke

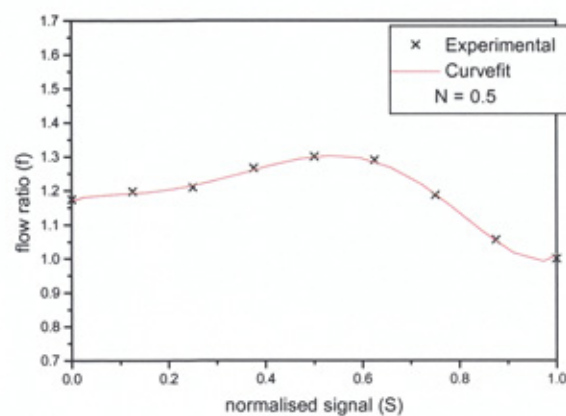


Fig.A3: 40mm valve, upstroke

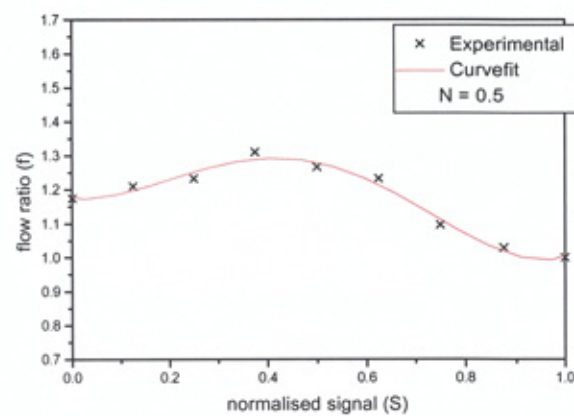


Fig.A4: 40mm valve, downstroke

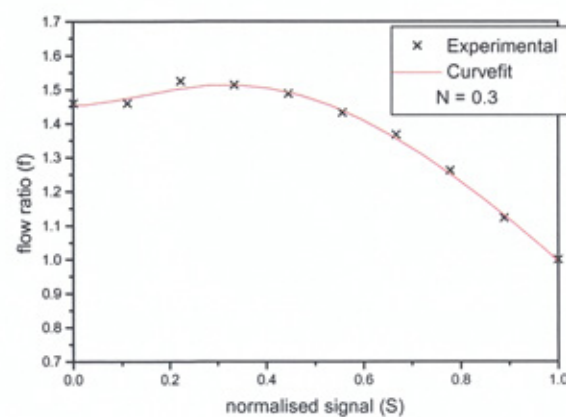


Fig.A5: 50mm valve, upstroke

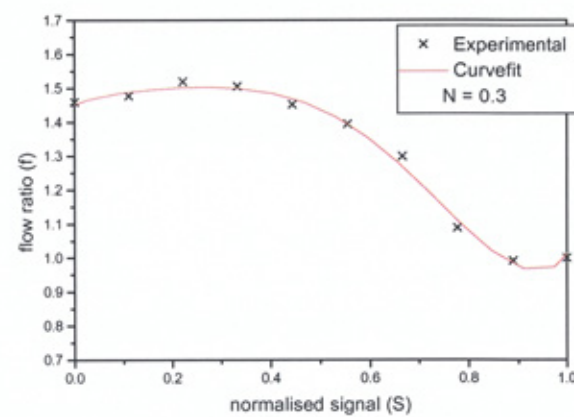


Fig.A6: 50mm valve, downstroke

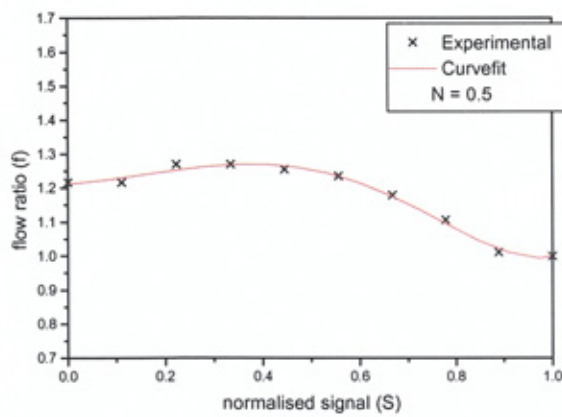


Fig.A7: 50mm valve, upstroke

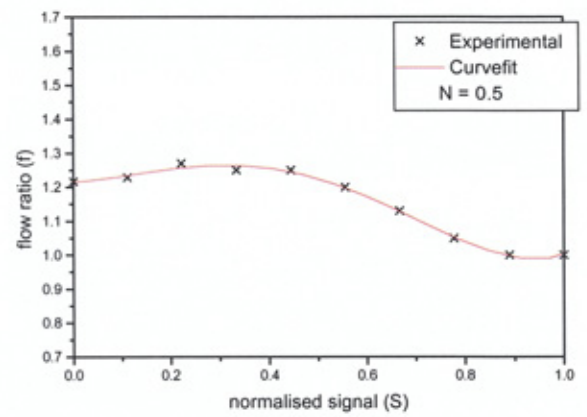


Fig.A8: 50mm valve, downstroke

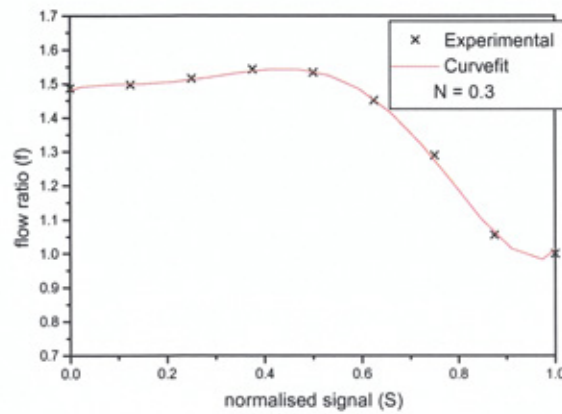


Fig.A9: 65mm valve, upstroke

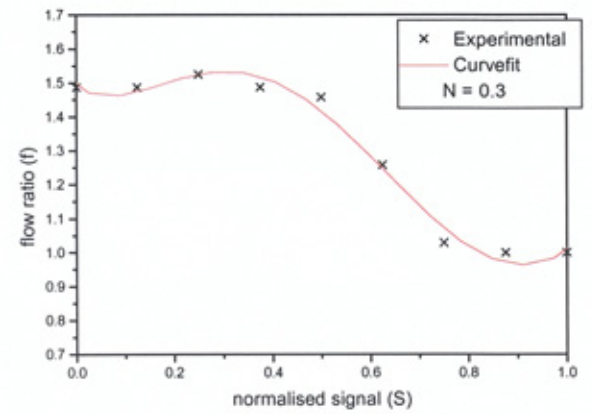


Fig.A10: 65mm valve, downstroke

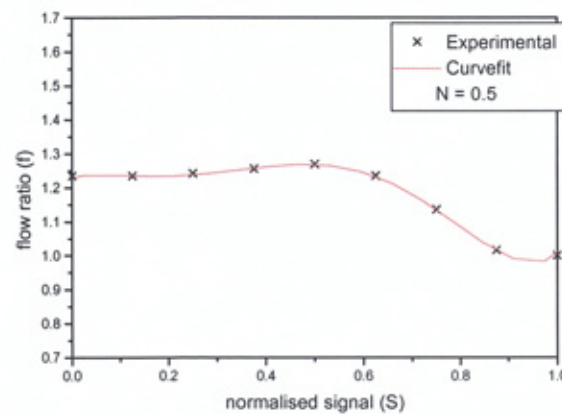


Fig.A11: 65mm valve, upstroke

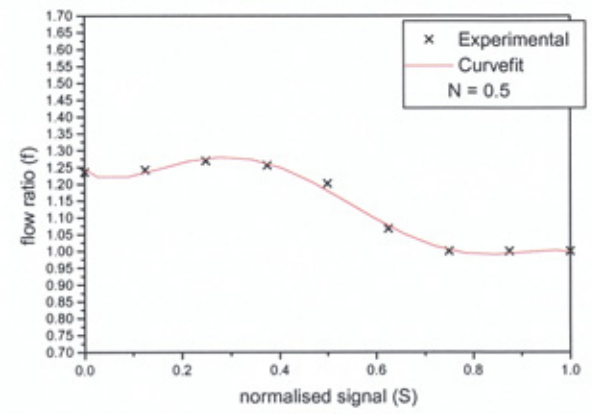


Fig.A12: 65mm valve, downstroke



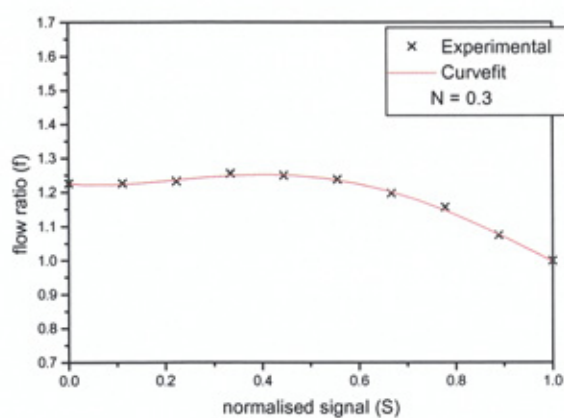


Fig.A13: 80mm valve, upstroke

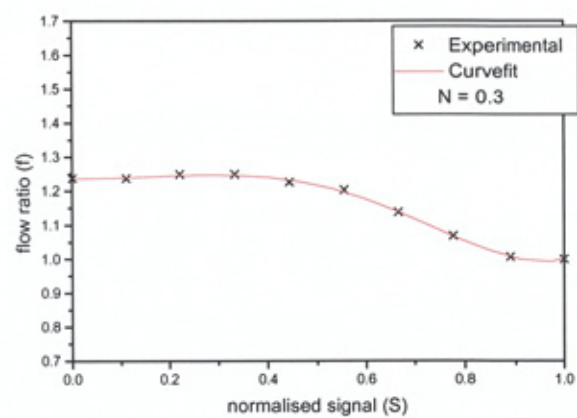


Fig.A14: 80mm valve, downstroke

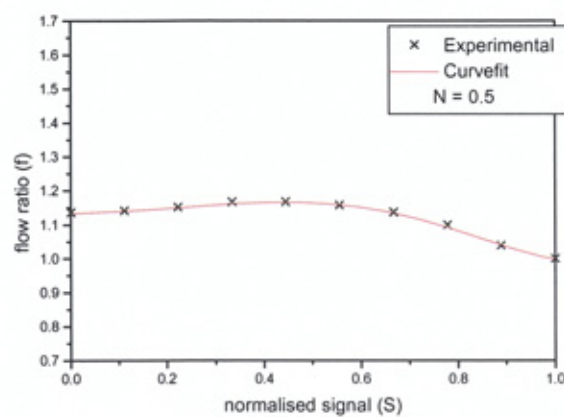


Fig.A15: 80mm valve, upstroke

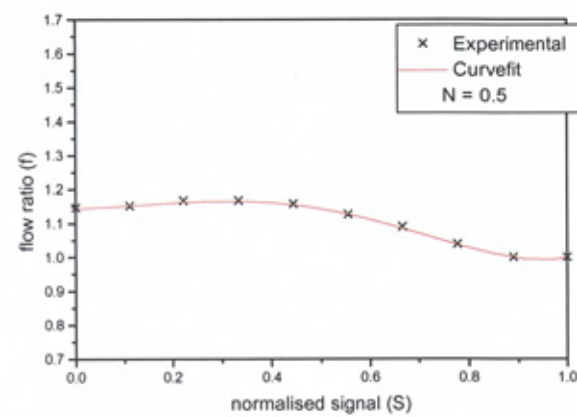


Fig.A16: 80mm valve, downstroke

## **Appendix 6. Curve Fits to Experimental Results (Tables of Statistical Data)**

Polynomial Regression for INITIALRESULT_I: $Y = A + B1*X + B2*X^2 + B3*X^3 + B4*X^4 + B5*X^5$			
Parameter	Value	Error	
A	1.39536	0.019	
B1	0.70632	0.49418	
B2	-6.53394	3.58753	
B3	24.85052	9.67329	
B4	-36.13978	10.89355	
B5	16.71973	4.33829	
R-Square(COD)	SD	N	
0.99591	0.01909	9	8.85906E-4

Table Curve fit Results for 40mm valve, N = 0.3, Upstroke

Polynomial Regression for INITIALRESULT_I: $Y = A + B1*X + B2*X^2 + B3*X^3 + B4*X^4 + B5*X^5$			
Parameter	Value	Error	
A	1.17514	0.00614	
B1	0.36171	0.15975	
B2	-3.1545	1.15971	
B3	14.30588	3.12701	
B4	-22.02192	3.52147	
B5	10.33437	1.4024	
R-Square(COD)	SD	N	
0.99862	0.00617	9	1.73041E-4

Table Curve fit Results for 40mm valve, N = 0.5, Upstroke

Polynomial Regression for INITIALRESULT_I: $Y = A + B1*X + B2*X^2 + B3*X^3 + B4*X^4 + B5*X^5$			
Parameter	Value	Error	
A	1.45505	0.0164	
B1	0.03363	0.4089	
B2	2.05367	2.91494	
B3	-6.62378	7.81315	
B4	5.98085	8.78071	
B5	-1.90248	3.49597	
R-Square(COD)	SD	N	
0.99619	0.01654	10	<0.0001

Table Curve fit Results for 50mm valve, N = 0.3, Upstroke

Polynomial Regression for INITIALRESULT_K: $Y = A + B1*X + B2*X^2 + B3*X^3 + B4*X^4 + B5*X^5$			
Parameter	Value	Error	
A	1.39572	0.01722	
B1	0.29715	0.44788	
B2	-1.7347	3.25139	
B3	10.38517	8.76694	
B4	-20.48838	9.87286	
B5	11.14648	3.93181	
R-Square(COD)	SD	N	
0.99717	0.01731	9	5.10877E-4

Table Curve fit Results for 40mm valve, N = 0.3, Downstroke

Polynomial Regression for INITIALRESULT_K: $Y = A + B1*X + B2*X^2 + B3*X^3 + B4*X^4 + B5*X^5$			
Parameter	Value	Error	
A	1.17665	0.02491	
B1	-0.1298	0.64764	
B2	3.25707	4.70159	
B3	-6.77142	12.67722	
B4	2.98368	14.27641	
B5	0.48588	5.68549	
R-Square(COD)	SD	N	
0.97986	0.02502	9	0.00953

Table Curve fit Results for 40mm valve, N = 0.5, Downstroke

Polynomial Regression for INITIALRESULT_K: $Y = A + B1*X + B2*X^2 + B3*X^3 + B4*X^4 + B5*X^5$			
Parameter	Value	Error	
A	1.45609	0.02365	
B1	0.50813	0.58975	
B2	-2.45719	4.20424	
B3	7.81003	11.26899	
B4	-13.88341	12.66451	
B5	7.56721	5.04227	
R-Square(COD)	SD	N	
0.9944	0.02385	10	1.36555E-4

Table Curve fit Results for 50mm valve, N = 0.3, Downstroke

Polynomial Regression for INITIALRESULT_I: $Y = A + B1*X + B2*X^2 + B3*X^3 + B4*X^4 + B5*X^5$			
Parameter	Value	Error	
A	1.21262	0.01459	
B1	0.12262	0.36374	
B2	0.4417	2.59302	
B3	-0.2802	6.9503	
B4	-2.51587	7.811	
B5	2.01631	3.10989	
R-Square(COD)	SD	N	P
0.99077	0.01471	10	3.69353E-4

Table Curve fit Results for 50mm valve, N = 0.5, Upstroke

Polynomial Regression for INITIALRESULT_K: $Y = A + B1*X + B2*X^2 + B3*X^3 + B4*X^4 + B5*X^5$			
Parameter	Value	Error	
A	1.21531	0.01061	
B1	0.10019	0.26458	
B2	1.0461	1.88613	
B3	-3.23737	5.05556	
B4	1.425	5.68163	
B5	0.45133	2.26209	
R-Square(COD)	SD	N	P
0.99554	0.0107	10	<0.0001

Table Curve fit Results for 50mm valve, N = 0.5, Downstroke

Polynomial Regression for INITIALRESULT_I: $Y = A + B1*X + B2*X^2 + B3*X^3 + B4*X^4 + B5*X^5$			
Parameter	Value	Error	
A	1.48607	0.00957	
B1	0.34863	0.24886	
B2	-3.43308	1.8066	
B3	15.39878	4.87127	
B4	-25.25667	5.48576	
B5	12.45471	2.18467	
R-Square(COD)	SD	N	P
0.99922	0.00962	9	<0.0001

Table Curve fit Results for 65mm valve, N = 0.3, Upstroke

Polynomial Regression for INITIALRESULT_K: $Y = A + B1*X + B2*X^2 + B3*X^3 + B4*X^4 + B5*X^5$			
Parameter	Value	Error	
A	1.49054	0.04388	
B1	-0.93335	1.14088	
B2	9.31809	8.2823	
B3	-25.42767	22.33213	
B4	23.24833	25.14926	
B5	-6.68937	10.01554	
R-Square(COD)	SD	N	P
0.98662	0.04408	9	0.00519

Table Curve fit Results for 65mm valve, N = 0.3, Downstroke

Polynomial Regression for INITIALRESULT_I: $Y = A + B1*X + B2*X^2 + B3*X^3 + B4*X^4 + B5*X^5$			
Parameter	Value	Error	
A	1.23502	0.00276	
B1	0.20818	0.07183	
B2	-2.78349	0.52148	
B3	12.22392	1.40611	
B4	-18.97086	1.58348	
B5	9.08718	0.63061	
R-Square(COD)	SD	N	P
0.99974	0.00278	9	<0.0001

Table Curve fit Results for 65mm valve, N = 0.5, Upstroke

Polynomial Regression for INITIALRESULT_K: $Y = A + B1*X + B2*X^2 + B3*X^3 + B4*X^4 + B5*X^5$			
Parameter	Value	Error	
A	1.23723	0.01562	
B1	-0.73275	0.40611	
B2	8.60985	2.94822	
B3	-26.92759	7.94948	
B4	29.95338	8.95229	
B5	-11.13846	3.56519	
R-Square(COD)	SD	N	P
0.99372	0.01569	9	0.00168

Table Curve fit Results for 65mm valve, N = 0.5, Downstroke

Polynomial Regression for INITIALRESULT_I: Y = A + B1*X + B2*X^2 + B3*X^3 + B4*X^4 + B5*X^5				Polynomial Regression for INITIALRESULT_K: Y = A + B1*X + B2*X^2 + B3*X^3 + B4*X^4 + B5*X^5			
Parameter	Value	Error		Parameter	Value	Error	
A	1.22645	0.0065		A	1.23717	0.00508	
B1	-0.13552	0.16217		B1	0.00202	0.12668	
B2	1.34779	1.15609		B2	0.25798	0.90309	
B3	-2.63155	3.09876		B3	0.11138	2.42063	
B4	1.36589	3.4825		B4	-2.53316	2.72039	
B5	-0.17396	1.38653		B5	1.92445	1.0831	
R-Square(COD)	SD	N	P	R-Square(COD)	SD	N	P
0.99735	0.00656	10	<0.0001	0.99886	0.00512	10	<0.0001

Table Curve fit Results for 80mm valve, N = 0.3, Upstroke

Table Curve fit Results for 80mm valve, N = 0.3, Downstroke

Polynomial Regression for INITIALRESULT_K: Y = A + B1*X + B2*X^2 + B3*X^3 + B4*X^4 + B5*X^5				Polynomial Regression for INITIALRESULT_I: Y = A + B1*X + B2*X^2 + B3*X^3 + B4*X^4 + B5*X^5			
Parameter	Value	Error		Parameter	Value	Error	
A	1.1461	0.00302		A	1.13572	0.00408	
B1	0.02347	0.07532		B1	0.03911	0.10163	
B2	0.57228	0.53697		B2	0.11502	0.72449	
B3	-1.45972	1.4393		B3	0.62305	1.94192	
B4	0.13258	1.61753		B4	-2.14731	2.1824	
B5	0.58488	0.64401		B5	1.23344	0.8689	
R-Square(COD)	SD	N	P	R-Square(COD)	SD	N	P
0.9991	0.00305	10	<0.0001	0.99768	0.00411	10	<0.0001

Table Curve fit Results for 80mm valve, N = 0.5, Upstroke

Table Curve fit Results for 80mm valve, N = 0.5, Downstroke

## **Appendix 7. Differential Pressure Transducer Readings Compared to Orifice Plate Readings**

**Appendix 7****TableA18: Error analysis of SITRANS P differential pressure transducer**

<u>Data logger and Manometer Results Comparison</u>						
mAd	Press	mandiff	manpress	loggerflow	manflow	%error
	(Pa)	(m)		(kg/s)	(kg/s)	
4.5	91.875	0.0008	98.8848	0.970291	1.001315	-3.09833
4.74	135.975	0.0012	148.3272	1.153937	1.20032	-3.86422
5.03	189.2625	0.0016	197.7696	1.339351	1.365365	-1.90528
5.62	297.675	0.0025	309.015	1.64284	1.671493	-1.71422
5.87	343.6125	0.0028	346.0968	1.755155	1.761488	-0.35953
6.63	483.2625	0.004	494.424	2.055059	2.075686	-0.99374
7.45	633.9375	0.0052	642.7512	2.330189	2.342946	-0.54449
8.15	762.5625	0.0062	766.3572	2.537236	2.543542	-0.24792
14.97	2015.738	0.0165	2039.499	4.011235	4.034807	-0.58422
11.32	1345.05	0.0109	1347.305	3.310936	3.31371	-0.08371
9.11	938.9625	0.0075	927.045	2.799078	2.781259	0.640681
7.39	622.9125	0.005	618.03	2.309838	2.300768	0.394216
5.56	286.65	0.0022	271.9332	1.616652	1.576808	2.526877
					Ave=	-0.75645

**Appendix 8. Mathematical Model Version 2.1, Comparison With Validation  
Test Rig Measurements (at a Hysteresis of 10%)**



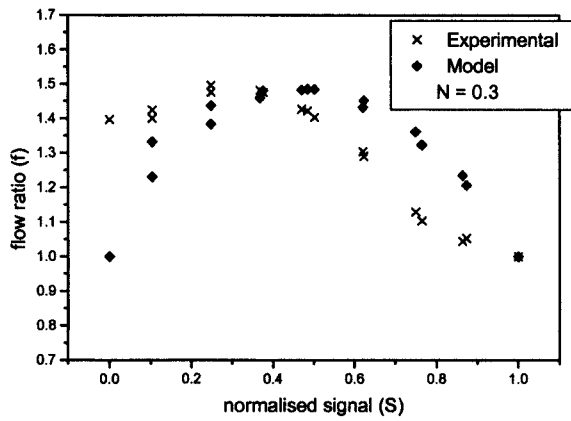


Fig.A17: 40mm valve,  $hys = 10\%$ ,  
 $G_0 = 0.05\%$  inlet port and  $0.065\%$  bypass port

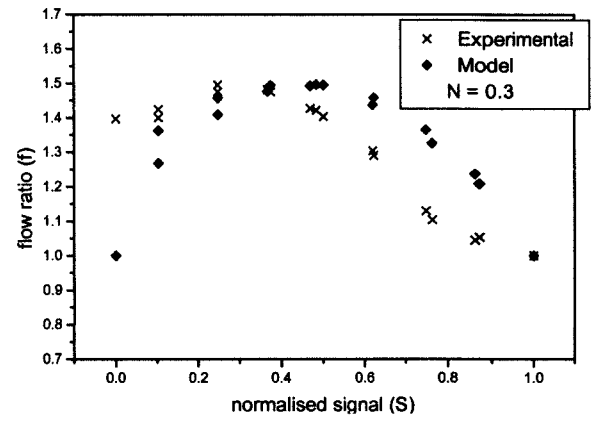


Fig.A18: 40mm valve,  $hys = 10\%$ ,  
 $G_0 = 0.05\%$  inlet port and  $0.075\%$  bypass port

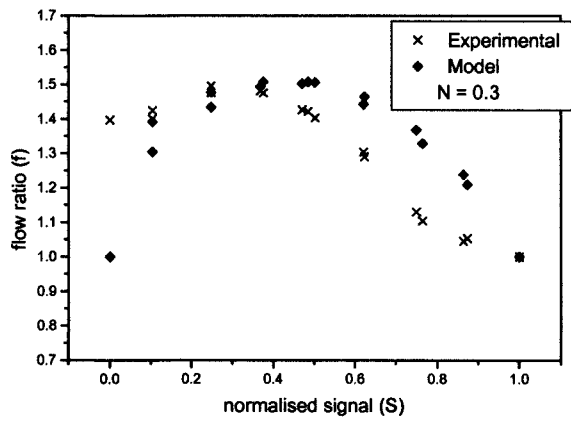


Fig.A19: 40mm valve,  $hys = 10\%$ ,  
 $G_0 = 0.05\%$  inlet port and  $0.1\%$  bypass port

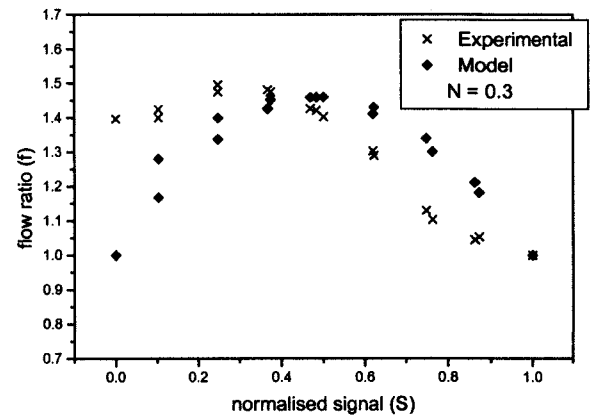


Fig.A20: 40mm valve,  $hys = 10\%$ ,  
 $G_0 = 0.01\%$  inlet and bypass ports

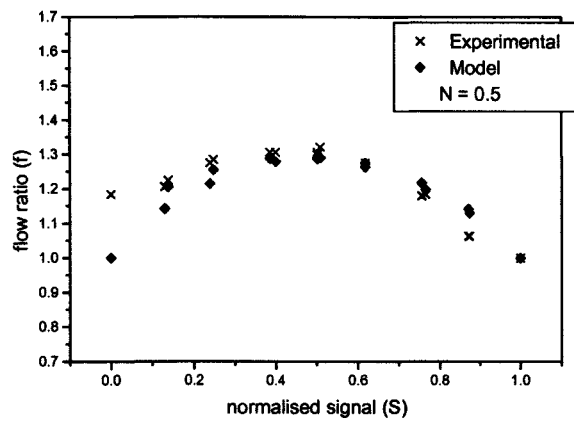


Fig.A21: 40mm valve,  $h_{ys} = 10\%$ ,  
 $G_0 = 0.05\%$  inlet and bypass ports

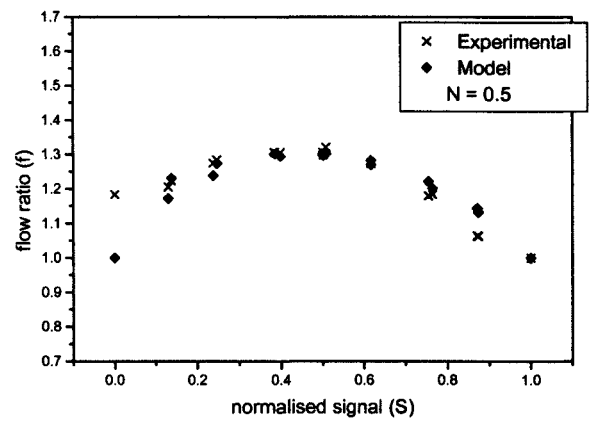


Fig.A22: 40mm valve,  $h_{ys} = 10\%$ ,  
 $G_0 = 0.05\%$  inlet port and 0.065% bypass port

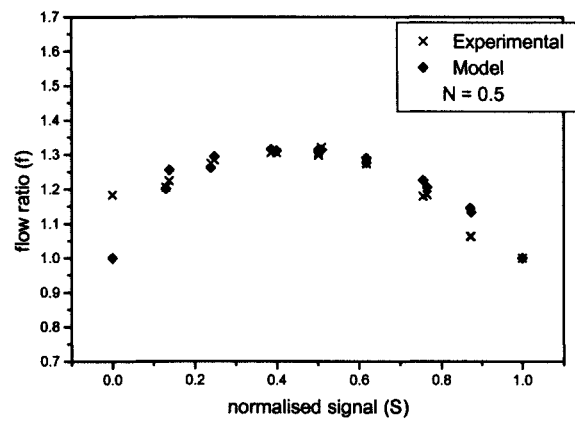


Fig.A23: 40mm valve,  $h_{ys} = 10\%$ ,  
 $G_0 = 0.05\%$  inlet port and 0.075% bypass port

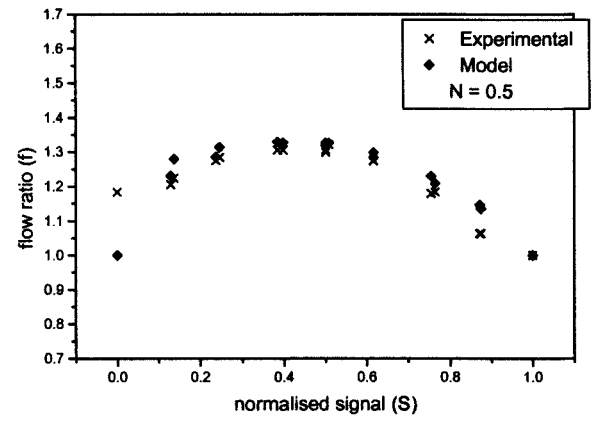


Fig.A24: 40mm valve,  $h_{ys} = 10\%$ ,  
 $G_0 = 0.05\%$  inlet port and 0.1% bypass port

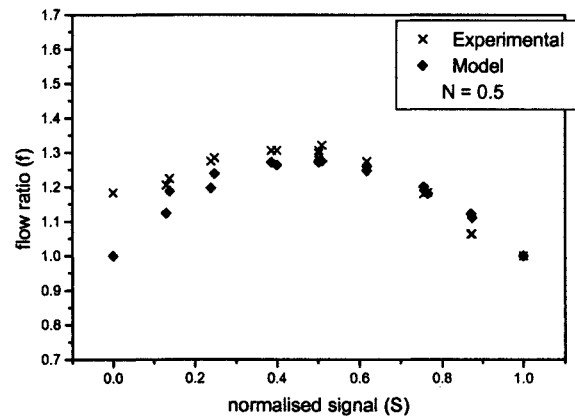


Fig.A25: 40mm valve,  $h_{ys} = 10\%$ ,  
 $G_0 = 0.01\%$  inlet and bypass ports

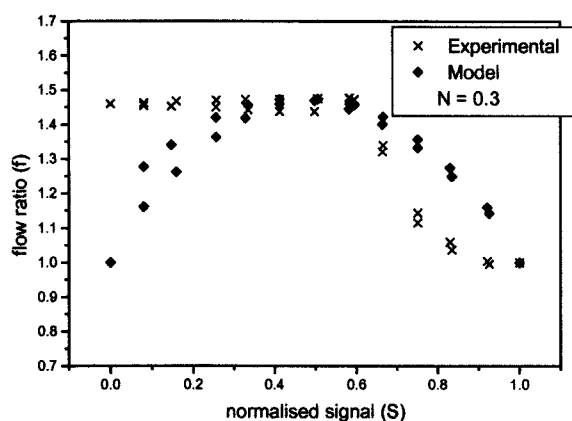


Fig.A26: 50mm valve,  $h_{ys} = 10\%$ ,  
 $G_0 = 0.05\%$  inlet and bypass ports

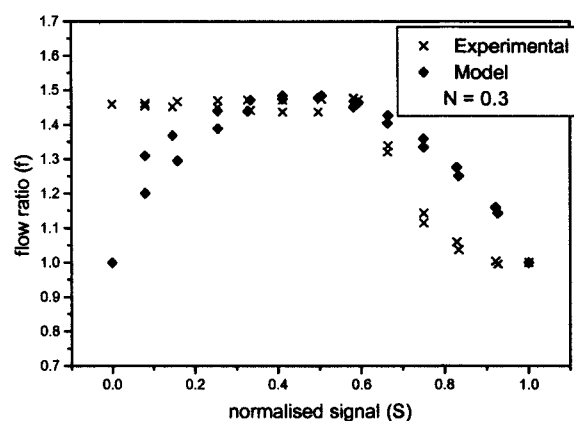


Fig. A27: 50mm valve,  $h_{ys} = 10\%$ ,  
 $G_0 = 0.05\%$  inlet port and 0.065% bypass port

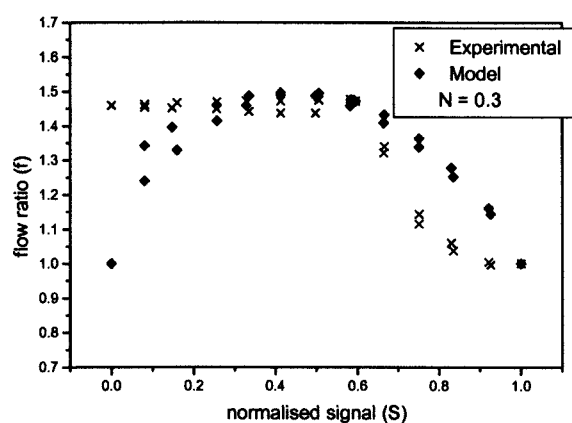


Fig.A28: 50mm valve,  $h_{ys} = 10\%$ ,  
 $G_0 = 0.05\%$  inlet port and 0.075% bypass port

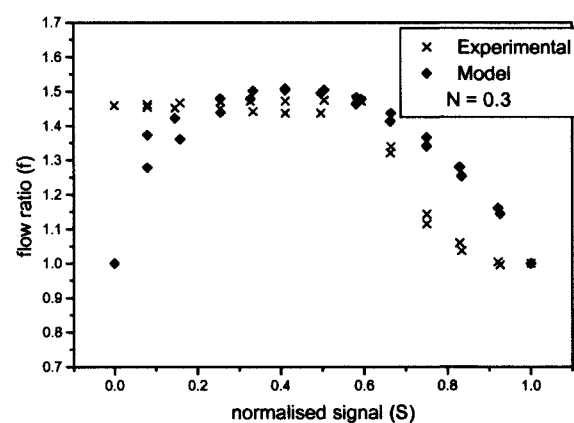


Fig.A29: 50mm valve,  $h_{ys} = 10\%$ ,  
 $G_0 = 0.05\%$  inlet port and 0.1% bypass port

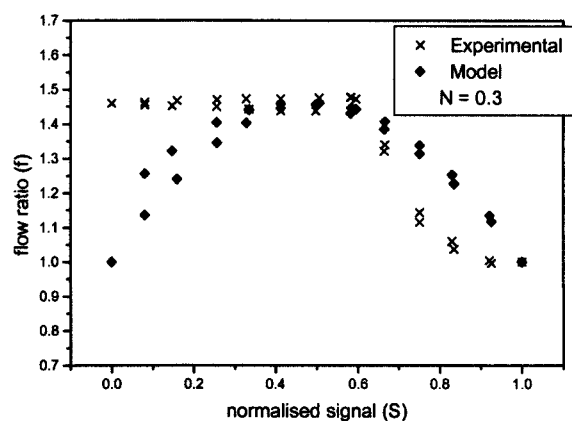


Fig.A30: 50mm valve,  $h_{ys} = 10\%$ ,  
 $G_0 = 0.01\%$  inlet and bypass ports

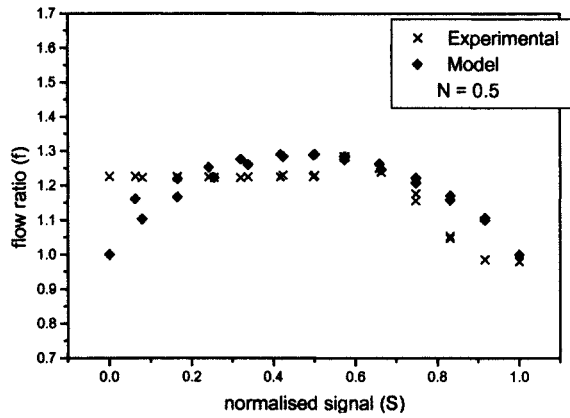


Fig.A31: 50mm valve,  $hys = 10\%$ ,  
 $G_0 = 0.05\%$  inlet and bypass ports

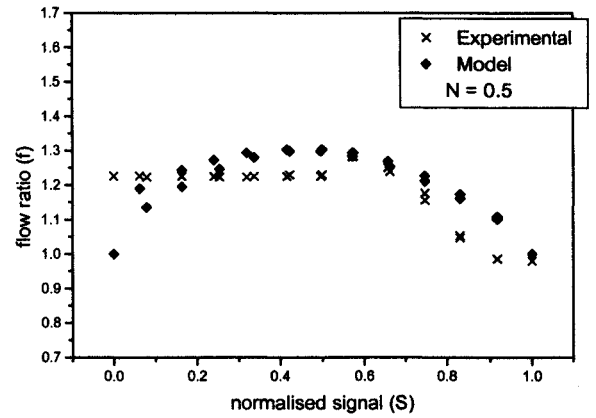


Fig.A32: 50mm valve,  $hys = 10\%$ ,  
 $G_0 = 0.05\%$  inlet port and 0.065% bypass port

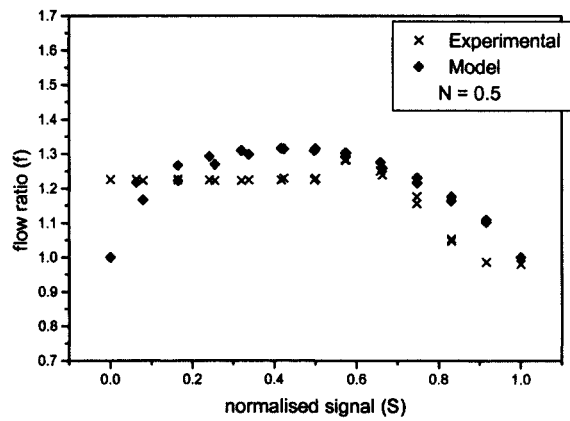


Fig.A33: 50mm valve,  $hys = 10\%$ ,  
 $G_0 = 0.05\%$  inlet port and 0.075% bypass port

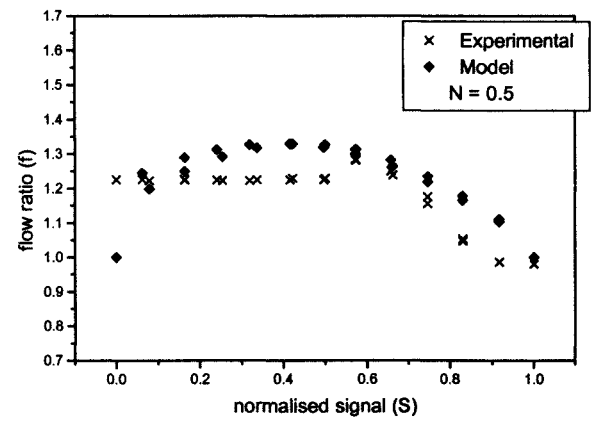


Fig.A34: 50mm valve,  $hys = 10\%$ ,  
 $G_0 = 0.05\%$  inlet port and 0.1% bypass port

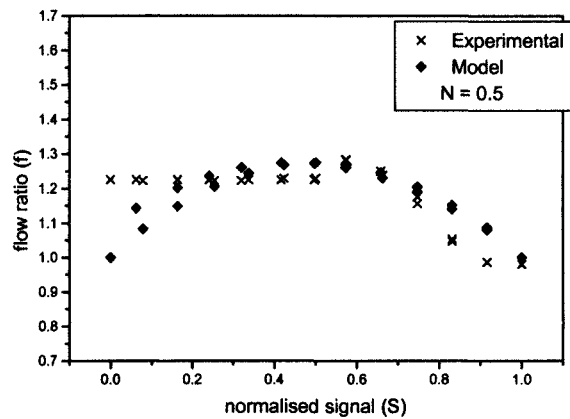


Fig.A35: 50mm valve,  $hys = 10\%$ ,  
 $G_0 = 0.01\%$  inlet and bypass ports

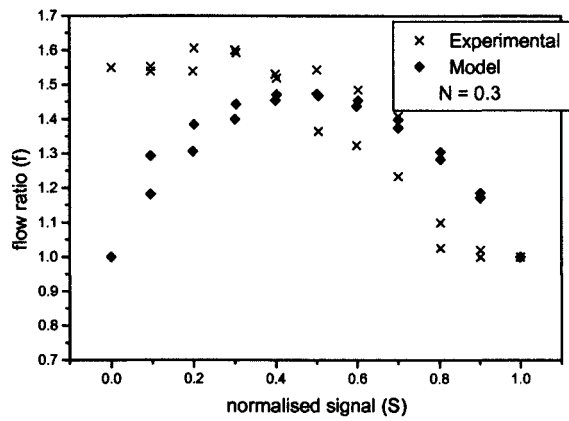


Fig.A36: 65mm valve,  $hys = 10\%$ ,  
 $G_0 = 0.05\%$  inlet and bypass ports

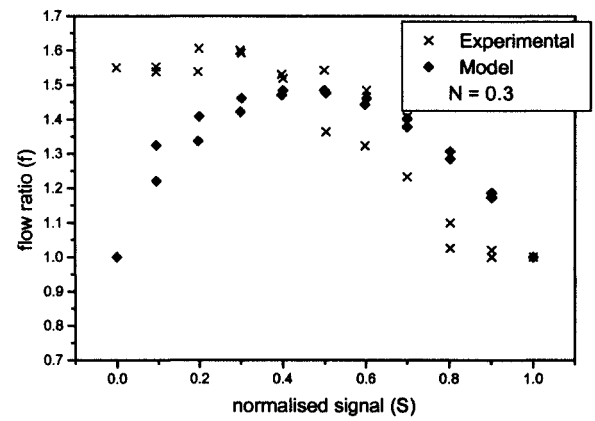


Fig.A37: 65mm valve,  $hys = 10\%$ ,  
 $G_0 = 0.05\%$  inlet port and 0.065% bypass port

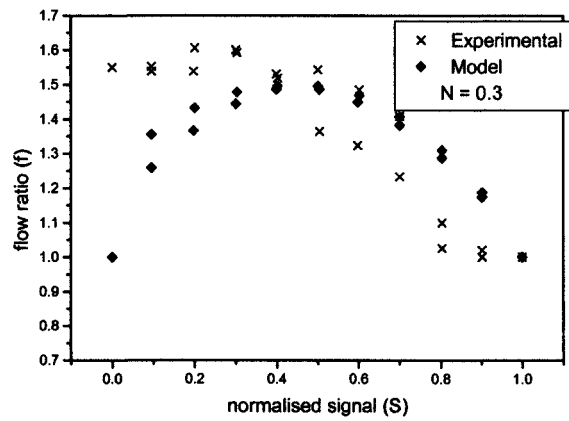


Fig.A38: 65mm valve,  $hys = 10\%$ ,  
 $G_0 = 0.05\%$  inlet port and 0.075% bypass port

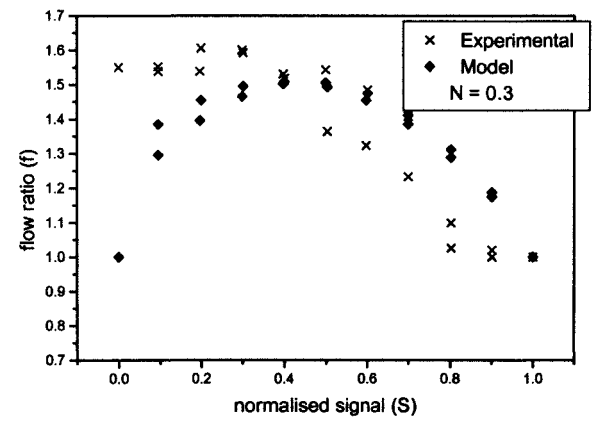


Fig.A39: 65mm valve,  $hys = 10\%$ ,  
 $G_0 = 0.05\%$  inlet port and 0.1% bypass port

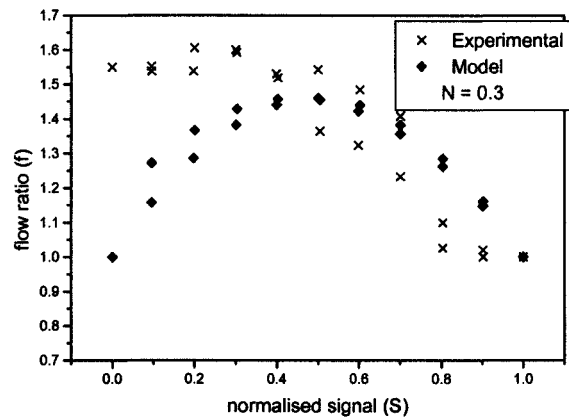


Fig.A40: 65mm valve,  $hys = 10\%$ ,  
 $G_0 = 0.01\%$  inlet and bypass ports

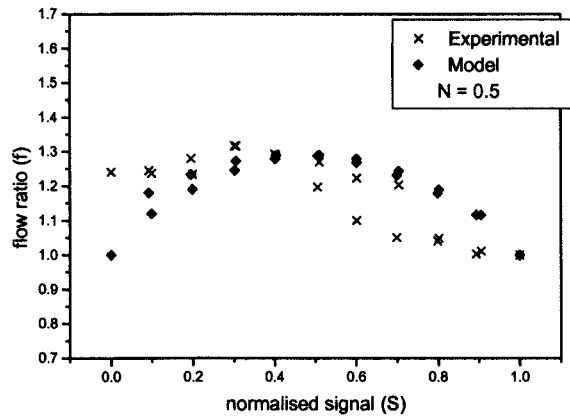


Fig.A41: 65mm valve,  $hys = 10\%$ ,  
 $G_0 = 0.05\%$  inlet and bypass ports

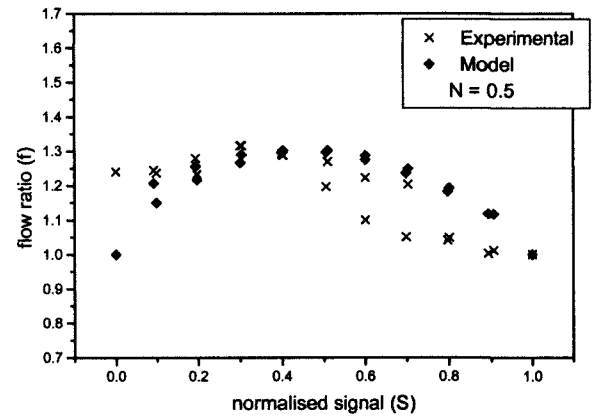


Fig.A42: 65mm valve,  $hys = 10\%$ ,  
 $G_0 = 0.05\%$  inlet port and 0.065% bypass port

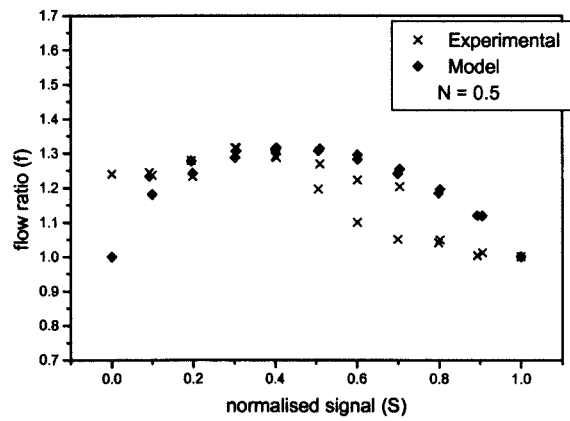


Fig.A43: 65mm valve,  $hys = 10\%$ ,  
 $G_0 = 0.05\%$  inlet port and 0.075% bypass port

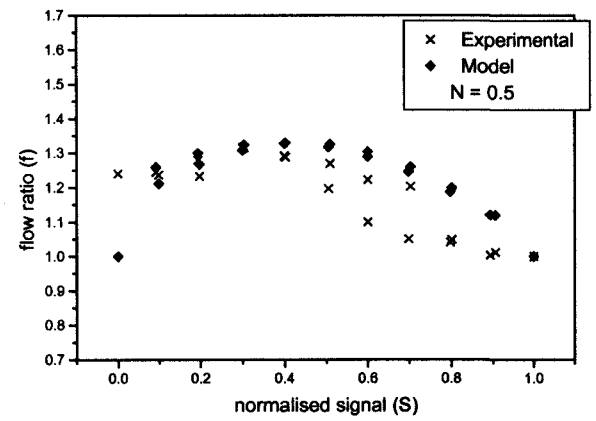


Fig.A44: 65mm valve,  $hys = 10\%$ ,  
 $G_0 = 0.05\%$  inlet port and 0.1% bypass port

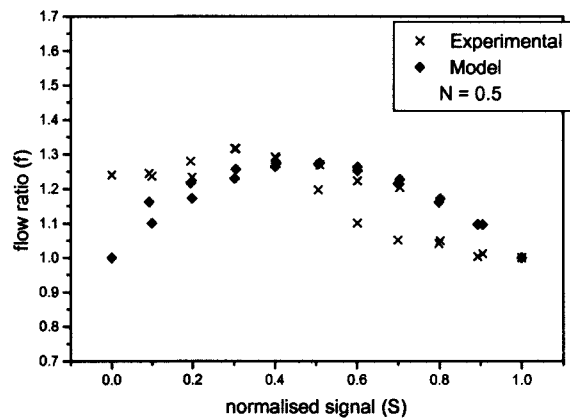


Fig.A45: 65mm valve,  $hys = 10\%$ ,  
 $G_0 = 0.01\%$  inlet and bypass ports

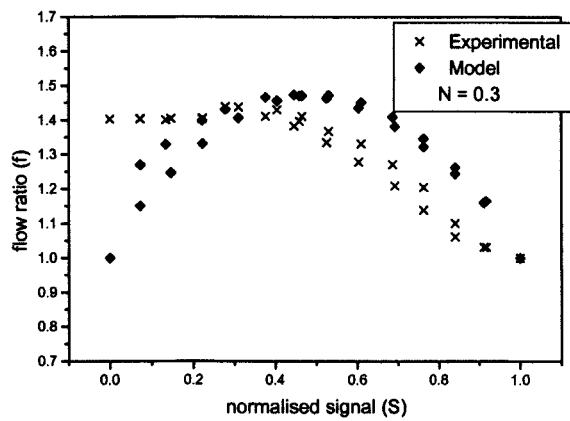


Fig.A46: 80mm valve,  $hys = 10\%$ ,  
 $G_0 = 0.05\%$  inlet and bypass ports

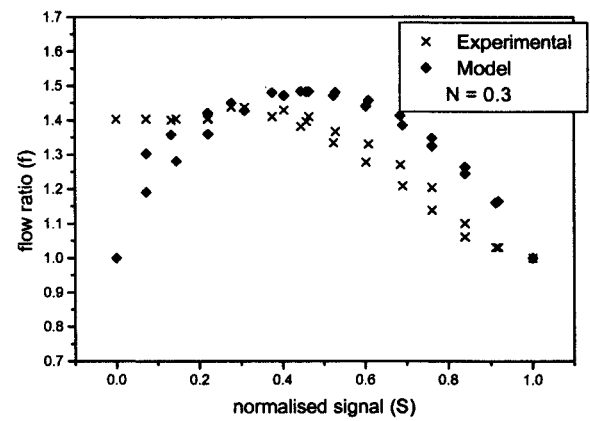


Fig.A47: 80mm valve,  $hys = 10\%$ ,  
 $G_0 = 0.05\%$  inlet port and 0.065% bypass port

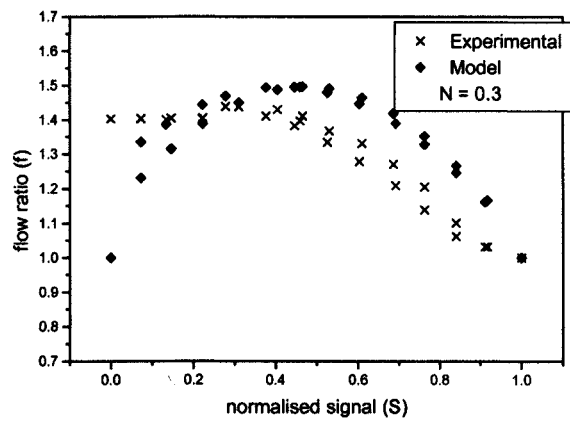


Fig.A48: 80mm valve,  $hys = 10\%$ ,  
 $G_0 = 0.05\%$  inlet port and 0.075% bypass port

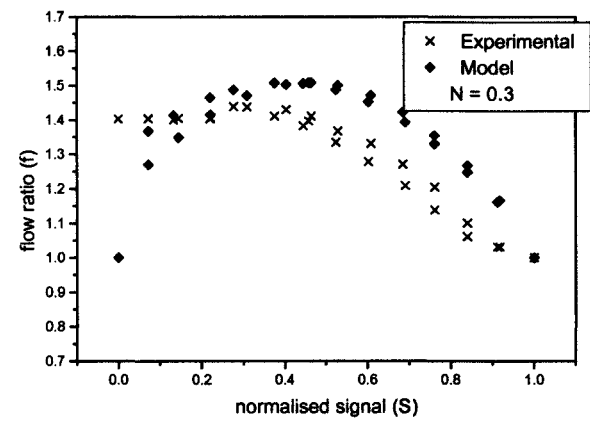


Fig.A49: 80mm valve,  $hys = 10\%$ ,  
 $G_0 = 0.05\%$  inlet port and 0.1% bypass port

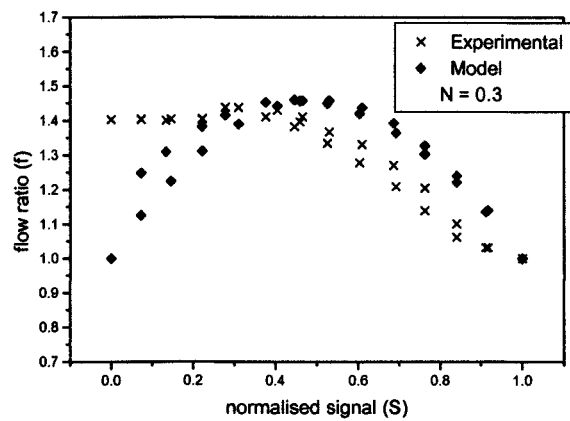


Fig.A50: 80mm valve,  $hys = 10\%$ ,  
 $G_0 = 0.01\%$  inlet and bypass ports

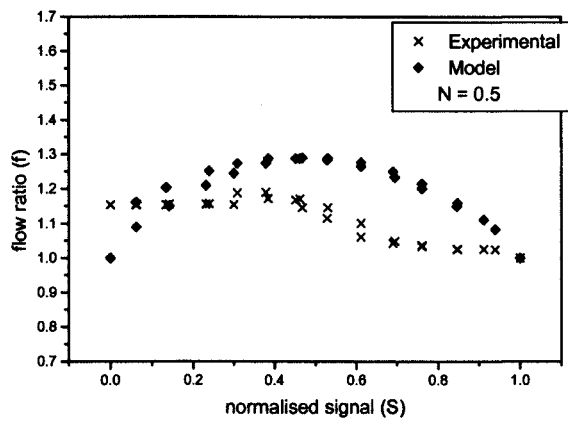


Fig.A51: 80mm valve,  $h_{ys} = 10\%$ ,  
 $G_0 = 0.05\%$  inlet and bypass ports

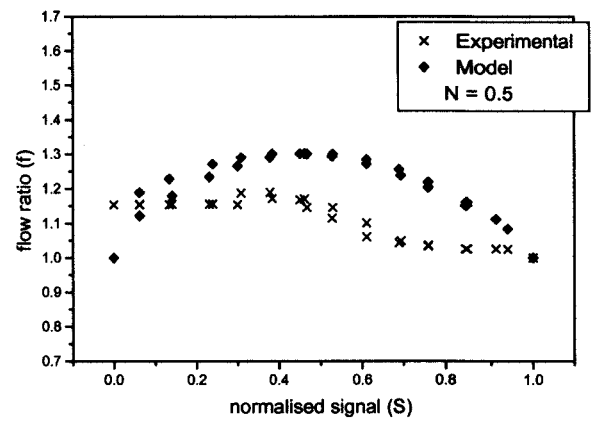


Fig.A52: 80mm valve,  $h_{ys} = 10\%$ ,  
 $G_0 = 0.05\%$  inlet port and 0.065% bypass port

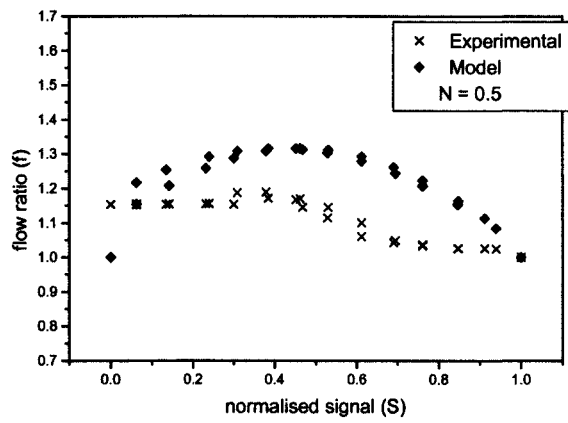


Fig.A53: 80mm valve,  $h_{ys} = 10\%$ ,  
 $G_0 = 0.05\%$  inlet port and 0.075% bypass port

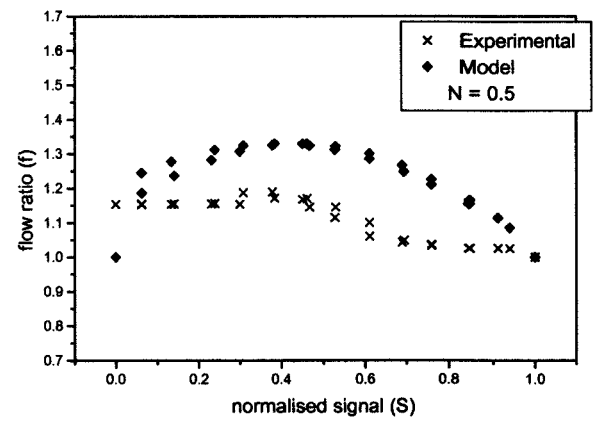


Fig.A54: 80mm valve,  $h_{ys} = 10\%$ ,  
 $G_0 = 0.05\%$  inlet port and 0.1% bypass port

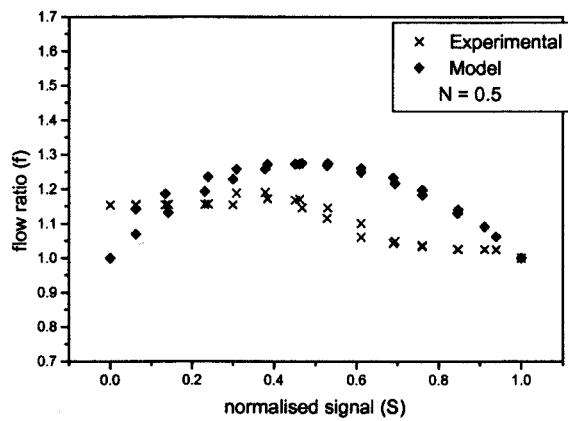


Fig.A55: 80mm valve,  $h_{ys} = 10\%$ ,  
 $G_0 = 0.01\%$  inlet and bypass ports